

Improvements in Methodologies for Radiographic Measurement of Diffusion Properties in Low-permeability Rocks, and Development of Methods for pH Measurement in Brines

NWMO-TR-2016-16

June 2016

Yan Xiang, Diana Loomer, Tom Al

University of New Brunswick

nwmo

NUCLEAR WASTE
MANAGEMENT
ORGANIZATION

SOCIÉTÉ DE GESTION
DES DÉCHETS
NUCLÉAIRES



Nuclear Waste Management Organization
22 St. Clair Avenue East, 6th Floor
Toronto, Ontario
M4T 2S3
Canada

Tel: 416-934-9814
Web: www.nwmo.ca

Improvements in Methodologies for Radiographic Measurement of Diffusion Properties in Low-permeability Rocks, and Development of Methods for pH Measurement in Brines

NWMO-TR-2016-16

June 2016

Yan Xiang, Diana Loomer, Tom Al
University of New Brunswick

This report has been prepared under contract to NWMO. The report has been reviewed by NWMO, but the views and conclusions are those of the authors and do not necessarily represent those of the NWMO.

All copyright and intellectual property rights belong to NWMO.

Document History

Title:	Improvements in Methodologies for Radiographic Measurement of Diffusion Properties in Low-permeability Rocks, and Development of Methods for pH Measurement in Brines		
Report Number:	NWMO-TR-2016-16		
Revision:	R000	Date:	June 2016
University of New Brunswick			
Authored by:	Yan Xiang, Diana Loomer, Tom Al		
Verified by:	Tom Al		
Approved by:	Tom Al		
Nuclear Waste Management Organization			
Reviewed by:	Tammy Yang		
Accepted by:	Mark Jensen		

ABSTRACT

Title: Improvements in Methodologies for Radiographic Measurement of Diffusion Properties in Low-permeability Rocks, and Development of Methods for pH Measurement in Brines

Report No.: NWMO-TR-2016-16

Author(s): Yan Xiang, Diana Loomer, Tom Al

Company: University of New Brunswick

Date: June 2016

Abstract

The objectives of this research are to develop and improve methodologies for measurement of diffusion properties in low-permeability sedimentary and crystalline rocks, and to develop methods for measurement of pH in high-ionic-strength aqueous solutions. Four separate projects are described.

The first project involved improvement and further development of the radiography method by using a monochromatic Am-241 γ -ray source. The use of monochromatic γ -radiation (γ -RAD) eliminates beam hardening which is a limitation to the precision and accuracy of the X-ray radiography technique. With the elimination of beam hardening, the γ -RAD technique allows for reliable calibration that is essentially independent of background matrix.

In the second project, diffusion coefficients for iodide (I^-) tracer were measured simultaneously using γ -RAD and through-diffusion on granite. Although only one test was conducted, the results indicate that the γ -RAD method will be a viable alternative to through-diffusion for measurements on very-low-porosity crystalline rocks.

The third project focused on the investigation of the effect of partial gas saturation on diffusion coefficients. A method has been developed to generate partial gas saturation in a rock sample by equilibrating the porewater with nitrogen (N_2) gas at high pressure (up to 7000 kPa) and then rapidly lowering the N_2 pressure to atmospheric. The degree of partial saturation is determined by the γ -RAD method. The effective diffusion coefficient (D_e) for iodide tracer at 100% brine saturation was compared to that at different degrees of partial gas saturation. A preliminary result from Queenston Formation shale indicates a 53% decrease in D_e as a result of 14.6% partial gas saturation. The results indicate good potential for evaluating the effect of partial saturation on diffusion in the low-permeability rocks that contain high salinity porewater.

The fourth project focussed on pH measurement in high-ionic-strength brine solutions. Buffers of varying composition and ionic strength were formulated and their pH values were determined by geochemical modelling using the Pitzer ion-interaction approach implemented in the geochemical program PHREEQC. These buffers were used to investigate two methods for pH measurement: potentiometric measurements with glass electrodes, and spectrophotometric measurements using the colorimetric indicator phenol red.

The pH electrode response is linear over a range from 1.4 to 9.1 and for ionic strengths up to 8.2 mol/kg. However, there is a systematic offset with increasing ionic strength such that an electrode calibrated with low-ionic-strength buffers will underestimate pH of a high-ionic-strength solution (8.2 mol/kg) by 0.6 to 0.7 pH units. For any given ionic strength, the potentiometric measurement is also sensitive to the ionic composition of the solution. Despite these effects, accurate potentiometric measurements are possible if the composition of the

calibration buffers is similar to the test solution. The results of spectrophotometric measurements indicate that the disassociation constant (pK'_a) of the phenol red indicator is virtually insensitive to the ionic composition of the solution. A maximum error of 0.2 units is possible for pH measured spectrophotometrically if the ionic strength of the buffers does not match the ionic strength of the test solution. However, the measurement range of phenol red is limited to a pH range from ~7 to 9; additional indicators can be used to increase the effective range for the spectrophotometric approach.

TABLE OF CONTENTS

	Page
ABSTRACT	iii
1. INTRODUCTION	1
2. γ-RADIOGRAPHY METHOD	1
2.1 CALIBRATION	5
2.2 SUMMARY	6
3. DIFFUSION MEASUREMENTS WITH GRANITE	7
3.1 METHODS	7
3.2 RESULTS	7
3.3 SUMMARY	10
4. EFFECT OF PARTIAL GAS SATURATION ON DIFFUSION	10
4.1 BACKGROUND: CREATING PARTIAL GAS SATURATION	10
4.2 EXPERIMENTAL PROCEDURES	13
4.3 RESULTS AND DISCUSSION	15
4.3.1 Partial Gas Saturation	15
4.3.1.1 Carbon Tan Sandstone	15
4.3.1.2 Queenston Formation Shale	16
4.3.2 Effect of Partial Gas Saturation on Diffusion Coefficients	17
4.3.2.1 Carbon Tan Sandstone	17
4.3.2.2 Queenston Formation Shale	21
4.4 SUMMARY	21
5. PH MEASUREMENT IN HIGH IONIC STRENGTH BRINE SOLUTIONS	23
5.1 HIGH-IONIC-STRENGTH BUFFERS	28
5.2 EXPERIMENTAL METHODS	34
5.2.1 Preparation of High Ionic Strength Buffers	34
5.2.2 Potentiometric pH Measurements	36
5.2.3 Spectrophotometric pH Measurements	36
5.3 RESULTS AND DISCUSSION	37
5.3.1 Potentiometric pH Measurements	37
5.3.2 Spectrophotometric pH Measurements	42
5.3.3 Uncertainty Assessment	44
5.4 SUMMARY	45
6. CONCLUDING REMARKS	46
ACKNOWLEDGEMENTS	47
REFERENCES	48

APPENDIX A: METHOD FOR ENSURING 100% BRINE SATURATION.....	57
APPENDIX B: PH MEASUREMENT IN BRINE SOLUTIONS	61

LIST OF TABLES

	Page
Table 1: Am-241 γ -RAD Operating Parameters	4
Table 2: γ -RAD Experimental Conditions	7
Table 3: Literature Values of Diffusion Properties Obtained by Through-diffusion Experiments for Crystalline Rocks	9
Table 4: Composition of Synthetic Porewater (SPW) Solutions Used at UNB	11
Table 5: Relationship between % Gas Saturation and Initial N ₂ Pressure (P ₁)	13
Table 6: Experimental Conditions Used for Partial Gas Saturation Experiments.....	14
Table 7: Properties of Variably Saturated Carbon Tan Sandstone.....	16
Table 8: Properties of Variably Saturated Queenston Formation Shale	17
Table 9: Additions Made to the PHREEQC v. 3.0.6 PITZER Database (pitzerUNB)	31
Table 10: Spectrophotometer Operating Conditions	36
Table 11: Measured Molar Absorptivities for Phenol Red in NaCl Solutions	42

LIST OF FIGURES

	Page
Figure 1: Sample Cell Designs for γ -RAD Experiments: (a) Sample Cell for Simultaneous Measurements Using γ -RAD and TD Techniques, (b) Sample Cell Used for Partial Saturation Experiments	2
Figure 2: Photograph of the γ -RAD System: The Am-241 γ -Ray Source is Visible at Left (Yellow), the Sample Cell is Mounted on a Computer-Controlled Stage in the Middle, and the Ti-NaI Detector is Encased in a Painted (Beige) Pb Brick at Right. Note that the Source Collimator was Removed for the Photo but the Detector Collimator is in Place.....	3
Figure 3: Estimation of Spatial Resolution (SR) for γ -RAD Technique	4
Figure 4: Calibration between $\Delta\mu$ and I ⁻ Concentration Using the γ -RAD Technique.....	6
Figure 5: Diffusion Profiles in Granite Obtained by γ -RAD with 4.0 M NaI Tracer. Inset: ϕ_i Profile of the Rock Sample	8
Figure 6: Results of Through-diffusion Experiment with Granite: (a) Flux of I ⁻ Tracer and (b) Cumulative I ⁻ Quantity as a Function of Time. This Experiment was Conducted Simultaneously with the γ -RAD Experiment (Figure 5)	8
Figure 7: Henry's Law Plots for N ₂ Gas at 25 °C in Water, 1.0 mol/L NaCl and 5.3 mol/L NaCl Solutions Calculated Using the Empirical Model Reported by Mao and Duan (2006). The Slopes Correspond to the Henry's Law Constants (K _H)	11
Figure 8: One Dimensional Profiles of a) $\Delta\mu$ and b) ϕ_i of 1 M I ⁻ Tracer in Carbon Tan Sandstone (Experiments CT-6A and CT-6B) before and after Establishment of Partial Gas Saturation. Error Bars Represent the Standard Deviation Measured on Replicate Scans over a Period of up to 7 Days	15
Figure 9: One Dimensional Profiles of a) $\Delta\mu$ and b) ϕ_i of 2 M I ⁻ Tracer in Queenston Shale Sample (DGR3-472) before and after Establishment of Partial Gas Saturation. Error Bars Represent the Standard Deviation Measured on Replicate Scans over a Period of 4 Days.....	16

Figure 10: Diffusion Profiles Obtained for Experiment CT-6A Using γ-RAD with 1.0 M NaI Tracer: a) In-Diffusion with 100% Brine (0% Gas) Saturation, b) Out-Diffusion with 15.2% Gas Saturation, and c) In-Diffusion following b). Inset Images are ϕ_I Profiles of the Rock Sample with I⁻ Tracer at Each Condition	19
Figure 11: Diffusion Profiles Obtained for Experiment CT-6B Using γ-RAD with 1.0 M NaI Tracer: a) In-Diffusion with 100% Brine (0% Gas) Saturation, b) Out-Diffusion with 13.5% Gas Saturation. Inset Images are ϕ_I Profiles of the Rock Sample with I⁻ Tracer at Each Condition	20
Figure 12: Diffusion Profiles Obtained for Sample DGR3-472 Using γ-RAD with 2.0 M NaI Tracer: a) In-Diffusion with 100% Brine (0% Gas) Saturation, b) Out-Diffusion with 14.6% Gas Saturation. Inset Images are ϕ_I Profiles of the Rock Sample with I⁻ Tracer at Each Condition.....	22
Figure 13: Schematic Example of a Modern Harned Cell, Based on the Diagram of Maksimov et al. (2008)	24
Figure 14: Glass Combination pH Electrode	26
Figure 15: Absorbance Spectra with Changing pH for Phenol Red in L-SPW Tris Buffer Solutions	27
Figure 16: Tris Buffer Data: a) Comparison of the pK'_a for Tris in Electrolyte Solutions Calculated Using PHREEQC (pitnerUNB Database) with Measured Values for Seawater and the Dead Sea from Millero et al. (1987, 1993). “MacInnes Convention” Means it was Used for Calculating pH in PHREEQC. The Filled Symbols Represent Measured Values and the Hollow Symbols Represent the Corresponding Calculated Values (Millero et al. 1987); (b) The Modelled pH of a 0.02 mol/kg Tris Buffer in the Same Solutions Shown in (a)	32
Figure 17: Acetate Buffer Data: (a) Comparison Between the Acetate pK'_a Calculated Using PHREEQC (pitnerUNB Database) and Values from Published Literature; (b) The Modelled pH of a 0.002 mol/kg Acetate Buffer in NaCl Solutions of Varying Ionic Strength. “MacInnes Convention” Means the MacInnes Convention was Used for Calculating pH in PHREEQC.....	33
Figure 18: Electrode Response to Changing pH for Selected Tris and HCl Buffer Solutions. Modelled pH Values Assume no Equilibrium with Atmospheric CO_{2(g)}. Inset: Filled Symbols Represent L-SPW Tris Buffer with No CO_{2(g)} and Hollow Symbols Represent Modelled pH Assuming Solution Equilibration with CO_{2(g)} (log PCO₂ = -3.4).....	38
Figure 19: Modelled Versus Measured pH for the Tris Buffer Data Set. Modelled pH Values Assume no Equilibrium with Atmospheric CO_{2(g)}. Data Series with the Identifier “Sureflow” were Measured with the Sureflow Electrode. Otherwise, the pH was Measured Using the Ross 815600 Electrode.....	39
Figure 20: The Difference Between Modelled pH and Potentiometrically Measured pH with Changing Ionic Strength and Solution Composition. Modelled Values Do Not Include Equilibration With Atmospheric CO_{2(g)}. Vertical Error Bars Represent the Standard Error in Potentiometric pH Measurements, ± 0.03 pH Units. Horizontal Error Bars Represent the Standard Deviation in Ionic Strength Across a Buffer Series; Where Not Visible, the Variation is Smaller than the Symbol.....	40
Figure 21: Measured pH of a L-SPW Tris Buffer Series Over Time. The Data Have	

Been Normalized to 25 °C. Error Bars Represent the Standard Error in Potentiometric pH Measurements, ± 0.03 pH Units	41
Figure 22: Plot of the Phenol Red Absorbance Ratio Versus pH in L-SPW. Filled Symbols Represent Modelled pH Assuming no Equilibrium with Atmospheric CO _{2(g)} ; Hollow Symbols Represent Modelled pH with Solutions at Equilibrium with Atmospheric CO _{2(g)} (log PCO ₂ = -3.4)	43
Figure 23: Variation in Phenol Red pK' _a with Ionic Strength and Solution Composition. Vertical Error Bars Represent 1σ . Horizontal Error Bars Represent the Standard Deviation in Ionic Strength Across a Tris Buffer Series; Where Not Visible, the Variation is Smaller than the Symbol	44

LIST OF ABBREVIATIONS

CT	Carbon Tan sandstone
D _p	Pore diffusion coefficient: $D_p = (\bar{\delta}/\tau) \cdot D_0$, where $\bar{\delta}$ is constrictivity, τ is tortuosity, and D_0 is the free water diffusion coefficient
D _e	Effective diffusion coefficient: $D_e = \phi D_p$.
DGR	Deep geological repository
ER	Edge Response
IUPAC	International Union of Pure and Applied Chemistry
L-SPW	DGR limestone synthetic porewater
MIN3P	Multicomponent reactive transport code
NIST	Nation Institute of Standards and Technology
NWMO	Nuclear Waste Management Organization
ODR	Optical Density Ratio
PHREEQC	A computer program for speciation, batch-reaction, one-dimensional transport, and inverse geochemical calculations
pK _a	Thermodynamic disassociation constant
pK' _a	Conditional disassociation constant
RAD	Radiography
γ-RAD	Gamma-radiography
RSD	Relative Standard Deviation
SNR	Signal-to-noise ratio
SP	Spatial Resolution
S-SPW	DGR shale synthetic porewater
TD	Through-diffusion
Tris	Tris-[hydroxymethyl]aminomethane
TrisHCl	Tris-[hydroxymethyl]aminomethane hydrochloride
UNB	University of New Brunswick
URL	Underground research laboratory
φ _i	Iodide-accessible porosity
φ _w	Water-loss porosity
Δμ	Change in attenuation coefficient
μ _{brine}	Attenuation coefficient of brine-saturated rock
μ _{PS}	Attenuation coefficient for the partially brine-saturated sample
μ _{PS-tracer}	Attenuation coefficient for the partially tracer-saturated sample
μ _{tracer}	Attenuation coefficient of the tracer-saturated rock

1. INTRODUCTION

This technical report documents activities and outcomes of research performed at the University of New Brunswick between March, 2012 and March, 2014 for the Nuclear Waste Management Organization. The research is intended to continue the development of new methodologies for laboratory measurements of diffusion properties in low permeability rocks and to gain a better understanding of the mechanisms controlling solute transport in diffusion-dominated sedimentary and crystalline rock systems. Such systems are under consideration in Canada as potential host and barrier rocks for a deep geological repository for the long-term management of radioactive waste.

The research is grouped into four projects that are presented separately in this report. The first involved improvement of the radiography method of tracer measurement in the estimation of diffusion properties in low permeability rocks by using a monochromatic γ -ray source (γ -RAD) instead of X-rays. One of the main advantages of the γ -RAD technique is to eliminate the beam hardening that occurs with a polychromatic X-ray source. A second advantage of the γ -RAD technique is that it allows for measurements on larger samples and provides greater flexibility in the experimental design. The second project involved development of methods for simultaneous measurement of diffusive tracer profiles in low permeability rocks using both γ -RAD and through-diffusion (TD) methods. This was tested for the first time using a granite sample. In the third project, a method was developed to create partial gas saturation conditions in porous sedimentary rock followed by the measurement of effective diffusion coefficient (D_e) values. The effect of partial gas saturation on diffusion coefficients was assessed by comparing the D_e values measured at full brine saturation with those measured at different degrees of partial gas saturation. The fourth project involved development of improved methods for pH measurement in high salinity natural porewaters. Accurate and precise measurement of pH at high ionic strength is important for a range of research activities that seek to quantify water-rock reaction processes (e.g. ion exchange, speciation, surface complexation, and mineral precipitation and dissolution), most of which are sensitive to pH.

2. γ -RADIOGRAPHY METHOD

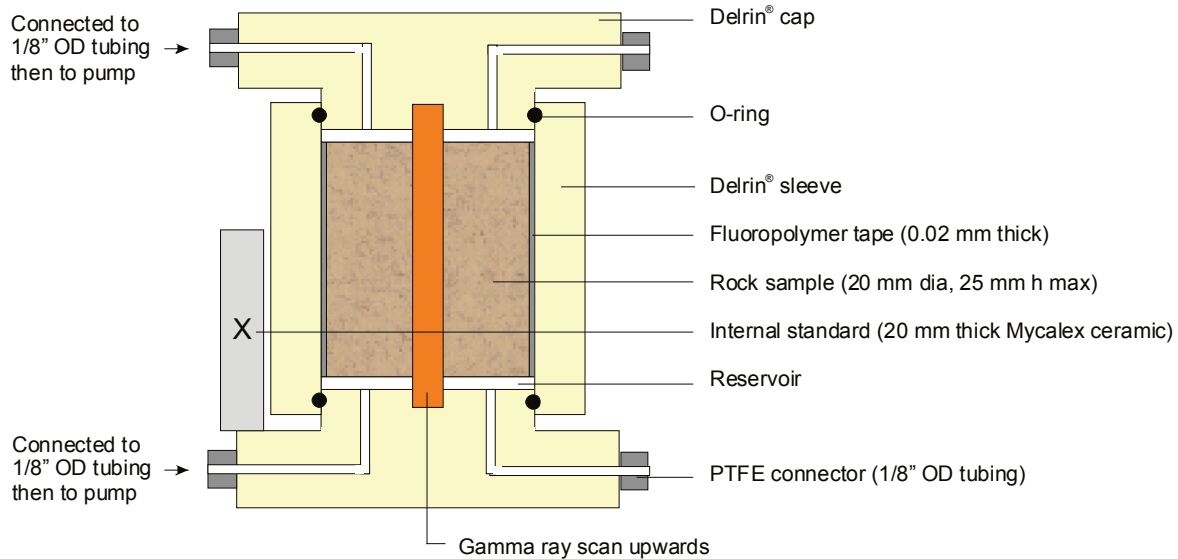
A γ -RAD technique was first developed by Subudhi (2009) and Subudhi et al. (2010) for measurement of porosity and diffusion coefficients of porous media. The method is similar in principle to the X-ray RAD technique (Al et al. 2010; Cavé et al. 2009, Cavé et al. 2010) except that it uses monochromatic gamma radiation from an Am-241 source. This has some advantages over the use of X-rays in that it minimizes or eliminates artefacts from beam hardening and X-ray-beam geometry and there are no restrictions on the sample size.

New sample cells were designed and constructed as shown in Figure 1. The cell shown in Figure 1a was used for simultaneous diffusion measurements with γ -RAD and TD methods, and the cell in Figure 1b was used for quantifying the degree of partial gas saturation and for measuring D_e on rock samples with variable brine-gas saturation states.

The circumference of the cylindrical sample (nominal 20 mm diameter, 13-25 mm height) was wrapped with a thin Teflon® tape (0.02 mm thickness, Green Belting Industries). The seam was sealed with a thin bead of silicone. The sample was pressed into the Delrin® sleeve

(Figure 1) and then saturated with a background brine solution (Appendix A). After sample saturation, the diffusion cell was assembled by installing Delrin® caps at each end (Figure 1).

a)



b)

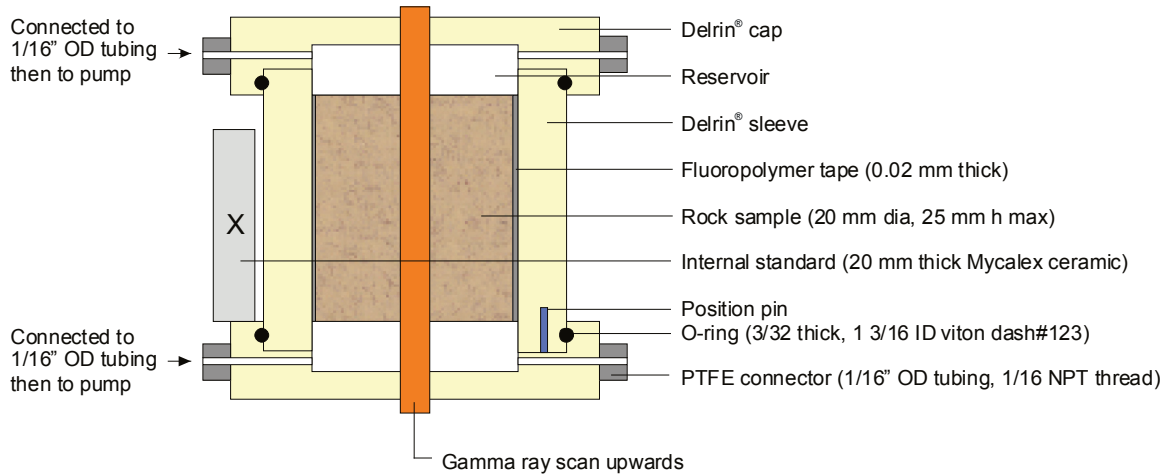


Figure 1: Sample Cell Designs for γ -RAD Experiments: (a) Sample Cell for Simultaneous Measurements Using γ -RAD and TD Techniques, (b) Sample Cell Used for Partial Saturation Experiments

Mycalex® ceramic was used for an internal standard because it has similar density and γ attenuation to the experimental rock materials (Loomer et al. 2013a). The internal standard was fixed to the side of the cell. The radiation path along the rock sample is shown in Figure 1. The length of the radiation path is 20 mm for both the rock samples and for the ceramic standard. The diffusion cell was mounted on a stage controlled by an automated stepping motor (BiSlide® Velmex Inc.; Figure 2). Positioning pins were constructed on the stage so that the cell can be removed and replaced in the same position during the experiments.

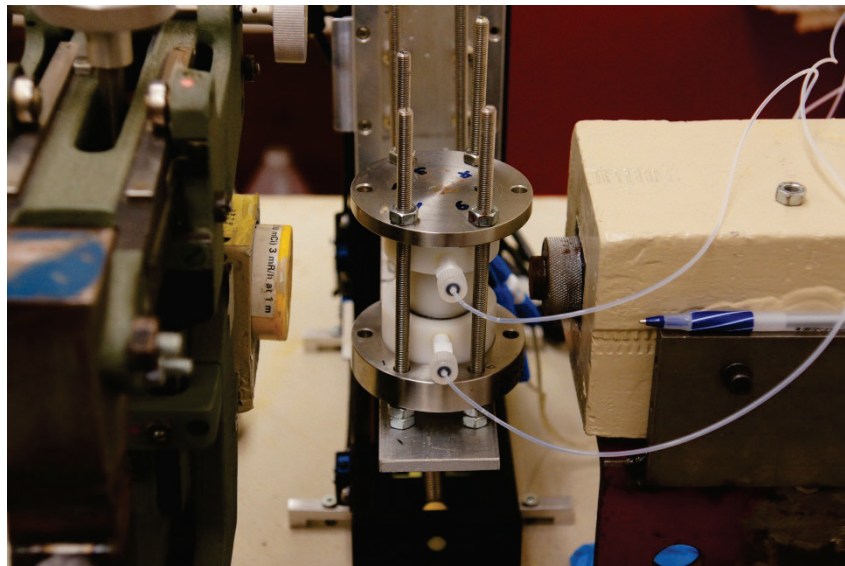
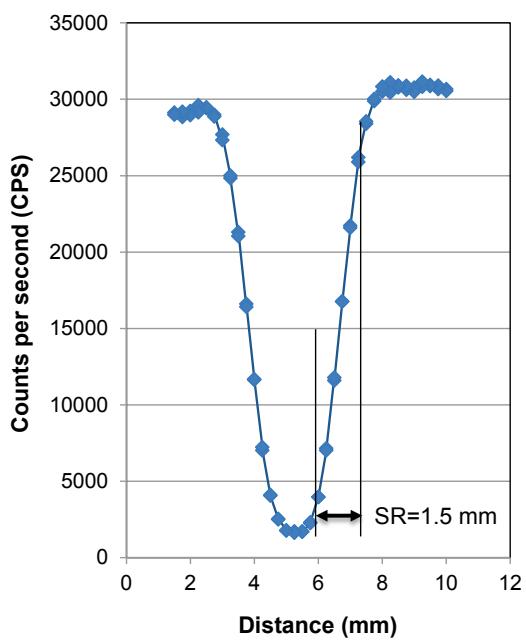


Figure 2: Photograph of the γ -RAD System: The Am-241 γ -Ray Source is Visible at Left (Yellow), the Sample Cell is Mounted on a Computer-Controlled Stage in the Middle, and the TI-Nal Detector is Encased in a Painted (Beige) Pb Brick at Right. Note that the Source Collimator was Removed for the Photo but the Detector Collimator is in Place

The system employs an Am-241 sealed source (11.1 GBq), a TI-Nal detector (Canberra model 802) powered by a Tennelec model TC950 detector bias supply, and a Tennelec model TC246 amplifier and single channel analyzer. The source and detector collimation, and the source-detector alignment are described by Subudhi et al. (2010). The operating parameters are presented in Table 1. The spatial resolution of the measurements (1.4 to 1.5 mm diameter) was determined using an Edge Response (ER) technique (Smith 2003; Hussein 2011). The ER measures how an instrument responds to a sharp discontinuity and involves collecting a line profile across the boundary of two sharply contrasting materials or media (such as the edge of a solid material and air). The spatial resolution is taken to be the distance required for the profile to rise from 10% to 90% of the difference in the values of the two contrasting materials or media. In this case the spatial resolution was determined by scanning (0.25 mm step size) across the sharp edge of a 3-mm-thick steel bar positioned on the sample stage (Figure 3).

Table 1: Am-241 γ -RAD Operating Parameters

Collimator diameter	3.0 mm
Sample thickness	20 mm
Source-detector distance	10 mm
Detector-sample distance	4 mm
Source collimator length	10.0 mm
Detector collimator length	95 mm
Detector Output voltage	1700 V
Coarse gain	50
Fine gain	8
Overall gain	$50 \times 0.8 = 40$
Stage increments (X,Z)	200 per 1.0 mm
Spatial resolution (diameter)	1.4 - 1.5 mm
Measurement step size (mm)	0.5 - 1.0
Scan time/point (s)	35 – 60

**Figure 3: Estimation of Spatial Resolution (SR) for γ -RAD Technique**

The radiography method for measuring diffusion coefficients uses a blank subtraction approach (Al et al. 2010; Cavé et al. 2009; Cavé et al. 2010) to remove the constant background attenuation effects of the porous matrix. Time-series radiographs (samples with tracer at $t > 0$) are subtracted from a reference radiograph (sample without tracer at $t = 0$) to determine the change in attenuation due to tracer mass in the pores, which we define as the parameter $\Delta\mu$:

$$\Delta\mu_x = \ln(I_{ref})_x - \ln(I_t)_x = (\mu_p|_{t=0} - \mu_p|_{t>0})_x \cdot \phi_x \quad (1)$$

where: t is time, $(I_{ref})_x$ is the transmitted γ -ray intensity at distance x on the $t = 0$ (reference) profile, $(I_t)_x$ is the transmitted γ -ray intensity at the same distance on one of the time-series profiles ($t > 0$), $\mu_p|_{t=0}$ and $\mu_p|_{t>0}$ are the attenuation coefficients of the pore fluids in the reference and time-series radiographs, respectively. The parameter $\Delta\mu$ is a function of the mass of tracer along the γ -ray path and is used to determine quantitative measurements of tracer concentration (Al et al. 2010; Cavé et al. 2009; Cavé et al. 2010).

There is significant ambiguity in the literature in terms of diffusion-related terms, so the following definitions are provided for clarity:

$$\text{Pore diffusion coefficient} = D_p = D_0 \cdot \tau_f \quad (2)$$

where: D_0 is the free-water diffusion coefficient and τ_f is the tortuosity factor,

$$\text{Effective diffusion coefficient} = D_e = D_p \cdot \phi \quad (3)$$

where: ϕ is porosity.

2.1 CALIBRATION

Calibration curves for $\Delta\mu$ as a function of I⁻ concentration were generated by the method reported by Cavé et al. (2009) using the sample cell (Figure 1) filled with a series of brine/tracer standard solutions. The $\Delta\mu$ values were normalized to the diameter of the rock samples, which is slightly smaller than the inner diameter of the Delrin® sleeve. Results of the calibration in a 1.0 M NaNO₃ matrix and in a much more saline S-SPW matrix (shale synthetic porewater, see Table 4) are presented in Figure 4. This relationship is linear over a range of $\Delta\mu$ up to approximately 2 and the slope is almost independent of the background matrix. In contrast, calibration curves obtained with X-ray radiation are affected by beam hardening which results in non-linear relationships and matrix dependency.

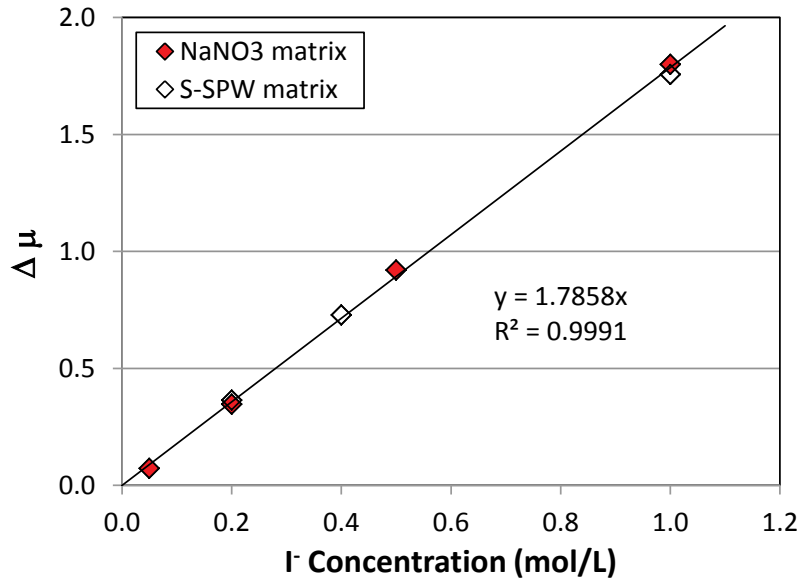


Figure 4: Calibration between $\Delta\mu$ and I^- Concentration Using the γ -RAD Technique

2.2 SUMMARY

The use of monochromatic Am-241 γ radiation eliminates beam hardening, providing a precise calibration function. Results of calibration indicate a linear function over a large range in $\Delta\mu$ that is not sensitive to the background matrix. The method is appropriate for measurements of tracer concentration in cases where spatial resolution on the order of 1 mm or greater is satisfactory.

3. DIFFUSION MEASUREMENTS WITH GRANITE

3.1 METHODS

A test was conducted to determine the potential for using the γ -RAD method for measuring diffusion coefficients of crystalline rocks such as granite. The testing was conducted on archived granite sample from the Atomic Energy of Canada Limited Whiteshell Research Area, specifically a segment of borehole 209-069-PH3 (sample OPG-10 from Cavé and Al 2006). A subsample, 20 mm in diameter, was prepared by diamond coring and then the sample was mounted in the modified diffusion cell (Figure 1a) which allows for simultaneous measurements by TD and by γ -RAD methods. The sample was saturated with NaNO_3 (4 mol/L) solution by immersion (mounted in the Delrin® sleeve) under vacuum for 3 days (Appendix A). The cell was then assembled and 4 mol/L NaNO_3 solution was circulated through both ends for 8 additional days. The concentration of the I^- tracer and the scanning parameters (Table 2) were selected to provide sufficient contrast for the γ -RAD method. The TD measurements were conducted according to the methods previously described by Cavé et al. (2010) and Xiang et al. (2013).

Table 2: γ -RAD Experimental Conditions

Sample	Carbon Tan	Queenston shale	Granite
Scan time/point (s)	35	35	60
Measurement Step Size (mm)	1.0	0.75	0.5
Synthetic Pore Fluid	1.0 M NaNO_3	S-SPW ^a	4.0 M NaNO_3
Tracer	1.0 M NaI	2.0 M I^- in S-SPW ^b	4.0 M NaI

^a Shale synthetic porewater, Table 4; ^b Equal moles of NaCl were substituted by NaI in S-SPW.

3.2 RESULTS

The γ -RAD measurements (Figure 5) display a large degree of scatter due to the low porosity and the resulting small mass of tracer contained in the sample. Efforts to enhance the signal to noise ratio (SNR) included the use of long counting times and high tracer concentration (Table 2). Despite the scatter in the data it is possible to identify tracer profiles that advance with time, and an average pore diffusion coefficient (D_p) value of $7.2 \times 10^{-11} \text{ m}^2/\text{s}$ is obtained. For the purpose of comparison, this D_p value can be multiplied by ϕ_i (0.0043) (iodide accessible porosity) to obtain a D_e value of $3.1 \times 10^{-13} \text{ m}^2/\text{s}$ which is consistent with measured diffusion coefficients for crystalline rocks from Manitoba Canada, Sweden and Finland (Table 3). A through-diffusion (TD) experiment was conducted simultaneously, and the early-time trends in the tracer flux and cumulative mass data (<13 days; Figure 6) evolved according to expectations. However, beyond 13 days the tracer flux decreases in a way that is inconsistent with steady-state diffusion. This behaviour is thought to result from gradual occlusion of diffusion pathways due to mineral-water reactions. Although the early time data (<13 days) indicate a D_e value of $3.0 \times 10^{-13} \text{ m}^2/\text{s}$ which is very close to the value obtained by γ -RAD,

confidence in this result is low because of the unexpected decline in the tracer flux after 13 days.

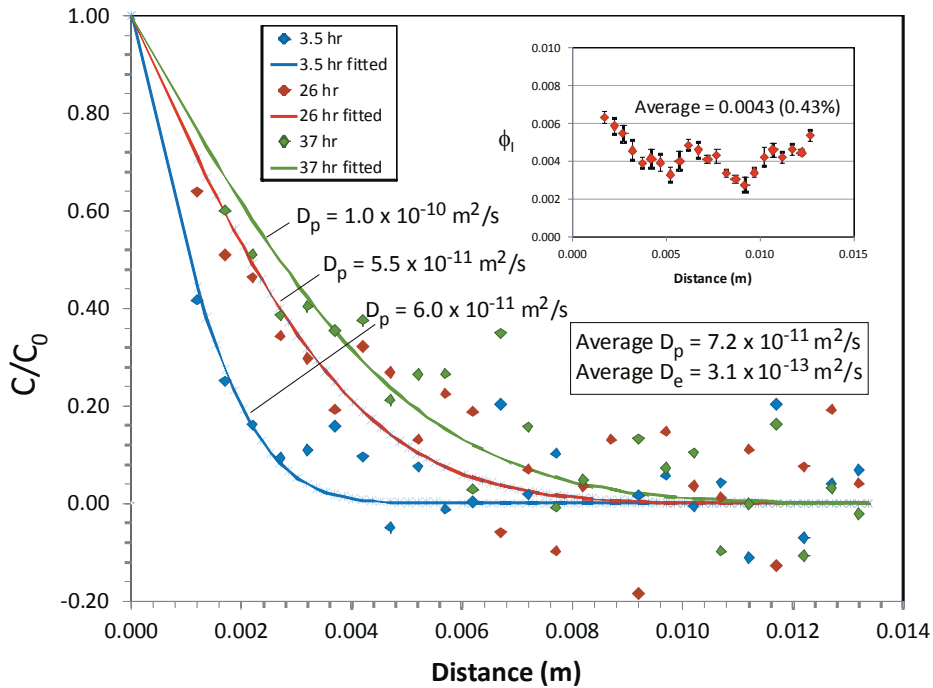


**Figure 5: Diffusion Profiles in Granite Obtained by γ -RAD with 4.0 M NaI Tracer.
Inset: ϕ_i Profile of the Rock Sample**

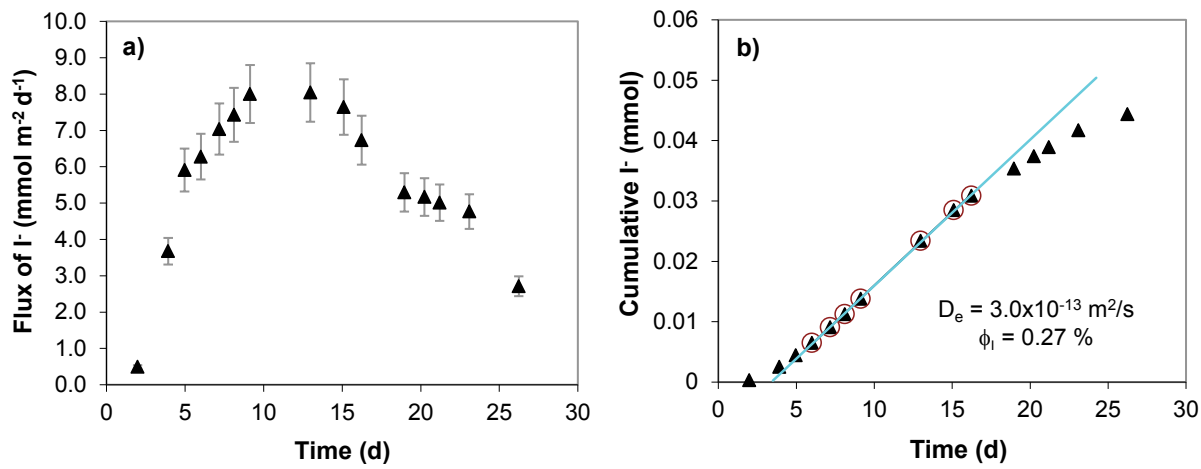


Figure 6: Results of Through-diffusion Experiment with Granite: (a) Flux of I^- Tracer and (b) Cumulative I^- Quantity as a Function of Time. This Experiment was Conducted Simultaneously with the γ -RAD Experiment (Figure 5)

Table 3: Literature Values of Diffusion Properties Obtained by Through-diffusion Experiments for Crystalline Rocks

Location	Rock type	Porosity	D_e (m²/s)	Exp. condition	Ref.
Canada, URL Manitoba	Granite, granodiorite	0.22-0.28% (H ₂ O immersion), 0.46 - 0.94% (I ⁻ ; TD)	2.1x10 ⁻¹² to 1.9x10 ⁻¹³	in situ, I ⁻	a
			2.2x10 ⁻¹² to 2.7x10 ⁻¹²	Lab, I ⁻	
Sweden central, east coast	Granite, granodiorite		7.0x10 ⁻¹² to 1.3x10 ⁻¹³	lab, I ⁻	b
			1.3x10 ⁻¹³ to 1.8x10 ⁻¹³	lab, HTO	
Sweden, Aspo lab	Diorite and granite	0.36 - 0.84%	1x10 ⁻¹³ to 9x10 ⁻¹³	lab, I ⁻ , HTO	c
Finland	Tonalite and mica gneiss	0.1 - 3% (tonalite)	3.0x10 ⁻¹² to 9x10 ⁻¹³	lab, TD, HTO	d
		0.2% (mica gneiss)	1.0x10 ⁻¹² to 6x10 ⁻¹³	lab, TD, Cl ⁻	

^a Vilks et al. 2003; ^b Skagius and Neretnieks 1986; ^c Xu et al. 2001 and Johansson et al. 1998; ^d Siitari-Kauppi et al 1997.

3.3 SUMMARY

The γ -RAD method has been tested for potential use in measurement of D_e values for crystalline rock samples. The result is consistent with the range of values obtained for crystalline rocks elsewhere. The result is also in good agreement with the D_e value obtained with simultaneous measurement by TD on the same sample ($3.0 \times 10^{-13} \text{ m}^2 \cdot \text{s}^{-1}$ and $3.1 \times 10^{-13} \text{ m}^2 \cdot \text{s}^{-1}$, respectively). However, there is low confidence in the TD measurement. This is the first and only test of the radiography method on low-porosity crystalline rocks and, although further improvements are possible, the results suggest that it is a viable approach.

4. EFFECT OF PARTIAL GAS SATURATION ON DIFFUSION

Results of site characterization studies at the Bruce nuclear site suggest that at some depths in the Ordovician shales and limestones the porewater saturation may be less than 100% and the pore volume may be occupied by a mixture of porewater and gas (Intera, 2011). Partial gas saturation may result from the formation of methane by thermogenic or biogenic mechanisms. Pore-scale changes in the volume ratio of gas and porewater are expected to affect D_e for both aqueous solutes and gases (Savoye et al. 2010).

In this study, our objectives are:

- to develop a method to create partial saturation in rock samples for use in testing of the γ -RAD technique;
- to determine the degree of the partial saturation using the γ -RAD technique; and,
- to investigate the effect of partial saturation on D_e in low permeability rocks.

Sedimentary rocks may contain highly saline porewater, and experimental methods for generating partial saturation must not cause dewatering which could lead to the precipitation of salts, occlusion of porosity and artefacts in D_e measurements.

4.1 BACKGROUND: CREATING PARTIAL GAS SATURATION

The approach to creating partial-gas-saturated conditions in rock samples uses N_2 gas and takes advantage of the variability of N_2 solubility versus pressure. The solubility of a gas in aqueous solution at a given temperature is proportional to its partial pressure. This is known as Henry's law:

$$S_i = K_H \cdot P_i \quad (4)$$

where S_i is the solubility of gas i (mol/L) in an aqueous solution; K_H is the Henry's law constant ($\text{mol} \cdot \text{L}^{-1} \cdot \text{atm}^{-1}$ or M/atm) for gas i in the solution; P_i is the partial pressure of gas i (atm). The constant K_H is dependent on the gas, the temperature and the solution composition. The partial saturation experiments described herein are conducted at 25 °C using N_2 gas and synthetic porewater solution (1.0 mol/L NaNO_3 solution for the Carbon Tan sandstone and shale synthetic porewater, S-SPW, for the Queenston Formation shale, Table 2). The composition of S-SPW (Table 4) was adapted from previous work on shale samples (Al et al. 2010, 2012; Cavé et al. 2010; Loomer et al. 2013b; Xiang et al. 2013). The solubility of N_2 at 25 °C as a

function of partial pressure (P_{N_2} ; Figure 7) was calculated with the empirical model reported by Mao and Duan (2006) for N_2 solubility in NaCl solutions up to 5.3 mol/L. Model calculations were conducted using 1.0 mol/L NaCl solution as a proxy for the 1.0 mol/L $NaNO_3$ Carbon Tan sandstone porewater. Model calculations for the Queenston shale porewater were conducted at the 5.3 mol/L (NaCl solution) limit of the model although the S-SPW is actually a Na-Ca-Cl solution with 5.8 mol/L Cl^- . As a result, the model calculations do not fully represent the experimental system, and particularly for the S-SPW case, it is expected that the N_2 solubility in S-SPW will be overestimated by the model.

Table 4: Composition of Synthetic Porewater (SPW) Solutions Used at UNB

	S-SPW (mol/kg)	L-SPW (mol/kg)
Na^+	2.71	2.18
K^+	0.56	0.49
Ca^{2+}	1.36	0.53
Mg^{2+}	0.28	0.22
Cl^-	6.55	4.16
SO_4^{2-}	0.001	0.005
Ionic Strength	8.2	4.9

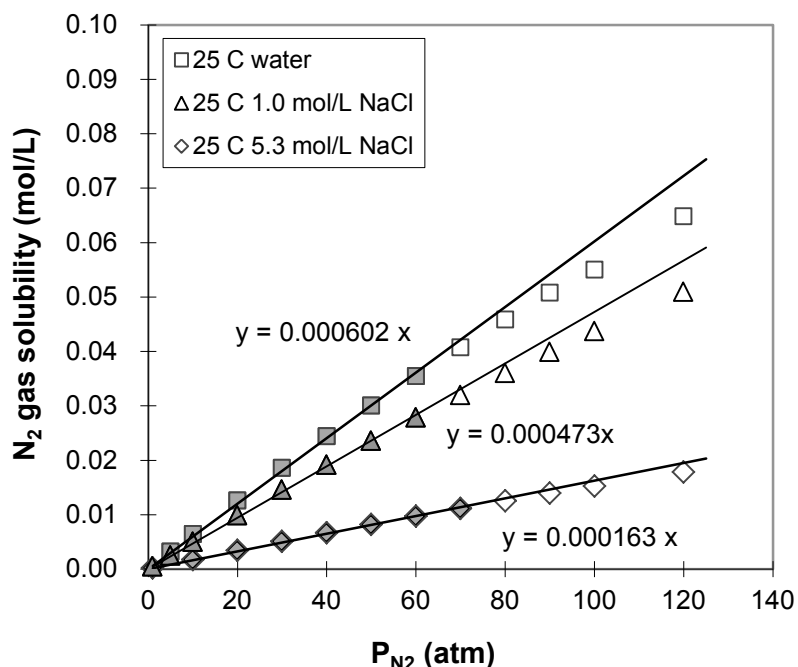


Figure 7: Henry's Law Plots for N_2 Gas at 25 °C in Water, 1.0 mol/L NaCl and 5.3 mol/L NaCl Solutions Calculated Using the Empirical Model Reported by Mao and Duan (2006). The Slopes Correspond to the Henry's Law Constants (K_H)

Data in Figure 7 indicate that N₂ solubility in 1.0-5.3 mol/L NaCl brines obeys Henry's law up to a partial pressure of 60-70 atm (filled symbols), after which (open symbols) there is a slight departure from linearity. The K_H values determined are 0.000473 M/atm for 1.0 mol/L NaCl brine and 0.000163 M/atm for 5.3 mol/L NaCl.

When a brine system undergoes a change in N₂ partial pressure from high (P₁) to low (P₂), the solubility of N₂ decreases correspondingly from S₁ to S₂. As a result, gas bubbles will form in the solution. For the brine solution occupying the pore spaces in a rock sample, gas bubbles should form in the pore spaces, causing partial brine saturation. Assuming equilibrium is established at P₂, the moles of N₂ bubbles, n, can be calculated according to:

$$n_{\text{bubble}} = K_H V_p (P_1 - P_2) \quad (5)$$

where V_p is the volume of the rock pores (L) initially occupied by brine. The volume of the gas bubbles (V_{bubble}) formed at P₂ can be calculated using the ideal gas law:

$$V_{\text{bubble}} = n_{\text{bubble}} RT / P_2 = K_H V_p (P_1 - P_2) RT / P_2 \quad (6)$$

The bubble volume calculated by this method was compared to the bubble volume calculated using Van der Waal's equation for non-ideal gases. A maximum difference between two methods of 0.07% was noted under the experimental conditions. Assuming bubbles are formed and remain in the rock pores (the volume change is accounted for by expulsion of brine from the pores), the relative pore volume occupied by gas (% gas saturation) will be:

$$\% \text{ gas saturation} = [K_H (P_1 - P_2) RT / P_2] \times 100\% \quad (7)$$

Experiments were designed so that P₂ was equal to 1 atm of N₂ (moisturized). Values for the % gas saturation as a function of P₁ (Table 5) were calculated using Equation 7. The calculations included P₁ values beyond the linear region in Figure 7 (>60-70 atm) assuming Henry's law still applies.

Table 5: Relationship between % Gas Saturation and Initial N₂ Pressure (P₁)

% gas sat.	1.0 M NaCl		5.3 M NaCl	
	P ₁ (atm)	P ₁ (kPa)	P ₁ (atm)	P ₁ (kPa)
2	2.6	268	5.8	591
5	5.2	522	13.1	1329
10	9.3	947	25.3	2560
20	17.7	1795	49.6	5022
25	21.9	2219	61.7	6253
30	26.1	2643	73.9	7484
35	30.3	3068	86.0	8715
40	34.5	3492	98.2	9946
45	38.6	3916	110.3	11177
50	42.8	4340	122.5	12408
55	47.0	4765	134.6	13639
60	51.2	5189	146.8	14870
70	59.6	6037	171.1	17332
80	68.0	6886	195.4	19794
90	76.3	7734	219.7	22256

^aData were calculated using Equation 7 under the following conditions: T = 25 °C, P₂ = 1.0 atm N₂, 1.0 mol/L or 5.3 mol/L NaCl brine with a K_H constant of 0.000473 mol L⁻¹ atm⁻¹ or 0.000163 mol L⁻¹ atm⁻¹ (Figure 7), respectively.

Estimates of % gas saturation from Equation 7 represent the maximum attainable values. The actual degree of partial saturation achieved by experiment is expected to be lower because some N₂ may be lost from the system by diffusion while the system re-equilibrates from P₁ to P₂. The actual degree of partial saturation is determined by the γ -RAD method.

4.2 EXPERIMENTAL PROCEDURES

Samples used in the investigation of partial gas saturation include one sample of Carbon Tan sandstone that was used in two experiments, one after the other (CT-6A and CT-6B) and a sample of Queenston Formation shale (DGR3-472). The experimental procedures are as follows:

- The samples were saturated according to the methods described in Appendix A using a synthetic pore fluid (1.0 mol/L NaNO₃ for the Carbon Tan sandstone and S-SPW for the Queenston Formation shale), installed in a Delrin® diffusion cell (Figure 1b).
- The initial reference scan was conducted prior to the introduction of tracer, which provides a measure of the γ attenuation properties of the brine–saturated rock (μ_{brine}).
- The samples were submerged in the tracer solution (Table 2) and allowed to saturate with l tracer after which γ -RAD scans were conducted to measure the γ attenuation properties of the tracer–saturated rock (μ_{tracer}).

- The solution containing the samples was then placed in a chamber pressurized with N₂ gas (P₁, Table 6). The system was allowed to equilibrate for up to 27 days, after which time the N₂ pressure in the chamber was decreased to one atmosphere (P₂), the sample was removed from the tracer solution and the diffusion cell was quickly re-assembled (<15 minutes).
- Moisturized N₂ gas (~1 atm) was pumped through both reservoirs (~15 mL/min) and radiography scans were recorded to monitor the displacement of tracer solution from the sample due to formation of N₂ gas bubbles. It took between five and ten hours for this process to stabilize in the Carbon Tan sandstone sample, and 48 hours in the Queenston shale sample.
- Fresh tracer solution (1.0 M I⁻ for Carbon Tan sandstone and 2.0 M I⁻ for Queenston Formation shale) was then allowed to circulate through both reservoirs for up to eleven days to ensure that the brine/gas saturation states had stabilized. Three scans were conducted before starting the diffusion experiment and the average of these scans ($\mu_{PS-tracer}$) provides a reference for the diffusion experiment to measure D_e for the partially saturated sample. This measurement was conducted as an “out-diffusion” experiment whereby synthetic pore fluid was introduced to one reservoir and tracer was allowed to diffuse out of the sample.
- After the out-diffusion measurement, the remaining I⁻ tracer was removed by circulating synthetic pore fluid through both reservoirs while recording radiography scans periodically to confirm complete removal.
- After tracer removal, three final scans were recorded ($\mu_{PS-brine}$) to complete the multi-step experiment.

A quantitative measure of the degree of partial gas saturation is obtained as:

$$\text{% gas saturation} = \left(1 - \frac{\Delta\mu_{ps}}{\Delta\mu_S}\right) 100\% \quad (8)$$

Where subscripts *ps* and *S* indicate partially-saturated and saturated conditions respectively.

For the purpose of comparison, an in-diffusion experiment was conducted following the out-diffusion experiment (CT-6A and CT-6B respectively).

Table 6: Experimental Conditions Used for Partial Gas Saturation Experiments

Experiment ID	CT-6A	CT-6B	DGR3-472
P ₁ (kPa)	4400	6600	7000
T (°C)	23 ± 2	22.5 ± 0.5	23 ± 1
Predicted % gas saturation (from Table 5)	50	80	28

4.3 RESULTS AND DISCUSSION

4.3.1 Partial Gas Saturation

4.3.1.1 Carbon Tan Sandstone

One-dimensional profiles of $\Delta\mu$ that reflect the distribution of I⁻ tracer mass in the rock samples are compared before and after establishment of partial gas saturation (Figure 8a). The concentration of I⁻ in the porewater remains constant so the systematic shift of the profiles to lower $\Delta\mu$ values is consistent with a decrease in porewater volume. Profiles of $\Delta\mu$ have been converted to that of ϕ_l (Figure 8b) using the calibration function of the γ -RAD method (Section 2.1). These results demonstrate that there is a near-uniform displacement of pore fluid due to formation of a discrete gas phase. Measurements indicate that the average partial gas saturation is 15.2% (84.8% brine) for experiment CT-6A and 13.5% (86.5% brine) for experiment CT-6B calculated by equation 8 (Table 7). These percentages are much lower than the predictions (50% and 80% respectively; Table 6). The discrepancy between predicted and measured values may be explained by non-ideal effects that are not accounted for in the ideal-gas law or the Van der Waal equation. Perhaps most importantly, the tendency to form a discrete gas phase in the pore space will be limited by the permeability, which controls the rate of pore fluid displacement by the expanding gas bubbles.

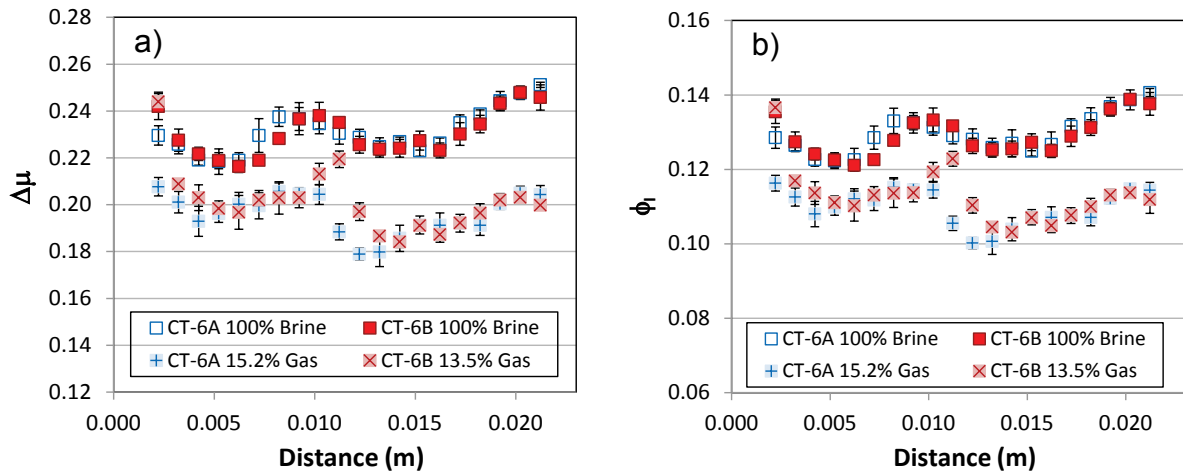


Figure 8: One Dimensional Profiles of a) $\Delta\mu$ and b) ϕ_l of 1 M I⁻ Tracer in Carbon Tan Sandstone (Experiments CT-6A and CT-6B) before and after Establishment of Partial Gas Saturation. Error Bars Represent the Standard Deviation Measured on Replicate Scans over a Period of up to 7 Days

Table 7: Properties of Variably Saturated Carbon Tan Sandstone

Experiment	CT-6A	CT-6A-PS ^a	CT-6B	CT-6B-PS ^a
$\Delta\mu$ (1 M I⁻)	0.231	0.196	0.230	0.199
ϕ_l (brine)^b	0.129	0.110	0.129	0.111
% Brine Saturation	100	84.8	100	86.5
% Gas Saturation	0	15.2	0	13.5
D_p (m²/s)	4.1E-10	3.9E-10 ^c	4.8E-10	2.4E-10
D_e (m²/s)	5.3E-11	4.2E-11 ^c	6.2E-11	2.7E-11

^a PS indicates samples with partial gas saturation; ^b brine-filled porosity determined by γ -RAD;^c average of values determined by in- and out-diffusion experiments.

4.3.1.2 Queenston Formation Shale

Profiles representing the distribution of I⁻ tracer in the shale sample before and after establishment of partial gas saturation (Figure 9) indicate a general shift to lower I⁻ mass, in a similar manner to the sandstone samples. Unfortunately, data in Figure 9 also indicate that sample breakage occurred at a distance of 0.015 m. The sample separated along the bedding plane, presumably due to the build-up of gas pressure that could not be relieved by pore fluid displacement because of the low permeability of the rock. This problem can be avoided with some minor modifications to the diffusion cell design. Results of measurements reported in Table 8 for this partially-gas saturated sample were obtained from the data collected in the 0-0.015 m portion of the sample. Measurement of the degree of partial gas saturation indicates 14.6% (85.4% brine). Once again, this percentage is lower than predicted (28%, Table 6).

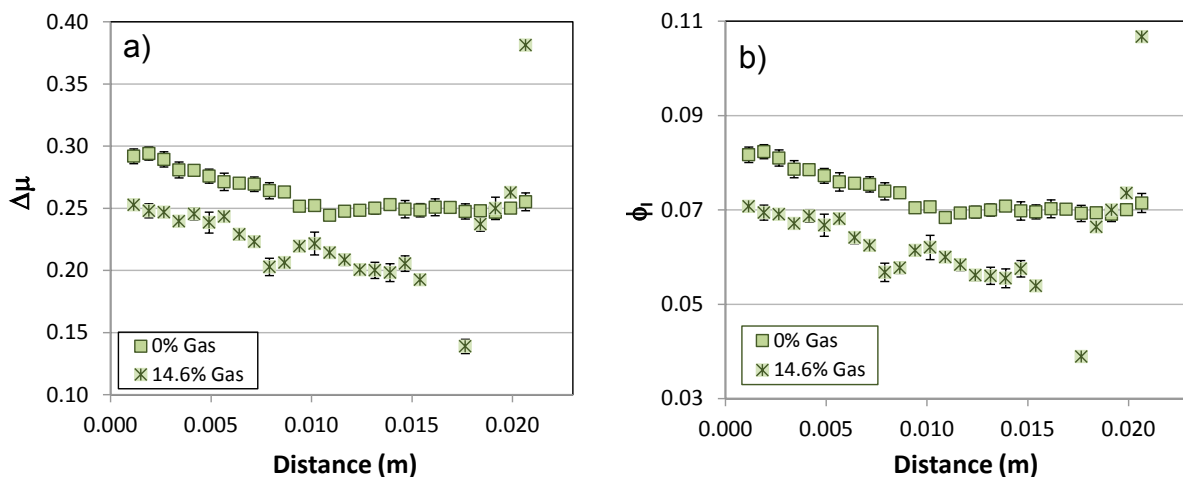


Figure 9: One Dimensional Profiles of a) $\Delta\mu$ and b) ϕ_l of 2 M I⁻ Tracer in Queenston Shale Sample (DGR3-472) before and after Establishment of Partial Gas Saturation. Error Bars Represent the Standard Deviation Measured on Replicate Scans over a Period of 4 Days

Table 8: Properties of Variably Saturated Queenston Formation Shale

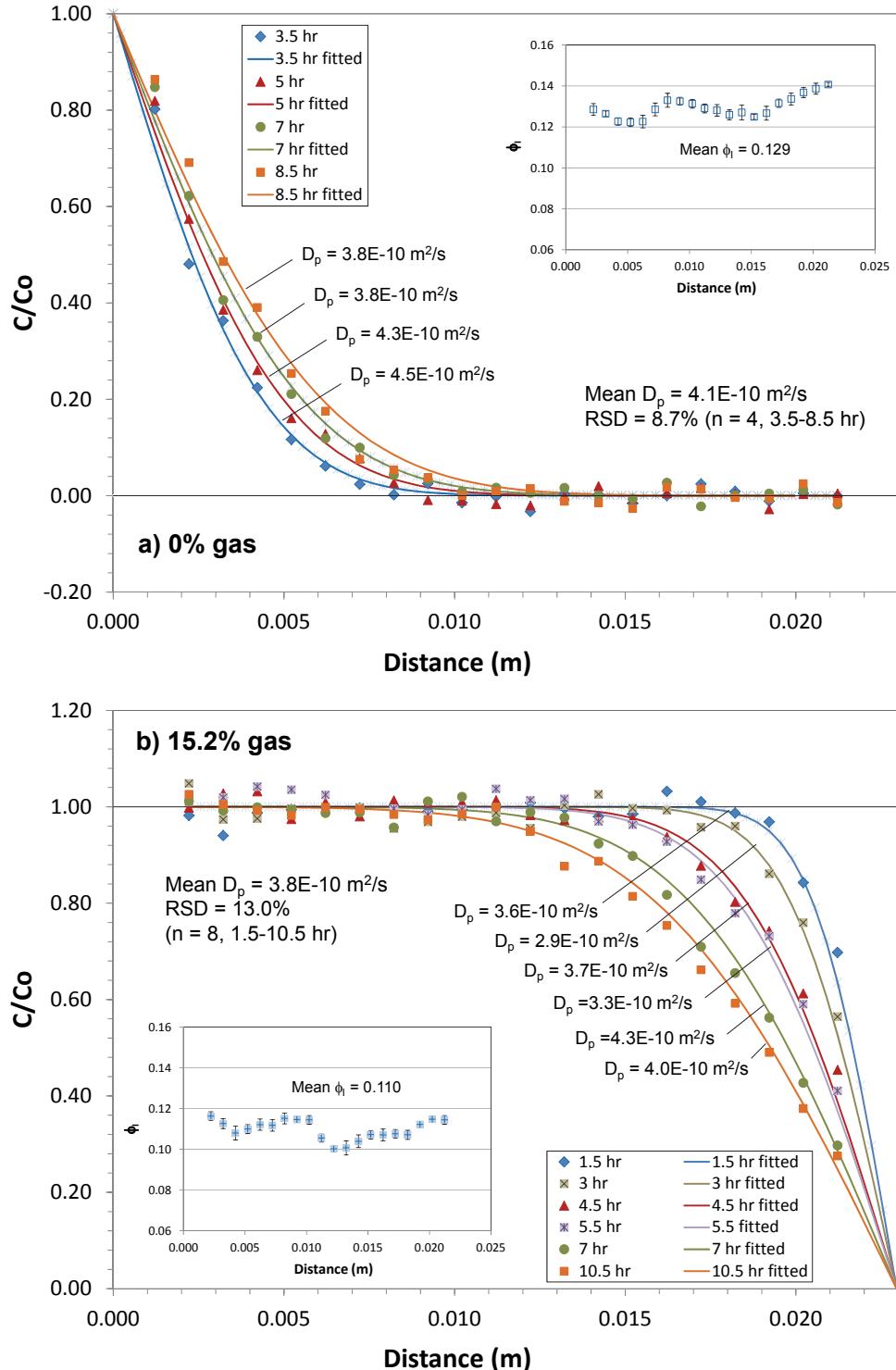
Sample	DGR3-472	DGR3-472-PS ^a
$\Delta\mu$ (2 M I ⁻)	0.261	0.223
ϕ_i (brine) ^b	0.073	0.063
% Brine Saturation	100	85.4
% Gas Saturation	0	14.6
D_p (m ² /s)	4.4E-11	2.3E-11
D_e (m ² /s)	3.2E-12	1.5E-12

^a PS indicates samples with partial gas saturation; ^b brine-filled porosity determined by γ -RAD.

4.3.2 Effect of Partial Gas Saturation on Diffusion Coefficients

4.3.2.1 Carbon Tan Sandstone

Measurements for experiment CT-6A indicate that D_p for I⁻ tracer in a 100% brine-saturated sample is 4.1×10^{-10} m²/s (Figure 10a), and at 15.2% gas saturation the D_p value decreases to 3.9×10^{-10} m²/s (average of results from out-diffusion and in-diffusion experiments; Figure 10b,c). These results suggest that the effect of approximately 15% gas is small - only a 5% decrease in D_p . In contrast, data for experiment CT-6B indicate a 50% decrease in D_p for the same sample at a slightly lower gas saturation (13.5%; Figure 11a, b). The large difference between two measurements using the same rock sample is surprising and suggests an unidentified source of error or a difference in the gas distribution at the pore scale that is not apparent in the ϕ_i profiles (Figures 8, 10 and 11). For example, a predominance of gas bubbles in the pore throats for experiment CT-6B could contribute to a relative decrease in the tortuosity factor (τ_f) and explain the lower D_p value observed for the partially saturated sandstone. The D_e values for aqueous solutes are further affected by the decrease in brine-filled porosity (Table 7) such that partial gas saturation resulted in decreases in D_e of 21% and 56% for experiments CT-6A and CT-6B respectively. The addition of a gas phase to the pores is also expected to cause an increase in diffusion coefficients for gases (Reardon and Moddle 1985), but this effect has not been quantified in these experiments.



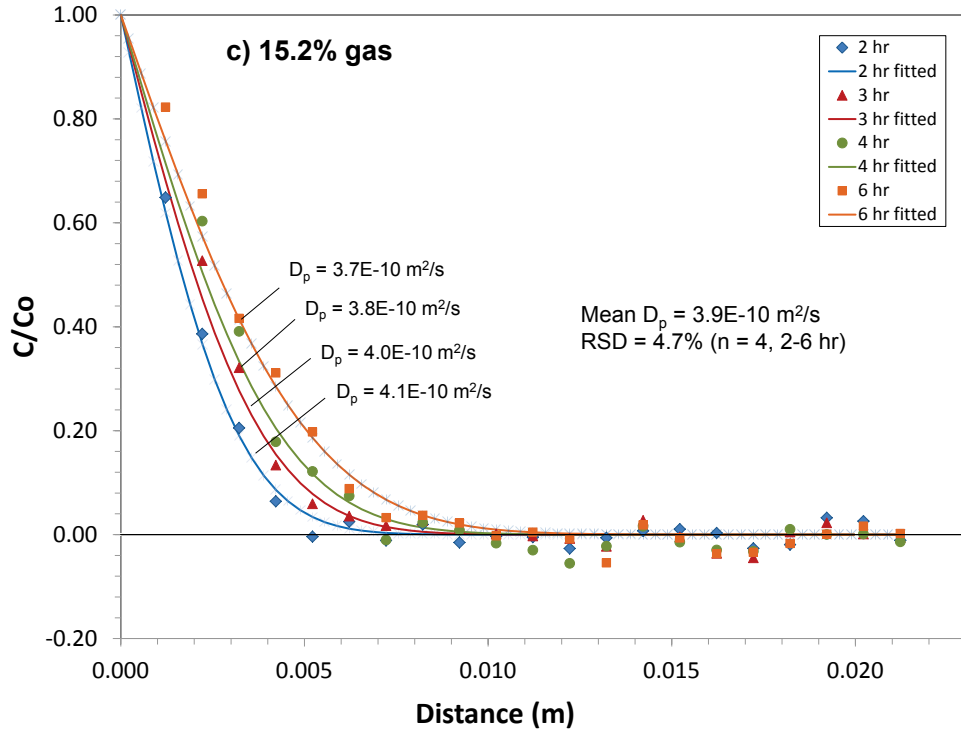


Figure 10: Diffusion Profiles Obtained for Experiment CT-6A Using γ -RAD with 1.0 M NaI Tracer: a) In-Diffusion with 100% Brine (0% Gas) Saturation, b) Out-Diffusion with 15.2% Gas Saturation, and c) In-Diffusion following b). Inset Images are ϕ_I Profiles of the Rock Sample with I⁻ Tracer at Each Condition

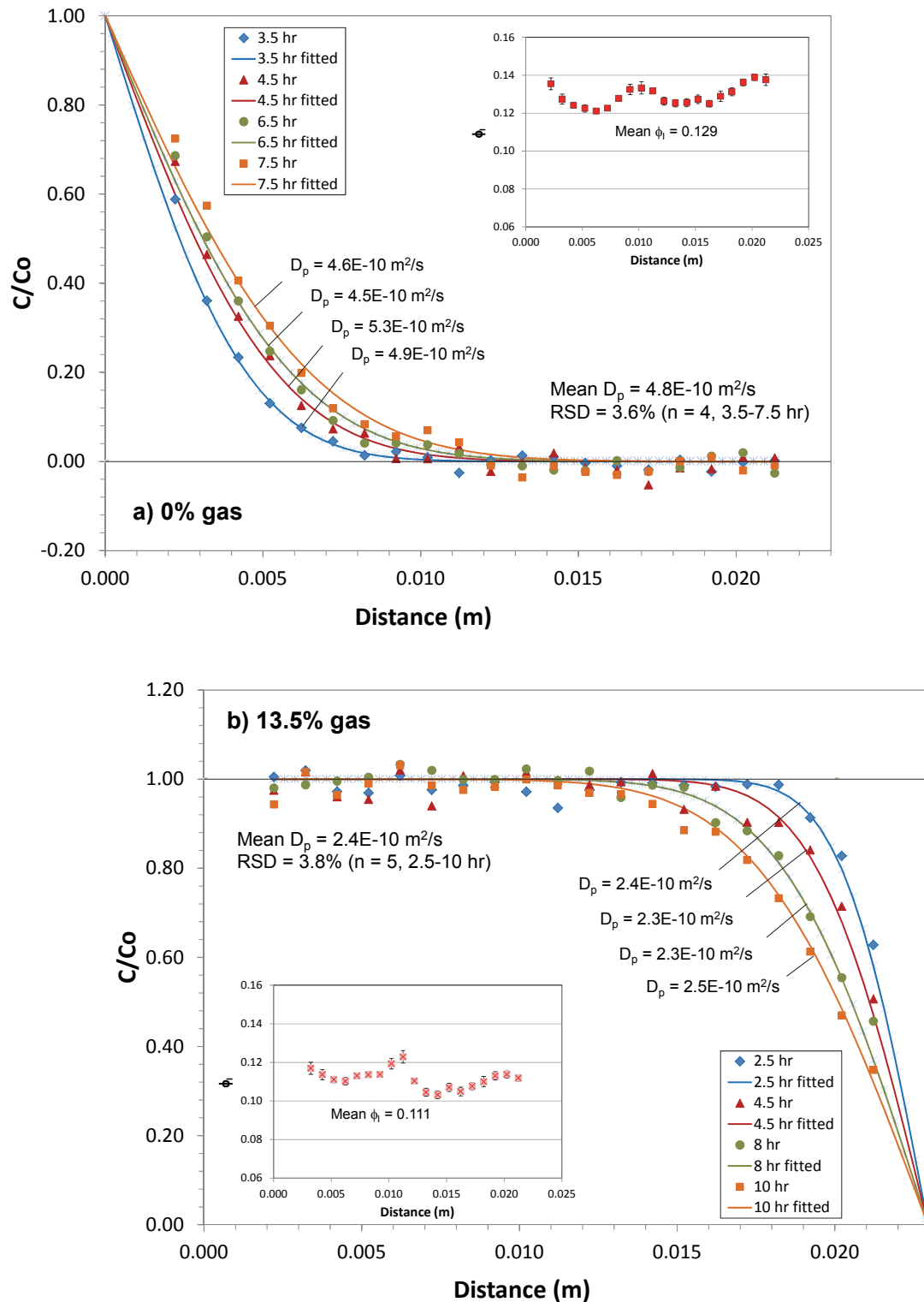


Figure 11: Diffusion Profiles Obtained for Experiment CT-6B Using γ -RAD with 1.0 M NaI Tracer: a) In-Diffusion with 100% Brine (0% Gas) Saturation, b) Out-Diffusion with 13.5% Gas Saturation. Inset Images are ϕ_I Profiles of the Rock Sample with I⁻ Tracer at Each Condition

4.3.2.2 Queenston Formation Shale

Measurements with the Queenston Formation shale (DGR3-472) are preliminary and must be viewed with caution because the problems experienced with sample breakage. The results indicate that D_p for I⁻ tracer at 100% brine-saturation is $4.4 \times 10^{-11} \text{ m}^2/\text{s}$ (Figure 12a) which is consistent with the range of values obtained by previous studies (Al et al. 2010, 2012; Cavé et al. 2010; Xiang et al. 2013). Measurements on the intact portion of the broken sample indicate that D_p decreases to $2.3 \times 10^{-11} \text{ m}^2/\text{s}$ at 14.6% gas saturation (Figure 12b). In terms of D_e , 14.6% gas saturation causes a decrease of 53%, from $3.2 \times 10^{-12} \text{ m}^2/\text{s}$ to $1.5 \times 10^{-12} \text{ m}^2/\text{s}$ (Table 8). This decrease is lower than that observed by Savoye et al. (2010) who report a 96.5% decrease in D_e for I⁻ in the Callovo-Oxfordian argillite at 14% gas saturation. Assuming these results can be supported by further work, it is apparent that the degree of partial saturation is one of the more important controls on the magnitude of aqueous diffusion coefficients. For comparison, previous work studying the effect of changes in confining pressure on D_e noted a maximum decrease in D_e of 44% for Georgian Bay Formation shale measured at ambient laboratory pressure versus a confining pressure of 15.1 MPa (Loomer et al. 2013a).

4.4 SUMMARY

A new method has been developed to generate partial gas and brine saturated conditions in rock samples containing highly concentrated brine without causing changes to the porosity and pore structure from precipitation of salts. The method is based on the relationship between N₂ gas solubility and pressure. The porewater system is equilibrated with N₂ gas at high pressure and then the pressure is rapidly decreased to atmospheric pressure. This causes a corresponding decrease in gas solubility, resulting in exsolution of N₂ to form gas bubbles in the pore spaces. The actual degree of partial gas saturation cannot be predicted accurately by calculations using theoretical P-V-T relationships for gases, but it can be quantified by γ -RAD. Results of D_e measurements for I⁻ tracer on partially saturated sandstone with gas fractions of 15.2% and 13.5% indicate decreases of 21% and 56% respectively. Preliminary results of measurements on the low-permeability Queenston Formation shale indicate a decrease in D_e from $3.2 \times 10^{-12} \text{ m}^2/\text{s}$ at 100% brine saturation to $1.5 \times 10^{-12} \text{ m}^2/\text{s}$ at 14.6% gas (85.4% brine) for an overall decrease of 53%.

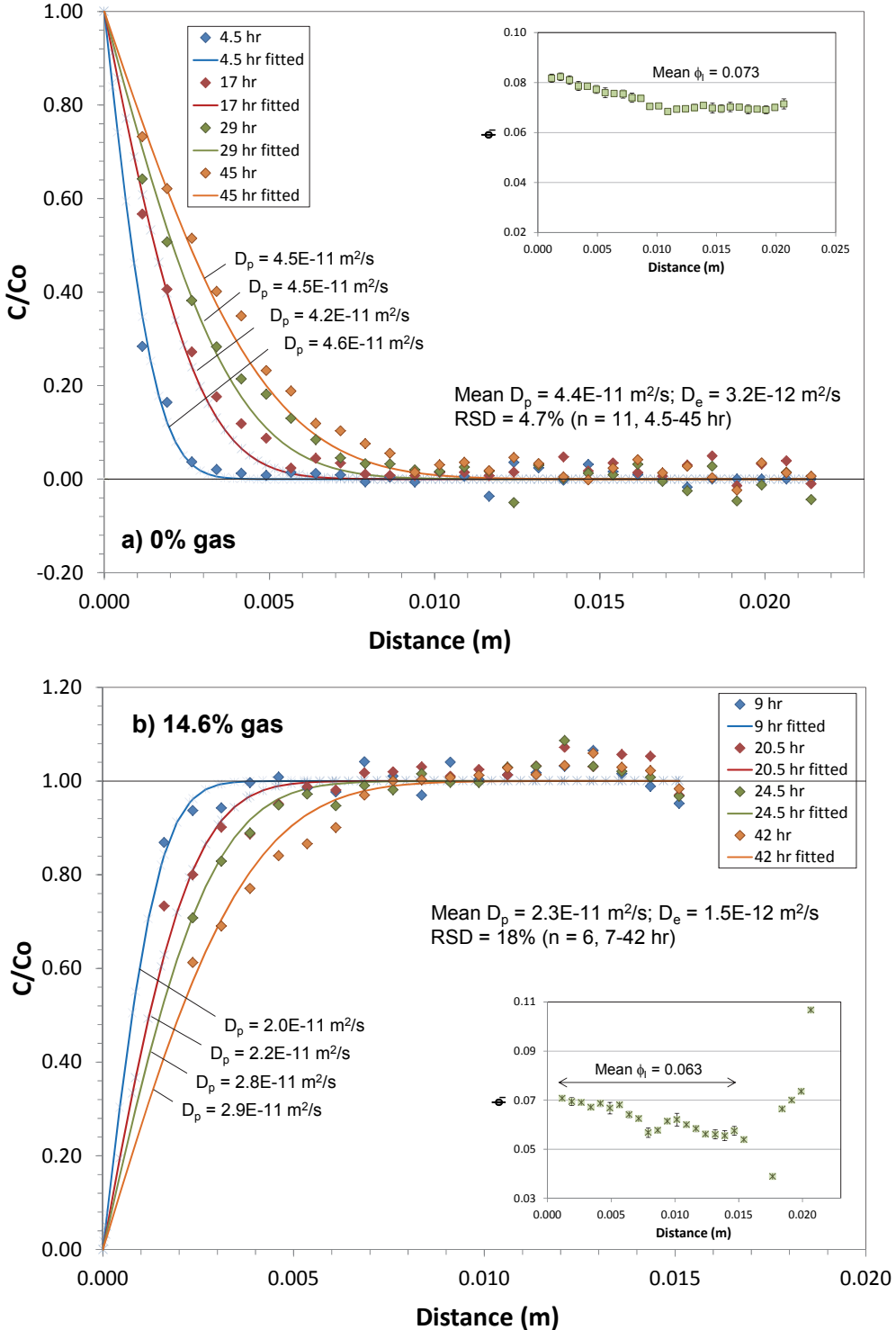


Figure 12: Diffusion Profiles Obtained for Sample DGR3-472 Using γ -RAD with 2.0 M NaI Tracer: a) In-Diffusion with 100% Brine (0% Gas) Saturation, b) Out-Diffusion with 14.6% Gas Saturation. Inset Images are ϕ_l Profiles of the Rock Sample with I⁻ Tracer at Each Condition

5. PH MEASUREMENT IN HIGH IONIC STRENGTH BRINE SOLUTIONS

Solution pH is a fundamental parameter for understanding the geochemical behaviour of many solutes in groundwater. Reliable pH measurements are important to support studies of speciation, solubility and sorption of radionuclides related to a deep geological repository (DGR) for radioactive nuclear waste. In Canada, Ordovician rocks in the Michigan Basin have been evaluated as possible host rocks for a DGR for low- and intermediate-level waste, and similar rocks are also under consideration as the possible host for a spent nuclear fuel repository. The porewater in these formations is highly saline (up to 28 wt% salinity), with ionic strengths up to 8 mol/kg or higher. The conventional potentiometric method for pH measurement is commonly used for dilute solutions (0.1 m or less), and there is a need for an evaluation of available methods for pH measurements in high salinity brine solutions.

Originally, pH was defined simply as the negative logarithm of the hydrogen ion concentration (mH) without consideration of ion interactions in the solution (Equation 9; Jensen 2004). The definition was subsequently modified to the negative logarithm of the H^+ activity (aH), but in practice, mH is easier to work with. Many researchers then created application-specific pH scales by adjusting mH to account for certain known interactions between anions and the H^+ ion in concentrated solutions (Covington and Ferra 1994; Dickson 1984; Hansson et al. 1973; Millero et al. 1993). This has led to multiple alternative pH scales and some confusion when comparing pH values reported in the published literature. Three common pH scales include the free hydrogen ion scale (pH_F), which is simply based on the concentration of free, or uncomplexed, H^+ ions (mH ; Equation 9); the total hydrogen ion scale (pH_T), which accounts for hydrogen ion complexation with sulphate (Equation 10); and the seawater scale (pH_{sws}), which accounts for H^+ interactions with both sulphate and fluoride ions (Equation 11) (Millero et al. 1993).

$$pH_F = -\log mH \quad (9)$$

$$pH_T = -\log mH^*, \text{ where } mH^* = mH + mHSO_4^- \quad (10)$$

$$pH_{sws} = -\log mH^{**}, \text{ where } mH^{**} = mH + mHSO_4^- + mHF^- \quad (11)$$

In 2002, the International Union of Pure and Applied Chemistry (IUPAC; Buck et al. 2002) provided an official definition of pH based on the activity of H^+ :

$$pH = -\log aH = -\log(mHyH/m^\circ) \quad (12)$$

where yH is the molal activity coefficient of the hydrogen ion, H^+ , and m° is the standard molality (1 mol/kg). In dilute solutions yH approaches 1 and, therefore $mH \approx aH$. However, as solutions become more saline and ion interactions become more important, yH changes and the difference between mH and aH increases.

The following discussion provides a brief introduction to the definition and measurement of pH as it was described by Buck et al. (2002).

The activity of the single H^+ ion in water cannot be measured. Instead, it is estimated from measurements of the combined activity of H^+ and Cl^- . The Harned cell (Harned and Owen 1958) is the only method for pH measurement that meets the IUPAC criteria for a primary method. The Harned cell is made up of the standard hydrogen electrode (SHE) coupled with a silver/silver-chloride electrode. It contains a standard buffer and chloride ions – in the form of potassium or sodium chloride (Figure 13). The Harned cell does not involve a liquid junction and, therefore, is not subject to the uncertainty resulting from variable liquid junction potentials.

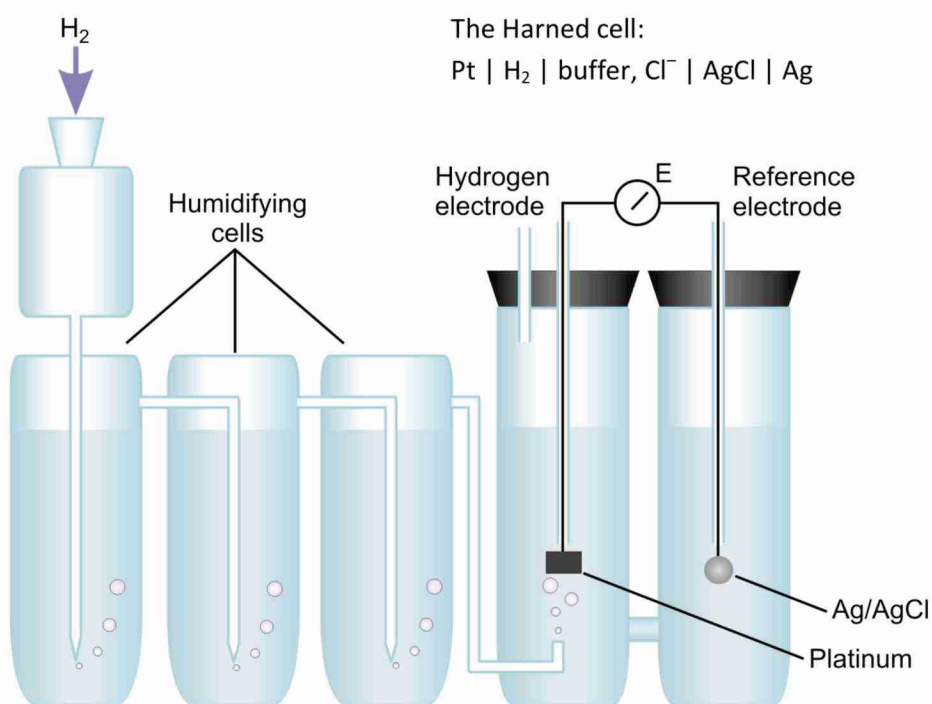


Figure 13: Schematic Example of a Modern Harned Cell, Based on the Diagram of Maksimov et al. (2008)

Potentiometrically, pH is determined according to the Nernst Equation:

$$E = E^\circ - \frac{2.3RT}{F} \log a_H \quad (13)$$

where E is the voltage of the cell, E° is the standard voltage of the cell, R is the universal gas constant, F is the Faraday constant, and T is the temperature in degrees Kelvin. In the Harned cell, the Nernst equation is modified to:

$$E = E^\circ - \frac{2.3(RT/F)}{\log[(m_{H_2}H/m^\circ)(m_{Cl}Cl/m^\circ)]} \quad (14)$$

The standard potential difference of the silver/silver-chloride electrode, E° , is determined from a Harned cell in which only HCl is present at a fixed molality (e.g., $m = 0.01 \text{ mol/kg}$).



Application of the Nernst equation to the HCl cell, written in a form convenient for pH determination is:

$$-\log[a\text{H}\cdot\gamma\text{Cl}] = \frac{\frac{E-E^{\circ}}{23RT}}{F} + \log\left[\frac{[\text{mCl}]}{[\text{m}^{\circ}]}\right] \quad (15)$$

To obtain a pH value, it is necessary to evaluate $\log\gamma\text{Cl}$ by independent means. This is done in two steps: (i) determination of the value of $\log(a\text{H}\gamma\text{Cl})$ at zero chloride molality, $\log(a\text{H}\gamma\text{Cl})^{\circ}$, and (ii) calculation of a value for the activity coefficient of the chloride ion at zero Cl molality, $\gamma^{\circ}\text{Cl}$. The activity coefficient of chloride is also an immeasurable quantity. However, in solutions of low ionic strength ($I < 0.1 \text{ mol/kg}$), it is possible to calculate the activity coefficient of the chloride ion using the Debye–Hückel theory. This assumes that $\gamma^{\circ}\text{Cl}$ is given by the expression:

$$\log\gamma_i = \frac{Az_i^2\sqrt{i}}{1+B\bar{a}_i\sqrt{i}} \quad (16)$$

where A and B are solvent parameters that are dependent on density, dielectric constant and temperature; z is the ionic charge, \bar{a} is the mean distance of closest approach of the ions (ion size parameter), and I is the ionic strength of the buffer. In practice, $B\bar{a}$ is set equal to $1.5 \text{ (mol/kg)}^{-1/2}$ at all temperatures in the range of 5–50 °C. While recognizing the importance of ion interaction approaches (e.g., Pitzer 1991) for determining pH (Covington and Ferra 1994; Buck et al. 2002), the IUPAC uses the Debye-Hückle ion-association approach because it has very small experimental uncertainty while the Pitzer ion-interaction approach involves more uncertainty that is difficult to assess in practical applications (Meinrath 2002; Spitzer et al. 2011). By employing the Debye-Hückle approach, the IUPAC (Buck et al. 2002) has limited the standard measurement of pH to solutions with ionic strengths less than 0.1 mol/kg.

Institutes worldwide, such as the National Institute of Standards and Technology (NIST), use the Harned cell to develop primary pH buffers. Chemical companies then use the primary buffers to make secondary, NIST-traceable, commercial pH buffers (NIST buffers) for general laboratory use.

The Harned cell is not practical for everyday laboratory pH measurements and more convenient methods are typically used. One conventional method is potentiometric measurement using glass combination electrodes (Figure 14). The potentiometric cell consists of a pH-sensitive glass electrode, a reference electrode (Ag/AgCl) and an inert filling solution (3.0 M KCl) that functions as a salt bridge connecting the two cells. The glass membrane responds to the H^+ activity in a solution (Pehrsson et al. 1976). The presence of the salt bridge introduces a liquid junction potential between the reference cell and the solution being measured. The magnitude of this potential is a function of the solution composition, temperature and ionic mobilities (Mesmer and Holmes 1992).

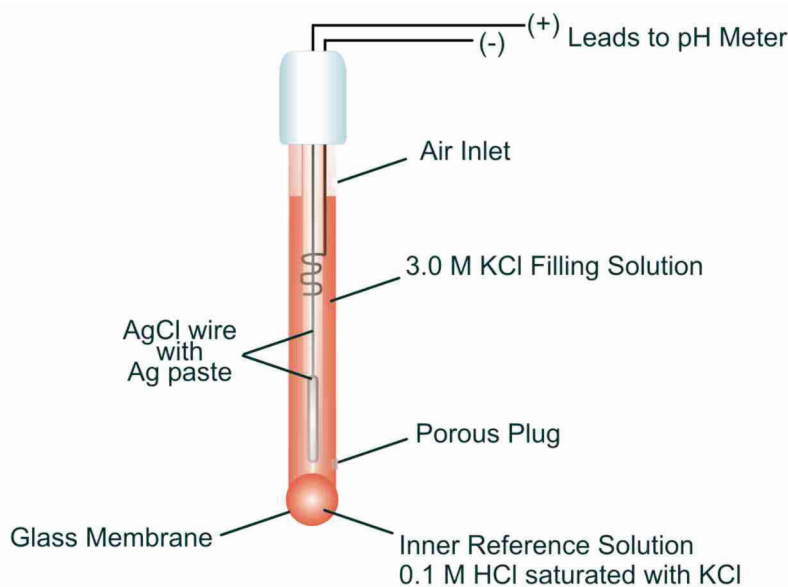


Figure 14: Glass Combination pH Electrode

The electrode is connected to a high impedance voltmeter. If the electrode behavior is Nernstian, for every unit change in pH, there should be a 59.16 mV response from the electrode. The conversion from millivolts to pH units is typically done internally by the meter based on calibration with standard, NIST-traceable buffers.

The experimental uncertainty for a typical primary pH (Harned Cell) measurement is of the order of ± 0.004 pH units, while the uncertainty arising from the use of the Debye-Hückle approach to determine γ_{Cl} is ± 0.01 pH units (Buck et al. 2002). It is acknowledged that typical pH measurement using a glass electrode can have an error of up to ± 0.03 pH units. Sources of error that contribute to this uncertainty include the uncertainty in the NIST calibration buffers (± 0.01 – 0.02 pH units), the precision and accuracy of the electrode (± 0.02 and ± 0.03 pH units, respectively) and the error in the meter (± 0.01 pH units). An additional source of error depends on the resolution of the temperature adjustment for the meter.

When measuring pH with a glass electrode, it is assumed that the liquid junction potential between the reference cell and the buffer is the same as the potential between the reference cell and the solution to be measured. However, this assumption is violated if there is a significant difference in the ionic strengths of the buffer solutions and the solution to be measured.

Ionic strengths as high as 8 mol/kg have been reported for porewaters in Ordovician rocks in the Michigan Basin in southern Ontario (Hobbs et al. 2011). At the University of New Brunswick (UNB), two synthetic porewater (SPW) formulations are commonly used when working with Michigan Basin drill core samples (Al et al. 2010, 2012; Cavé et al. 2010). The Shale SPW (S-SPW) has ionic strength (I) equal to 8.2 mol/kg and the Limestone SPW (L-SPW) has ionic strength equal to 4.9 mol/kg (Table 4). There must then be a difference in liquid junction potential for measurements in the SPW versus the NIST buffers that would add systematic error to potentiometric pH measurements in these solutions. One alternative to the use of NIST buffers for measuring pH in high ionic strength solutions is to calibrate the electrode in terms of

mH rather than aH using a Gran plot (Gran 1950, 1952; Hansson 1973). In this application, the Gran plot involves the titration of a solution of known strong-acid concentration with a solution of known strong base concentration in the presence of a relatively high concentration of background electrolyte. The background electrolyte allows the assumption of constant γH^+ during the titration. The Gran plot provides a calibration for an electrode that can be used for pH measurements in solutions with the same electrolyte composition as the calibration solution, assuming negligible electrode drift between the titration and the measurements. However, this method is time consuming and impractical for everyday laboratory and field applications, and it is prone to complication in the presence of weak acids (Pehrsson et al. 1976). Furthermore, if defining pH in terms of mH rather than aH, the measured pH would not be consistent with geochemical models that are employed within the DGR context such as PHREEQC (Parkhurst and Appelo 1999, 2013) or MIN3P (Mayer et al. 2002; Bea et al. 2010, 2011). For this study, it was decided to evaluate pH measurement in brine solutions as a function of aH, consistent with IUPAC recommendations (Buck et al. 2002) and standard geochemical practice.

Solution pH can also be measured spectrophotometrically. Spectrophotometric measurements using colorimetric indicators have been used as an alternative to potentiometric measurements by a variety of researchers (King and Kester 1989; Martz et al. 2003; Millero et al. 2009; Raghuraman et al. 2006a,b). Colorimetric pH indicators are weak acids or bases – analogous to pH buffers – and are sensitive to the activity, rather than the concentration of H^+ . With colorimetric indicators such as phenol red, the acid (A) and base (B) forms of the indicator, absorb light at different wavelengths (Figure 15). Spectrophotometric pH measurements take advantage of the change in absorbance ratio, or optical density ratio (ODR), between the basic and acidic peaks as pH changes. Raghuraman et al. (2006a) have applied the spectrophotometric method to the measurement of pH in NaCl brines up to an ionic strength of 3.0 mol/kg. In this work, we follow their approach, but extend the range of pK_a' measurements to higher ionic strengths and more complex solutions.

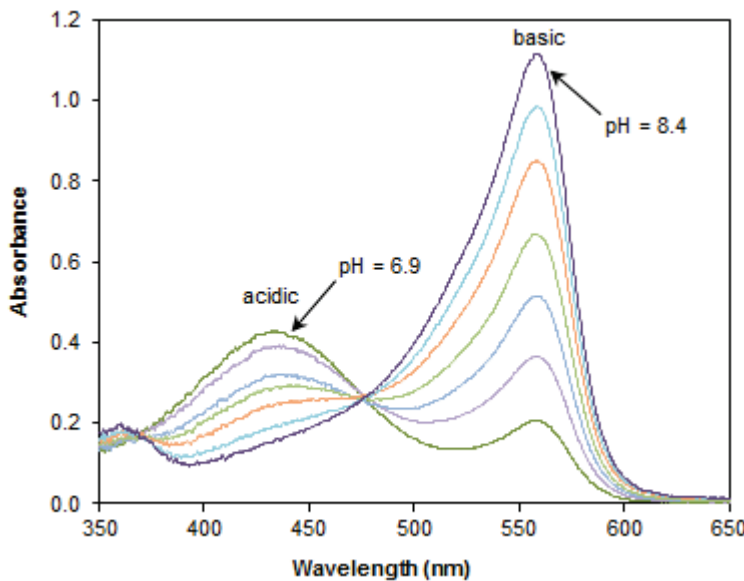


Figure 15: Absorbance Spectra with Changing pH for Phenol Red in L-SPW Tris Buffer Solutions

In spectrometry, the pH of a solution can be determined based on: (1) the thermodynamic disassociation constant (pK_a) of the indicator, a weak acid (HA) or base (A⁻) and its disassociation equilibrium is represented as $HA \rightleftharpoons A^- + H^+$; and (2) the ratio of basic to acid peaks in the spectra (Figure 15).

$$pH = pK_a + \log \frac{[\gamma_B]}{[\gamma_A]} + \log \frac{[B]}{[A]} \quad (17)$$

where γ_A and γ_B are the activity coefficients of the acid (A) and base (B) forms of the indicator. Equation 17 can be rewritten such that pH is a function of the measured concentration ratio for the acid (A) and base (B) forms of the indicator, and the conditional disassociation constant pK'_a which varies with γ_A and γ_B .

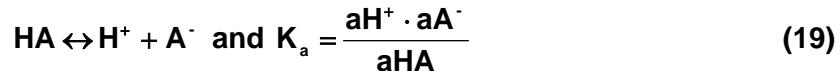
$$pH = pK'_a + \log \frac{[B]}{[A]} \quad (18)$$

The pK'_a is therefore a function of ionic strength, temperature and pressure (King and Kester 1989; Raghuraman et al. 2006a). Pitzer ion interaction coefficients for the phenol red indicator are not available in the published literature and its pK'_a values in high ionic strength solutions can not be determined by geochemical modelling. Therefore, it is necessary to empirically determine the variation of pK'_a with ionic strength and solution composition. A common method involves the collection of spectra to measure $\log [B]/[A]$ over a range of pH. The pK'_a of an indicator is then determined at the pH value where $\log [B]/[A] = 0$ in a straight-line plot of $\log [B]/[A]$ versus pH. This method was described in detail by Raghuraman et al. (2006a).

The objectives of this work were to: 1) characterize the glass electrode response in increasingly saline solutions; 2) evaluate a spectrophotometric approach as a possible alternative method for pH measurements in brine solutions; and 3) present an approach for improved confidence in pH determination when working with brine solutions. The approach developed to meet these objectives was to create high-ionic-strength buffers with known pH to: a) test the glass electrode response in solutions of varying ionic strength; and b) determine the ionic-strength dependence of the association constant (pK'_a) for a colorimetric pH indicator.

5.1 HIGH-IONIC-STRENGTH BUFFERS

The standard NIST buffers have low ionic strength (<0.1 mol/kg) and there are no NIST-certified high-ionic-strength pH buffers commercially available. A pH buffer is an aqueous solution consisting of a mixture of a weak acid (HA) and its conjugate base (A⁻) or a weak base and its conjugate acid. The equilibrium between the acid and base (Equation 19) resists changes in pH in response to minor changes in solution composition.



As noted above, determination of single-ion activity coefficients with the Debye-Hückle ion-association model makes it possible to assign a pH value to a buffer solution, but that method is not suitable for solutions with ionic strength much greater than 0.1 mol/kg. In order to extend pH measurement to high-ionic-strength solutions, the ion interaction approach (Pitzer 1991), is

required. Several geochemical speciation codes (e.g. PHREEQC, MIN3P-THCm) implement the Pitzer equations for ion activity calculations (Bea et al. 2011; Parkhurst and Appelo 1999, 2013; Wall et al. 2006).

The publicly available geochemical code PHREEQC (Parkhurst and Appelo 1999, 2013; USGS 2013) includes the numerical implementation of the Pitzer equations of Plummer et al. (1988) and a limited thermodynamic database containing virial Pitzer coefficients. PHREEQC Interactive, version 3.0.6.7757, was used in this work. The buffer protonation-deprotonation reaction is an association-disassociation reaction. The geochemical equilibrium code is used to calculate a conditional disassociation constant (pK'_a) according to Equation 20.

$$pK'_a = pK_{a(\text{thermodynamic})} \cdot \frac{\gamma(\text{reactants})}{\gamma(\text{products})} \quad (20)$$

Two pH buffers were chosen for this work: acetate – acetic acid (acetate; pH ≈ 4) and Tris-[hydroxymethyl]aminomethane – Tris-[hydroxymethyl]aminomethane hydrochloride (Tris and TrisHCl; pH ≈ 8). The Pitzer ion interaction coefficients for these buffer components were added to the PHREEQC-Pitzer database (pitzer.dat). The choice of these buffers was constrained by the need to avoid buffers that react with the components of the brine. For example, citrate and phosphate buffers are not recommended for solutions with significant concentrations of Ca because of the significant complexation with Ca and the insolubility of Ca-phosphate complexes. Tris is known to be compatible with Ca- and Mg- containing solutions (ANGUS Chemical Company 2000; McFarland and Norris 1958; Mohan 2006). Tris is also highly soluble in aqueous solutions, chemically stable and readily available in purified form. Furthermore, Tris has low hygroscopicity, does not readily absorb CO_{2(g)} from the atmosphere and has insignificant light absorbance characteristics between 240 nm and 700 nm, so its use will not interfere in colorimetric measurements (ANGUS Chemical Company 2000). Another benefit to using Tris is that the base and acid forms are both salts, and therefore, there is no dilution from adding acidic or basic solutions to adjust the pH of a buffer. However, the Tris association reaction is such that changing the relative Tris:TrisHCl concentrations results in variable ionic strength for a given buffer series.

In addition, the Tris buffer is temperature sensitive. In dilute buffer solutions the pH changes ±0.03 pH units/°C inversely with temperature (AppliChem 2008). Foti et al. (1999) and Millero et al. (2009) reported the same temperature dependency of the Tris buffer system (±0.03 pH unit/°C) in the temperature range 0-100 °C for ionic strengths ranging from 0-5 mol/kg NaCl solution. Because of the limitations in the availability of verifiable Pitzer parameters in the peer-reviewed literature, the Pitzer ion interaction coefficients added to the PHREEQC-Pitzer database for Tris buffer are limited to a temperature of 25 °C.

Multiple references were considered and included in the modified Pitzer database (pitzerUNB; Appendix B.1) and the modified database was verified against published pK'_a data (Figure 16a; Figure 17a). The parameters (or combination of parameters) that could best reproduce the published pK'_a data have been activated in the database (Table 9). The maximum difference between the PHREEQC-calculated and the literature values (Millero et al. 1987) for the pK'_a of Tris was 0.02 units. Novak et al. (1996) reported Pitzer coefficients for the acetate-NaCl system and was the main source used for model calculations involving the acetate buffer. The maximum difference in the pK'_a of acetate calculated with PHREEQC and the values reported by Novak et al. (1996) was 0.03 units (Figure 16). Mesmer et al. (1989) and Mizera et al. (1999) also measured the pK'_a of acetate in NaCl solutions and their results were included in

the model verification. The pK'_a values calculated using PHREEQC were similar to those from Mesmer et al. (1989) and Mizera et al. (1999) (Figure 17) with a maximum difference in pK'_a of 0.06 units.

The MacInnes convention for scaling activity coefficients is the default in PHREEQC. It was not used in this work, either for verification of results against literature values or for any other PHREEQC calculations. The MacInnes convention (MacInnes 1919) assumes that $\gamma K^+ = \gamma Cl^- = \gamma \pm KCl$. With this assumption one can determine the single-ion activity coefficients of other salts in a KCl solution by substitution. While the MacInnes convention is recognized as being convenient and is widely used, the IUPAC (Bates and Robinson 1974) have stated that the assumption that Cl^- will have a constant activity coefficient at a given ionic strength across a range of solution compositions is implausible. There is a considerable difference in calculated pH if the MacInnes convention is used in PHREEQC (Nordstrom et al., 2000; Figure 16b; Figure 17b), highlighting the sensitivity of the calculated pH values to the convention used.

The Pitzer interaction parameters for the acetate buffer are well characterized in NaCl solutions (up to an ionic strength of 5 mol/kg) and for the Tris buffer in NaCl, KCl, $CaCl_2$ and $MgCl_2$ solutions (up to an ionic strength of 6 mol/kg). However, Millero et al. (1987) indicated that for solutions with ≥ 1 mol/kg Ca there is increasing uncertainty in the Pitzer parameters for Tris, and that additional parameters may be required. These ionic strength and Ca-concentration limitations place constraints on the use of Tris buffer in pH measurement for brine from the Michigan Basin which commonly contains Ca^{2+} in excess of 1 mol/kg, and in some cases has ionic strength greater than 6 mol/kg (Al et al. 2010; Hobbs et al. 2011; Koroleva et al. 2009).

There are few data for Pitzer parameters in Ca-acetate buffer solutions, and none were found for Mg-acetate solutions, which limits the use of PHREEQC to calculate the pH of acetate buffer solutions at high ionic strength. Loos et al. (2004) determined interaction parameters for Ca with acetate but they did not report pH values, therefore modelled pH values for Ca-acetate buffer solutions cannot be verified. Because of these limitations, it was decided not to use the acetate buffer for this work, but it is recognized that the acetate buffer can be used reliably in NaCl solutions.

Table 9: Additions Made to the PHREEQC v. 3.0.6 PITZER Database (pitzerUNB)

Name	Master Species	Alkalinity	FWT (Formula Weight)	
Tris	Tris	1	121.138	
Acetate	Acetate ⁻	1	59.045	
Solution Species	pK _a ¹	Temperature (°C)	Delta H (kcal)	Ref
Tris + H ⁺ = (Tris)H ⁺	8.075	25	11.36 kcal	1
H ⁺ + Acetate ⁻ = H(Acetate)	4.757	25	0.098	2
Na ⁺ + Acetate ⁻ = Na(Acetate)	-0.18	25	2.87	2
K ⁺ + Acetate ⁻ = K(Acetate)	-0.1955	25	1	2
Ca ⁺² + Acetate ⁻ = Ca(Acetate) ⁺	1.18	25	0.96	2
Mg ⁺² + Acetate ⁻ = Mg(Acetate) ⁺	1.27	25	0	2

Binary Pitzer ion-interaction coefficients:

Ion-pair		B ₀	B ₁	C ₀	θ	λ	Ref
(Tris)H ⁺	Cl ⁻	0.0395	0.20978	-0.00236	-	-	3
(Tris)H ⁺	SO ₄ ²⁻	0.09393	0.59829	-0.004316	-	-	3
(Tris)H ⁺	H ⁺	-	-	-	0.0027	-	3
Na ⁺	Tris	-	-	-	-	0.0239	8
K ⁺	Tris	-	-	-	-	0.0262	8
Mg ⁺²	Tris	-	-	-	-	-0.0594	8
Ca ⁺²	Tris	-	-	-	-	-0.2327	8
H ⁺	Acetate ⁻	0	0	0	-	-	4
Na ⁺	Acetate ⁻	0.1426	0.3237	-0.00629	-	-	4/5
K ⁺	Acetate ⁻	0.155	0.3	-0.005	-	-	6
Ca ⁺²	Acetate ⁻	0.269	1.134	-0.031	-	-	7
Acetate ⁻	Cl ⁻	-	-	-	-0.09	-	4

Ternary Pitzer ion-interaction coefficients:

Ion group		ζ	ψ	Ref
Tris	Na ⁺	Cl ⁻	0	-
H ⁺	(Tris)H ⁺	Cl ⁻	-	-0.013
Na ⁺	H ⁺	Acetate ⁻	-	0
Na ⁺	Acetate ⁻	Cl ⁻	-	0.01029

¹Zero ionic strength pK_a; PHREEQC calculates pK_a internally.

References: 1. Foti et al. (1999); 2. PHREEQC v. 3.0.6 minteq.v4 database (Parkhurst and Appelo 2013); 3. Bates and Macaskill (1985); 4. Novak et al. (1996); 5. Pitzer and Mayorga (1973); 6. Spitzer et al. (2011); 7. Loos et al. (2004); 8. Millero et al. (1987).

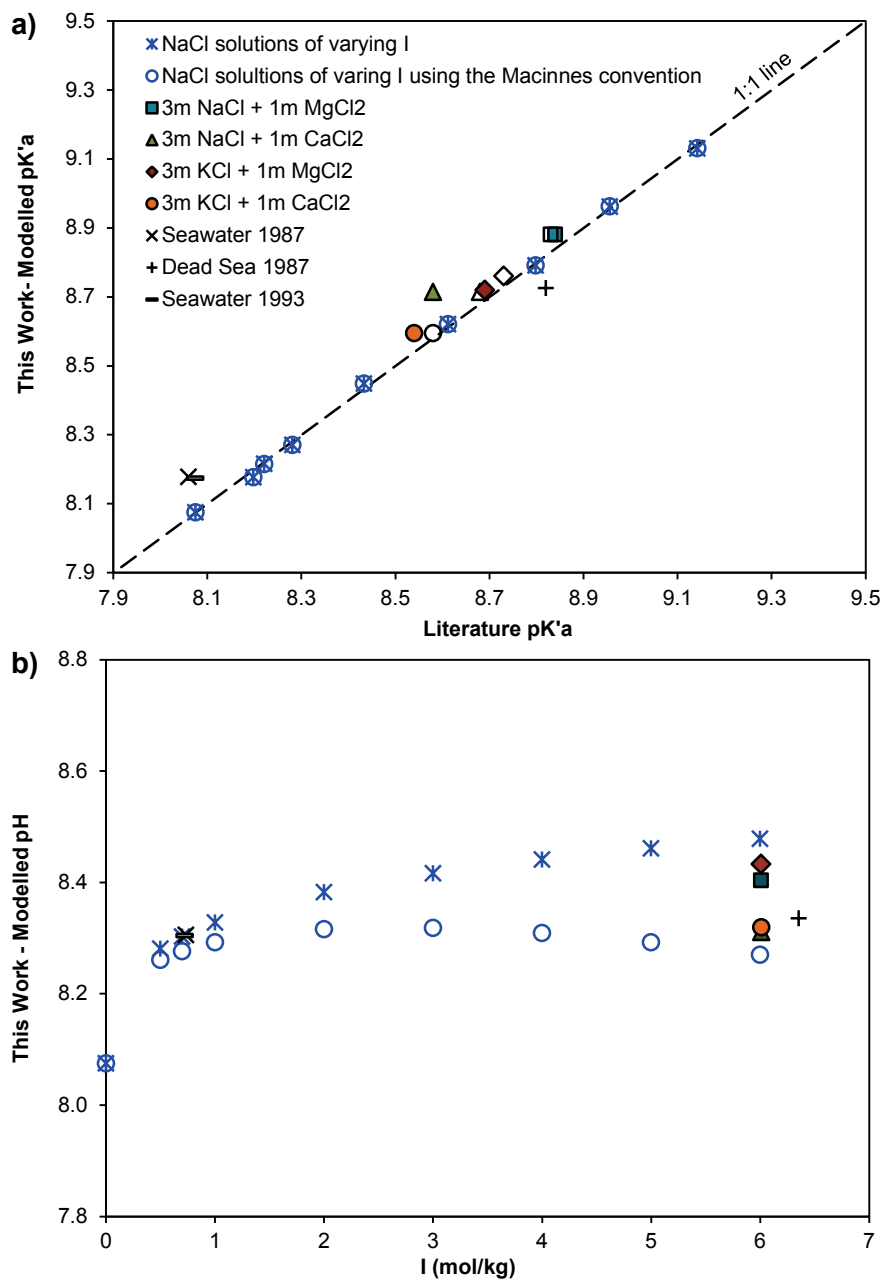


Figure 16: Tris Buffer Data: a) Comparison of the pK'_a for Tris in Electrolyte Solutions Calculated Using PHREEQC (pitzeUNB Database) with Measured Values for Seawater and the Dead Sea from Millero et al. (1987, 1993). “MacInnes Convention” Means it was Used for Calculating pH in PHREEQC. The Filled Symbols Represent Measured Values and the Hollow Symbols Represent the Corresponding Calculated Values (Millero et al. 1987); (b) The Modelled pH of a 0.02 mol/kg Tris Buffer in the Same Solutions Shown in (a)

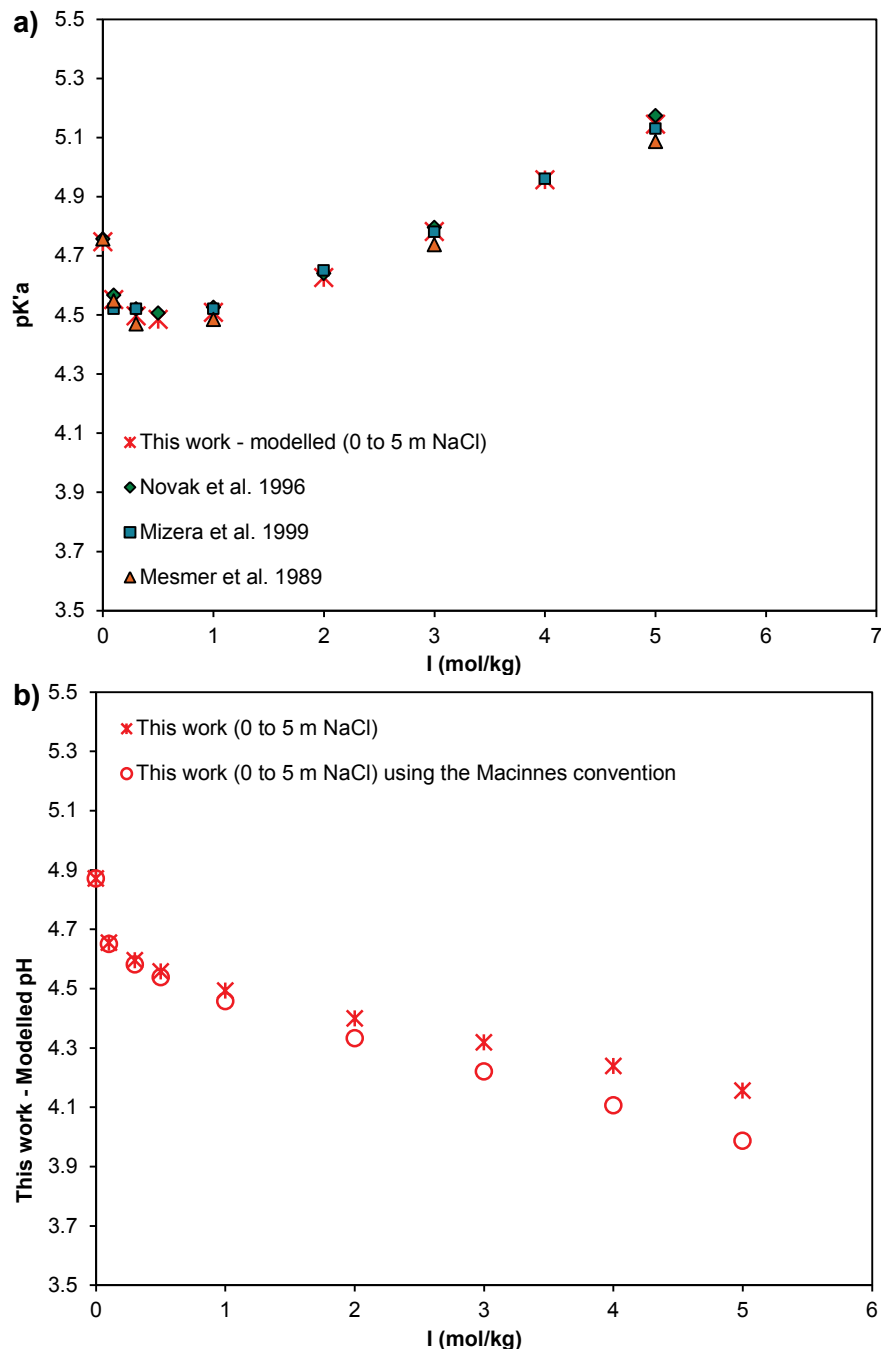


Figure 17: Acetate Buffer Data: (a) Comparison Between the Acetate pK'_a Calculated Using PHREEQC (pitlerUNB Database) and Values from Published Literature; (b) The Modelled pH of a 0.002 mol/kg Acetate Buffer in NaCl Solutions of Varying Ionic Strength. “MacInnes Convention” Means the MacInnes Convention was Used for Calculating pH in PHREEQC

5.2 EXPERIMENTAL METHODS

5.2.1 Preparation of High Ionic Strength Buffers

Buffered solutions at varying ionic strengths and solution compositions were developed by using PHREEQC with the pitzerUNB database. The buffer solutions were designed to simultaneously test the glass electrode response (potentiometric pH measurements) and collect the spectral data necessary to determine the pK_a' of the phenol red indicator for spectrophotometric pH measurements.

The pK_a (infinite dilution) at 25 °C for the Tris buffer is 8.075 (Foti et al. 1999). The pK_a (infinite dilution) at 25 °C for the phenol red (phenolsulfonphthalein) indicator is 8.0 (Drummond et al. 1989). The MERK Index (MERK 2014) lists a pK_a of 7.9 for phenolsulfonphthalein, but does not specify a temperature and the relevant references in the monograph date back to the late 1800's or early 1900's. Therefore, the Drummond et al. (1989) value is considered the more reliable of the two. Both pH buffers and pH-sensitive colorimetric indicators are reliable within ± 1 pH unit of their pK_a . Therefore, it is appropriate to use Tris and phenol red in the pH range 7 to 9, and in this work we extended the working range down to pH 6.5.

Tris buffers were prepared with total Tris concentrations of 0.05 or 0.06 mol/kg which is near the lower limit of Tris concentrations that are reliable for maintaining the desired pH (Millero et al. 2009). The range of pH values was achieved by varying the relative proportions of Tris and TrisHCl. A series of 5-8 Tris buffers were prepared for each ionic strength. On average, the effect of the Tris on ionic strength across a series of Tris buffers was 0.03 mol/kg, with a maximum effect of 0.06 mol/kg.

The Tris buffers were prepared in 4 types of aqueous media: pure water, NaCl solutions of varying ionic strength, concentrated and diluted forms of L-SPW solution with varying ionic strength, and S-SPW dilutions of varying ionic strength. All salts used for the buffer solutions were ACS grade: NaCl, KCl, $\text{CaCl}_2 \cdot 2\text{H}_2\text{O}$, $\text{MgCl}_2 \cdot 6\text{H}_2\text{O}$, CaSO_4 , Tris and TrisHCl.

The range in difference between the measured and calculated Tris pK_a' in mixed electrolyte solutions reported by Millero et al. (1987) was 0.01 to 0.1 unit, with the maximum discrepancy reported from a solution of 3 mol/kg NaCl + 1 mol/kg CaCl_2 (Figure 16a). Millero et al. (1987) suggested that Ca^{2+} -Tris- Na^+ and Ca^{2+} -Trish $^+$ - Na^+ ternary Pitzer coefficients would be necessary to account for the Ca^{2+} -Tris interactions. Such ternary Pitzer coefficients are not available in the published literature. However, there is debate in the literature about whether the ternary Pitzer coefficients are statistically different from zero (Meinrath 2002; Spitzer et al. 2011). Without the ternary Pitzer parameters it was decided that this work would focus on L-SPW solution because of its relatively low Ca content relative to that of the S-SPW (Table 4).

One goal of the work was to extend the colorimetric pK_a' determinations and potentiometric pH measurements from ionic strength of ≈ 0.1 mol/kg to 8.2 mol/kg, the ionic strength of the S-SPW. To do this, the L-SPW matrix was either diluted or concentrated while maintaining the relative proportions of the major ions. The one exception is the SO_4^{2-} concentration which was held to a maximum of 0.001 mol/kg to prevent gypsum precipitation.

The L-SPW-based pH buffers covered a wide range of ionic strengths, from 0.09-7.67 mol/kg. At most, the buffer was 1.6 times more concentrated than L-SPW, with a Ca concentration of

0.81 mol/kg, less than the 1 mol/kg limitation discussed by Millero et al. (1987). The Ca concentration in S-SPW is higher than the measurements reported by Millero et al. (1987) and, therefore, greater uncertainty in the modelled pH values for S-SPW is unavoidable. Four buffer series based on dilutions of S-SPW were also prepared. All buffers were undersaturated with respect to halite and gypsum.

Example PHREEQC input and output files are provided in Appendices B.2 and B.3. The solution compositions, modelled pH values and ionic strengths are provided in Appendix B.4. In the modelling, the pH of the solutions was calculated by assuming that there was no effect from CO₍₂₎ in the solutions and also by equilibrating the solutions with CO_{2(g)} (log PCO₂ = -3.4; equivalent to the 2012 global average atmospheric concentration of 393 ppm; Dlugokencky and Tans 2014).

The solutions were prepared in deionized water (18 MΩ•cm) which had been bubbled vigorously with N_{2(g)} for 1.5 to 3.0 hours to remove CO_{2(g)}. The Tris buffers were made by adding the appropriate amounts of Tris and TrisHCl to the solution. This approach ensured that the only difference within a series of Tris buffers was the relative proportions of Tris and TrisHCl. Each buffer series consisted of 5-8 buffer solutions of varying pH. A series of Tris buffers made up in pure deionized water (Just Tris; ionic strength = 0.04 ± 0.01 mol/kg) was also prepared.

After the Tris buffers were made, a phenol red indicator solution (made from phenol red sodium salt, ACS grade; Amresco®) was added. Because the colorimetric method is based on the ratio of base to acid peaks in the spectra, measurements are independent of the concentration of the indicator (King and Kester 1989; Raghuraman 2006b). However, low indicator concentrations (2-3 × 10⁻⁶ mol/L) were used in order to stay within the linear range of the spectrophotometer, to prevent changes in the pH of the solutions from the indicator itself, and to reduce the risk of indicator dimerization (King and Kester 1989). The same stock indicator solution, 3.2×10⁻³ mol/L, was used for most of the pK'_a determinations which were performed over a period of 6 months. The stock solution was stored in a double-sealed amber glass bottle at room temperature. Replicate pK'_a measurements using both freshly made and 6-month-old phenol red indicator stock solution gave the same value, within the uncertainty of the pK'_a measurements.

The buffer solutions were made, the indicator added, spectra collected and pH measured potentiometrically on the same day. The buffers were then measured at least twice more at 1 to 3 day intervals. The pH of one set of L-SPW buffers was monitored potentiometrically over a period of 2 months to assess buffer stability with time. The buffer solutions were capped and stored at room temperature between measurements.

Replicate solutions were prepared as part of the quality assurance/quality control (QAQC) protocol. Three complete Tris buffer series were prepared in duplicate. Eight individual solutions within buffer series were prepared in either duplicate or triplicate and 15 phenol red additions to the buffer solutions were performed in duplicate.

To test the range in linearity of the potentiometric electrodes, five sets of low pH (pH = 1.4-3.4) HCl buffers were prepared in high-ionic-strength matrices (Appendix B.4). The buffering capacity of HCl is strongest below a pH of 2. The pH of the solutions was adjusted using either standardized 0.0101 mol/kg hydrochloric acid (HCl) or concentrated HCl (\approx 16.6 mol/kg) as the buffering agent. The Pitzer coefficients for ions in HCl systems have been well characterized

and are included in the standard PHREEQC-PITZER database. Dilution of high ionic strength solutions with the 0.0101 mol/kg HCl solution was accounted for in the modelling.

5.2.2 Potentiometric pH Measurements

pH measurements were made with two electrode/meter combinations: an Orion Ross 815600 electrode (Ross 815600) with a Barnant 20 meter and a Ross Sureflow 8165BNWP electrode (Sureflow) with a Jenco M-5005 meter. Both electrodes have low-sodium error and are suitable for use with the Tris buffer. The Sureflow electrode is recommended by the manufacturer for pH measurements in high ionic strength solutions because the flowing junction should reduce the liquid junction potential compared to a standard porous-plug junction (Ross 815600).

The meters were calibrated using low-ionic strength pH 4 and pH 7 NIST buffers immediately before each set of measurements. The linear range of the calibration was checked using a pH 9.18 commercial buffer. The stability of calibration was checked by re-measuring the calibration buffers after the measurements were completed. In all cases, both the pH and the mV reading were recorded. Ambient laboratory temperature was recorded and the pH measurements were made with manual temperature compensation.

5.2.3 Spectrophotometric pH Measurements

Absorbance measurements were made using an Ocean Optics USB4000 spectrophotometer coupled with an Ocean Optics deuterium-halogen light source. The spectrophotometric measurements were in a FIALab® Instruments SMA Z-flow cell with a 10-cm path length. Dark spectra and reference spectra were collected immediately prior to each set of measurements. For a consistent background matrix between reference and test solution spectra, the reference spectrum for each series of measurements was collected using one of the test solutions without the addition of the phenol red indicator. Spectra were collected in triplicate for all of the Tris buffer solutions. The spectrophotometer operating conditions are summarized in Table 10.

Table 10: Spectrophotometer Operating Conditions

Integration Time (μsec):	15000
Spectra Averaged:	10
Boxcar Smoothing:	2
Correct for Electrical Dark:	No
Strobe/Lamp Enabled:	No
Correct for Detector Non-linearity:	No
Correct for Stray Light:	No
Number of Pixels in Processed Spectrum:	3648

The phenol red molal absorption coefficients, ϵ , for the acid and base forms were measured at their maximum absorbance wavelengths 431 nm (λ_1) and 559 nm (λ_2), respectively. To do this, spectra were acquired for phenol red when it was 99.9% in its acid form (3 pH units below pK_a')

and also 99.9% in its base form (3 pH units above pK'_a) (King and Kester 1989). In L-SPW and S-SPW, an increase of 3 pH units resulted in the formation of precipitates and the ϵ measurements are not possible. As a result, ϵ measurements were determined in NaCl solutions only, at three ionic strengths: 0.05, 1.0, and 5.0 mol/kg. The maximum difference in a calculated pK'_a , if based on ϵ values determined at either the 0.05, 1.0 or 5.0 mol/kg ionic strength solutions, was small (0.03 units). Therefore, the average values of the ϵ measurements (acid and base forms) were used for the pK'_a calculations at all ionic strengths. This approach is consistent with that of King and Kester (1989) and Raghuraman et al. (2006b).

5.3 RESULTS AND DISCUSSION

The mean ambient laboratory temperature for all measurements was 24.9 °C, and ranged between 23.5 and 25.8 °C. The mean variation in ambient temperature over the course of a single experiment was 0.4 °C and the maximum variation was 1.5 °C. Any change in the solution temperature during an experiment would be less than these values. For both the potentiometric pH measurements and the phenol red pK'_a determinations, the modelled pH values were corrected (± 0.03 unit/°C; Millero et al. 2009) by post modelling to account for the difference between the mean laboratory temperature and 25.0 °C.

5.3.1 Potentiometric pH Measurements

The glass electrode is linear across a modelled pH range of 1.4 to 9.1 (Figure 18) and the linearity of the electrode response is consistent over the range of ionic strengths tested (Figure 19). The measured pH values from the Ross 815600 and the Sureflow electrodes are the same within error, ± 0.03 units (Figure 19; Appendix B.5). Despite the expectation that uncertainty increases with Ca concentration (Section 5.2.1), the linear response observed for the S-SPW across the pH range suggests that the modelled values are reasonable.

There is a linear relationship between mV and modelled pH ($R^2 = 0.9997$) when CO_2 is not included in the model calculations. In contrast, if equilibration with $\text{CO}_{2(\text{g})}$ is accounted for, the relationship is nonlinear (Figure 18 Inset) because of the increase in CO_2 solubility at high pH. The linearity observed in the experimental data across the pH range of 1.4 to 9.1 suggests that any influence on the solution pH from atmospheric $\text{CO}_{2(\text{g})}$ in these solutions over the course of the experiments was negligible.

Although the electrode response is linear, an offset from the NIST buffer calibration line is observed with increasing ionic strength for all solutions (Figure 19, Figure 20). Measured pH values are either equal to (within error) or lower than modelled values. The 0.2 pH unit offset for the 5 mol/kg NaCl buffers is consistent with the finding of Hinds et al. (2009), who compared glass electrode pH measurements against the standard hydrogen electrode (SHE) in NaCl solutions. The magnitude of the offset is not only affected by ionic strength, but also by the solution composition. For example, the offset in the 4.89 mol/kg L-SPW solution is 0.39 units, double that of the NaCl solution of similar ionic strength. The offset is even greater, 0.45 units, with the S-SPW diluted to an ionic strength of 4.95 mol/kg. These differences indicate that the offset is a function of both ionic strength and solution composition.

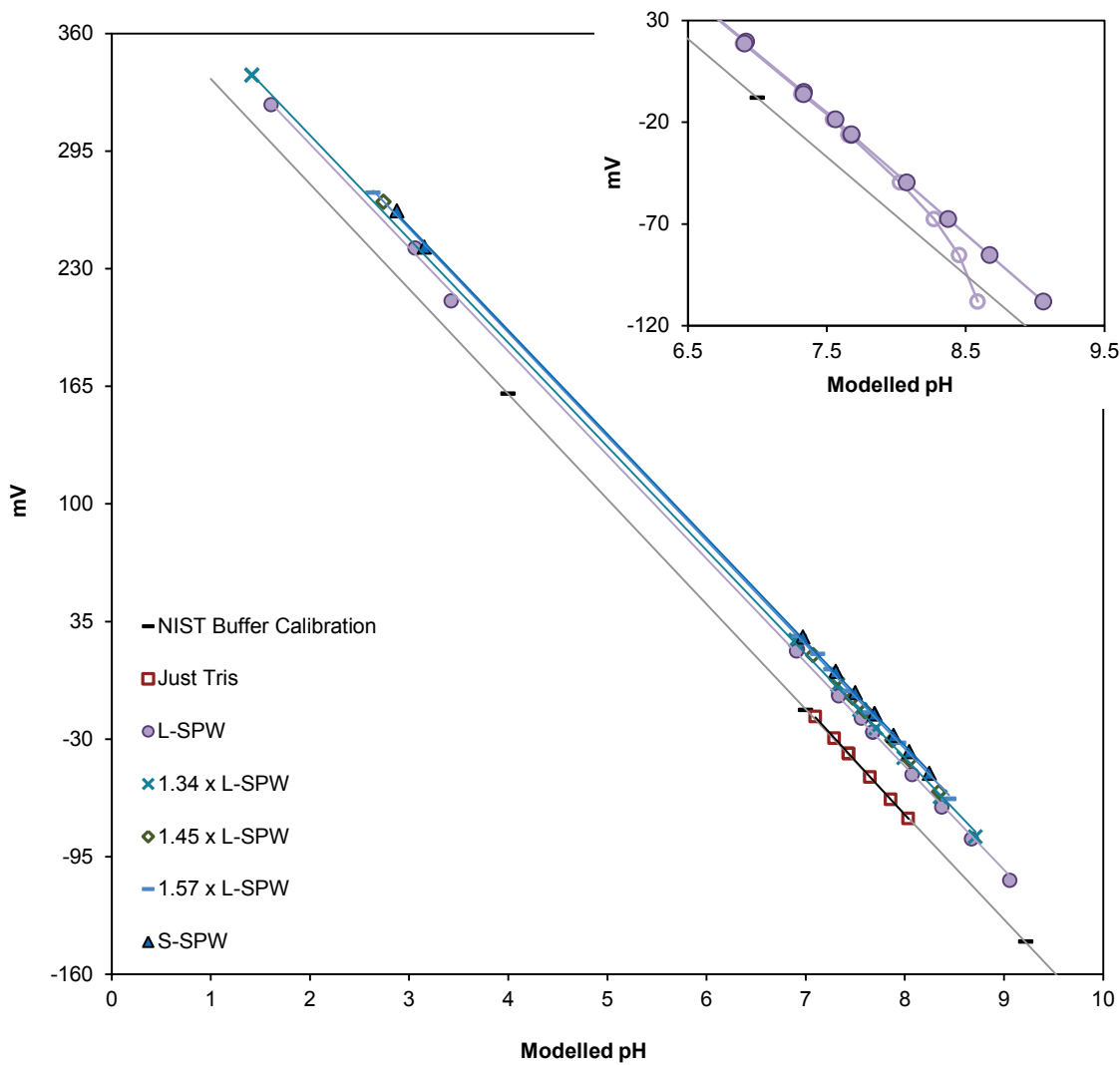


Figure 18: Electrode Response to Changing pH for Selected Tris and HCl Buffer Solutions. Modelled pH Values Assume no Equilibrium with Atmospheric $\text{CO}_{2(\text{g})}$. Inset: Filled Symbols Represent L-SPW Tris Buffer with No $\text{CO}_{2(\text{g})}$ and Hollow Symbols Represent Modelled pH Assuming Solution Equilibration with $\text{CO}_{2(\text{g})}$ ($\log \text{PCO}_2 = -3.4$)

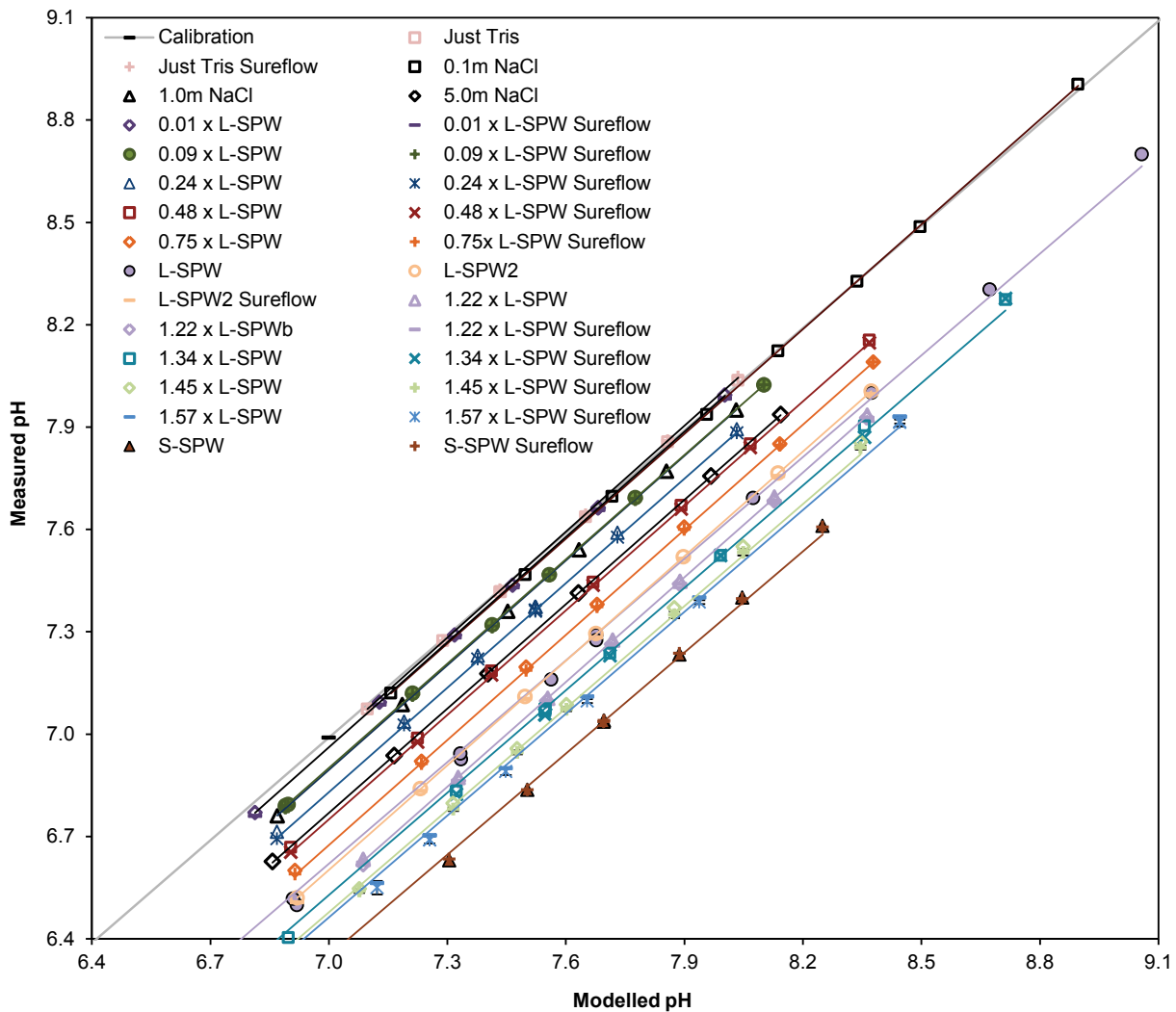


Figure 19: Modelled Versus Measured pH for the Tris Buffer Data Set. Modelled pH Values Assume no Equilibrium with Atmospheric $\text{CO}_{2(g)}$. Data Series with the Identifier “Sureflow” were Measured with the Sureflow Electrode. Otherwise, the pH was Measured Using the Ross 815600 Electrode

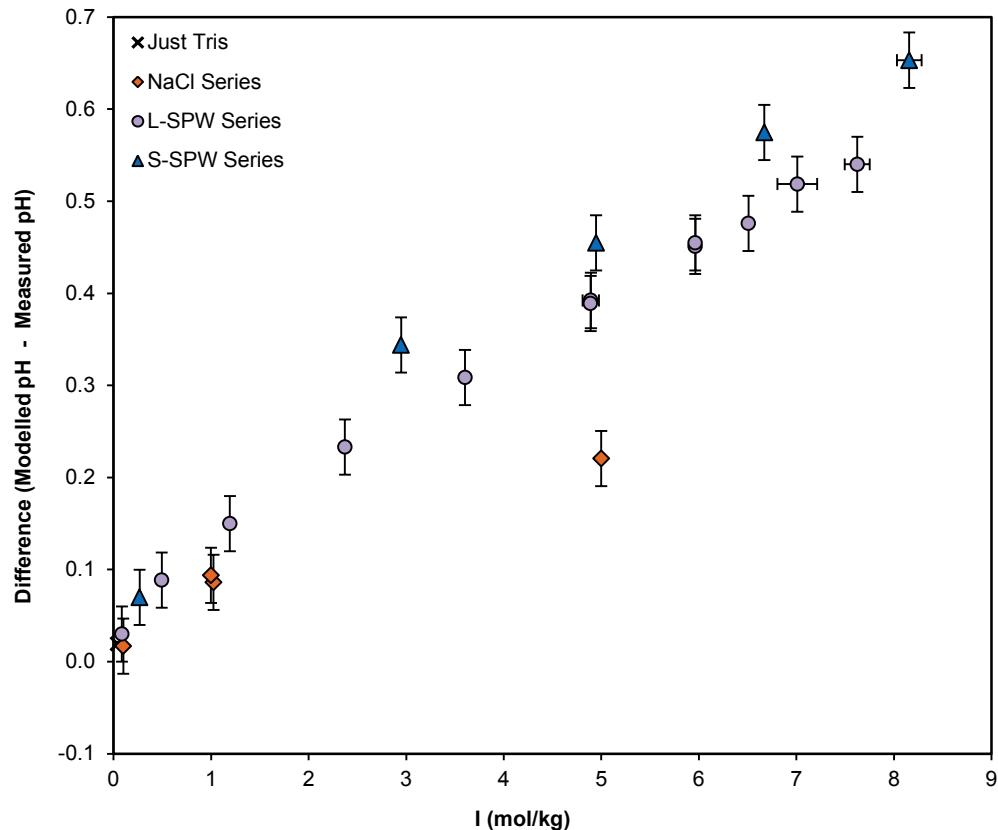


Figure 20: The Difference Between Modelled pH and Potentiometrically Measured pH with Changing Ionic Strength and Solution Composition. Modelled Values Do Not Include Equilibration With Atmospheric CO_{2(g)}. Vertical Error Bars Represent the Standard Error in Potentiometric pH Measurements, ±0.03 pH Units. Horizontal Error Bars Represent the Standard Deviation in Ionic Strength Across a Buffer Series; Where Not Visible, the Variation is Smaller than the Symbol

Periodic pH measurements for a Tris buffer series stored over a period of 60 days display very little change (standard deviation = 0.02; Figure 21), indicating that the Tris buffers are stable over that amount of time. Millero et al. (1993) also reported that the Tris buffer is stable over similar time periods.

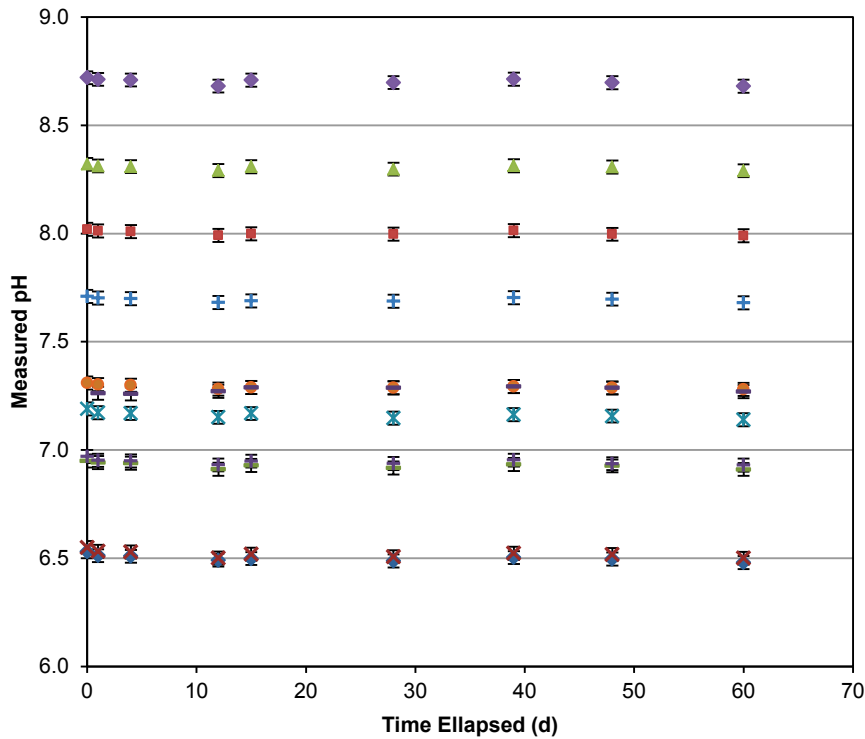


Figure 21: Measured pH of a L-SPW Tris Buffer Series Over Time. The Data Have Been Normalized to 25 °C. Error Bars Represent the Standard Error in Potentiometric pH Measurements, ± 0.03 pH Units

The time series measurements, the agreement between the two pH electrodes used in this study and the results of replicate pH measurements all suggest that the offsets are consistent and reproducible. The millivolt response and the E° of the potentiometric cells are different with different electrode/meter combinations and will change over time; they are not reproducible. However, as long as the composition of the buffers used to calibrate the potentiometric cell is consistent, the measured pH values will also be consistent.

In practice, when working in the laboratory, the composition of test solutions will be known and, provided model parameters are available for all solution components, calibration buffers can be prepared to match the matrix. In cases where the test-solution composition is not known, such as with field sampling of groundwater, there may be a mismatch between the ionic strength and composition of the calibration buffers and the test solution. The magnitude of these mismatches will determine any offset (error) in the measurement (Figure 18, Figure 20) that is over and above the standard error of ± 0.03 pH units. A field measurement strategy that includes collection of the raw data (mV) for any calibrations and for the test solutions would make it possible to make corrections to field measurements at a later time, after the composition and ionic strength of the solution becomes known.

Two-point calibrations are required for reliable pH measurement. Therefore, in practice, one Tris buffer and one HCl buffer should be prepared in the same matrix as the test solutions. The buffers should be prepared so that the pH is well within their effective range; for Tris this means

using Tris and TrisHCl salts at or near equal molar quantities. This would give, for example, a pH of 8.25 in S-SPW (Appendix B.4). The HCl buffer should have a pH <2.0.

5.3.2 Spectrophotometric pH Measurements

The measured molar absorptivities for the phenol red indicator (Table 11) are not the same as those reported by Raghuraman et al. (2006b) because different wavelengths were used. Raghuraman et al. (2006b) used 445 nm and 570 nm wavelengths, and 431 nm and 559 nm wavelengths were used in this work. Furthermore, Raghuraman (2006b) used different instrumentation and it has also been reported that impurities in indicators, which can vary by manufacture and even by batch, can affect the molar absorptivities of the indicator and result in differences in measured pH by up to 0.01 unit (Yao et al. 2007). To put it in context, that magnitude of error from indicator impurities is similar to the magnitude of error associated with commercial NIST pH buffers. If required, the error from indicator impurities can be reduced by taking extra steps to purify each dye batch used (Liu et al. 2011), or molar absorptivities can be measured each time a new batch of indicator is used. The pK_a' for phenol red in 0.1 mol/kg NaCl was recalculated at the wavelengths used by Raghuraman et al. (2006b) and with the molar absorptivities they reported. Raghuraman et al. (2006b) reported a pK_a' of 7.79 at 20 °C and the corresponding pK_a' measured in this study would be 7.74 at 25 °C. The uncertainty in the method developed by Raghuraman et al. (2006b) is ± 0.1 unit. Therefore, the effect of differences in measured ϵ values between the studies is considered negligible.

Table 11: Measured Molar Absorptivities for Phenol Red in NaCl Solutions

	0.05 mol/kg NaCl		1.0 mol/kg NaCl		5.0 mol/kg NaCl		All Measurements	
	Mean	σ	Mean	σ	Mean	σ	Mean	σ
$\epsilon_{559,B}$	59,975	279	59,170	1,477	55,823	583	58,323	2,039
$\epsilon_{559,A}$	74	29	-11	63	66	75	43	69
$\epsilon_{431,B}$	4,077	78	3,529	135	3,771	201	3,792	269
$\epsilon_{431,A}$	19,303	205	20,246	1,367	19,393	440	19,647	914

ϵ in units of $(\text{mol}/\text{kg})^{-1}\text{cm}^{-1}$; σ is standard deviation

The effect of equilibration with atmospheric $\text{CO}_{2(g)}$ on plots of $\log[\text{B}]/[\text{A}]$ versus modelled pH is presented in (Figure 22). The addition of $\text{CO}_{2(g)}$ adds a small degree of nonlinearity at the higher pH values, and this in-turn would contribute to error on the order of 0.02 to 0.03 in the pK_a' measurement (intercept with the X axis). However, on the basis of arguments presented in Section 5.3.1, any effect from the presence of $\text{CO}_{2(g)}$ is expected to be negligible and all pK_a' determinations were made with pH values obtained from the model without equilibrating with atmospheric $\text{CO}_{2(g)}$ (Appendix B.6).

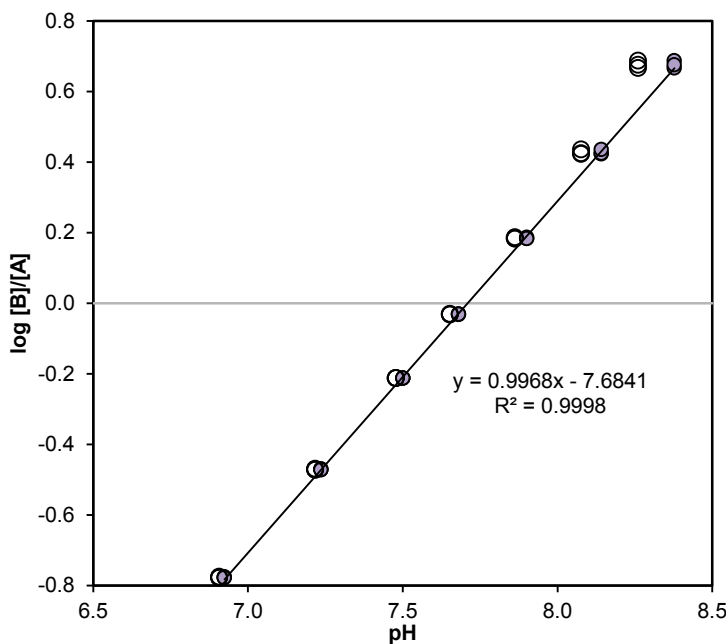


Figure 22: Plot of the Phenol Red Absorbance Ratio Versus pH in L-SPW. Filled Symbols Represent Modelled pH Assuming no Equilibrium with Atmospheric $\text{CO}_{2(\text{g})}$; Hollow Symbols Represent Modelled pH with Solutions at Equilibrium with Atmospheric $\text{CO}_{2(\text{g})}$ ($\log \text{PCO}_2 = -3.4$)

The pK'_{a} of phenol red is sensitive to the ionic strength of the solution, but the data indicate that it is not sensitive to solution composition (Figure 23; Appendix B.6). With increasing ionic strength there is a rapid drop from the pK'_{a} of 8.0 (Drummond et al. 1989) to a pK'_{a} of 7.8 at 0.04 mol/kg. There is a minimum ($\text{pK}'_{\text{a}} = 7.6$) in the ionic strength range of 1.0 to 2.5 mol/kg and then a gradual increase back to a pK'_{a} of 7.8 at 8.2 mol/kg. This indicates that the maximum possible error in measured pH would be 0.2 units if the ionic strength of the test solution did not match the ionic strength of the buffer solutions. Therefore, the maximum error in pH measured spectrophotometrically is lower than that from potentiometric measurements (Section 5.3.1). Furthermore, there is an advantage in that the spectrophotometric measurements are not sensitive to variations in ionic composition. In this case, the difference in the measured pK'_{a} for three solutions of similar ionic strength (~5.0 mol/kg) but different composition ranged from 0.01 to 0.04 (Figure 23).

The useful range for the phenol red indicator is approximately ± 1 pH unit from the pK'_{a} value (Figure 22) and the measurement is therefore a function of ionic strength. The pH range for the spectrophotometric method in high-ionic-strength solutions could be extended by developing similar datasets for pK'_{a} for multiple indicators that cover a broad pH range. Raghuraman (2006b) used a combination of colorimetric indicators in NaCl solutions, however NaCl buffer solutions limit the upper end of ionic strength to approximately 6 mol/kg. To extend the ionic strength range beyond 6 mol/kg requires the use of divalent cation salts, but this is only possible for a limited range of conditions because the Pitzer ion interaction parameters are not available to model pH for all buffers and for solutions with high Ca and Mg concentrations (Section 5.1, Figure 20). For DGR-related work it is desirable to have the ability to measure pH

in the range 4 to 9 and, until additional spectrophotometric datasets become available, the only available option is to use the potentiometric approach as outlined in Section 5.3.1.

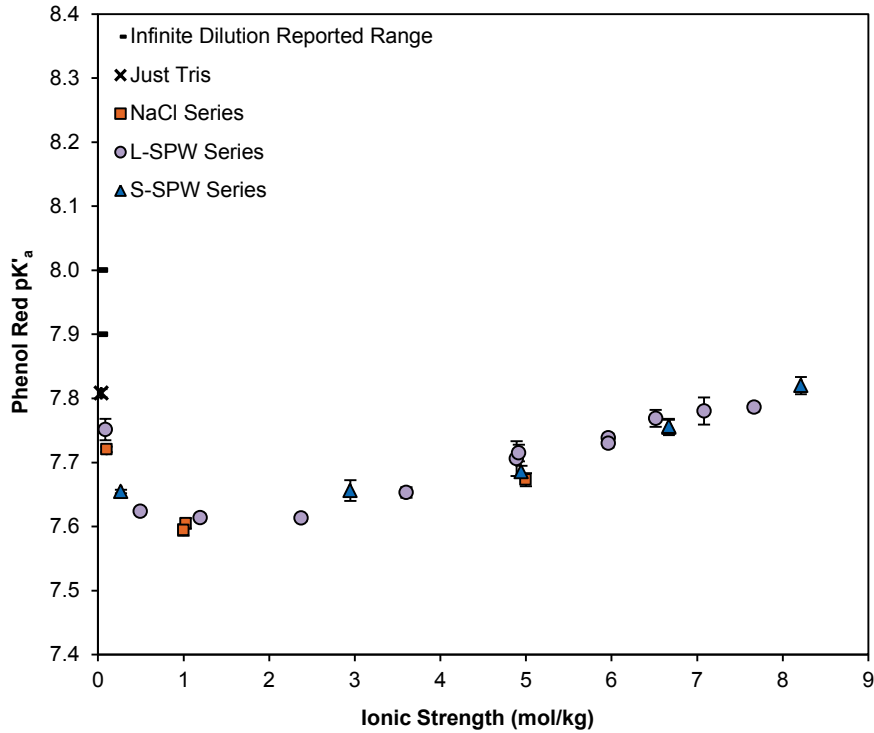


Figure 23: Variation in Phenol Red pK'_a with Ionic Strength and Solution Composition. Vertical Error Bars Represent 1σ . Horizontal Error Bars Represent the Standard Deviation in Ionic Strength Across a Tris Buffer Series; Where Not Visible, the Variation is Smaller than the Symbol

5.3.3 Uncertainty Assessment

To evaluate what effect weighing errors could have had on the buffer pH, and therefore on the measured pK'_a , a sensitivity analysis was conducted. The L-SPW2 buffer series was modelled for an additional 4 times considering:

- The maximum discrepancy that could occur if the actual mass of Tris and TrisHCl was in error by a factor of 5 times the precision of the balances used to weigh the Tris salts; and
- +5% and -5% of the molal values for the components of the L-SPW2 matrix (Na^+ , K^+ , Ca^{2+} , Mg^{2+} , Cl^- and SO_4^{2-}).

The differences in both buffer pH and pK'_a were apparent at the third decimal point, less than the resolution of the glass electrodes, ± 0.01 unit. The pK'_a for phenol red in L-SPW2 ranged from 7.705 to 7.709 – a difference of 0.004 units. This is almost an order of magnitude smaller

than the standard deviation from replicate pK'_a measurements, which was up to 0.03 units. Therefore, effects from possible errors in solution preparation are considered negligible.

5.4 SUMMARY

Pitzer coefficients for two buffers, Tris and acetate, were added to the PHREEQC-Pitzer database and the model-calculated pK'_a values were verified against literature data. The Pitzer coefficient data were more complete and considered more reliable for the Tris buffer – effective pH range of 6.5-9.0 – than for the acetate data – effective pH range of 3.0-5.6 units. pH buffers were also prepared using HCl. The Pitzer coefficients for the HCl system are well known and included in the standard PHREEQC-Pitzer database. It was decided to use Tris and HCl buffers to evaluate two methods for pH ($-\log a_H$) measurement in brine solutions: potentiometric measurements with glass electrodes, and spectrophotometric measurements using the colorimetric indicator phenol red ($pK_a = 8.0$). The experiments involved a range of ionic strengths from 0.04 to 8.2 mol/kg, and solution compositions ranging from NaCl to the more complex S-SPW. Uncertainty in the modelled pH values for the buffer solutions increases for ionic strengths >6.0 mol/kg and for solutions that are more complex than just NaCl because Pitzer parameters for the Tris and acetate buffers have not been measured in such conditions. Extrapolation beyond these conditions could result in errors in modelled pH of up to 0.1 pH unit.

The potentiometric pH electrode response is linear over a pH range from 1.4 to 9.1 and for ionic strengths up to 8.2 mol/kg. However, there is a systematic offset with increasing ionic strength such that an electrode calibrated with low ionic strength buffers will underestimate the pH of the highest ionic strength solution tested (8.2 mol/kg) by 0.6 to 0.7 pH units. For any given ionic strength, the potentiometric measurement is also sensitive to the ionic composition of the solution. Despite these effects, accurate potentiometric measurements are possible if the composition of the calibration buffers is similar to the test solution.

The results of spectrophotometric measurements indicate that the stoichiometric disassociation constant (pK'_a) of the phenol red indicator is sensitive to ionic strength but virtually insensitive to the composition of the solution. A maximum error of 0.2 units is possible for pH measured spectrophotometrically, if the ionic strength of the buffers does not match the ionic strength of the test solution. Because of the lower sensitivity of the spectrophotometric data to both ionic strength and solution composition, spectrophotometric measurements may prove more reliable than potentiometric measurements in unknown solutions, e.g., for pH measured in the field. However, the measurement range of phenol red is limited to pH \approx 7-9. Additional indicators can be combined to increase the effective range of the spectrophotometric approach. The choice in additional indicators must be considered in the context of the availability and reliability of the appropriate Pitzer ion interaction coefficient data for the buffer as well as the logical combination of indicators to extract unique pH values from multi-indicator spectra (Raghuraman et al. 2006b).

Both methods for pH measurement, potentiometric and spectrophotometric, can be adapted to reliably measure pH in high ionic strength solutions. The two methods offer distinct advantages and limitations. Therefore, the selection of which method to use will depend on the application.

6. CONCLUDING REMARKS

A γ -RAD technique has been established for use in measurement of D_e and ϕ_l values for low-permeability sedimentary and crystalline rock samples. The γ -RAD method is free of beam-hardening artefacts and a linear calibration function is obtained that is essentially independent of background matrix.

The γ -RAD method has been tested for measurement of porosity and diffusion coefficients of granite (<1% porosity; $D_e = 3.1 \times 10^{-13} \text{ m}^2/\text{s}$) using an experimental design that allows for simultaneous TD (through-diffusion) measurements ($D_e = 3.0 \times 10^{-13} \text{ m}^2/\text{s}$). Only one test has been conducted to date and the results of the two techniques are in good agreement, but there were problems identified in the TD experiment probably due to gradual occlusion of diffusion pathways by mineral-water reactions and the SNR (signal to noise ratio) is low for the γ -RAD measurements. These results demonstrate that the γ -RAD technique will be viable for crystalline rocks but further method development is required to demonstrate full confidence.

A new method has been developed to generate partial gas saturation conditions in low-permeability rocks. The method is based on the relationship between gas solubility and pressure, whereby a rock sample that is initially 100% brine saturated is equilibrated with N₂ gas at high pressure (up to 7000 kPa), and then the pressure is rapidly decreased to atmospheric pressure. This causes a corresponding decrease in gas solubility, resulting in exsolution of N₂ to form gas bubbles in the pore spaces. The degree of partial saturation is determined by γ -RAD. During method development, the initial partial saturation work has been conducted on sandstone (13.0% porosity). Results of repeat experiments on the same sandstone sample display decrease in D_e values ranging from 21-56% for very similar degrees of partial saturation (15% and 13.5%, respectively). This is an unexpected result and it suggests that there is either an unidentified source of error in the measurements, or an effect from pore-scale variations in the distribution of the gas phase that cannot be resolved in the γ -RAD measurements. A preliminary result from Queenston Formation shale indicates a 53% decrease in D_e as a result of 14.6% partial gas saturation. This method shows great potential for evaluating the effect of partial saturation on diffusion in the Michigan Basin rocks that contain very high salinity porewater. However, these are challenging, multistep experiments and the technique requires further testing and development in order to gain full confidence in the results.

Two techniques for measuring pH were evaluated – potentiometric and spectrophotometric pH measurement – in the context of high-ionic-strength brines. As part of the study, Pitzer coefficients for two buffers, Tris and acetate, were added to the PHREEQC-Pitzer database to calculate the pH of high-ionic-strength buffers. Using these buffers, it was found that the potentiometric measurement is sensitive to both the ionic strength and the ionic composition of the solution. Despite these effects, accurate potentiometric measurements are possible if the composition of the calibration buffers is similar to the test solution. The results of spectrophotometric measurements indicate that the association constant (pK'_a) of the phenol red indicator is sensitive to ionic strength but virtually insensitive to the composition of the solution. The magnitude of the possible error in pH measurement using unmatched calibration buffers is larger for the potentiometric method than the spectrophotometric method. However, the range of pH that can be measured using the spectrophotometric method is limited by the narrow working range of the colorimetric indicators, whereas the potentiometric method is

applicable across the pH range. From this work, we have determined that both methods for pH measurement can be adapted to reliably measure pH in high ionic strength solutions. The two methods offer certain advantages and limitations. Therefore, the selection of which method to use will depend on the application.

ACKNOWLEDGEMENTS

We thank Professor Sean McGrady, Department of Chemistry, UNB, who provided access to a high-pressure chamber, and Sandra Riley for assisting with its operation.

REFERENCES

- AI, T., Y. Xiang and L. Cavé. 2010. Measurement of Diffusion Properties by X-ray Radiography and by Through-Diffusion Techniques Using Iodide and Tritium Tracers: Core Samples from OS-1 and DGR-2. Intera Engineering Ltd., Technical Report TR-07-17 Revision 3. (Available at www.nwmo.ca)
- AI, T., Y. Xiang, L. Cavé and D. Loomer. 2012. Measurement of Diffusion Properties by X-Ray Radiography and by Through-Diffusion Techniques Using Iodide and Tritium Tracers: Core Samples from DGR-3 and DGR-4. Geofirma Engineering Ltd., Technical Report TR-08-27 Revision 2. (Available at www.nwmo.ca)
- ANGUS Chemical Company. 2000. ANGUS Chemical Company Technology Review: Biotechnology applications of Tris Amino® (Tris Buffer). TR 10, 12 p.
- AppliChem. 2008. Biological Buffers. A brochure providing information on biological buffers. www.applichem.com.
- Bates, R.G. and J.B. Macaskill. 1985. Activity and osmotic coefficients of t-butylammonium chloride; Activity coefficients of HCl in mixtures with Tris hydrochloride or t-butylammonium chloride at 25 °C. Journal of Solution Chemistry 14, 723-734.
- Bates, R.G. and R.A. Robinson. 1974. An approach to conventional scales of ionic activity for the standardization of ion-selective electrodes. Pure and Applied Chemistry 37, 573-577.
- Bea, S.A., J. Carrera, C. Ayora, F. Batlle. 2010. Pitzer Algorithm: efficient implementation of Pitzer equations in geochemical and reactive transport models. Computers & Geosciences 36, 526-538.
- Bea Jofré, S.A., K.U. Mayer and K.T.B. MacQuarrie. 2011. Modelling Reactive Transport in Sedimentary Rock Environments - Phase II MIN3P code enhancements and illustrative simulations for a glaciation scenario. Nuclear Waste Management Organization Report NWMO TR-2011-13. Toronto, Canada. (Available at www.nwmo.ca)
- Buck, R.P., S. Rondinini, A.K. Covington, F.G.K. Bauke, C.M.A. Brett, M.F. Camoes, M.J.T. Milton, T. Mussini, R. Naumann, K.W. Pratt, P. Spitzer and G.S. Wilson. 2002. Measurement of pH. Definition, standards, and procedures – IUPAC Recommendations 2002. Pure and Applied Chemistry 74, 2169-2200.
- Cavé, L. and T. AI. 2006. Paleohydrogeology – Analytical TEM investigation of mineral weathering in the Whiteshell research area. OPG Nuclear Waste Management Division, Report No: 06819-REP-01200-10156-R00.
- Cavé, L., T. AI, Y. Xiang and P. Vilks. 2009. A technique for estimating one-dimensional diffusion coefficients in low permeability sedimentary rock using X-ray radiography: Comparison with through-diffusion measurements. Journal of Contaminant Hydrology 103, 1-12.

- Cavé, L., T. Al, Y. Xiang and D. Loomer. 2010. Investigations of Diffusive Transport Processes in Sedimentary Rock. Nuclear Waste Management Organization Report NWMO TR-2010-04. Toronto, Canada. (Available at www.nwmo.ca)
- Covington, A.K. and M.I.A. Ferra. 1994. A Pitzer mixed electrolyte solution theory approach to assignment of pH to standard buffer solutions. *Journal of Solution Chemistry* 23, 1-10.
- Dickson, A.G. 1984. pH scales and proton-transfer reactions in saline media such as sea water. *Geochimica et Cosmochimica Acta* 48, 2299-2308.
- Slagokenky, E. and P. Tans. 2014. Recent global monthly mean carbon dioxide concentrations over marine surface sites. NOAA/ESRL (www.esrl.noaa.gov/gmd/ccgg/trends/).
- Drummond, C.J., F. Grieser and T.W. Healy. 1989. Acid-base equilibria in aqueous micellar solutions. Part 2: Sulphonaphthalene indicators. *Journal of the Chemical Society, Faraday Transactions 1* 85, 537-550.
- Foti, C., C. Rigano and S. Sammartano. 1999. Analysis of thermodynamic data for complex formation: Protonation of tham and fluoride ion at different temperature and ionic strengths. *Annali di Chimica* 89, 87-98.
- Gran, G. 1950. Determination of the equivalence point in potentiometric titrations. *Acta Chemica Scandinavica* 4, 559-577.
- Gran, G. 1952. Determination of the equivalence point in potentiometric titrations. Part II. *Analyst* 77, 661-671.
- Hansson, I. 1973. A new set of pH-scales and standard buffers for sea water. *Deep-Sea Research* 20, 479-491.
- Harned, H.S. and B.B. Owen. 1958. *The Physical Chemistry of Electrolytic Solutions*, Reinhold, New York, 803p.
- Hinds, G, P. Cooling, A. Wain, S. Zhou and A. Turnbill. 2009. Technical Note: Measurement of pH in Concentrated Brines. *Corrosion* 65, 635-638.
- Hobbs, M., A. de Haller, M. Koroleva, M. Mazurek, J. Spangenberg, U. Mäder and D. Meier. 2011. Borehole DGR-3 and DGR-4 Porewater Investigations, R0. Geofirma Engineering Ltd. Technical Report TR-08-40, Toronto, Canada.
- Hussein, E. M. A. 2011. *Computer Radiation Imaging: Physics and Mathematics of Forward and Inverse Problems*, Elsevier, Amsterdam.
- Intera 2011. Descriptive Geosphere Site Model. Intera Engineering Ltd. report for the Nuclear Waste Management Organization NWMO DGR-TR-2011-24 R000. Toronto, Canada. (available at www.nwmo.ca/dgrgeoscientificsitecharacterization)
- Jensen, W.B. 2004. The symbol for *pH*. *Journal of Chemical Education* 81, 21.

- Johansson, H., M. Siitari-Kauppi, M. Skalberg and E.L. Tullborg. 1998. Diffusion pathways in crystalline rock – examples from Aspo-diorite and fine-grained granite. *Journal of Contaminant Hydrology* 35, 41-53.
- King, D.W. and D.R. Kester. 1989. Determination of seawater pH from 1.5 to 8.5 using colorimetric indicators. *Marine Chemistry* 26, 5-20.
- Koroleva, M., A. de Haller, U. Mader, H.N. Waber and M. Mazurek. 2009. Borehole DGR-2: Pore-water investigations. Intera Engineering Ltd., Technical Report TR-08-06, August 4, Institute of Geological Sciences, University of Bern, Switzerland.
- Liu, X., M.C Patsavas and R.H. Byrne. 2011. Purification and characterization of meta-cresol purple for spectrophotometric seawater pH measurements. *Environmental Science & Technology* 45, 4862-4868.
- Loomer, D., Y. Xiang and T. Al. 2013a. Investigations of methods for quantifying diffusive transport processes in sedimentary rock. Nuclear Waste Management Organization Report NWMO TR-2013-18. Toronto, Canada.
- Loomer, D., L. Scott, T. Al, K.U. Mayer and S. Bea. 2013b. Diffusion–reaction studies in low permeability shale using X-ray radiography with cesium. *Applied Geochemistry* 39, 49-58.
- Loos, D., C. Pasel, M. Luckas, K.G. Schmidt and J.-D. Herbell. 2004. Experimental investigation and modelling of the solubility of calcite and gypsum in aqueous systems at higher ionic strength. *Fluid Phase Equilibria* 219, 219-229.
- MacInnes, D.A. 1919. The activities of the ions of strong electrolytes. *Journal of the American Chemical Society*, 41, 1086-1092.
- Maksimov, I., M. Ohata, S. Nakamura, A. Hioki, K. Chiba and P. Spitzer. 2008. pH determination on a carbonate buffer by Harned cells of different designs. *Accreditation and Quality Assurance* 13, 381-387.
- Mao, S. and Z. Duan. 2006. A thermodynamic model for calculating nitrogen solubility, gas phase composition and density of the N₂-H₂O-NaCl system. *Liquid Phase Equilibria* 248, 103-114.
- Martz, T.R., J.J. Carr, C.R. French and M.D. DeGrandpre. 2003. A submersible autonomous sensor for spectrophotometric pH measurements of natural waters. *Analytical Chemistry* 75, 1844-1850.
- Mayer, K.U., E.O. Frind and D.W. Blowes. 2002. Multicomponent reactive transport modeling in variably saturated porous media using a generalized formulation for kinetically controlled reactions. *Water Resource Research* 38, 1174, doi:10.1029/2001WR000862.
- McFarland, W.N. and K.S. Norris. 1958. The control of pH by buffers in fish transport. *California Fish and Game* 44, 4291.

- Meinrath, G. 2002. Extended traceability of pH: an evaluation of the role of Pitzer's equations. *Analytical and Bioanalytical Chemistry*, 374, 796-805.
- MERK. 2014. The MERK Index, 14th Ed. Merck Sharp & Dohme Corp., a subsidiary of Merck & Co., Inc., Whitehouse Station, NJ, USA.
- Mesmer, R.E., C. S. Patterson, R. H. Busey and H. F. Holmes. 1989. Ionization of acetic acid in NaCl(aq) media: A potentiometric study to 573 K and 130 bar. *The Journal of Physical Chemistry* 93, 7483-7490.
- Mesmer, R.E. and H.F. Holmes. 1992. pH, definition and measurement at high temperatures. *Journal of Solution Chemistry* 21, 725-744.
- Millero, F.J., J.P. Hershey and M. Fernandez. 1987. The pK* of TRISH⁺ in Na-K-Mg-Ca-Cl-SO₄ brines – pH scales. *Geochimica et Cosmochimica Acta* 51, 707-711.
- Millero, F.J., J.-Z. Zhang, S. Fiol, S. Sotolongo, R.N. Roy, K. Lee and S. Mane. 1993. The use of buffers to measure the pH of seawater. *Marine Chemistry* 44, 143-152.
- Millero, F.J., B. DiTrolio, A.F. Suarez and G. Lando. 2009. Spectroscopic measurements of the pH in NaCl brines. *Geochimica et Cosmochimica Acta* 73, 3109-3114.
- Mizera, J., A.H. Bond, G.R. Choppin and R.C. Moore. 1999. Dissociation constants of carboxylic acids at high ionic strengths. In *Actinide Speciation in High Ionic Strength Media: Experimental and Modeling Approaches to Predicting Actinide Speciation and Migration in the Subsurface*, Reed, D.T.; Clark, S. B.; Linfeng R. (Eds.). Proceedings of an American Chemical Society Symposium, August 26-28, 1996, Orlando, Florida, Kluwer Academic/Plenum Publishers, New York, 113-124.
- Mohan, C. 2006. Calbiochem®: A guide for the preparation and use of buffers in biological systems, CB0052-2006 USD Buffers Booklet., EMD, San Diego, California.
- Nordstrom, D.K., C.N. Alpers, C.J. Ptacek and D. W. Blowes. 2000. Negative pH and extremely acidic mine waters from Iron Mountain, California. *Environmental Science & Technology* 34, 254-258.
- Novak, C.F., M. Borkowski and G.R. Choppin. 1996. Thermodynamic modeling of Neptunium(V)-acetate complexation in concentrated NaCl media. *Radiochimica Acta* 74, 111-116.
- Parkhurst, D.L. and C.A.J. Appelo. 1999. User's Guide to PHREEQC (Version 2) – A Computer Program for Speciation, Batch-Reaction, One-Dimensional Transport and Inverse Geochemical Calculations. Water-Resources Investigations Report 99-4259. U.S. Department of the Interior, U.S. Geological Survey, Denver, Colorado.
- Parkhurst, D.L. and C.A.J. Appelo. 2013. Description of input and examples for PHREEQC version 3 — A computer program for speciation, batch-reaction, one-dimensional transport, and inverse geochemical calculations. In: U.S. Geological Survey Techniques and Methods, book 6, chap. A43, 497 p., available online at <http://pubs.usgs.gov/tm/06/a43>.

- Pehrsson, L., F. Ingman and A. Johansson. 1976. Acid-base titrations by stepwise additions of equal volumes of titrant with special reference to automatic titrations I: Theory, discussion of the Gran functions, the Hofstee method and two proposed methods for calculating equivalence volumes. *Talanta* 23, 769-780.
- Plummer, L.N., D.L. Parkhurst, G.W. Fleming and S.A. Dunkle. 1988. A computer program incorporating Pitzer's equations for calculation of geochemical reactions in brines. USGS Water-Resources Investigations Report 88-4153, Reston, Virginia.
- Pitzer, K.S. 1991. Ion interaction approach: theory and data correlation. In *Activity Coefficients in Electrolyte Solutions* (2nd ed.), Pitzer, K.S. (ed). C.R.C. Press., Boca Raton, Florida, 542p.
- Pitzer, K.S. and G. Mayorga. 1973. Thermodynamics of electrolytes. II. Activity and osmotic coefficients for strong electrolytes with one or both ions univalent. *The Journal of Physical Chemistry* 77, 2300-2308.
- Raghuraman, B., G. Gustavson, O. C. Mullins and P. Rabbitto. 2006a. Spectroscopic pH measurement for high temperatures, pressures and ionic strength. *AIChE Journal* 52, 3257-3265.
- Raghuraman, B., G. Gustavson, R.E.G. van Hal, E. Dressaire and O. Zhdaneev. 2006b. Extended-range spectroscopic pH measurement using optimized mixtures of dyes. *Applied Spectroscopy* 60, 1461-1469.
- Reardon, E.J. and P.M. Moddle. 1985. Gas diffusion coefficient measurements on uranium mill tailings: implications to cover layer design. *Uranium* 2, 111-131.
- Savoye, S., J. Page, C. Puente, C. Imbert and D. Coelho. 2010. New experimental approach for studying diffusion through an intact and unsaturated medium: A case study with Callovian-Oxfordian argillite. *Environmental Science and Technology* 44, 3698–3704.
- Siitari-Kauppi, M., A. Lindberg, K.H. Hellmuth, J. Timonen, K. Vaatainen, J. Hartikainen and K. Hartikainen. 1997. The effect of microscale pore structure on matrix diffusion – a site-specific study on tonalite. *Journal of Contaminant Hydrology* 26, 147-158.
- Skagius, K. and I. Neretnieks. 1986. Porosities and diffusivities of some nonsorbing species in crystalline rocks. *Water Resources Research* 22, 389-398.
- Smith, S.W. 2003. *The Scientist and Engineer's Guide to Digital Signal Processing*, California Technical Publishing, San Diego.
- Spitzer, P., P. Fisicaro, G. Meinrath and D. Stoica. 2011. pH buffer assessment and Pitzer's equations. *Accreditation and Quality Assurance* 16, 191-198.
- Subudhi, R.K. 2009. A radiation transmission technique for the spatially-resolved measurement of porosity and diffusion properties of porous media. M. Sc. Thesis, University of New Brunswick.

- Subudhi, R.K., E.A. Hussein and T. Al. 2010. Measurement of spatial distribution of total and accessible porosity in sedimentary rocks using isotopic radiation transmission: Device design and testing. *Applied Radiation and Isotopes* 68, 496-504.
- USGS. 2013. PHREEQC Interactive v. 3.0.6, June 2013.
http://wwwbrr.cr.usgs.gov/projects/GWC_coupled/phreeqc/.
- Vilks, P., J.J. Cramer, M. Jensen and N.H. Miller. 2003. In situ diffusion experiment in granite: Phase I. *Journal of Contaminant Hydrology* 61, 191-202.
- Wall, D.E., N.A. Wall and L.H. Brush. 2006. Speciation and Solubility Modeling of Actinides in the Waste Isolation Pilot Plant. In *Separations for the Nuclear Fuel Cycle in the 21st Century*, Chapter 20, 313–334. ACS Symposium Series 933.
- Xiang, Y., T. Al, L. Scott and D. Loomer. 2013. Diffusive anisotropy in low-permeability Ordovician sedimentary rocks from the Michigan Basin in southwest Ontario. *Journal of Contaminant Hydrology* 155, 31-45.
- Xiang, Y. and T. Al. in prep. Effect of confining pressure on diffusion coefficients in low-permeability Ordovician sedimentary rocks from the Michigan Basin in southwest Ontario. Manuscript in preparation.
- Xu, S., A. Worman and B. Dverstorp. 2001. Heterogeneous matrix diffusion in crystalline rock – implications for geosphere retardation of migrating radionuclides. *Journal of Contaminant Hydrology* 47, 365-378.
- Yao, W., X. Liu and R. H. Byrne. 2007. Impurities in indicator used for spectrophotometric seawater pH measurements: Assessment and remedies. *Marine Chemistry* 107, 167-172.

APPENDIX A: METHOD FOR ENSURING 100% BRINE SATURATION

CONTENTS

	Page
A.1 SAMPLE DESCRIPTION.....	57
A.1.1 Sandstones	57
A.1.2 Queenston Formation Shale.....	57
A.2 IMPROVED EXPERIMENTAL PROCEDURES FOR ENSURING 100% BRINE SATURATION.....	57
A.2.1 Sandstones	58
A.2.2 Queenston Formation Shale.....	58
A.3 RESULTS.....	59

LIST OF TABLES

	Page
Table A.1: Water-Loss Porosity Data.....	59

LIST OF FIGURES

	Page
Figure A.1: Carbon Tan Sandstone Sample Partially Immersed in Water in a Vacuum Chamber: a) Immediately after Adding Water; and b) 30 min later	58

APPENDIX A: METHOD FOR ENSURING 100% BRINE SATURATION

In conducting measurements of diffusion coefficients under partially brine-saturated conditions, the 100% brine-saturated condition represents a baseline against which all data will be compared.

Saturation of a rock sample with a background brine solution is required for measurements of water-accessible porosity (ϕ_w) and D_e . The method for brine saturation used in previous work (Al et al. 2010, 2012; Cavé et al. 2009; Loomer et al. 2013b; Xiang et al. 2013; Xiang and Al, in prep.) involves submersing the sample in a brine solution followed by evacuation of the head space in a large (5 L) desiccator. This step is intended to remove the gas (air) initially present in the system, including dissolved air in the aqueous phase and trapped air in the rock pore spaces, and thereby maximize brine saturation of the sample.

A.1 SAMPLE DESCRIPTION

A.1.1 Sandstones

Well characterized natural sandstone (Carbon Tan from Utah from Ohio) was purchased from Kocurek Industries, Inc. (Caldwell, TX). The porosities of the sandstone were reported to be 12.2-17.7% for Carbon Tan at purchase. They were used previously in our research lab as calibration matrices for the X-ray radiography method (Loomer et al. 2013a). The water-loss porosity measured at UNB was 12.8% for Carbon Tan , which is in the reported range.

A.1.2 Queenston Formation Shale

The Queenston Formation shale sample (DGR3-472) used in this study was prepared from a preserved core segment obtained during a drilling and coring program for characterization of the Deep Geologic Repository (DGR) site for low- and intermediate-level waste at the Bruce nuclear site near Tiverton, Ontario. Samples from the Queenston Formation are dominantly red-brown shale with minor green and grey shale. Clay minerals comprise 50-60% of these shales, 70-80% of which are illite and illite-smectite mixed layers. Chlorite is also present. Carbonates (calcite and dolomite, 30-40%) and quartz (approximately 10%) are the other major mineral components in these shales (Koroleva et al., 2009). The previously measured ϕ_w value for sample DGR3-472 was 8.6%.

A.2 IMPROVED EXPERIMENTAL PROCEDURES FOR ENSURING 100% BRINE SATURATION

Modification of the saturation procedure involves use of a smaller (approximately 100 mL) vacuum chamber to minimize water mass lost to evaporation (Figure A.1). Such a system allows the following two equilibria to be established and maintained.

- 1) $\text{Air}_{(\text{aq})} \leftrightarrow \text{Air}_{(\text{g, head space})}$
- 2) $\text{Air}_{(\text{g, rock pores})} \leftrightarrow \text{Air}_{(\text{aq})}$

If a vacuum is maintained in the headspace by removal of $\text{Air}_{(\text{g, head space})}$ these coupled equilibria lead to removal of pore gas from the rock.

A.2.1 Sandstones

The first step was to replace air in the rock pore space with a water soluble gas, CO₂. Dry sandstone samples were placed in the vacuum chamber and the system was evacuated to approximately 90 kPa below atmospheric pressure (capacity of the pump) for an hour, after which CO₂ gas was introduced and allowed to flow through the chamber for 10-20 min. The CO₂ source was removed and the rock samples were allowed to equilibrate with the CO₂ atmosphere for approximately 30 min. The chamber was then evacuated. This procedure of adding CO₂ followed by evacuation of the chamber was repeated 3 times to ensure complete replacement of the air.

After CO₂ treatment, tap water was introduced into the chamber under vacuum to a level approximately 1/4 of the sample height (Figure A.1a), following which the chamber was evacuated. Within 30 minutes, the sandstone samples appeared wet as a result of capillary rise of water in the pores (Figure A.1b). Additional water was added under vacuum to completely submerge the samples, and then the system was allowed to sit in vacuum for 7 days. After water saturation, the ϕ_w values for the replicates of Carbon Tan sample were measured using the method outlined in Al et al. (2010, 2012) and Loomer et al. (2013a).

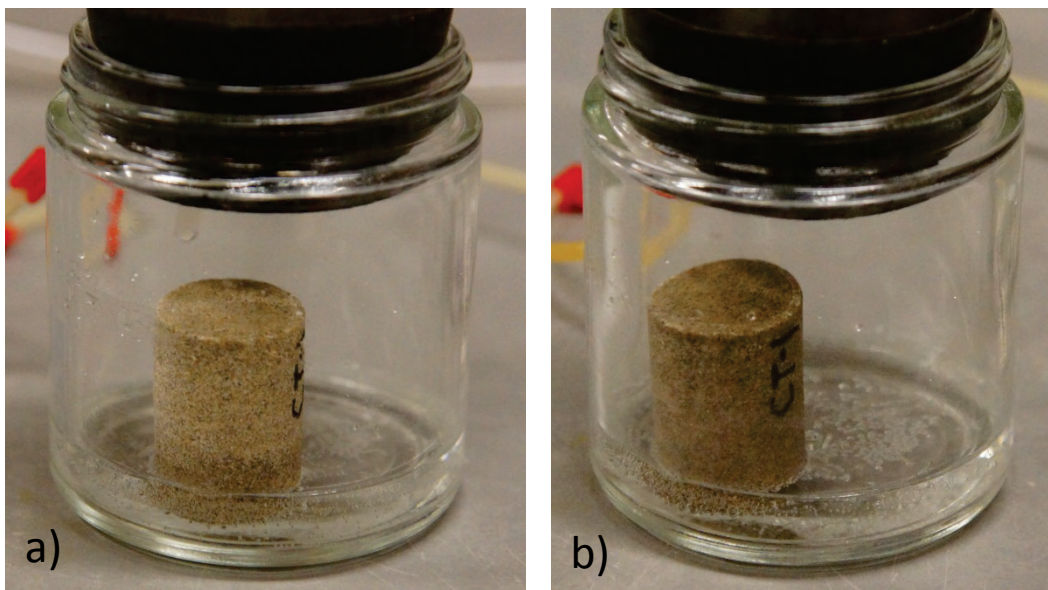


Figure A.1: Carbon Tan Sandstone Sample Partially Immersed in Water in a Vacuum Chamber: a) Immediately after Adding Water; and b) 30 min Later

A.2.2 Queenston Formation Shale

Triplicates of DGR3-472 were prepared from preserved drill cores. During the preparation it is expected that some water loss occurs from the surface of the samples. In order to resaturate them they were placed in the 100-mL vacuum chamber and the chamber was evacuated to approximately 90 kPa below atmospheric pressure for 1 hour. Shale synthetic porewater (S-SPW, Table 4) was introduced into the chamber under vacuum to reach approximately 1/4 of

the sample height. Partially immersed samples were allowed to sit in vacuum until samples were visibly wet – this commonly required 5-6 hours. Additional S-SPW was added under vacuum to submerge the samples completely. Submerged samples were allowed to sit in vacuum for 19 days, during which time the S-SPW solution was replaced 3-4 times with fresh solution to ensure constant concentration.

After brine saturation, the ϕ_w values were measured using the method outlined in Al et al. (2010, 2012); Xiang and Al (in prep.).

A.3 RESULTS

Measurements of ϕ_w , using this method are 9.0% for Queenston Formation shale, and 13.0% for Carbon Tan sandstone. Comparison of these values with those previously reported (Al et al. 2010, 2012; Loomer et al. 2013a; Xiang and Al, in prep.) indicates that the new porosity values are 2-4 % higher (Table A.1). The fact that the present results consistently display higher values suggests some improvement in the method of saturating samples.

Table A.1: Water-Loss Porosity Data

Sample ID	DGR3-472		Carbon Tan	
Description	Queenston shale		Sandstone	
Method	Ref ^a	This work	Ref ^b	This work
Porosity, ϕ_w (%)	8.6 ± 0.1	9.0 ± 0.03	12.8 ± 0.2	13.0 ± 0.1
ϕ_w (Ref)/ ϕ_w (This work)		0.96		0.98

^a Xiang and Al, in prep.; ^b Loomer et al. 2013a.

APPENDIX B: PH MEASUREMENT IN BRINE SOLUTIONS**CONTENTS**

	Page
B.1 MODIFIED PHREEQC-PITZER DATABASE.....	63
B.2 EXAMPLE PHREEQC INPUT FILE FOR pH BUFFER SOLUTIONS	79
B.3 EXAMPLE PHREEQC OUTPUT FILE FOR pH BUFFER SOLUTIONS	80
B.4 pH BUFFER SOLUTIONS.....	109
B.5 POTENTIOMETRIC pH MEASUREMENTS	118
B.6 PHENOL RED pK_a DETERMINATION RESULTS	129

B.1 MODIFIED PHREEQC-PITZER DATABASE

The PHREEQC-PITZER database as modified at UNB (pitzerUNB.dat). "#" marks in front of an entry indicate that the entry is inactive (ignored) in the file.

```
# PHREEQCI v.3.0.0-7430 PITZER database modified to include the Tris and Acetate buffer system and Cesium Pitzer parameters
# Date: 22 March 2013
# Personnel: Diana Loomer (DL), UNB Fredericton
# Parameter values listed after a "#" were considered and are included here for reference but the parameters (or combination of)
# that resulted in the best fit and/or could be verified best are set as active in the file.
# Data were verified with literature using "macinnes=false" which must be specified in input file.
# The Pitzer parameters for TRISHCl and TRIS are only known at 25 °C(Millero 2009).
# Millero et al. 1987 indicate reduced reliability in the Ca+2 and Mg+2 Pitzer parameters and/or that additional parameters
# are required to fully define a solution with 1(or greater) mol/kg Ca or Mg.
# For Millero's SO4 considerations, his calculations included using Harvie et al. 1984 values which are the same used in the
# PHREEQC-Pitzer database.
# Generally, Millero's data could be best reproduced for Tris and is considered the best for use.
# Tishchenko 2000 determined several temp dependant Tris Pitzer parameters (included here) based on the same eqn PHREEQC
# uses, but did not extend to the last 2 PHREEQC coefficients so PHREEQC would assume are zero.
# Generally, it was found Novak's acetate data could be reproduced best for acetate.
#
# Using "analytic" instead of delta h for Tris pK temperature dependence
#
# Pitzer.DAT for calculating pressure dependence of reactions, with
# molal volume of aqueous species and of minerals, and
# critical temperatures and pressures of gases used in Peng-Robinson's EOS.
# Details are given at the end of this file.

SOLUTION_MASTER_SPECIES
Tris          Tris      1.0      121.138  121.138#DL
Acetate       Acetate- 1.0      59.045  59.045      #DL - From minteq.v4
Cs   Cs+      0.0    132.91  132.91      #DL
H   H+        -1.     H       1.008
H(1)  H+        -1.     0.0
E   e-        0.0    0.0      0.0
O   H2O       0.0    O       16.00
O(-2) H2O      0.0    0.0
Ca  Ca+2      0.0    Ca      40.08
Mg  Mg+2      0.0    Mg      24.305
Na  Na+       0.0    Na      22.9898
K   K+        0.0    K       39.0983
Fe  Fe+2      0.0    Fe      55.847
Mn  Mn+2      0.0    Mn      54.938
Ba  Ba+2      0.0    Ba      137.33
Sr  Sr+2      0.0    Sr      87.62
Cl  Cl-       0.0    Cl      35.453
C   CO3-2      2.0    HCO3     12.0111
C(4) CO3-2      2.0    HCO3     12.0111
Alkalinity CO3-2  1.0    Ca0.5(CO3)0.5 50.05
S   SO4-2      0.0    SO4      32.064
S(6) SO4-2      0.0    SO4
B   B(OH)3     0.0    B       10.81
Li  Li+       0.0    Li      6.941
Br  Br-       0.0    Br      79.904
# redox-uncoupled gases
Hdg          Hdg      0      Hdg      2.016 # H2 gas
Oxg          Oxg      0      Oxg      32 # Oxygen gas
Mtg          Mtg      0.0    Mtg      16.032 # CH4 gas
Sg            H2Sg     1.0    H2Sg     34.08
Ntg          Ntg      0      Ntg      28.0134 # N2 gas

SOLUTION_SPECIES
Tris = Tris          #DL
      log_k      0.0      #DL
Tris + H+ = (Tris)H+ #DL
#      log_k      8.075    #DL - zero ionic strength pKa @ 25 deg C - Bates and Hetzer 1961: J. Phys. Chem.
65.667-67 1
      log_k      8.070    #DL - zero ionic stregh pKa @ 25 deg C - Foti et al. 1999: Ann. di Chim. 89, 87-98
(recommended value from compiled references)
```

```

#      delta_h  11.377 kcal      #DL - zero ionic strength delta h @ 25 deg C = 47,600 J/mol valid 0-50 deg C - Bates and
Hetzer 1961: J. Phys. Chem. 65,667-67 1
      delta_h  11.36      kcal      #DL - zero ionic strength pKa @ 25 deg C - Foti et al. 1999: Ann. di Chim. 89, 87-98
(recommended value from compiled references)
#      delta_h  11.395 kcal      #DL - Tishchenko 2000
#      -analytic 75.6853  0.0153422      -4884.31 -29.0765
Acetate- = Acetate-      #DL - From minteq.v4
      log_k      0.0      #DL - From minteq.v4
H+ + Acetate- = H(Acetate)      #DL - acetic acid
      log_k      4.757      #DL - From minteq.v4 (zero ionic strength pKa for acetate/acetic acid (0.001m))
#      log_k      4.756      #DL - From Handbook of Chemistry and Physics, 93rd Ed., 2012-2013
      delta_h  0.098 kcal      #DL - From minteq.v4
      -gamma  0.0      0.0      #DL - From minteq.v4 (Debye-Hückel a, Debye-Hückel b coefficients - not relevant here)
          #DL -      Id: 3309921
          #DL -      log K source: NIST46.4
          #DL -      Delta H source: NIST46.4
          #DL -      T and ionic strength: 0.00 25.0
#      log_k      4.757      #DL - From Mesmer et al.: J. Phys. Chem. 1989, 93, 7483-7490(ionic strength 0 m NaCl;
25 deg C)
#      delta_h  -0.12 kcal #DL - From Mesmer et al.: J. Phys. Chem. 1989, 93, 7483-7490(ionic strength 0 m NaCl; 25 deg C -
different at different temperatures)
Na+ + Acetate- = Na(Acetate) #DL - From minteq.v4
      log_k      -0.18      #DL - From minteq.v4 -0.18: corrected to zero ionic strength, if necessary. Original NIST
database now discontinued
      delta_h  2.87 kcal #DL - From minteq.v4
          #DL -      Id: 5009920
          #DL -      log K source: NIST46.4
          #DL -      Delta H source: NIST46.4
          #DL -      T and ionic strength: 0.00 25.0
K+ + Acetate- = K(Acetate) #DL - From minteq.v4
      log_k      -0.1955 #DL - From minteq.v4
      delta_h  1      kcal      #DL - From minteq.v4
      -gamma  0      0      #DL - From minteq.v4
          #DL -      Id: 4109921
          #DL -      log K source: NIST46.4
          #DL -      Delta H source: NIST46.2
          #DL -      T and ionic strength: 0.10 25.0
Ca+2 + Acetate- = Ca(Acetate)+      #DL - From minteq.v4
      log_k      1.18      #DL - From minteq.v4
      delta_h  0.96 kcal #DL - From minteq.v4
      -gamma  0      0      #DL - From minteq.v4
          #DL -      Id: 1509920
          #DL -      log K source: NIST46.4
          #DL -      Delta H source: NIST46.4
          #DL -      T and ionic strength: 0.00 25.0
Mg+2 + Acetate- = Mg(Acetate)+      #DL - From minteq.v4
      log_k      1.27      #DL - From minteq.v4
      delta_h  0      kcal      #DL - From minteq.v4
      -gamma  0      0      #DL - From minteq.v4
          #DL -      Id: 4609920
          #DL -      log K source: NIST46.4
          #DL -      Delta H source: NIST46.2
          #DL -      T and ionic strength: 0.00 25.0
Cs+ = Cs+      #DL
      log_k      0.000      #DL
      -gamma  1.81      0.01      #DL - a,b parameters from Parkhurst 1990 cited in Langmuir 1997 p 133
H+ = H+
      -dw      9.31e-9
e- = e-
H2O = H2O
Li+ = Li+
      -dw      1.03e-9
      -Vm      -.0237   -.0690   11.5800   -2.7761 .4862 6 # supcrt
Na+ = Na+
      -dw      1.33e-9
      -Vm      1.403   -2.285   4.419   -2.726   -5.125e-5  4.0  0.162  47.67   -3.09e-3  0.725 # supcrt modified
# for calculating densities (rho) when l > 3...
#      -Vm      1.403   -2.285   4.419   -2.726   -5.125e-5  2.0  0.162  47.67   -3.09e-3  0.4
K+ = K+
      -dw      1.96e-9

```

-Vm 3.322 -1.473 6.534 -2.712 9.06e-2 3.5 0 29.70 0 1 # supcrt modified
Mg+2 = Mg+2
 -dw 0.705e-9
 -Vm -1.410 -8.6 11.13 -2.39 1.332 5.5 1.29 -32.9 -5.86e-3 1 # supcrt modified
Ca+2 = Ca+2
 -dw 0.793e-9
 -Vm -0.3456 -7.252 6.149 -2.479 1.239 5 1.60 -57.1 -6.12e-3 1 # supcrt modified
Sr+2 = Sr+2
 -dw 0.794e-9
 -Vm -1.57e-2 -10.15 10.18 -2.36 0.860 5.26 0.859 -27.0 -4.1e-3 1.97 # supcrt modified
Ba+2 = Ba+2
 -dw 0.848e-9
 -Vm 2.063 -10.06 1.9534 -2.36 0.4218 5 1.58 -12.03 -8.35e-3 1 # supcrt modified
Mn+2 = Mn+2
 -dw 0.688e-9
 -Vm -.1016 -8.0295 8.9060 -2.4471 1.4006 6 # supcrt
Fe+2 = Fe+2
 -dw 0.719e-9
 -Vm -0.3255 -9.687 1.536 -2.379 0.3033 5.5 -4.21e-2 37.96 0 1 # supcrt modified
Cl- = Cl-
 -dw 2.03e-9
 -Vm 4.465 4.801 4.325 -2.847 1.748 0 -0.331 20.16 0 1 # supcrt modified
CO3-2 = CO3-2
 -dw 0.955e-9
 -Vm 5.052 0 0 -5.447 4.927 0 0.103 94.9 -1.30e-2 1 # supcrt modified
SO4-2 = SO4-2
 -dw 1.07e-9
 -Vm 5.0 9.06 -8.36 -3.14 3.773 0 6.61 -27.9 -6.32e-2 0.428 # supcrt modified
B(OH)3 = B(OH)3
 -dw 1.1e-9
 -Vm 7.0643 8.8547 3.5844 -3.1451 -.2000 # supcrt
Br- = Br-
 -dw 2.01e-9
 -Vm 5.2690 6.5940 4.7450 -3.1430 1.3858 # supcrt
redox-uncoupled gases
Hdg = Hdg # H2
 -dw 5.13e-9
 -Vm 6.52 0.78 0.12 # supcrt
Oxg = Oxg # O2
 -dw 2.35e-9
 -Vm 5.7889 6.3536 3.2528 -3.0417 -0.3943 # supcrt
Mtg = Mtg # CH4
 -dw 1.85e-9
 -Vm 7.7 # CH4 solubility, 25-100C, 1-700atm
Ntg = Ntg # N2
 -dw 1.96e-9
 -Vm 7 # Pray et al., 1952, IEC 44. 1146
H2Sg = H2Sg # H2S
 -dw 2.1e-9
 -Vm 7.81 2.96 -0.46 # supcrt
aqueous species
H2O = OH- + H+
 -analytic 68.547 0 -6199.8 -24.955
 -dw 5.27e-9
 -Vm 1.776 0.0738 1.417 -2.782 2.347 0 0.906 0 0 1 # supcrt modified
CO3-2 + H+ = HCO3-
 log_k 10.3393
 delta_h -3.561 kcal
 -analytic 107.8975 0.03252849 -5151.79 -38.92561 563713.9
 -dw 1.18e-9
 -Vm 8.625 0 -11.90 0 1.695 0 0 124 0 1 # supcrt modified
CO3-2 + 2 H+ = CO2 + H2O
 log_k 16.6767
 delta_h -5.738 kcal
 -analytic 464.1965 0.09344813 -26986.16 -165.75951 2248628.9
 -dw 1.92e-9
 -Vm 21.78 -49.4 -91.7 31.96 # supcrt modified
SO4-2 + H+ = HSO4-
 log_k 1.979
 delta_h 4.91 kcal

```

-analytic -5.3585 0.0183412 557.2461
-dw 1.33e-9
-Vm 8.2 9.2590 2.1108 -3.1618 1.1748 0 -0.3 15 0 1 # supcrt modified
H2Sg = HSg- + H+
    log_k -6.994
    delta_h 5.30 kcal
    -analytical 11.17 -0.02386 -3279.0
    -dw 2.1e-9
    -Vm 5.0119 4.9799 3.4765 -2.9849 1.4410 # supcrt
B(OH)3 + H2O = B(OH)4- + H+
    log_k -9.239
    delta_h 0 kcal
3B(OH)3 = B3O3(OH)4- + 2H2O + H+
    log_k -7.528
    delta_h 0 kcal
4B(OH)3 = B4O5(OH)4-2 + 3H2O + 2H+
    log_k -16.134
    delta_h 0 kcal
Ca+2 + B(OH)3 + H2O = CaB(OH)4+ + H+
    log_k -7.589
    delta_h 0 kcal
Mg+2 + B(OH)3 + H2O = MgB(OH)4+ + H+
    log_k -7.840
    delta_h 0 kcal
#Ca+2 + CO3-2 = CaCO3
#    log_k 3.151
#    delta_h 3.547 kcal
#    -analytic -1228.806 -0.299440 35512.75 485.818
#    -dw 4.46e-10 # complexes: calc'd with the Pikal formula
#    -Vm -.2430 -8.3748 9.0417 -2.4328 -.0300 # supcrt
Mg+2 + H2O = MgOH+ + H+
    log_k -11.809
    delta_h 15.419 kcal
Mg+2 + CO3-2 = MgCO3
    log_k 2.928
    delta_h 2.535 kcal
    -analytic -32.225 0.0 1093.486 12.72433
    -dw 4.21e-10
    -Vm -.5837 -9.2067 9.3687 -2.3984 -.0300 # supcrt

```

PHASES

```

CsCl #DL
    CsCl = Cs+ + Cl- #DL
    log_k 1.515 #DL - Hu et al 2007 CCPDTC 31:541-544 (note: they give solubility as ln Ksp, not log K - to
convert: log K = ln K/2.303 = 3.488/2.303 = 1.515)
CsBr #DL
    CsBr = Cs+ + Br- #DL
    log_k 0.817 #DL - Hu et al 2007 CCPDTC 31:541-544 (note: they give solubility as ln Ksp, not log K - to
convert: log K = ln K/2.303 = 1.881/2.303 = 0.817)

```

Anhydrite

```

CaSO4 = Ca+2 + SO4-2
log_k -4.362
-anal 87.836 0 -3136.79 -32.953 # 50 - 160oC, 1 - 1e3 atm, anhydrite dissolution, Blount and Dickson, 1973, Am.

```

Mineral. 58, 323.

```

-Vm 46.1 # 136.14 / 2.95

```

Aragonite

```

CaCO3 = CO3-2 + Ca+2
log_k -8.336
delta_h -2.589 kcal
-analytic -171.8607 -.077993 2903.293 71.595
-Vm 34.04

```

Arcanite

```

K2SO4 = + 1.0000 SO4-- + 2.0000 K+
log_k -1.776
-analytic 2.823 0.0 -1371.2
-Vm 65.5

```

Bischofite

```

MgCl2:6H2O = + 1.0000 Mg++ + 2.0000 Cl- + 6.0000 H2O
log_k 4.455
-analytic 3.524 0.0 277.6

```

Vm 127.1
 Bloedite
 $\text{Na}_2\text{Mg}(\text{SO}_4)_2 \cdot 4\text{H}_2\text{O} = + 1.0000 \text{Mg}^{++} + 2.0000 \text{Na}^+ + 2.0000 \text{SO}_4^{--} + 4.0000 \text{H}_2\text{O}$
 $\log_k -2.347$
 $-\delta_H 0$ # Not possible to calculate enthalpy of reaction Bloedite
 Vm 147

Brucite
 $\text{Mg}(\text{OH})_2 = + 1.0000 \text{Mg}^{++} + 2.0000 \text{OH}^-$
 $\log_k -10.88$
 $-\delta_H 4.85 \text{ kcal/mol}$
-analytic -1.0280e+002 -1.9759e-002 9.0180e+003 3.8282e+001 1.4075e+002
-Range: 0-300
 Vm 24.6

Burkeite
 $\text{Na}_6\text{CO}_3(\text{SO}_4)_2 = + 1.0000 \text{CO}_3^{--} + 2.0000 \text{SO}_4^{--} + 6.0000 \text{Na}^+$
 $\log_k -0.772$
 Vm 152

Calcite
 $\text{CaCO}_3 = \text{CO}_3^{--} + \text{Ca}^{++}$
 $\log_k -8.406$
 $\delta_H -2.297 \text{ kcal}$
-analytic -171.8329 -0.077993 2839.319 71.595
-Vm 36.9

Carnallite
 $\text{KMgCl}_3 \cdot 6\text{H}_2\text{O} = \text{K}^+ + \text{Mg}^{++} + 3\text{Cl}^- + 6\text{H}_2\text{O}$
 $\log_k 4.330$
 Vm 173.7

Celestite
 $\text{SrSO}_4 = \text{Sr}^{++} + \text{SO}_4^{--}$
 $\log_k -6.630$
-analytic -7.14 6.11E-03 75 0 0 -1.79E-05 # Howell et al., 1992, JCED 37, 464.
-Vm 46.4

Dolomite
 $\text{CaMg}(\text{CO}_3)_2 = \text{Ca}^{++} + \text{Mg}^{++} + 2\text{CO}_3^{--}$
 $\log_k -17.083$
 $\delta_H -9.436 \text{ kcal}$
-Vm 64.5

Epsomite
 $\text{MgSO}_4 \cdot 7\text{H}_2\text{O} = \text{Mg}^{++} + \text{SO}_4^{--} + 7\text{H}_2\text{O}$
 $\log_k -1.881$
-analytical 1.718 0.0 -1073.
 Vm 147

Gaylussite
 $\text{CaNa}_2(\text{CO}_3)_2 \cdot 5\text{H}_2\text{O} = \text{Ca}^{++} + 2\text{CO}_3^{--} + 2\text{Na}^+ + 5\text{H}_2\text{O}$
 $\log_k -9.421$

Glaserite
 $\text{NaK}_3(\text{SO}_4)_2 = \text{Na}^+ + 3\text{K}^+ + 2\text{SO}_4^{--}$
 $\log_k -3.803$

Glauberite
 $\text{Na}_2\text{Ca}(\text{SO}_4)_2 = \text{Ca}^{++} + 2\text{Na}^+ + 2\text{SO}_4^{--}$
 $\log_k -5.245$
 Vm 99

Gypsum
 $\text{CaSO}_4 \cdot 2\text{H}_2\text{O} = \text{Ca}^{++} + \text{SO}_4^{--} + 2\text{H}_2\text{O}$
 $\log_k -4.581$
 $\delta_H -0.109 \text{ kcal}$
-analytic 90.318 0.0 -4213. -32.641
-Vm 73.9

Barite
 $\text{BaSO}_4 = \text{Ba}^{++} + \text{SO}_4^{--}$
 $\log_k -9.97$
 $\delta_H 6.35 \text{ kcal}$
-analytic 136.035 0.0 -7680.41 -48.595
-Vm 51.9

Halite
 $\text{NaCl} = \text{Cl}^- + \text{Na}^+$
 $\log_k 1.570$
-analytic -713.4616 -1.201241 37302.21 262.4583 -2106915.
-Vm 27.1

Hexahydrite

	MgSO4:6H2O = Mg+2 + SO4-2 + 6 H2O
	log_k -1.635
	-analytic -62.666 0.0 1828. 22.187
	Vm 132
Kainite	KMgClSO4:3H2O = Cl- + K+ + Mg+2 + SO4-2 + 3 H2O
	log_k -0.193
Kalicinrite	KHCO3 = K+ + H+ + CO3-2
	log_k -10.058
Kieserite	MgSO4:H2O = Mg+2 + SO4-2 + H2O
	log_k -0.123
	Vm 53.8
Labile_S	Na4Ca(SO4)3:2H2O = 4Na+ + Ca+2 + 3SO4-2 + 2H2O
	log_k -5.672
Leonardite	MgSO4:4H2O = Mg+2 + SO4-2 + 4H2O
	log_k -0.887
Leonite	K2Mg(SO4)2:4H2O = Mg+2 + 2 K+ + 2 SO4-2 + 4 H2O
	log_k -3.979
Magnesite	MgCO3 = CO3-2 + Mg+2
	log_k -7.834
	delta_h -6.169
	Vm 28.3
Mirabilite	Na2SO4:10H2O = SO4-2 + 2 Na+ + 10 H2O
	log_k -1.214
	-analytic -3862.234 -1.19856 93713.54 1577.756 0.
	Vm 216
Misenite	K8H6(SO4)7 = 6 H+ + 7 SO4-2 + 8 K+
	log_k -10.806
Nahcolite	NaHCO3 = CO3-2 + H+ + Na+
	log_k -10.742
Natron	Na2CO3:10H2O = CO3-2 + 2 Na+ + 10.0000 H2O
	log_k -0.825
Nesquehonite	MgCO3:3H2O = CO3-2 + Mg+2 + 3 H2O
	log_k -5.167
Pentahydrite	MgSO4:5H2O = Mg+2 + SO4-2 + 5 H2O
	log_k -1.285
Pirssonite	Na2Ca(CO3)2:2H2O = 2Na+ + Ca+2 + 2CO3-2 + 2 H2O
	log_k -9.234
Polyhalite	K2MgCa2(SO4)4:2H2O = 2K+ + Mg+2 + 2 Ca+2 + 4SO4-2 + 2 H2O
	log_k -13.744
	Vm 218
Portlandite	Ca(OH)2 = Ca+2 + 2 OH-
	log_k -5.190
Schoenite	K2Mg(SO4)2:6H2O = 2K+ + Mg+2 + 2 SO4-2 + 6H2O
	log_k -4.328
Sylvite	KCl = K+ + Cl-
	log_k 0.900
	-analytic 3.984 0.0 -919.55
	Vm 37.5
Syngenite	K2Ca(SO4)2:H2O = 2K+ + Ca+2 + 2SO4-2 + H2O
	log_k -7.448
Trona	

$\text{Na3H}(\text{CO}_3)_2 \cdot 2\text{H}_2\text{O} = 3\text{Na}^+ + \text{H}^+ + 2\text{CO}_3^{2-} + 2\text{H}_2\text{O}$
 log_k -11.384
 Vm 106

Borax
 $\text{Na}_2(\text{B}_4\text{O}_5(\text{OH})_4) \cdot 8\text{H}_2\text{O} + 2\text{H}^+ = 4\text{B}(\text{OH})_3 + 2\text{Na}^+ + 5\text{H}_2\text{O}$
 log_k 12.464
 Vm 223

Boric_acid,s
 $\text{B}(\text{OH})_3 = \text{B}(\text{OH})_3$
 log_k -0.030

KB5O8:4H2O
 $\text{KB5O8:4H}_2\text{O} + 3\text{H}_2\text{O} + \text{H}^+ = 5\text{B}(\text{OH})_3 + \text{K}^+$
 log_k 4.671

K2B4O7:4H2O
 $\text{K}_2\text{B}_4\text{O}_7 \cdot 4\text{H}_2\text{O} + \text{H}_2\text{O} + 2\text{H}^+ = 4\text{B}(\text{OH})_3 + 2\text{K}^+$
 log_k 13.906

NaBO2:4H2O
 $\text{NaBO}_2 \cdot 4\text{H}_2\text{O} + \text{H}^+ = \text{B}(\text{OH})_3 + \text{Na}^+ + 3\text{H}_2\text{O}$
 log_k 9.568

NaB5O8:5H2O
 $\text{NaB}_5\text{O}_8 \cdot 5\text{H}_2\text{O} + 2\text{H}_2\text{O} + \text{H}^+ = 5\text{B}(\text{OH})_3 + \text{Na}^+$
 log_k 5.895

Teepleite
 $\text{Na}_2\text{B}(\text{OH})_4\text{Cl} + \text{H}^+ = \text{B}(\text{OH})_3 + 2\text{Na}^+ + \text{Cl}^- + \text{H}_2\text{O}$
 log_k 10.840

CO2(g)
 $\text{CO}_2 = \text{CO}_2$
 log_k -1.468
 delta_h -4.776 kcal
 -analytic 119.87356 2.185434e-2 -7337.8 -44.7652 669371
 -T_c 304.2 # critical T, K
 -P_c 72.80 # critical P, atm
 -Omega 0.225 # acentric factor

H2O(g)
 $\text{H}_2\text{O} = \text{H}_2\text{O}$
 log_k 1.506; delta_h -44.03 kJ
 -T_c 647.3 # critical T, K
 -P_c 217.60 # critical P, atm
 -Omega 0.344 # acentric factor
 -analytic -16.5066 -2.0013E-3 2710.7 3.7646 0 2.24E-6

redox-uncoupled gases

Oxg(g)
 $\text{Oxg} = \text{Oxg}$
 -analytic -7.5001 7.8981e-003 0.0 0.0 2.0027e+005
 T_c 154.6 ; -P_c 49.80 ; -Omega 0.021

Hdg(g)
 $\text{Hdg} = \text{Hdg}$
 -analytic -9.3114e+000 4.6473e-003 -4.9335e+001 1.4341e+000 1.2815e+005
 -T_c 33.2 ; -P_c 12.80 ; -Omega 0.225

Ntg(g)
 $\text{Ntg} = \text{Ntg}$
 -analytic -58.453 1.81800E-03 3199 17.909 -27460
 T_c 126.2 ; -P_c 33.50 ; -Omega 0.039

Mtg(g)
 $\text{Mtg} = \text{Mtg}$
 -analytic -2.4027e+001 4.7146e-003 3.7227e+002 6.4264e+000 2.3362e+005
 T_c 190.6 ; -P_c 45.40 ; -Omega 0.008

H2Sg(g)
 $\text{H}_2\text{Sg} = \text{H}^+ + \text{HSg}$
 -analytic -9.7354e+001 -3.1576e-002 1.8285e+003 3.7440e+001 2.8560e+001
 T_c 373.2 ; -P_c 88.20 ; -Omega 0.1

PITZER
-B0
(Tris)H+ Cl- 0.0395 #DL - Bates and Macaskill 1985: J. Solution Chem. 1985, 14, 723-734.
(Tris)H+ SO4-2 0.09393 #DL - Bates and Macaskill 1986: J. Chem. Eng. Data 31, 416-418.
(Tris)H+ Cl- 0.03574 0 0 0.00013 #DL - Tishchenko 2000: Russ. Chem. Bull. 49, No 4, April, 2000
H+ Cl- 0.17527 #DL - Bates and Macaskill 1985: J. Solution Chem. 14, 723-734 (Tris)
Na+ Cl- 0.075373 #DL - Manohar and Ananthaswamy 1991: CAN. J. CHEM. 69, 111-115 (acetate)

H+ OH- O #DL - not listed, so same in PHREEQC Pitzer database, Novak et al 1996:
 Radiochimica Acta 74, 111-116 (acetate)

H+	Acetate-	0	#DL - Novak et al 1996: Radiochimica Acta 74, 111-116		
Na+	Acetate-	0.1426	#DL - Novak et al 1996: Radiochimica Acta 74, 111-116/Pitzer and Mayorga 1973: J. Phys. Chem. 77, 2300-2307/Pitzer 1991: Activity Coefficients in Electrolyte Solutions		
# Na+	Acetate-	0.13723	#DL - Manohar and Ananthaswamy 1991: CAN. J. CHEM. 69, 111-115		
# K+	Acetate-	0.1587	#DL - Pitzer and Mayorga 1973: J. Phys. Chem. 77, 2300-2307/Pitzer 1991: Activity Coefficients in Electrolyte Solutions		
# K+	Acetate-	0.15343	#DL - (+/-0.00204)Marshall et al 1995: J. Chem. Eng. Data 40, 1041-1052		
# K+	Acetate-	0.15283	#DL - Kim and Frederick 1988: J. Chem. Eng. Data 33, 177-184		
# K+	Acetate-	0.161	#DL - Ferra et al 2011: J. Chem. Eng. Data 56, 3673-3678		
# K+	Acetate-	0.228	#DL - DeRobertis et al (1999) J. Chem. Eng. Data 1999, 44, 262-270		
K+	Acetate-	0.155	#DL - (+/-0.005)Spitzer et al 2011: Accred. Qual. Assur. 16, 191-198		
Ca+2	Acetate-	0.269	#DL - Loos et al. 2004: Fluid Phase Equilibria 219, 219-229		
# Ca+2	HCO3-	-0.104	#DL - different than PHREEQC Pitzer database: Loos et al 2004: Fluid Phase Equilibria 219, 219-229 (acetate)		
# Ca+2	SO4-2	0.128	#DL - different in PHREEQC Pitzer database: Loos et al 2004: Fluid Phase Equilibria 219, 219-229 (acetate)		
Cs+	Cl-	0.030	#DL - Pitzer and Mayorga 1973: J Phys Chem 77, 2300-2307		
Cs+	Br-	0.0279	#DL - Pitzer and Mayorga 1973: J Phys Chem 77, 2300-2307		
Cs+	SO4-2	0.0888	#DL - Pitzer and Mayorga 1973: J Phys Chem 77, 2300-2307		
Cs+	OH-	0.150	#DL - Pitzer and Mayorga 1973: J Phys Chem 77, 2300-2307		
Na+	Cl-	0.0765	-777.03	-4.4706	0.008946 -3.3158E-6
K+	Cl-	0.04835	0	0	5.794E-4
Mg+2	Cl-	0.35235	0	0	-1.943E-4
Ca+2	Cl-	0.3159	0	0	-1.725E-4
MgOH+	Cl-	-0.1			
H+	Cl-	0.1775	0	0	-3.081E-4
Li+	Cl-	0.1494	0	0	-1.685E-4
Sr+2	Cl-	0.2858	0	0	0.717E-3
Fe+2	Cl-	0.335925			
Mn+2	Cl-	0.327225			
Ba+2	Cl-	0.2628	0	0	0.6405E-3
CaB(OH)4+	Cl-	0.12			
MgB(OH)4+	Cl-	0.16			
Na+	Br-	0.0973	0	0	7.692E-4
K+	Br-	0.0569	0	0	7.39E-4
H+	Br-	0.1960	0	0	-2.049E-4
Mg+2	Br-	0.4327	0	0	-5.625E-5
Ca+2	Br-	0.3816	0	0	-5.2275E-4
Li+	Br-	0.1748	0	0	-1.819E-4
Sr+2	Br-	0.331125	0	0	-0.32775E-3
Ba+2	Br-	0.31455	0	0	-0.33825E-3
Na+	SO4-2	0.01958	0	0	2.367E-3
K+	SO4-2	0.04995	0	0	1.44E-3
Mg+2	SO4-2	0.221	0	0	-0.69E-3
Ca+2	SO4-2	0.2			
H+	SO4-2	0.0298			
Li+	SO4-2	0.136275	0	0	0.5055E-3
Sr+2	SO4-2	0.200	0	0	-2.9E-3
Fe+2	SO4-2	0.2568			
Mn+2	SO4-2	0.2065			
Na+	HSO4-	0.0454			
K+	HSO4-	-0.0003			
Mg+2	HSO4-	0.4746			
Ca+2	HSO4-	0.2145			
H+	HSO4-	0.2065			
Fe+2	HSO4-	0.4273			
Na+	OH-	0.0864	0	0	7.00E-4
K+	OH-	0.1298			
Ca+2	OH-	-0.1747			
Li+	OH-	0.015			
Ba+2	OH-	0.17175			
Na+	HCO3-	0.0277	0	0	1.00E-3
K+	HCO3-	0.0296	0	0	0.996E-3
Mg+2	HCO3-	0.329			
Ca+2	HCO3-	0.4			
Sr+2	HCO3-	0.12			
Na+	CO3-2	0.0399	0	0	1.79E-3
K+	CO3-2	0.1488	0	0	1.788E-3

Na+ B(OH)4- -0.0427
 Na+ B3O3(OH)4- -0.056
 Na+ B4O5(OH)4-2 -0.11
 K+ B(OH)4- 0.035
 K+ B3O3(OH)4- -0.13
 K+ B4O5(OH)4-2 -0.022
 -B1
 (Tris)H+ Cl- 0.20978 #DL - Bates and Macaskill 1985: J. Solution Chem. 1985 14, 723-734.
 (Tris)H+ SO4-2 0.59829 #DL - Bates and Macaskill 1986: J. Chem. Eng. Data 31, 416-418.
 # (Tris)H+ Cl- 0.21452 -5875.10 -36.291 0.05613 #DL - The A0 coeff
 is a different value in the temp dependance table than for the value listed at 25 deg C (0.21488), Tishchenko 2000 Russ.Chem.Bull. 49, No 4, April, 2000
 # H+ Cl- 0.30197 #DL - Bates and Macaskill 1985: J. Solution Chem. 1985 14, 723-734 (Tris)
 # Na+ Cl- 0.277031 #DL - Manohar and Ananthaswamy 1991: CAN. J. CHEM. 69, 111-115 (acetate)
 H+ OH- 0 #DL - not listed, so same in PHREEQC Pitzer database, Novak et al 1996:
 Radiochimica Acta 74, 111-116 (acetate)
 H+ Acetate- 0 #DL - Novak et al 1996: Radiochimica Acta 74, 111-116/Mesmer et al 1989: J. Phys. Chem. 93, 7483-7490
 # Na+ Acetate- 0.22 #DL - Novak et al 1996: Radiochimica Acta 74, 111-116/Mesmer et al 1989: J. Phys. Chem. 93, 7483-7490
 Na+ Acetate- 0.3237 #DL - Pitzer and Mayorga 1973: J. Phys. Chem. 77, 2300-2307/Pitzer 1991:
 Activity Coefficients in Electrolyte Solutions
 # Na+ Acetate- 0.34915 #DL - Manohar and Ananthaswamy 1991: CAN. J. CHEM. 69, 111-115
 # K+ Acetate- 0.3251 #DL - Pitzer and Mayorga 1973: J. Phys. Chem. 77, 2300-2307/Pitzer 1991:
 Activity Coefficients in Electrolyte Solutions
 # K+ Acetate- 0.34323 #DL - (+/-0.01102)Marshall et al 1995: J. Chem. Eng. Data 40, 1041-1052
 # K+ Acetate- 0.35513 #DL - Kim and Frederick 1988: J. Chem. Eng. Data 33, 177-184
 # K+ Acetate- 0.143 #DL - DeRobertis et al 1999: J. Chem. Eng. Data 44, 262-270
 # K+ Acetate- 0.342 #DL - Ferrá et al 2011: J. Chem. Eng. Data 56, 3673-3678
 K+ Acetate- 0.3 #DL - Spitzer et al 2011: Accred. Qual. Assur. 16, 191-198
 Ca+2 Acetate- 1.134 #DL - Loos et al 2004: Fluid Phase Equilibria 219, 219-229
 # Ca+2 HCO3- 1.68 #DL - different in PHREEQC Pitzer database: Loos et al 2004: Fluid Phase Equilibria 219, 219-229 (acetate)
 # Ca+2 SO4-2 2.76 #DL - different in PHREEQC Pitzer database: Loos et al 2004: Fluid Phase Equilibria 219, 219-229 (acetate)
 Cs+ Cl- 0.0558 #DL - Pitzer and Mayorga 1973: J. Phys. Chem. 77, 2300-2307
 Cs+ Br- 0.0139 #DL - Pitzer and Mayorga 1973: J. Phys. Chem. 77, 2300-2307
 Cs+ SO4-2 1.11075 #DL - Pitzer and Mayorga 1973: J. Phys. Chem. 77, 2300-2307
 Cs+ OH- 0.30 #DL - Pitzer and Mayorga 1973: J. Phys. Chem. 77, 2300-2307
 Na+ Cl- 0.2664 0 0 6.1608E-5 1.0715E-6
 K+ Cl- 0.2122 0 0 10.71E-4
 Mg+2 Cl- 1.6815 0 0 3.6525E-3
 Ca+2 Cl- 1.614 0 0 3.9E-3
 MgOH+ Cl- 1.658
 H+ Cl- 0.2945 0 0 1.419E-4
 Li+ Cl- 0.3074 0 0 5.366E-4
 Sr+2 Cl- 1.667 0 0 2.8425E-3
 Fe+2 Cl- 1.53225
 Mn+2 Cl- 1.55025
 Ba+2 Cl- 1.49625 0 0 3.2325E-3
 Na+ Br- 0.2791 0 0 10.79E-4
 K+ Br- 0.2212 0 0 17.40E-4
 H+ Br- 0.3564 0 0 4.467E-4
 Mg+2 Br- 1.753 0 0 3.8625E-3
 Ca+2 Br- 1.613 0 0 6.0375E-3
 Li+ Br- 0.2547 0 0 6.636E-4
 Sr+2 Br- 1.7115 0 0 6.5325E-3
 Ba+2 Br- 1.56975 0 0 6.78E-3
 Na+ SO4-2 1.113 0 0 5.6325E-3
 K+ SO4-2 0.7793 0 0 6.6975E-3
 Mg+2 SO4-2 3.343 0 0 1.53E-2
 Ca+2 SO4-2 3.1973 0 0 5.46E-2
 Li+ SO4-2 1.2705 0 0 1.41E-3
 Sr+2 SO4-2 3.1973 0 0 27.0E-3
 Fe+2 SO4-2 3.063
 Mn+2 SO4-2 2.9511
 Na+ HSO4- 0.398
 K+ HSO4- 0.1735
 Mg+2 HSO4- 1.729
 Ca+2 HSO4- 2.53

H+ HSO4- 0.5556
 Fe+2 HSO4- 3.48
 Na+ OH- 0.253 0 0 1.34E-4
 K+ OH- 0.32
 Ca+2 OH- -0.2303
 Li+ OH- 0.14
 Ba+2 OH- 1.2
 Na+ HCO3- 0.0411 0 0 1.10E-3
 K+ HCO3- -0.013 0 0 1.104E-3
 Mg+2 HCO3- 0.6072
 Ca+2 HCO3- 2.977
 Na+ CO3-2 1.389 0 0 2.05E-3
 K+ CO3-2 1.43 0 0 2.051E-3
 Na+ B(OH)4- 0.089
 Na+ B3O3(OH)4- -0.910
 Na+ B4O5(OH)4-2 -0.40
 K+ B(OH)4- 0.14
 -B2
 Mg+2 SO4-2 -37.23 0 0 -0.253
 Ca+2 SO4-2 -54.24 0 0 -0.516
 Sr+2 SO4-2 -54.24 0 0 -0.42
 Fe+2 SO4-2 -42.0
 Mn+2 SO4-2 -40.0
 Ca+2 OH- -5.72
 # (Tris)H+ Cl- -1.93 #DL - Tishchenko 2000: Russ. Chem. Bull. 49, No 4, April, 2000
 # Ca+2 SO4-2 -51.09 #DL - different than PHREEQC Pitzer database: Loos et al 2004: Fluid Phase Equilibria 219, 219–229 (acetate)
 -C0
 (Tris)H+ Cl- -0.00236 #DL - Bates and Macaskill 1985: J. Solution Chem. 14, 723–734
 (Tris)H+ SO4-2 -0.004316 #DL - Bates and Macaskill 1986: J. Chem. Eng. Data 31, 416-418
 # (Tris)H+ Cl- -0.000693 251.30 1.775 -0.00313 #DL - The A0 coeff is a different value in the temp dependance table than for the value listed at 25 deg C (0.000695), Tishchenko 2000 Russ. Chem. Bull. 49, No 4, April, 2000
 # H+ Cl- 0.001467 #DL - Bates and Macaskill 1985: J. Solution Chem. 1985, 14, 723–734 (Tris)
 # Na+ Cl- 0.001407 #DL - Manohar and Ananthaswamy 1991: CAN. J. CHEM. 69, 111-115 (acetate)
 H+ OH- 0 #DL - not listed so same in PHREEQC Pitzer database, Novak et al 1996: Radiochimica Acta 74, 111-116 (acetate)
 H+ Acetate- 0 #DL - Novak et al 1996: Radiochimica Acta 74, 111-116
 Na+ Acetate- -0.00629 #DL - Novak et al 1996: Radiochimica Acta 74, 111-116/Pitzer 1991: Activity Coefficients in Electrolyte Solutions
 # Na+ Acetate- -0.00523 #DL - Pitzer and Mayorga 1973: J. Phys. Chem. 77, 2300-2307
 # Na+ Acetate- -0.00474 #DL - Manohar and Ananthaswamy 1991: CAN. J. CHEM. 69, 111-115
 # K+ Acetate- -0.00660 #DL - Pitzer and Mayorga 1973: J. Phys. Chem. 77, 2300-2307/Pitzer 1991: Activity Coefficients in Electrolyte Solutions
 # K+ Acetate- -0.00452 #DL - (+/-0.00058)Marshall et al 1995: J. Chem. Eng. Data 40, 1041–1052
 # K+ Acetate- -0.00432 #DL - Kim and Frederick 1988: J. Chem. Eng. Data 33, 177–184
 # K+ Acetate- -0.0021 #DL - Ferra et al 2011: J. Chem. Eng. Data 56, 3673–3678
 # K+ Acetate- -0.0033 #DL - DeRobertis et al 1999: J. Chem. Eng. Data 44, 262–270 in Ferra et al 2011: J. Chem. Eng. Data 56, 3673–3678
 K+ Acetate- -0.005 #DL - (+/-0.002)Spitzer et al 2011: Accred. Qual. Assur. 2011 16, 191–198
 Ca+2 Acetate- -0.031 #DL - Loos et al 2004: Fluid Phase Equilibria 219, 219–229
 Cs+ Cl- 0.00038 #DL - Pitzer and Mayorga 1973: J. Phys. Chem. 77, 2300-2307
 Cs+ Br- 0.00004 #DL - Pitzer and Mayorga 1973: J. Phys. Chem. 77, 2300-2307
 Cs+ SO4-2 -0.00599803 #DL - Pitzer and Mayorga 1973: J. Phys. Chem. 77, 2300-2307
 Na+ Cl- 0.00127 33.317 0.09421 -4.655E-5
 K+ Cl- -0.00084 0 0 -5.095E-5
 Mg+2 Cl- 0.00519 0 0 -1.64933E-4
 Ca+2 Cl- -0.00034
 H+ Cl- 0.0008 0 0 6.213E-5
 Li+ Cl- 0.00359 0 0 -4.520E-5
 Sr+2 Cl- -0.00130
 Fe+2 Cl- -0.00860725
 Mn+2 Cl- -0.0204972
 Ba+2 Cl- -0.0193782 0 0 -1.53796E-4
 Na+ Br- 0.00116 0 0 -9.30E-5
 K+ Br- -0.00180 0 0 -7.004E-5
 H+ Br- 0.00827 0 0 -5.685E-5
 Mg+2 Br- 0.00312
 Ca+2 Br- -0.00257
 Li+ Br- 0.0053 0 0 -2.813E-5

Sr+2 Br- 0.00122506
 Ba+2 Br- -0.0159576
 Na+ SO4-2 0.00497 0 0 -4.87904E-4
 Mg+2 SO4-2 0.025 0 0 0.523E-3
 H+ SO4-2 0.0438
 Li+ SO4-2 -0.00399338 0 0 -2.33345E-4
 Fe+2 SO4-2 0.0209
 Mn+2 SO4-2 0.01636
 Na+ OH- 0.0044 0 0 -18.94E-5
 K+ OH- 0.0041
 K+ HCO3- -0.008
 Na+ CO3-2 0.0044
 K+ CO3-2 -0.0015
 Na+ B(OH)4- 0.0114
-THETA
 # H+ Na+ 0.0289 #DL - Different than PHREEQC Pitzer database: used in Millero 2009 - ref
 Campell et al 1993: Mar. Chem. 44, 221–234: (0.0342-0.000209*25degC =0.0290)(Tris)
 (Tris)H+ H+ 0.0027 #DL - Bates and Macaskill 1985: J. Solution Chem. 14, 723–734. Can't tell if
 higher-order electrostatic terms were considered, but is from same paper as B and C values
 # (Tris)H+ Na+ -0.00055 -17353.52 -118.9707 0.2031 #DL - The A0 coeff
 is a different value in the temp dependance table than for the value listed at 25 deg C (-0.00086), Tishchenko 2000 Russ. Chem.
 Bull. 49, No 4, April, 2000
 Acetate- Cl- -0.09 #DL - Novak et al 1996: Radiochimica Acta 74, 111-116
 # Acetate- Cl- -0.00545 #DL - Manohar and Ananthaswamy 1991: CAN. J. CHEM. 69, 111-115/Ferra et
 al 2011: J. Chem. Eng. Data 56, 3673–3678
 OH- Acetate- 0 #DL - Novak et al 1996: Radiochimica Acta 74, 111-116
 Na+ Cs+ -0.033 #DL - Pitzer and Kim 1974: J. Am. Chem. Soc. 96, 5701-5707
 K+ Cs+ 0.0 #DL - Pitzer and Kim 1974: J. Am. Chem. Soc. 96, 5701-5707
 H+ Cs+ -0.044 #DL - Pitzer and Kim 1974: J. Am. Chem. Soc. 96, 5701-5707
 K+ Na+ -0.012
 Mg+2 Na+ 0.07
 Ca+2 Na+ 0.07
 Sr+2 Na+ 0.051
 H+ Na+ 0.036
 Ca+2 K+ 0.032
 H+ K+ 0.005
 Ca+2 Mg+2 0.007
 H+ Mg+2 0.1
 H+ Ca+2 0.092
 SO4-2 Cl- 0.02
 HSO4- Cl- -0.006
 OH- Cl- -0.05
 HCO3- Cl- 0.03
 CO3-2 Cl- -0.02
 B(OH)4- Cl- -0.065
 B3O3(OH)4- Cl- 0.12
 B4O5(OH)4-2 Cl- 0.074
 OH- Br- -0.065
 OH- SO4-2 -0.013
 HCO3- SO4-2 0.01
 CO3-2 SO4-2 0.02
 B(OH)4- SO4-2 -0.012
 B3O3(OH)4- SO4-2 0.10
 B4O5(OH)4-2 SO4-2 0.12
 CO3-2 OH- 0.1
 CO3-2 HCO3- -0.04
 B3O3(OH)4- HCO3- -0.10
 B4O5(OH)4-2 HCO3- -0.087
-LAMDA
 Tris Na+ 0.0239 #DL - Millero et al 1987: Geochim. Cosmochim. Acta 51, 707–711
 Tris Cl- 0 #DL - Millero et al 1987: Geochim. Cosmochim. Acta 51, 707–711
 Tris K+ 0.0262 #DL - Millero et al 1987: Geochim. Cosmochim. Acta 51, 707–711
 Tris Mg+2 -0.0594 #DL - Lower reliability indicated, Millero et al 1987: Geochim. Cosmochim. Acta 51, 707–
 711
 Tris Ca+2 -0.2327 #DL - Lower reliability indicated, Millero et al 1987: Geochim. Cosmochim. Acta 51, 707–
 711
 # Tris Tris 0.02617 -1692.47 -10.151 0.01524 #DL - The A0 coeff
 is a different value in the temp dependance table than for the value listed at 25 deg C (0.02591), Tishchenko 2000: Russ. Chem.
 Bull. 49, No 4, April, 2000
 # H+ H(Acetate) 0.08 #DL - Partanen 1998: Acta Chem. Scand. 52, 985-994

Na+ H(Acetate) 0.087 #DL - Partanen 1998: Acta Chem. Scand. 52, 985-994
Cl- H(Acetate) 0 #DL - Partanen 1998: Acta Chem. Scand. 52, 985-994
Acetate- H(Acetate) -0.09 #DL - Partanen 1998: Acta Chem. Scand. 52, 985-994
H(Acetate) H(Acetate) -0.06 #DL - Partanen 1998: Acta Chem. Scand. 52, 985-994
K+ H(Acetate) 0.044 #DL - Partanen 1998: Acta Chem. Scand. 52, 985-994/Ferra et al
2011: J. Chem. Eng. Data 56, 3673-3678
K+ H(Acetate) 0.094 #DL - DeRobertis et al 1999: J. Chem. Eng. Data 44, 262-270 in Ferra et al
2011: J. Chem. Eng. Data 56, 3673-3678
Na+ CO2 0.085
K+ CO2 0.051
Mg+2 CO2 0.183
Ca+2 CO2 0.183
Cl- CO2 -0.005
SO4-2 CO2 0.097
HSO4- CO2 -0.003
Na+ B(OH)3 -0.097
K+ B(OH)3 -0.14
Cl- B(OH)3 0.091
SO4-2 B(OH)3 0.018
B3O3(OH)4- B(OH)3 -0.20
-ZETA
Tris Na+ Cl- 0 #DL - Millero et al 1987: Geochim. Cosmochim. Acta 51, 707-711
Tris (Tris)H+ Cl- -0.02747 2899.40 20.379 -0.03546 #DL - The A0 coeff
is a different value in the temp dependance table than for the value listed at 25 deg C (-0.02741), Tishchenko 2000: Russ. Chem. Bull. 49, No 4, April, 2000
Tris Na+ Cl- 0.02067 2475.34 17.384 -0.03045 #DL - The A0 coeff
is a different value in the temp dependance table than for the value listed at 25 deg C (0.02097), Tishchenko 2000: Russ. Chem. Bull. 49, No 4, April, 2000
H+ Cl- B(OH)3 -0.0102
Na+ SO4-2 B(OH)3 0.046
Na+ SO4-2 CO2 -0.015
-PSI
H+ Na+ Cl- 0.0002 #DL - Different than PHREEQC Pitzer database: used in Millero 2009 ref
Campbell et al. 1993: Mar. Chem. 44, 221-234: psi HNaCl = 0? (Tris)
H+ Na+ Cl- -0.004 #DL - as listed in PHREEQC Pitzer database: Millero 1983: Geochim. Cosmochim. Acta 41, 2121-2129 (Tris)
H+ (Tris)H+ Cl- -0.013 #DL - Bates and Macaskill 1985: J. Solution Chem. 14, 723-734. Can't tell if higher-order electrostatic terms were considered, but is from same paper as B and C values
Na+ (Tris)H+ Cl- -0.00095 3920.1 27.114 -0.04657 #DL - The A0 coeff is a different value in the temp dependance table than for the value listed at 25 deg C (-0.000405), Tishchenko 2000: Russ. Chem. Bull. 49, No 4, April, 2000
Na+ H+ OH- 0 #DL - not listed so same in PHREEQC Pitzer database, Novak et al 1996:
Radiochimica Acta 74, 111-116
Na+ H+ Acetate- 0 # DL - Novak et al 1996: Radiochimica Acta 74, 111-116
Na+ Acetate- Cl- 0.01029 #DL - Novak et al 1996: Radiochimica Acta 74, 111-116
Na+ Acetate- Cl- -0.00205 #DL - Manohar and Ananthaswamy 1991: CAN. J. CHEM. 69, 111-115
H+ Acetate- Cl- 0 #DL - Novak et al 1996: Radiochimica Acta 74, 111-116
H+ Cl- OH- 0 #DL - not listed so same in PHREEQC Pitzer database, Novak et al
1996: Radiochimica Acta 74, 111-116
Na+ Cs+ Cl- -0.003 #DL - Pitzer and Kim 1974: J. Am. Chem. Soc. 96, 5701-5707
K+ Cs+ Cl- -0.0013 #DL - Pitzer and Kim 1974: J. Am. Chem. Soc. 96, 5701-5707
H+ Cs+ Cl- -0.019 #DL - Pitzer and Kim 1974: J. Am. Chem. Soc. 96, 5701-5707
Na+ K+ Cl- -0.0018
Na+ K+ Br- -0.0022
Na+ K+ SO4-2 -0.010
Na+ K+ HCO3- -0.003
Na+ K+ CO3-2 0.003
Na+ Ca+2 Cl- -0.007
Na+ Sr+2 Cl- -0.0021
Na+ Ca+2 SO4-2 -0.055
Na+ Mg+2 Cl- -0.012
Na+ Mg+2 SO4-2 -0.015
Na+ H+ Cl- -0.004
Na+ H+ Br- -0.012
Na+ H+ HSO4- -0.0129
K+ Ca+2 Cl- -0.025
K+ Mg+2 Cl- -0.022
K+ Mg+2 SO4-2 -0.048
K+ H+ Cl- -0.011
K+ H+ Br- -0.021

K+ H+ SO4-2 0.197
 K+ H+ HSO4- -0.0265
 Ca+2 Mg+2 Cl- -0.012
 Ca+2 Mg+2 SO4-2 0.024
 Ca+2 H+ Cl- -0.015
 Mg+2 MgOH+ Cl- 0.028
 Mg+2 H+ Cl- -0.011
 Mg+2 H+ HSO4- -0.0178
 Cl- Br- K+ 0.0000
 Cl- SO4-2 Na+ 0.0014
 Cl- SO4-2 Ca+2 -0.018
 Cl- SO4-2 Mg+2 -0.004
 Cl- HSO4- Na+ -0.006
 Cl- HSO4- H+ 0.013
 Cl- OH- Na+ -0.006
 Cl- OH- K+-0.006
 Cl- OH- Ca+2 -0.025
 Cl- HCO3- Na+ -0.015
 Cl- HCO3- Mg+2 -0.096
 Cl- CO3-2 Na+ 0.0085
 Cl- CO3-2 K+ 0.004
 Cl- B(OH)4- Na+ -0.0073
 Cl- B3O3(OH)4- Na+ -0.024
 Cl- B4O5(OH)4-2 Na+ 0.026
 SO4-2 HSO4- Na+ -0.0094
 SO4-2 HSO4- K+ -0.0677
 SO4-2 HSO4- Mg+2 -0.0425
 SO4-2 OH- Na+ -0.009
 SO4-2 OH- K+ -0.050
 SO4-2 HCO3- Na+ -0.005
 SO4-2 HCO3- Mg+2 -0.161
 SO4-2 CO3-2 Na+ -0.005
 SO4-2 CO3-2 K+ -0.009
 OH- CO3-2 Na+ -0.017
 OH- CO3-2 K+ -0.01
 OH- Br- Na+ -0.018
 OH- Br- K+ -0.014
 HCO3- CO3-2 Na+ 0.002
 HCO3- CO3-2 K+ 0.012

#MU

Tris Tris Tris -0.003707 -95.29 -0.854 0.00175 #DL - The A0 coeff is a different value in the temp dependance table than for the value listed at 25 deg C (-0.003734), Tishchenko 2000: Russ. Chem. Bull. 49, No 4, April, 2000

EXCHANGE_MASTER_SPECIES
X X-

EXCHANGE_SPECIES
X- = X-
log_k 0.0

Cs+ + X- = CsX #DL
log_k 1.10 #DL - from Appelo and Postma p160, log K(Na/Cs)
log_k 7.239 #DL - K(Vaneslow) for Cs-Na exch on strong sites (illite) at 5M ionic strength from Liu et al 2004 JCH 68 217-238
log_k 2.302 #DL - K(Vaneslow) for Cs-Na exch on weak sites at 5M ionic strength from Liu et al 2004 JCH 68 217-238
log_k 4.64 #DL - average K(Gaines-Thomas?) for Cs-Na exch on weak sites in Bure mudrock Melkior et al 2005
log_k 1.5 #DL - determined at UNB using 1 mol/l Cs+ in Shale SPW through MIN3P-PEST fitting, Loomer et al 2013: Applied Geochemistry 39, 49-58

Na+ + X- = NaX
log_k 0.0

K+ + X- = KX
log_k 0.7
delta_h -4.3 # Jardine & Sparks, 1984

Li+ + X- = LiX

```

log_k -0.08
delta_h 1.4 # Merriam & Thomas, 1956

Ca+2 + 2X- = CaX2
log_k 0.8
delta_h 7.2 # Van Bladel & Gheyl, 1980

Mg+2 + 2X- = MgX2
log_k 0.6
delta_h 7.4 # Laudelout et al., 1968

Sr+2 + 2X- = SrX2
log_k 0.91
delta_h 5.5 # Laudelout et al., 1968

Ba+2 + 2X- = BaX2
log_k 0.91
delta_h 4.5 # Laudelout et al., 1968

Mn+2 + 2X- = MnX2
log_k 0.52

Fe+2 + 2X- = FeX2
log_k 0.44

SURFACE_MASTER_SPECIES
Hfo_s Hfo_sOH
Hfo_w Hfo_wOH
SURFACE_SPECIES
# All surface data from
# Dzombak and Morel, 1990
#
#
# Acid-base data from table 5.7
#
# strong binding site--Hfo_s,
Hfo_sOH = Hfo_sOH
log_k 0.0

Hfo_sOH + H+ = Hfo_sOH2+
log_k 7.29 # = pKa1,int

Hfo_sOH = Hfo_sO- + H+
log_k -8.93 # = -pKa2,int

# weak binding site--Hfo_w
Hfo_wOH = Hfo_wOH
log_k 0.0

Hfo_wOH + H+ = Hfo_wOH2+
log_k 7.29 # = pKa1,int

Hfo_wOH = Hfo_wO- + H+
log_k -8.93 # = -pKa2,int

#####
# CATIONS #
#####
#
# Cations from table 10.1 or 10.5
#
# Calcium
Hfo_sOH + Ca+2 = Hfo_sOHCa+2
log_k 4.97

Hfo_wOH + Ca+2 = Hfo_wOCa+ + H+
log_k -5.85
# Strontium

```

```

Hfo_sOH + Sr+2 = Hfo_sOHSr+2
log_k 5.01

Hfo_wOH + Sr+2 = Hfo_wOSr+ + H+
log_k -6.58

Hfo_wOH + Sr+2 + H2O = Hfo_wOSrOH + 2H+
log_k -17.60
# Barium
Hfo_sOH + Ba+2 = Hfo_sOHBa+2
log_k 5.46

Hfo_wOH + Ba+2 = Hfo_wOBa+ + H+
log_k -7.2          # table 10.5
#
# Derived constants table 10.5
#
# Magnesium
Hfo_wOH + Mg+2 = Hfo_wOMg+ + H+
log_k -4.6
# Manganese
Hfo_sOH + Mn+2 = Hfo_sOMn+ + H+
log_k -0.4          # table 10.5

Hfo_wOH + Mn+2 = Hfo_wOMn+ + H+
log_k -3.5          # table 10.5
# Iron
# Hfo_sOH + Fe+2 = Hfo_sOFe+ + H+
# log_k 0.7  # LFER using table 10.5

#      Hfo_wOH + Fe+2 = Hfo_wOFe+ + H+
# log_k -2.5  # LFER using table 10.5

# Iron, strong site: Appelo, Van der Weiden, Tournassat & Charlet, subm.
Hfo_sOH + Fe+2 = Hfo_sOFe+ + H+
log_k -0.95
# Iron, weak site: Liger et al., GCA 63, 2939, re-optimized for D&M
Hfo_wOH + Fe+2 = Hfo_wOFe+ + H+
log_k -2.98

Hfo_wOH + Fe+2 + H2O = Hfo_wOFeOH + 2H+
log_k -11.55

#####
#           ANIONS          #
#####

# Anions from table 10.6
#
#
# Anions from table 10.7
#
#
# Borate
Hfo_wOH + B(OH)3 = Hfo_wh2BO3 + H2O
log_k 0.62
#
# Anions from table 10.8
#
#
# Sulfate
Hfo_wOH + SO4-2 + H+ = Hfo_wSO4- + H2O
log_k 7.78

Hfo_wOH + SO4-2 = Hfo_wOHSO4-2
log_k 0.79

#
# Carbonate: Van Geen et al., 1994 reoptimized for HFO
# 0.15 g HFO/L has 0.344 mM sites == 2 g of Van Geen's Goethite/L
#
#
#      Hfo_wOH + CO3-2 + H+ = Hfo_wCO3- + H2O
# log_k 12.56

```

```

#
#      Hfo_wOH + CO3-2 + 2H+= Hfo_wHCO3 + H2O
#      log_k  20.62

END
MEAN GAM
CaCl2
CaSO4
CaCO3
Ca(OH)2
MgCl2
MgSO4
MgCO3
Mg(OH)2
NaCl
Na2SO4
NaHCO3
Na2CO3
NaOH
KCl
K2SO4
KHCO3
K2CO3
KOH
HCl
H2SO4
HBr

END

# For the reaction aA + bB = cC + dD,
# with delta_v = c*Vm(C) + d*Vm(D) - a*Vm(A) - b*Vm(B),
# PHREEQC adds the pressure term to log_k: -= delta_v * (P - 1) / (2.3RT).
# Vm(A) is volume of A, cm3/mol, P is pressure, atm, R is the gas constant, T is Kelvin.
# Gas-pressure and fugacity coefficients are calculated with Peng-Robinson's EOS.
# Binary interaction coefficients from Soreide and Whitson, 1992, FPE 77, 217 are
# hard-coded in calc_PR():
#   kij  CH4  CO2  H2S  N2
#   H2O  0.49  0.19  0.19  0.49
# =====
# The molar volumes of solids are entered with
#   -Vm vm cm3/mol
#   vm is the molar volume, cm3/mol (default), but dm3/mol and m3/mol are permitted.
# Data for minerals' vm (= MW (g/mol) / rho (g/cm3)) are defined using rho from
# Deer, Howie and Zussman, The rock-forming minerals, Longman.
#
# Temperature- and pressure-dependent volumina of aqueous species are calculated with a Redlich-
# type equation (cf. Redlich and Meyer, Chem. Rev. 64, 221), from parameters entered with
#   -Vm a1 a2 a3 a4 W a0 i1 i2 i3 i4
# The volume (cm3/mol) is
#   Vm(T, pb, I) = 41.84 * (a1 * 0.1 + a2 * 100 / (2600 + pb) + a3 / (T - 228) +
#                      a4 * 1e4 / (2600 + pb) / (T - 228) - W * QBrn)
#                      + z^2 / 2 * Av * f(I^0.5)
#                      + (i1 + i2 / (T - 228) + i3 * (T - 228)) * I^i4
# Volumina at I = 0 are obtained using supcrt92 formulas (Johnson et al., 1992, CG 18, 899).
# 41.84 transforms cal/bar/mol into cm3/mol.
# pb is pressure in bar.
# W * QBrn is the Born volume, calculated from Wref and the pressure dependence of the
# dielectric constant of water (f(P, T), see below).
# z is charge of the solute species.
# Av is the Debye-Hueckel limiting slope.
# a0 is the ion-size parameter in the extended Debye-Hueckel parameter:
#   f(I^0.5) = I^0.5 / (1 + a0 * DH_B * I^0.5),
#   a0 = -gamma x for cations, = 0 for anions.
# Av (P, T) is calculated using the dielectric constant of water from Bradley and Pitzer, 1979, JPC 83, 1599,
# and the compressibility of pure water.
# The density of pure water at water saturation pressure is calculated with eqn 2.6 from
# Wagner and Pruss, 2002, J. Phys. Chem. Ref. Data 31, 387. At higher P,T with polynomials
# interpolated from IAPWS table 3 (2007).

```

```

#
# Data for species' parameters, commented with '# supcrt modified', were fitted from data
# compiled by Laliberte, 2009, J. Chem. Eng. Data 54, 1725, + additions, see Appelo, Parkhurst and Post (in prep.)
# H+ has the reference volume of 0 at all P, T and I.
# For Cl-, parameters were obtained from densities of HCl solutions up to 176 oC, 1 - 280 atm.
# The numbers for cations were extracted from the densities of cation-Cl-solutions.
# Other anions and OH- then follow from the measured densities of cation-anion solutions.
# Water dissociation was fitted from Bandura and Lvov, 2006, J. Phys. Chem. Ref. Data, 35, 15, 0-200 oC, 1-2000 atm.
#
# -----
# If -Vm is not defined, the a-f values from -Millero a b c d e f (if available) will be used for calculating
# Vm(t, I) = a + b * t + c * t^2 + z^2 / 2 * Av * I^0.5 + (d + e * t + f * t^2) * I
# t is temperature in oC.
#
# redox-uncoupled gases have been added for H2 (Hdg), O2 (Oxg), CH4 (Mtg), N2 (Ntg),
# H2S (H2Sg, species HSg-, etc.).
#
# =====
# It remains the responsibility of the user to check the calculated results, for example with
# measured solubilities as a function of (P, T).

```

B.2 EXAMPLE PHREEQC INPUT FILE FOR pH BUFFER SOLUTIONS

```

TITLE Tris Buffer solutions (ionic strength 6 m)
#Part of a series of L-SPW based solutions to cover a large range of ionic strengths

```

```

SELECTED_OUTPUT
-file 12xLSPWBuffersAsMade20131203.csv
-reset false
-solution true
-ionic_strength true
-percent_error true
-pH true
-totals Na K Ca Mg Cl S(6) Tris
-saturation_indices halite gypsum

```

```
END
```

```
PITZER
-macinnies false
```

SOLUTION_SPREAD

Number	Na	K	Ca	Mg	Cl	S(6)	Tris	pH charge
1	2.64240	0.59453	0.62866	0.26424	5.0775349	0.00110	0.0600	7.00000
2	2.64240	0.59453	0.62866	0.26424	5.0755069	0.00110	0.0600	7.00000
3	2.64240	0.59453	0.62866	0.26424	5.0725195	0.00110	0.0600	7.00000
4	2.64240	0.59453	0.62866	0.26424	5.0695803	0.00110	0.0601	7.00000
5	2.64240	0.59453	0.62866	0.26424	5.0655326	0.00110	0.0600	7.00000
6	2.64240	0.59453	0.62866	0.26424	5.0585272	0.00110	0.0600	7.00000
7	2.64240	0.59453	0.62866	0.26424	5.0505570	0.00110	0.0600	7.00000

```
Save Solution 1-7
END
```

```
Solution 8 Just 1.2x's LSPW (no Tris)
```

```
-pe 11
-units mol/L
-pH 7 charge
-density 1.17505
Na 2.40000
K 0.54000
Ca 0.5710
Mg 0.24000
Cl 4.56000
```

```
S(6)      0.00100
Save Solution 8
END
```

```
USE solution 1
EQUILIBRIUM_PHASES 1
CO2(g) -3.4 10
END
```

```
USE solution 2
EQUILIBRIUM_PHASES 2
CO2(g) -3.4 10
END
```

```
USE solution 3
EQUILIBRIUM_PHASES 3
CO2(g) -3.4 10
END
```

```
USE solution 4
EQUILIBRIUM_PHASES 4
CO2(g) -3.4 10
END
```

```
USE solution 5
EQUILIBRIUM_PHASES 5
CO2(g) -3.4 10
END
```

```
USE solution 6
EQUILIBRIUM_PHASES 6
CO2(g) -3.4 10
END
```

```
USE solution 7
EQUILIBRIUM_PHASES 7
CO2(g) -3.4 10
END
```

```
USE solution 8
EQUILIBRIUM_PHASES 8
CO2(g) -3.4 10
```

B.3 EXAMPLE PHREEQC OUTPUT FILE FOR pH BUFFER SOLUTIONS

Input file: D:\NWMO\pH measurement\PRpKa\PHREEQC\12xLSPWBuffersAsMade20131203.pqi
 Output file: D:\NWMO\pH measurement\PRpKa\PHREEQC\12xLSPWBuffersAsMade20131203.pqo
 Database file: C:\Program Files\USGS\Phreeqc Interactive 3.0.0-7430\database\pitzerUNB.dat

 Reading data base.

```
SOLUTION_MASTER_SPECIES
SOLUTION_SPECIES
PHASES
PITZER
EXCHANGE_MASTER_SPECIES
EXCHANGE_SPECIES
SURFACE_MASTER_SPECIES
SURFACE_SPECIES
END
```

 Reading input data for simulation 1.

DATABASE C:\Program Files\USGS\Phreeqc Interactive 3.0.0-7430\database\pitzerUNB.dat
 TITLE Tris Buffer solutions (ionic strength 6 m)
 SELECTED_OUTPUT
 file 12xLSPWBuffersAsMade20131203.csv
 reset false
 solution true
 ionic_strength true
 percent_error true
 ph true
 totals Na K Ca Mg Cl S(6) Tris
 saturation_indices halite gypsum
 END

 TITLE

Tris Buffer solutions (ionic strength 6 m)

 End of simulation.

 Reading input data for simulation 2.

PITZER
 macinnes false
 SOLUTION_SPREAD
 pe 11
 units mol/kgw

Number	Na	K	Ca	Mg	Cl	S(6)	Tris	pH charge
1	2.64240	0.59453	0.62866	0.26424	5.0775349	0.00110	0.0600	7.00000
2	2.64240	0.59453	0.62866	0.26424	5.0755069	0.00110	0.0600	7.00000
3	2.64240	0.59453	0.62866	0.26424	5.0725195	0.00110	0.0600	7.00000
4	2.64240	0.59453	0.62866	0.26424	5.0695803	0.00110	0.0601	7.00000
5	2.64240	0.59453	0.62866	0.26424	5.0655326	0.00110	0.0600	7.00000
6	2.64240	0.59453	0.62866	0.26424	5.0585272	0.00110	0.0600	7.00000
7	2.64240	0.59453	0.62866	0.26424	5.0505570	0.00110	0.0600	7.00000

Save Solution 1-7
 END

 Beginning of initial solution calculations.

Initial solution 1.

 Solution composition-----

Elements	Molality	Moles
Ca	6.287e-001	6.287e-001
Cl	5.078e+000	5.078e+000
K	5.945e-001	5.945e-001
Mg	2.642e-001	2.642e-001
Na	2.642e+000	2.642e+000
S(6)	1.100e-003	1.100e-003
Tris	6.000e-002	6.000e-002

 Description of solution-----

pH = 7.087 Charge balance
 pe = 11.000

Specific Conductance (uS/cm, 25 oC) = 511867
 Density (g/cm3) = 1.18218
 Volume (L) = 1.10231
 Activity of water = 0.808
 Ionic strength = 5.974e+000
 Mass of water (kg) = 1.000e+000
 Total alkalinity (eq/kg) = 2.995e-003

Total carbon (mol/kg) = 0.000e+000
 Total CO₂ (mol/kg) = 0.000e+000
 Temperature (deg C) = 25.00
 Electrical balance (eq) = 7.034e-016
 Percent error, 100*(Cat-|An|)/(Cat+|An|) = 0.00
 Iterations = 12
 Gamma iterations = 5
 Osmotic coefficient = 1.27364
 Density of water = 0.99704
 Total H = 1.110695e+002
 Total O = 5.551063e+001

-----Distribution of species-----

Species	Molality	Unscaled			Gamma	cm ³ /mol
		Activity	Molality	Activity		
OH-	3.968e-007	9.957e-008	-6.401	-7.002	-0.600	3.81
H+	3.290e-008	8.180e-008	-7.483	-7.087	0.396	0.00
H ₂ O	5.551e+001	8.084e-001	1.744	-0.092	0.000	18.07
Ca	6.287e-001					
Ca+2	6.287e-001	3.118e-001	-0.202	-0.506	-0.305	-14.28
Cl	5.078e+000					
Cl-	5.078e+000	5.850e+000	0.706	0.767	0.062	20.09
K	5.945e-001					
K+	5.945e-001	2.470e-001	-0.226	-0.607	-0.381	12.11
Mg	2.642e-001					
Mg+2	2.642e-001	1.983e-001	-0.578	-0.703	-0.125	-17.78
MgOH+	8.228e-006	3.042e-006	-5.085	-5.517	-0.432	(0)
Na	2.642e+000					
Na+	2.642e+000	2.016e+000	0.422	0.304	-0.118	1.41
S(6)	1.100e-003					
SO ₄ -2	1.100e-003	2.412e-005	-2.959	-4.618	-1.659	26.83
HSO ₄ -	2.131e-010	1.880e-010	-9.671	-9.726	-0.055	42.04
Tris	6.000e-002					
(Tris)H+	5.701e-002	2.430e-002	-1.244	-1.614	-0.370	(0)
Tris	2.987e-003	2.528e-003	-2.525	-2.597	-0.072	(0)

-----Saturation indices-----

Phase	SI	log IAP	log K(298 K, 1 atm)	
Anhydrite	-0.90	-5.12	-4.22	CaSO ₄
Arcanite	-4.06	-5.83	-1.78	K ₂ SO ₄
Bischofite	-4.18	0.28	4.46	MgCl ₂ :6H ₂ O
Bloedite	-7.35	-9.70	-2.35	Na ₂ Mg(SO ₄) ₂ :4H ₂ O
Brucite	-3.83	-14.71	-10.88	Mg(OH) ₂
Carnallite	-3.89	0.44	4.33	KMgCl ₃ :6H ₂ O
Epsomite	-4.09	-5.97	-1.88	MgSO ₄ :7H ₂ O
Glaserite	-6.95	-10.75	-3.80	NaK ₃ (SO ₄) ₂
Glauberite	-3.89	-9.13	-5.25	Na ₂ Ca(SO ₄) ₂
Gypsum	-0.73	-5.31	-4.58	CaSO ₄ :2H ₂ O
H ₂ O(g)	-1.60	-0.09	1.50	H ₂ O
Halite	-0.50	1.07	1.57	NaCl
Hexahydrite	-4.24	-5.87	-1.63	MgSO ₄ :6H ₂ O
Kainite	-5.24	-5.44	-0.19	KMgCl ₃ O ₄ :3H ₂ O
Kieserite	-5.29	-5.41	-0.12	MgSO ₄ :H ₂ O
Labile_S	-7.65	-13.33	-5.67	Na ₄ Ca(SO ₄) ₃ :2H ₂ O
Leonardite	-4.80	-5.69	-0.89	MgSO ₄ :4H ₂ O
Leonite	-7.54	-11.52	-3.98	K ₂ Mg(SO ₄) ₂ :4H ₂ O
Mirabilite	-3.72	-4.93	-1.21	Na ₂ SO ₄ :10H ₂ O
Misenite	-68.90	-79.71	-10.81	K ₈ H ₆ (SO ₄) ₇
Pentahydrite	-4.50	-5.78	-1.28	MgSO ₄ :5H ₂ O
Polyhalite	-7.84	-21.58	-13.74	K ₂ MgCa ₂ (SO ₄) ₄ :2H ₂ O
Portlandite	-9.32	-14.51	-5.19	Ca(OH) ₂
Schoenite	-7.38	-11.71	-4.33	K ₂ Mg(SO ₄) ₂ :6H ₂ O
Sylvite	-0.74	0.16	0.90	KCl
Syngenite	-3.60	-11.05	-7.45	K ₂ Ca(SO ₄) ₂ :H ₂ O

Initial solution 2.

-----Solution composition-----

Elements	Molality	Moles
Ca	6.287e-001	6.287e-001
Cl	5.076e+000	5.076e+000
K	5.945e-001	5.945e-001
Mg	2.642e-001	2.642e-001
Na	2.642e+000	2.642e+000
S(6)	1.100e-003	1.100e-003
Tris	6.000e-002	6.000e-002

-----Description of solution-----

$$\text{pH} = 7.327 \quad \text{Charge balance}$$

$$\text{pe} = 11.000$$

Specific Conductance ($\mu\text{S}/\text{cm}$, 25 oC) = 511605
 Density (g/cm^3) = 1.18216
 Volume (L) = 1.10227
 Activity of water = 0.808
 Ionic strength = 5.972e+000
 Mass of water (kg) = 1.000e+000
 Total alkalinity (eq/kg) = 5.023e-003
 Total carbon (mol/kg) = 0.000e+000
 Total CO₂ (mol/kg) = 0.000e+000
 Temperature (deg C) = 25.00
 Electrical balance (eq) = -5.523e-014
 Percent error, $100 * (\text{Cat}-|\text{An}|)/(\text{Cat}+|\text{An}|)$ = -0.00
 Iterations = 11
 Gamma iterations = 5
 Osmotic coefficient = 1.27350
 Density of water = 0.99704
 Total H = 1.110674e+002
 Total O = 5.551063e+001

-----Distribution of species-----

Species	Molality	Unscaled			Gamma	cm^3/mol
		Activity	Unscaled log	log log		
OH-	6.897e-007	1.731e-007	-6.161	-6.762	-0.600	3.81
H+	1.893e-008	4.705e-008	-7.723	-7.327	0.395	0.00
H ₂ O	5.551e+001	8.085e-001	1.744	-0.092	0.000	18.07
Ca	6.287e-001					
Ca+2	6.287e-001	3.113e-001	-0.202	-0.507	-0.305	-14.29
Cl	5.076e+000					
Cl-	5.076e+000	5.848e+000	0.705	0.767	0.062	20.09
K	5.945e-001					
K+	5.945e-001	2.470e-001	-0.226	-0.607	-0.381	12.11
Mg	2.642e-001					
Mg+2	2.642e-001	1.980e-001	-0.578	-0.703	-0.125	-17.79
MgOH+	1.428e-005	5.283e-006	-4.845	-5.277	-0.432	(0)
Na	2.642e+000					
Na+	2.642e+000	2.016e+000	0.422	0.304	-0.118	1.41
S(6)	1.100e-003					
SO ₄ -2	1.100e-003	2.413e-005	-2.959	-4.618	-1.659	26.83
HSO ₄ -	1.226e-010	1.081e-010	-9.912	-9.966	-0.054	42.04
Tris	6.000e-002					
(Tris)H+	5.499e-002	2.344e-002	-1.260	-1.630	-0.370	(0)
Tris	5.008e-003	4.240e-003	-2.300	-2.373	-0.072	(0)

-----Saturation indices-----

Phase	SI	log IAP	log K(298 K, 1 atm)
-------	----	---------	---------------------

Anhydrite	-0.90	-5.12	-4.22	CaSO4
Arcanite	-4.06	-5.83	-1.78	K2SO4
Bischofite	-4.18	0.28	4.46	MgCl2:6H2O
Bloedite	-7.35	-9.70	-2.35	Na2Mg(SO4)2:4H2O
Brucite	-3.35	-14.23	-10.88	Mg(OH)2
Carnallite	-3.89	0.44	4.33	KMgCl3:6H2O
Epsomite	-4.09	-5.97	-1.88	MgSO4:7H2O
Glaserite	-6.95	-10.75	-3.80	NaK3(SO4)2
Glauberite	-3.89	-9.13	-5.25	Na2Ca(SO4)2
Gypsum	-0.73	-5.31	-4.58	CaSO4:2H2O
H2O(g)	-1.60	-0.09	1.50	H2O
Halite	-0.50	1.07	1.57	NaCl
Hexahydrite	-4.24	-5.87	-1.63	MgSO4:6H2O
Kainite	-5.25	-5.44	-0.19	KMgClSO4:3H2O
Kieserite	-5.29	-5.41	-0.12	MgSO4:H2O
Labile_S	-7.65	-13.33	-5.67	Na4Ca(SO4)3:2H2O
Leonhardite	-4.80	-5.69	-0.89	MgSO4:4H2O
Leonite	-7.54	-11.52	-3.98	K2Mg(SO4)2:4H2O
Mirabilite	-3.72	-4.93	-1.21	Na2SO4:10H2O
Misenite	-70.34	-81.15	-10.81	K8H6(SO4)7
Pentahydrite	-4.50	-5.78	-1.28	MgSO4:5H2O
Polyhalite	-7.84	-21.59	-13.74	K2MgCa2(SO4)4:2H2O
Portlandite	-8.84	-14.03	-5.19	Ca(OH)2
Schoenite	-7.38	-11.71	-4.33	K2Mg(SO4)2:6H2O
Sylvite	-0.74	0.16	0.90	KCl
Syngenite	-3.60	-11.05	-7.45	K2Ca(SO4)2:H2O

Initial solution 3.

-----Solution composition-----

Elements	Molality	Moles
Ca	6.287e-001	6.287e-001
Cl	5.073e+000	5.073e+000
K	5.945e-001	5.945e-001
Mg	2.642e-001	2.642e-001
Na	2.642e+000	2.642e+000
S(6)	1.100e-003	1.100e-003
Tris	6.000e-002	6.000e-002

-----Description of solution-----

$$\text{pH} = 7.554 \quad \text{Charge balance}$$

$$\text{pe} = 11.000$$

Specific Conductance (uS/cm, 25 oC) = 511221
 Density (g/cm3) = 1.18213
 Volume (L) = 1.10220
 Activity of water = 0.809
 Ionic strength = 5.969e+000
 Mass of water (kg) = 1.000e+000
 Total alkalinity (eq/kg) = 8.011e-003
 Total carbon (mol/kg) = 0.000e+000
 Total CO2 (mol/kg) = 0.000e+000
 Temperature (deg C) = 25.00
 Electrical balance (eq) = -1.444e-013
 Percent error, 100*(Cat-|An|)/(Cat+|An|) = -0.00
 Iterations = 12
 Gamma iterations = 5
 Osmotic coefficient = 1.27330
 Density of water = 0.99704
 Total H = 1.110645e+002
 Total O = 5.551064e+001

-----Distribution of species-----

Species	Molality	Unscaled			Gamma	cm3/mol
		Unscaled	log	log		

OH-	1.162e-006	2.919e-007	-5.935	-6.535	-0.600	3.81
H+	1.124e-008	2.791e-008	-7.949	-7.554	0.395	0.00
H2O	5.551e+001	8.086e-001	1.744	-0.092	0.000	18.07
Ca	6.287e-001					
Ca+2	6.287e-001	3.105e-001	-0.202	-0.508	-0.306	-14.29
Cl	5.073e+000					
Cl-	5.073e+000	5.844e+000	0.705	0.767	0.062	20.09
K	5.945e-001					
K+	5.945e-001	2.470e-001	-0.226	-0.607	-0.381	12.11
Mg	2.642e-001					
Mg+2	2.642e-001	1.977e-001	-0.578	-0.704	-0.126	-17.79
MgOH+	2.403e-005	8.892e-006	-4.619	-5.051	-0.432	(0)
Na	2.642e+000					
Na+	2.642e+000	2.015e+000	0.422	0.304	-0.118	1.41
S(6)	1.100e-003					
SO4-2	1.100e-003	2.413e-005	-2.959	-4.617	-1.659	26.83
HSO4-	7.270e-011	6.416e-011	-10.138	-10.193	-0.054	42.04
Tris	6.000e-002					
(Tris)H+	5.201e-002	2.217e-002	-1.284	-1.654	-0.370	(0)
Tris	7.985e-003	6.761e-003	-2.098	-2.170	-0.072	(0)

-----Saturation indices-----

Phase	SI	log IAP	log K(298 K, 1 atm)	
Anhydrite	-0.90	-5.13	-4.22	CaSO4
Arcanite	-4.06	-5.83	-1.78	K2SO4
Bischofite	-4.18	0.28	4.46	MgCl2:6H2O
Bloedite	-7.35	-9.70	-2.35	Na2Mg(SO4)2:4H2O
Brucite	-2.89	-13.77	-10.88	Mg(OH)2
Carnallite	-3.89	0.44	4.33	KMgCl3:6H2O
Epsomite	-4.09	-5.97	-1.88	MgSO4:7H2O
Glaserite	-6.95	-10.75	-3.80	NaK3(SO4)2
Glauberite	-3.89	-9.13	-5.25	Na2Ca(SO4)2
Gypsum	-0.73	-5.31	-4.58	CaSO4:2H2O
H2O(g)	-1.60	-0.09	1.50	H2O
Halite	-0.50	1.07	1.57	NaCl
Hexahydrite	-4.24	-5.88	-1.63	MgSO4:6H2O
Kainite	-5.25	-5.44	-0.19	KMgClSO4:3H2O
Kieserite	-5.29	-5.41	-0.12	MgSO4:H2O
Labile_S	-7.66	-13.33	-5.67	Na4Ca(SO4)3:2H2O
Leonardite	-4.80	-5.69	-0.89	MgSO4:4H2O
Leonite	-7.54	-11.52	-3.98	K2Mg(SO4)2:4H2O
Mirabilite	-3.72	-4.93	-1.21	Na2SO4:10H2O
Misenite	-71.70	-82.51	-10.81	K8H6(SO4)7
Pentahydrite	-4.50	-5.78	-1.28	MgSO4:5H2O
Polyhalite	-7.84	-21.59	-13.74	K2MgCa2(SO4)4:2H2O
Portlandite	-8.39	-13.58	-5.19	Ca(OH)2
Schoenite	-7.38	-11.71	-4.33	K2Mg(SO4)2:6H2O
Sylvite	-0.74	0.16	0.90	KCl
Syngenite	-3.60	-11.05	-7.45	K2Ca(SO4)2:H2O

Initial solution 4.

-----Solution composition-----

Elements	Molality	Moles
Ca	6.287e-001	6.287e-001
Cl	5.070e+000	5.070e+000
K	5.945e-001	5.945e-001
Mg	2.642e-001	2.642e-001
Na	2.642e+000	2.642e+000
S(6)	1.100e-003	1.100e-003
Tris	6.010e-002	6.010e-002

-----Description of solution-----

pH = 7.719 Charge balance
 pe = 11.000
 Specific Conductance (uS/cm, 25 oC) = 510842
 Density (g/cm3) = 1.18211
 Volume (L) = 1.10214
 Activity of water = 0.809
 Ionic strength = 5.966e+000
 Mass of water (kg) = 1.000e+000
 Total alkalinity (eq/kg) = 1.105e-002
 Total carbon (mol/kg) = 0.000e+000
 Total CO2 (mol/kg) = 0.000e+000
 Temperature (deg C) = 25.00
 Electrical balance (eq) = -2.426e-013
 Percent error, 100*(Cat-|An|)/(Cat+|An|) = -0.00
 Iterations = 13
 Gamma iterations = 5
 Osmotic coefficient = 1.27310
 Density of water = 0.99704
 Total H = 1.110616e+002
 Total O = 5.551065e+001

-----Distribution of species-----

Species	Molality	Unscaled		Unscaled		cm3/mol
		Activity	Molality	Activity	Gamma	
OH-	1.698e-006	4.267e-007	-5.770	-6.370	-0.600	3.80
H+	7.696e-009	1.909e-008	-8.114	-7.719	0.395	0.00
H2O	5.551e+001	8.086e-001	1.744	-0.092	0.000	18.07
Ca	6.287e-001					
Ca+2	6.287e-001	3.097e-001	-0.202	-0.509	-0.307	-14.29
Cl	5.070e+000					
Cl-	5.070e+000	5.841e+000	0.705	0.766	0.062	20.09
K	5.945e-001					
K+	5.945e-001	2.470e-001	-0.226	-0.607	-0.381	12.11
Mg	2.642e-001					
Mg+2	2.642e-001	1.973e-001	-0.578	-0.705	-0.127	-17.79
MgOH+	3.504e-005	1.297e-005	-4.455	-4.887	-0.432	(0)
Na	2.642e+000					
Na+	2.642e+000	2.015e+000	0.422	0.304	-0.118	1.41
S(6)	1.100e-003					
SO4-2	1.100e-003	2.414e-005	-2.959	-4.617	-1.659	26.83
HSO4-	4.974e-011	4.391e-011	-10.303	-10.357	-0.054	42.04
Tris	6.010e-002					
(Tris)H+	4.909e-002	2.092e-002	-1.309	-1.679	-0.370	(0)
Tris	1.101e-002	9.324e-003	-1.958	-2.030	-0.072	(0)

-----Saturation indices-----

Phase	SI	log IAP	log K(298 K, 1 atm)
Anhydrite	-0.90	-5.13	-4.22 CaSO4
Arcanite	-4.06	-5.83	-1.78 K2SO4
Bischofite	-4.18	0.27	4.46 MgCl2:6H2O
Bloedite	-7.35	-9.70	-2.35 Na2Mg(SO4)2:4H2O
Brucite	-2.56	-13.44	-10.88 Mg(OH)2
Carnallite	-3.90	0.43	4.33 KMgCl3:6H2O
Epsomite	-4.09	-5.97	-1.88 MgSO4:7H2O
Glaserite	-6.95	-10.75	-3.80 NaK3(SO4)2
Glauberite	-3.89	-9.14	-5.25 Na2Ca(SO4)2
Gypsum	-0.73	-5.31	-4.58 CaSO4:2H2O
H2O(g)	-1.60	-0.09	1.50 H2O
Halite	-0.50	1.07	1.57 NaCl
Hexahydrite	-4.24	-5.88	-1.63 MgSO4:6H2O
Kainite	-5.25	-5.44	-0.19 KMgClSO4:3H2O
Kieserite	-5.29	-5.41	-0.12 MgSO4:H2O
Labile_S	-7.66	-13.33	-5.67 Na4Ca(SO4)3:2H2O
Leonardite	-4.80	-5.69	-0.89 MgSO4:4H2O
Leonite	-7.54	-11.52	-3.98 K2Mg(SO4)2:4H2O

Mirabilite	-3.72	-4.93	-1.21	Na ₂ SO ₄ :10H ₂ O
Misenite	-72.69	-83.49	-10.81	K ₈ H ₆ (SO ₄) ₇
Pentahydrite	-4.50	-5.78	-1.28	MgSO ₄ :5H ₂ O
Polyhalite	-7.85	-21.59	-13.74	K ₂ MgCa ₂ (SO ₄) ₄ :2H ₂ O
Portlandite	-8.06	-13.25	-5.19	Ca(OH) ₂
Schoenite	-7.38	-11.71	-4.33	K ₂ Mg(SO ₄) ₂ :6H ₂ O
Sylvite	-0.74	0.16	0.90	KCl
Syngenite	-3.60	-11.05	-7.45	K ₂ Ca(SO ₄) ₂ :H ₂ O

Initial solution 5.

-----Solution composition-----

Elements	Molality	Moles
Ca	6.287e-001	6.287e-001
Cl	5.066e+000	5.066e+000
K	5.945e-001	5.945e-001
Mg	2.642e-001	2.642e-001
Na	2.642e+000	2.642e+000
S(6)	1.100e-003	1.100e-003
Tris	6.000e-002	6.000e-002

-----Description of solution-----

pH = 7.889 Charge balance
pe = 11.000
Specific Conductance (uS/cm, 25 oC) = 510323
Density (g/cm³) = 1.18206
Volume (L) = 1.10205
Activity of water = 0.809
Ionic strength = 5.962e+000
Mass of water (kg) = 1.000e+000
Total alkalinity (eq/kg) = 1.500e-002
Total carbon (mol/kg) = 0.000e+000
Total CO₂ (mol/kg) = 0.000e+000
Temperature (deg C) = 25.00
Electrical balance (eq) = -3.915e-013
Percent error, 100*(Cat-|An|)/(Cat+|An|) = -0.00
Iterations = 14
Gamma iterations = 5
Osmotic coefficient = 1.27283
Density of water = 0.99704
Total H = 1.110575e+002
Total O = 5.551067e+001

-----Distribution of species-----

Species	Molality	Unscaled			Gamma	cm ³ /mol
		Unscaled	log	log		
OH-	2.508e-006	6.309e-007	-5.601	-6.200	-0.599	3.80
H+	5.211e-009	1.292e-008	-8.283	-7.889	0.394	0.00
H ₂ O	5.551e+001	8.088e-001	1.744	-0.092	0.000	18.07
Ca	6.287e-001					
Ca+2	6.287e-001	3.087e-001	-0.202	-0.511	-0.309	-14.29
Cl	5.066e+000					
Cl-	5.066e+000	5.836e+000	0.705	0.766	0.062	20.09
K	5.945e-001					
K+	5.945e-001	2.471e-001	-0.226	-0.607	-0.381	12.11
Mg	2.642e-001					
Mg+2	2.642e-001	1.968e-001	-0.578	-0.706	-0.128	-17.79
MgOH+	5.165e-005	1.913e-005	-4.287	-4.718	-0.431	(0)
Na	2.642e+000					
Na+	2.642e+000	2.014e+000	0.422	0.304	-0.118	1.41
S(6)	1.100e-003					
SO ₄ -2	1.100e-003	2.415e-005	-2.959	-4.617	-1.658	26.82
HSO ₄ -	3.364e-011	2.972e-011	-10.473	-10.527	-0.054	42.04

Tris	6.000e-002
(Tris)H+	4.506e-002
Tris	1.494e-002

1.920e-002 -1.346 -1.717 -0.371 (0)
 1.265e-002 -1.826 -1.898 -0.072 (0)

-----Saturation indices-----

Phase	SI	log IAP	log K(298 K, 1 atm)
Anhydrite	-0.90	-5.13	-4.22 CaSO4
Arcanite	-4.06	-5.83	-1.78 K2SO4
Bischofite	-4.18	0.27	4.46 MgCl2:6H2O
Bloedite	-7.35	-9.70	-2.35 Na2Mg(SO4)2:4H2O
Brucite	-2.23	-13.11	-10.88 Mg(OH)2
Carnallite	-3.90	0.43	4.33 KMgCl3:6H2O
Epsomite	-4.09	-5.97	-1.88 MgSO4:7H2O
Glaserite	-6.95	-10.75	-3.80 NaK3(SO4)2
Glauberite	-3.89	-9.14	-5.25 Na2Ca(SO4)2
Gypsum	-0.73	-5.31	-4.58 CaSO4:2H2O
H2O(g)	-1.60	-0.09	1.50 H2O
Halite	-0.50	1.07	1.57 NaCl
Hexahydrite	-4.24	-5.88	-1.63 MgSO4:6H2O
Kainite	-5.25	-5.44	-0.19 KMgClSO4:3H2O
Kieserite	-5.29	-5.42	-0.12 MgSO4:H2O
Labile_S	-7.66	-13.33	-5.67 Na4Ca(SO4)3:2H2O
Leonhardite	-4.80	-5.69	-0.89 MgSO4:4H2O
Leonite	-7.54	-11.52	-3.98 K2Mg(SO4)2:4H2O
Mirabilite	-3.72	-4.93	-1.21 Na2SO4:10H2O
Misenite	-73.70	-84.51	-10.81 K8H6(SO4)7
Pentahydrite	-4.50	-5.78	-1.28 MgSO4:5H2O
Polyhalite	-7.85	-21.59	-13.74 K2MgCa2(SO4)4:2H2O
Portlandite	-7.72	-12.91	-5.19 Ca(OH)2
Schoenite	-7.38	-11.71	-4.33 K2Mg(SO4)2:6H2O
Sylvite	-0.74	0.16	0.90 KCl
Syngenite	-3.60	-11.05	-7.45 K2Ca(SO4)2:H2O

Initial solution 6.

-----Solution composition-----

Elements	Molality	Moles
Ca	6.287e-001	6.287e-001
Cl	5.059e+000	5.059e+000
K	5.945e-001	5.945e-001
Mg	2.642e-001	2.642e-001
Na	2.642e+000	2.642e+000
S(6)	1.100e-003	1.100e-003
Tris	6.000e-002	6.000e-002

-----Description of solution-----

pH = 8.128 Charge balance
 pe = 11.000
 Specific Conductance (uS/cm, 25 oC) = 509425
 Density (g/cm3) = 1.18200
 Volume (L) = 1.10189
 Activity of water = 0.809
 Ionic strength = 5.955e+000
 Mass of water (kg) = 1.000e+000
 Total alkalinity (eq/kg) = 2.200e-002
 Total carbon (mol/kg) = 0.000e+000
 Total CO2 (mol/kg) = 0.000e+000
 Temperature (deg C) = 25.00
 Electrical balance (eq) = -7.137e-013
 Percent error, 100*(Cat-|An|)/(Cat+|An|) = -0.00
 Iterations = 15
 Gamma iterations = 5
 Osmotic coefficient = 1.27236
 Density of water = 0.99704

Total H = 1.110506e+002
 Total O = 5.551071e+001

-----Distribution of species-----

Species	Molality	Unscaled		Unscaled		Gamma	cm3/mol
		Activity	Molality	log	log		
		Activity	Molality	log	log		
OH-	4.347e-006	1.095e-006	-5.362	-5.961	-0.599	3.79	
H+	3.009e-009	7.446e-009	-8.522	-8.128	0.393	0.00	
H2O	5.551e+001	8.090e-001	1.744	-0.092	0.000	18.07	
Ca	6.287e-001						
Ca+2	6.287e-001	3.069e-001	-0.202	-0.513	-0.311	-14.29	
Cl	5.059e+000						
Cl-	5.059e+000	5.828e+000	0.704	0.766	0.062	20.09	
K	5.945e-001						
K+	5.945e-001	2.471e-001	-0.226	-0.607	-0.381	12.11	
Mg	2.642e-001						
Mg+2	2.642e-001	1.960e-001	-0.578	-0.708	-0.130	-17.79	
MgOH+	8.911e-005	3.306e-005	-4.050	-4.481	-0.431	(0)	
Na	2.642e+000						
Na+	2.642e+000	2.013e+000	0.422	0.304	-0.118	1.40	
S(6)	1.100e-003						
SO4-2	1.100e-003	2.417e-005	-2.959	-4.617	-1.658	26.81	
HSO4-	1.938e-011	1.714e-011	-10.713	-10.766	-0.053	42.04	
Tris	6.000e-002						
(Tris)H+	3.809e-002	1.623e-002	-1.419	-1.790	-0.371	(0)	
Tris	2.191e-002	1.855e-002	-1.659	-1.732	-0.072	(0)	

-----Saturation indices-----

Phase	SI	log IAP	log K(298 K, 1 atm)
Anhydrite	-0.90	-5.13	-4.22 CaSO4
Arcanite	-4.05	-5.83	-1.78 K2SO4
Bischofite	-4.18	0.27	4.46 MgCl2:6H2O
Bloedite	-7.35	-9.70	-2.35 Na2Mg(SO4)2:4H2O
Brucite	-1.75	-12.63	-10.88 Mg(OH)2
Carnallite	-3.90	0.43	4.33 KMgCl3:6H2O
Epsomite	-4.09	-5.97	-1.88 MgSO4:7H2O
Glaserite	-6.95	-10.75	-3.80 NaK3(SO4)2
Glauberite	-3.89	-9.14	-5.25 Na2Ca(SO4)2
Gypsum	-0.73	-5.31	-4.58 CaSO4:2H2O
H2O(g)	-1.59	-0.09	1.50 H2O
Halite	-0.50	1.07	1.57 NaCl
Hexahydrite	-4.24	-5.88	-1.63 MgSO4:6H2O
Kainite	-5.25	-5.44	-0.19 KMgCISO4:3H2O
Kieserite	-5.29	-5.42	-0.12 MgSO4:H2O
Labile_S	-7.66	-13.33	-5.67 Na4Ca(SO4)3:2H2O
Leonardite	-4.81	-5.69	-0.89 MgSO4:4H2O
Leonite	-7.54	-11.52	-3.98 K2Mg(SO4)2:4H2O
Mirabilite	-3.72	-4.93	-1.21 Na2SO4:10H2O
Misenite	-75.14	-85.94	-10.81 K8H6(SO4)7
Pentahydrite	-4.50	-5.78	-1.28 MgSO4:5H2O
Polyhalite	-7.86	-21.60	-13.74 K2MgCa2(SO4)4:2H2O
Portlandite	-7.24	-12.43	-5.19 Ca(OH)2
Schoenite	-7.38	-11.71	-4.33 K2Mg(SO4)2:6H2O
Sylvite	-0.74	0.16	0.90 KCl
Syngenite	-3.60	-11.05	-7.45 K2Ca(SO4)2:H2O

Initial solution 7.

-----Solution composition-----

Elements	Molality	Moles
Ca	6.287e-001	6.287e-001
Cl	5.051e+000	5.051e+000

K	5.945e-001	5.945e-001
Mg	2.642e-001	2.642e-001
Na	2.642e+000	2.642e+000
S(6)	1.100e-003	1.100e-003
Tris	6.000e-002	6.000e-002

-----Description of solution-----

pH = 8.363 Charge balance
pe = 11.000
Specific Conductance (uS/cm, 25 oC) = 508405
Density (g/cm3) = 1.18193
Volume (L) = 1.10171
Activity of water = 0.809
Ionic strength = 5.947e+000
Mass of water (kg) = 1.000e+000
Total alkalinity (eq/kg) = 2.997e-002
Total carbon (mol/kg) = 0.000e+000
Total CO2 (mol/kg) = 0.000e+000
Temperature (deg C) = 25.00
Electrical balance (eq) = -1.229e-012
Percent error, 100*(Cat-|An|)/(Cat+|An|) = -0.00
Iterations = 16
Gamma iterations = 5
Osmotic coefficient = 1.27181
Density of water = 0.99704
Total H = 1.110428e+002
Total O = 5.551078e+001

-----Distribution of species-----

Species	Molality	Unscaled		Unscaled		Gamma	cm3/mol
		Activity	Molality	Activity	log		
OH-	7.456e-006	1.880e-006	-5.128	-5.726	-0.598	3.78	
H+	1.756e-009	4.336e-009	-8.756	-8.363	0.393	0.00	
H2O	5.551e+001	8.092e-001	1.744	-0.092	0.000	18.07	
Ca	6.287e-001						
Ca+2	6.287e-001	3.048e-001	-0.202	-0.516	-0.314	-14.30	
Cl	5.051e+000						
Cl-	5.051e+000	5.819e+000	0.703	0.765	0.061	20.09	
K	5.945e-001						
K+	5.945e-001	2.472e-001	-0.226	-0.607	-0.381	12.10	
Mg	2.642e-001						
Mg+2	2.641e-001	1.950e-001	-0.578	-0.710	-0.132	-17.80	
MgOH+	1.521e-004	5.650e-005	-3.818	-4.248	-0.430	(0)	
Na	2.642e+000						
Na+	2.642e+000	2.012e+000	0.422	0.304	-0.118	1.40	
S(6)	1.100e-003						
SO4-2	1.100e-003	2.419e-005	-2.959	-4.616	-1.658	26.80	
HSO4-	1.128e-011	9.990e-012	-10.948	-11.000	-0.053	42.04	
Tris	6.000e-002						
(Tris)H+	3.019e-002	1.286e-002	-1.520	-1.891	-0.371	(0)	
Tris	2.981e-002	2.524e-002	-1.526	-1.598	-0.072	(0)	

-----Saturation indices-----

Phase	SI	log IAP	log K(298 K, 1 atm)
Anhydrite	-0.91	-5.13	-4.22 CaSO4
Arcanite	-4.05	-5.83	-1.78 K2SO4
Bischofite	-4.19	0.27	4.46 MgCl2:6H2O
Bloedite	-7.36	-9.70	-2.35 Na2Mg(SO4)2:4H2O
Brucite	-1.28	-12.16	-10.88 Mg(OH)2
Carnallite	-3.90	0.43	4.33 KMgCl3:6H2O
Epsomite	-4.09	-5.97	-1.88 MgSO4:7H2O
Glaserite	-6.95	-10.75	-3.80 NaK3(SO4)2
Glauberite	-3.90	-9.14	-5.25 Na2Ca(SO4)2
Gypsum	-0.74	-5.32	-4.58 CaSO4:2H2O

H2O(g)	-1.59	-0.09	1.50	H2O
Halite	-0.50	1.07	1.57	NaCl
Hexahydrite	-4.24	-5.88	-1.63	MgSO4:6H2O
Kainite	-5.25	-5.44	-0.19	KMgClSO4:3H2O
Kieserite	-5.30	-5.42	-0.12	MgSO4:H2O
Labile_S	-7.66	-13.33	-5.67	Na4Ca(SO4)3:2H2O
Leonhardite	-4.81	-5.69	-0.89	MgSO4:4H2O
Leonite	-7.55	-11.52	-3.98	K2Mg(SO4)2:4H2O
Mirabilite	-3.72	-4.93	-1.21	Na2SO4:10H2O
Misenite	-76.54	-87.35	-10.81	K8H6(SO4)7
Pentahydrite	-4.50	-5.79	-1.28	MgSO4:5H2O
Polyhalite	-7.86	-21.61	-13.74	K2MgCa2(SO4)4:2H2O
Portlandite	-6.78	-11.97	-5.19	Ca(OH)2
Schoenite	-7.38	-11.71	-4.33	K2Mg(SO4)2:6H2O
Sylvite	-0.74	0.16	0.90	KCl
Syngenite	-3.61	-11.05	-7.45	K2Ca(SO4)2:H2O

End of simulation.

Reading input data for simulation 3.

```
Solution 8 Just 1.2x's LSPW (no Tris)
pe    11
units mol/L
ph    7 charge
density 1.17505
Na    2.40000
K     0.54000
Ca    0.5710
Mg    0.24000
Cl    4.56000
S(6)  0.00100
Save Solution 8
END
```

Beginning of initial solution calculations.

Initial solution 8. Just 1.2x's LSPW (no Tris)

-----Solution composition-----

Elements	Molality	Moles
Ca	6.287e-001	6.287e-001
Cl	5.020e+000	5.020e+000
K	5.945e-001	5.945e-001
Mg	2.642e-001	2.642e-001
Na	2.642e+000	2.642e+000
S(6)	1.101e-003	1.101e-003

-----Description of solution-----

```
pH = 5.889   Charge balance
pe = 11.000
Specific Conductance (uS/cm, 25 oC) = 505299
Density (g/cm3) = 1.17504
Volume (L) = 1.10105
Activity of water = 0.811
Ionic strength = 5.917e+000
Mass of water (kg) = 1.000e+000
Total alkalinity (eq/kg) = 7.689e-016
Total carbon (mol/kg) = 0.000e+000
Total CO2 (mol/kg) = 0.000e+000
Temperature (deg C) = 25.00
```

Electrical balance (eq) = 7.859e-014
 Percent error, 100*(Cat-|An|)/(Cat+|An|) = 0.00
 Iterations = 12
 Gamma iterations = 5
 Osmotic coefficient = 1.27274
 Density of water = 0.99704
 Total H = 1.110124e+002
 Total O = 5.551062e+001

-----Distribution of species-----

Species	Molality	Unscaled		Unscaled		cm3/mol
		Activity	Molality	log	log	
H+	5.261e-007	1.290e-006	-6.279	-5.889	0.389	0.00
OH-	2.497e-008	6.333e-009	-7.603	-8.198	-0.596	3.75
H2O	5.551e+001	8.107e-001	1.744	-0.091	0.000	18.07
Ca	6.287e-001					
Ca+2	6.287e-001	3.056e-001	-0.202	-0.515	-0.313	-14.31
Cl	5.020e+000					
Cl-	5.020e+000	5.785e+000	0.701	0.762	0.062	20.08
K	5.945e-001					
K+	5.945e-001	2.465e-001	-0.226	-0.608	-0.382	12.09
Mg	2.642e-001					
Mg+2	2.642e-001	1.930e-001	-0.578	-0.714	-0.136	-17.81
MgOH+	5.045e-007	1.884e-007	-6.297	-6.725	-0.428	(0)
Na	2.642e+000					
Na+	2.642e+000	2.001e+000	0.422	0.301	-0.121	1.39
S(6)	1.101e-003					
SO4-2	1.101e-003	2.429e-005	-2.958	-4.615	-1.656	26.78
HSO4-	3.354e-009	2.985e-009	-8.474	-8.525	-0.051	42.03

-----Saturation indices-----

Phase	SI	log IAP	log K(298 K, 1 atm)
Anhydrite	-0.90	-5.13	-4.22 CaSO4
Arcanite	-4.05	-5.83	-1.78 K2SO4
Bischofite	-4.19	0.26	4.46 MgCl2:6H2O
Bloedite	-7.36	-9.71	-2.35 Na2Mg(SO4)2:4H2O
Brucite	-6.23	-17.11	-10.88 Mg(OH)2
Carnallite	-3.91	0.42	4.33 KMgCl3:6H2O
Epsomite	-4.09	-5.97	-1.88 MgSO4:7H2O
Glaserite	-6.95	-10.75	-3.80 NaK3(SO4)2
Glauberite	-3.90	-9.14	-5.25 Na2Ca(SO4)2
Gypsum	-0.73	-5.31	-4.58 CaSO4:2H2O
H2O(g)	-1.59	-0.09	1.50 H2O
Halite	-0.51	1.06	1.57 NaCl
Hexahydrite	-4.24	-5.88	-1.63 MgSO4:6H2O
Kainite	-5.26	-5.45	-0.19 KMgCISO4:3H2O
Kieserite	-5.30	-5.42	-0.12 MgSO4:H2O
Labile_S	-7.66	-13.34	-5.67 Na4Ca(SO4)3:2H2O
Leonardite	-4.81	-5.69	-0.89 MgSO4:4H2O
Leonite	-7.55	-11.52	-3.98 K2Mg(SO4)2:4H2O
Mirabilite	-3.71	-4.92	-1.21 Na2SO4:10H2O
Misenite	-61.70	-72.50	-10.81 K8H6(SO4)7
Pentahydrite	-4.50	-5.78	-1.28 MgSO4:5H2O
Polyhalite	-7.86	-21.60	-13.74 K2MgCa2(SO4)4:2H2O
Portlandite	-11.72	-16.91	-5.19 Ca(OH)2
Schoenite	-7.38	-11.71	-4.33 K2Mg(SO4)2:6H2O
Sylvite	-0.75	0.15	0.90 KCl
Syngenite	-3.60	-11.05	-7.45 K2Ca(SO4)2:H2O

End of simulation.

Reading input data for simulation 4.

```
USE solution 1
EQUILIBRIUM_PHASES 1
CO2(g) -3.4 10
END
```

Beginning of batch-reaction calculations.

Reaction step 1.

Using solution 1.

Using pure phase assemblage 1.

-----Phase assemblage-----

Phase	Moles in assemblage					
	SI	log IAP	log K(T, P)	Initial	Final	Delta
CO2(g)	-3.40	-4.86	-1.46	1.000e+001	1.000e+001	-8.234e-005

-----Solution composition-----

Elements	Molality	Moles
C	8.234e-005	8.234e-005
Ca	6.287e-001	6.287e-001
Cl	5.078e+000	5.078e+000
K	5.945e-001	5.945e-001
Mg	2.642e-001	2.642e-001
Na	2.642e+000	2.642e+000
S	1.100e-003	1.100e-003
Tris	6.000e-002	6.000e-002

-----Description of solution-----

pH = 7.074 Charge balance
pe = 11.000 Adjusted to redox equilibrium
Specific Conductance (uS/cm, 25 oC) = 511871
Density (g/cm3) = 1.18218
Volume (L) = 1.10232
Activity of water = 0.808
Ionic strength = 5.974e+000
Mass of water (kg) = 1.000e+000
Total alkalinity (eq/kg) = 2.995e-003
Total CO2 (mol/kg) = 8.234e-005
Temperature (deg C) = 25.00
Electrical balance (eq) = -5.591e-015
Percent error, 100*(Cat-|An|)/(Cat+|An|) = -0.00
Iterations = 16
Gamma iterations = 4
Osmotic coefficient = 1.27364
Density of water = 0.99704
Total H = 1.110695e+002
Total O = 5.551079e+001

-----Distribution of species-----

Species	Unscaled					
	Unscaled	log	log	log		
	Molality	Activity	Molality	Activity	Gamma	cm3/mol
OH-	3.850e-007	9.661e-008	-6.415	-7.015	-0.600	3.81
H+	3.391e-008	8.430e-008	-7.470	-7.074	0.396	0.00
H2O	5.551e+001	8.084e-001	1.744	-0.092	0.000	18.07
C(4)	8.234e-005					
HCO3-	6.737e-005	6.027e-005	-4.172	-4.220	-0.048	37.58
CO2	6.287e-006	1.380e-005	-5.202	-4.860	0.341	30.26

MgCO3	5.501e-006	5.501e-006	-5.260	-5.260	0.000	-17.09
CO3-2	3.183e-006	3.274e-008	-5.497	-7.485	-1.988	8.69
Ca	6.287e-001					
Ca+2	6.287e-001	3.118e-001	-0.202	-0.506	-0.304	-14.28
Cl	5.078e+000					
Cl-	5.078e+000	5.850e+000	0.706	0.767	0.062	20.09
K	5.945e-001					
K+	5.945e-001	2.470e-001	-0.226	-0.607	-0.381	12.11
Mg	2.642e-001					
Mg+2	2.642e-001	1.983e-001	-0.578	-0.703	-0.125	-17.78
MgOH+	7.984e-006	2.952e-006	-5.098	-5.530	-0.432	(0)
MgCO3	5.501e-006	5.501e-006	-5.260	-5.260	0.000	-17.09
Na	2.642e+000					
Na+	2.642e+000	2.016e+000	0.422	0.304	-0.118	1.41
S(6)	1.100e-003					
SO4-2	1.100e-003	2.412e-005	-2.959	-4.618	-1.659	26.83
HSO4-	2.197e-010	1.937e-010	-9.658	-9.713	-0.055	42.04
Tris	6.000e-002					
(Tris)H+	5.710e-002	2.434e-002	-1.243	-1.614	-0.370	(0)
Tris	2.902e-003	2.457e-003	-2.537	-2.610	-0.072	(0)

-----Saturation indices-----

Phase	SI	log IAP	log K(298 K, 1 atm)		
Anhydrite	-0.90	-5.12	-4.22	CaSO4	
Aragonite	0.23	-7.99	-8.22	CaCO3	
Arcanite	-4.06	-5.83	-1.78	K2SO4	
Bischofite	-4.18	0.28	4.46	MgCl2:6H2O	
Bloedite	-7.35	-9.70	-2.35	Na2Mg(SO4)2:4H2O	
Brucite	-3.85	-14.73	-10.88	Mg(OH)2	
Burkeite	-14.12	-14.89	-0.77	Na6CO3(SO4)2	
Calcite	0.42	-7.99	-8.41	CaCO3	
Carnallite	-3.89	0.44	4.33	KMgCl3:6H2O	
CO2(g)	-3.40	-4.86	-1.46	CO2	Pressure 0.0 atm, phi 1.000
Dolomite	0.90	-16.18	-17.08	CaMg(CO3)2	
Epsomite	-4.09	-5.97	-1.88	MgSO4:7H2O	
Gaylussite	-5.91	-15.33	-9.42	CaNa2(CO3)2:5H2O	
Glaserite	-6.95	-10.75	-3.80	NaK3(SO4)2	
Glauberite	-3.89	-9.13	-5.25	Na2Ca(SO4)2	
Gypsum	-0.73	-5.31	-4.58	CaSO4:2H2O	
H2O(g)	-1.60	-0.09	1.50	H2O	
Halite	-0.50	1.07	1.57	NaCl	
Hexahydrite	-4.24	-5.87	-1.63	MgSO4:6H2O	
Kainite	-5.24	-5.44	-0.19	KMgCISO4:3H2O	
Kalichinit	-5.11	-15.17	-10.06	KHCO3	
Kieserite	-5.29	-5.41	-0.12	MgSO4:H2O	
Labile_S	-7.65	-13.33	-5.67	Na4Ca(SO4)3:2H2O	
Leonhardite	-4.80	-5.69	-0.89	MgSO4:4H2O	
Leonite	-7.54	-11.52	-3.98	K2Mg(SO4)2:4H2O	
Magnesite	-0.35	-8.19	-7.83	MgCO3	
Mirabilite	-3.72	-4.93	-1.21	Na2SO4:10H2O	
Misenite	-68.82	-79.63	-10.81	K8H6(SO4)7	
Nahcolite	-3.51	-14.25	-10.74	NaHCO3	
Natron	-6.97	-7.80	-0.82	Na2CO3:10H2O	
Nesquehonite	-3.30	-8.46	-5.17	MgCO3:3H2O	
Pentahydrite	-4.50	-5.78	-1.28	MgSO4:5H2O	
Pirssonite	-5.82	-15.05	-9.23	Na2Ca(CO3)2:2H2O	
Polyhalite	-7.84	-21.58	-13.74	K2MgCa2(SO4)4:2H2O	
Portlandite	-9.35	-14.54	-5.19	Ca(OH)2	
Schoenite	-7.38	-11.71	-4.33	K2Mg(SO4)2:6H2O	
Sylvite	-0.74	0.16	0.90	KCl	
Syngenite	-3.60	-11.05	-7.45	K2Ca(SO4)2:H2O	
Trona	-9.93	-21.32	-11.38	Na3H(CO3)2:2H2O	

End of simulation.

Reading input data for simulation 5.

```
USE solution 2
EQUILIBRIUM_PHASES 2
CO2(g) -3.4 10
END
```

Beginning of batch-reaction calculations.

Reaction step 1.

Using solution 2.

Using pure phase assemblage 2.

-----Phase assemblage-----

Phase	Moles in assemblage					
	SI	log IAP	log K(T, P)	Initial	Final	Delta
CO2(g)	-3.40	-4.86	-1.46	1.000e+001	1.000e+001	-1.485e-004

-----Solution composition-----

Elements	Molality	Moles
C	1.485e-004	1.485e-004
Ca	6.287e-001	6.287e-001
Cl	5.076e+000	5.076e+000
K	5.945e-001	5.945e-001
Mg	2.642e-001	2.642e-001
Na	2.642e+000	2.642e+000
S	1.100e-003	1.100e-003
Tris	6.000e-002	6.000e-002

-----Description of solution-----

pH = 7.311	Charge balance
pe = 11.000	Adjusted to redox equilibrium
Specific Conductance (uS/cm, 25 oC) = 511613	
Density (g/cm3) = 1.18216	
Volume (L) = 1.10228	
Activity of water = 0.808	
Ionic strength = 5.972e+000	
Mass of water (kg) = 1.000e+000	
Total alkalinity (eq/kg) = 5.023e-003	
Total CO2 (mol/kg) = 1.485e-004	
Temperature (deg C) = 25.00	
Electrical balance (eq) = -9.226e-011	
Percent error, 100*(Cat-[Anl])/(Cat+[Anl]) = -0.00	
Iterations = 17	
Gamma iterations = 5	
Osmotic coefficient = 1.27350	
Density of water = 0.99704	
Total H = 1.110674e+002	
Total O = 5.551093e+001	

-----Distribution of species-----

Species	Unscaled					
	Molality	Activity	Unscaled log	log	log	
OH-	6.646e-007	1.668e-007	-6.177	-6.778	-0.600	3.81
H+	1.965e-008	4.882e-008	-7.707	-7.311	0.395	0.00
H2O	5.551e+001	8.085e-001	1.744	-0.092	0.000	18.07
C(4)	1.485e-004					
HCO3-	1.163e-004	1.041e-004	-3.934	-3.983	-0.048	37.57

MgCO3	1.638e-005	1.638e-005	-4.786	-4.786	0.000	-17.09
CO3-2	9.484e-006	9.761e-008	-5.023	-7.010	-1.987	8.69
CO2	6.287e-006	1.380e-005	-5.202	-4.860	0.341	30.26
Ca	6.287e-001					
Ca+2	6.287e-001	3.113e-001	-0.202	-0.507	-0.305	-14.29
Cl	5.076e+000					
Cl-	5.076e+000	5.848e+000	0.705	0.767	0.062	20.09
K	5.945e-001					
K+	5.945e-001	2.470e-001	-0.226	-0.607	-0.381	12.11
Mg	2.642e-001					
Mg+2	2.642e-001	1.980e-001	-0.578	-0.703	-0.125	-17.79
MgCO3	1.638e-005	1.638e-005	-4.786	-4.786	0.000	-17.09
MgOH+	1.376e-005	5.091e-006	-4.861	-5.293	-0.432	(0)
Na	2.642e+000					
Na+	2.642e+000	2.016e+000	0.422	0.304	-0.118	1.41
S(6)	1.100e-003					
SO4-2	1.100e-003	2.413e-005	-2.959	-4.618	-1.659	26.83
HSO4-	1.272e-010	1.122e-010	-9.895	-9.950	-0.054	42.04
Tris	6.000e-002					
(Tris)H+	5.516e-002	2.351e-002	-1.258	-1.629	-0.370	(0)
Tris	4.841e-003	4.098e-003	-2.315	-2.387	-0.072	(0)

-----Saturation indices-----

Phase	SI	log IAP	log K(298 K, 1 atm)		
Anhydrite	-0.90	-5.12	-4.22	CaSO4	
Aragonite	0.70	-7.52	-8.22	CaCO3	
Arcanite	-4.06	-5.83	-1.78	K2SO4	
Bischofite	-4.18	0.28	4.46	MgCl2:6H2O	
Bloedite	-7.35	-9.70	-2.35	Na2Mg(SO4)2:4H2O	
Brucite	-3.38	-14.26	-10.88	Mg(OH)2	
Burkeite	-13.65	-14.42	-0.77	Na6CO3(SO4)2	
Calcite	0.89	-7.52	-8.41	CaCO3	
Carnallite	-3.89	0.44	4.33	KMgCl3:6H2O	
CO2(g)	-3.40	-4.86	-1.46	CO2	Pressure 0.0 atm, phi 1.000
Dolomite	1.85	-15.23	-17.08	CaMg(CO3)2	
Epsomite	-4.09	-5.97	-1.88	MgSO4:7H2O	
Gaylussite	-4.96	-14.38	-9.42	CaNa2(CO3)2:5H2O	
Glaserite	-6.95	-10.75	-3.80	NaK3(SO4)2	
Glauberite	-3.89	-9.13	-5.25	Na2Ca(SO4)2	
Gypsum	-0.73	-5.31	-4.58	CaSO4:2H2O	
H2O(g)	-1.60	-0.09	1.50	H2O	
Halite	-0.50	1.07	1.57	NaCl	
Hexahydrite	-4.24	-5.87	-1.63	MgSO4:6H2O	
Kainite	-5.25	-5.44	-0.19	KMgClSO4:3H2O	
Kalichinit	-4.87	-14.93	-10.06	KHCO3	
Kieserite	-5.29	-5.41	-0.12	MgSO4:H2O	
Labile_S	-7.65	-13.33	-5.67	Na4Ca(SO4)3:2H2O	
Leonardite	-4.80	-5.69	-0.89	MgSO4:4H2O	
Leonite	-7.54	-11.52	-3.98	K2Mg(SO4)2:4H2O	
Magnesite	0.12	-7.71	-7.83	MgCO3	
Mirabilite	-3.72	-4.93	-1.21	Na2SO4:10H2O	
Misenite	-70.24	-81.05	-10.81	K8H6(SO4)7	
Nahcolite	-3.28	-14.02	-10.74	NaHCO3	
Natron	-6.50	-7.32	-0.82	Na2CO3:10H2O	
Nesquehonite	-2.82	-7.99	-5.17	MgCO3:3H2O	
Pentahydrite	-4.50	-5.78	-1.28	MgSO4:5H2O	
Pirssonite	-4.87	-14.10	-9.23	Na2Ca(CO3)2:2H2O	
Polyhalite	-7.84	-21.59	-13.74	K2MgCa2(SO4)4:2H2O	
Portlandite	-8.87	-14.06	-5.19	Ca(OH)2	
Schoenite	-7.38	-11.71	-4.33	K2Mg(SO4)2:6H2O	
Sylvite	-0.74	0.16	0.90	KCl	
Syngenite	-3.60	-11.05	-7.45	K2Ca(SO4)2:H2O	
Trona	-9.22	-20.60	-11.38	Na3H(CO3)2:2H2O	

End of simulation.

Reading input data for simulation 6.

```
USE solution 3
EQUILIBRIUM_PHASES 3
CO2(g) -3.4 10
END
```

Beginning of batch-reaction calculations.

Reaction step 1.
Using solution 3.
Using pure phase assemblage 3.

-----Phase assemblage-----

Phase	SI	log IAP	log K(T, P)	Initial	Final	Delta
CO2(g)	-3.40	-4.86	-1.46	1.000e+001	1.000e+001	-2.715e-004

-----Solution composition-----

Elements	Molality	Moles
C	2.715e-004	2.715e-004
Ca	6.287e-001	6.287e-001
Cl	5.073e+000	5.073e+000
K	5.945e-001	5.945e-001
Mg	2.642e-001	2.642e-001
Na	2.642e+000	2.642e+000
S	1.100e-003	1.100e-003
Tris	6.000e-002	6.000e-002

-----Description of solution-----
 pH = 7.533 Charge balance
 pe = 11.000 Adjusted to redox equilibrium
 Specific Conductance (uS/cm, 25 oC) = 511233
 Density (g/cm3) = 1.18214
 Volume (L) = 1.10222
 Activity of water = 0.809
 Ionic strength = 5.969e+000
 Mass of water (kg) = 1.000e+000
 Total alkalinity (eq/kg) = 8.011e-003
 Total CO2 (mol/kg) = 2.715e-004
 Temperature (deg C) = 25.00
 Electrical balance (eq) = -2.200e-010
 Percent error, 100*(Cat-|An|)/(Cat+|An|) = -0.00
 Iterations = 17
 Gamma iterations = 5
 Osmotic coefficient = 1.27329
 Density of water = 0.99704
 Total H = 1.110645e+002
 Total O = 5.551118e+001

-----Distribution of species-----

Species	Molality	Unscaled			Gamma	cm3/mol
		Activity	Molality	Activity		
OH-	1.106e-006	2.779e-007	-5.956	-6.556	-0.600	3.81
H+	1.181e-008	2.932e-008	-7.928	-7.533	0.395	0.00
H2O	5.551e+001	8.086e-001	1.744	-0.092	0.000	18.07

C(4)	2.715e-004					
HCO3-	1.936e-004	1.733e-004	-3.713	-3.761	-0.048	37.57
MgCO3	4.534e-005	4.534e-005	-4.344	-4.344	0.000	-17.09
CO3-2	2.627e-005	2.707e-007	-4.580	-6.568	-1.987	8.68
CO2	6.287e-006	1.380e-005	-5.202	-4.860	0.341	30.26
Ca	6.287e-001					
Ca+2	6.287e-001	3.106e-001	-0.202	-0.508	-0.306	-14.29
Cl	5.073e+000					
Cl-	5.073e+000	5.844e+000	0.705	0.767	0.062	20.09
K	5.945e-001					
K+	5.945e-001	2.470e-001	-0.226	-0.607	-0.381	12.11
Mg	2.642e-001					
Mg+2	2.642e-001	1.977e-001	-0.578	-0.704	-0.126	-17.79
MgCO3	4.534e-005	4.534e-005	-4.344	-4.344	0.000	-17.09
MgOH+	2.287e-005	8.462e-006	-4.641	-5.073	-0.432	(0)
Na	2.642e+000					
Na+	2.642e+000	2.015e+000	0.422	0.304	-0.118	1.41
S(6)	1.100e-003					
SO4-2	1.100e-003	2.413e-005	-2.959	-4.617	-1.659	26.83
HSO4-	7.638e-011	6.741e-011	-10.117	-10.171	-0.054	42.04
Tris	6.000e-002					
(Tris)H+	5.235e-002	2.231e-002	-1.281	-1.652	-0.370	(0)
Tris	7.650e-003	6.476e-003	-2.116	-2.189	-0.072	(0)

-----Saturation indices-----

Phase	SI	log IAP	log K(298 K, 1 atm)			
Anhydrite	-0.90	-5.13	-4.22	CaSO4		
Aragonite	1.14	-7.08	-8.22	CaCO3		
Arcanite	-4.06	-5.83	-1.78	K2SO4		
Bischofite	-4.18	0.28	4.46	MgCl2:6H2O		
Bloedite	-7.35	-9.70	-2.35	Na2Mg(SO4)2:4H2O		
Brucite	-2.94	-13.82	-10.88	Mg(OH)2		
Burkeite	-13.20	-13.98	-0.77	Na6CO3(SO4)2		
Calcite	1.33	-7.08	-8.41	CaCO3		
Carnallite	-3.89	0.44	4.33	KMgCl3:6H2O		
CO2(g)	-3.40	-4.86	-1.46	CO2	Pressure	0.0 atm, phi 1.000
Dolomite	2.74	-14.35	-17.08	CaMg(CO3)2		
Epsomite	-4.09	-5.97	-1.88	MgSO4:7H2O		
Gaylussite	-4.07	-13.50	-9.42	CaNa2(CO3)2:5H2O		
Glaserite	-6.95	-10.75	-3.80	NaK3(SO4)2		
Glauberite	-3.89	-9.13	-5.25	Na2Ca(SO4)2		
Gypsum	-0.73	-5.31	-4.58	CaSO4:2H2O		
H2O(g)	-1.60	-0.09	1.50	H2O		
Halite	-0.50	1.07	1.57	NaCl		
Hexahydrite	-4.24	-5.88	-1.63	MgSO4:6H2O		
Kainite	-5.25	-5.44	-0.19	KMgClSO4:3H2O		
Kalicinitite	-4.65	-14.71	-10.06	KHCO3		
Kieserite	-5.29	-5.41	-0.12	MgSO4:H2O		
Labile_S	-7.66	-13.33	-5.67	Na4Ca(SO4)3:2H2O		
Leonardite	-4.80	-5.69	-0.89	MgSO4:4H2O		
Leonite	-7.54	-11.52	-3.98	K2Mg(SO4)2:4H2O		
Magnesite	0.56	-7.27	-7.83	MgCO3		
Mirabilite	-3.72	-4.93	-1.21	Na2SO4:10H2O		
Misenite	-71.57	-82.38	-10.81	K8H6(SO4)7		
Nahcolite	-3.05	-13.80	-10.74	NaHCO3		
Natron	-6.06	-6.88	-0.82	Na2CO3:10H2O		
Nesquehonite	-2.38	-7.55	-5.17	MgCO3:3H2O		
Pentahydrite	-4.50	-5.78	-1.28	MgSO4:5H2O		
Pirssonite	-3.98	-13.22	-9.23	Na2Ca(CO3)2:2H2O		
Polyhalite	-7.84	-21.59	-13.74	K2MgCa2(SO4)4:2H2O		
Portlandite	-8.43	-13.62	-5.19	Ca(OH)2		
Schoenite	-7.38	-11.71	-4.33	K2Mg(SO4)2:6H2O		
Sylvite	-0.74	0.16	0.90	KCl		
Syngenite	-3.60	-11.05	-7.45	K2Ca(SO4)2:H2O		
Trona	-8.56	-19.94	-11.38	Na3H(CO3)2:2H2O		

End of simulation.

Reading input data for simulation 7.

```
USE solution 4
EQUILIBRIUM_PHASES 4
CO2(g) -3.4 10
END
```

Beginning of batch-reaction calculations.

Reaction step 1.

Using solution 4.

Using pure phase assemblage 4.

-----Phase assemblage-----

Phase	Moles in assemblage					
	SI	log IAP	log K(T, P)	Initial	Final	Delta
CO2(g)	-3.40	-4.86	-1.46	1.000e+001	1.000e+001	-4.329e-004

-----Solution composition-----

Elements	Molality	Moles
C	4.329e-004	4.329e-004
Ca	6.287e-001	6.287e-001
Cl	5.070e+000	5.070e+000
K	5.945e-001	5.945e-001
Mg	2.642e-001	2.642e-001
Na	2.642e+000	2.642e+000
S	1.100e-003	1.100e-003
Tris	6.010e-002	6.010e-002

-----Description of solution-----

pH = 7.691 Charge balance
pe = 11.000 Adjusted to redox equilibrium
Specific Conductance (uS/cm, 25 oC) = 510860
Density (g/cm3) = 1.18213
Volume (L) = 1.10216
Activity of water = 0.809
Ionic strength = 5.966e+000
Mass of water (kg) = 1.000e+000
Total alkalinity (eq/kg) = 1.105e-002
Total CO2 (mol/kg) = 4.329e-004
Temperature (deg C) = 25.00
Electrical balance (eq) = -3.834e-010
Percent error, 100*(Cat-|An|)/(Cat+|An|) = -0.00
Iterations = 18
Gamma iterations = 5
Osmotic coefficient = 1.27308
Density of water = 0.99704
Total H = 1.110616e+002
Total O = 5.551152e+001

-----Distribution of species-----

Species	Unscaled					
	Molality	Activity	Unscaled	log	log	log
OH-	1.591e-006	3.998e-007	-5.798	-6.398	-0.600	3.80
H+	8.212e-009	2.038e-008	-8.086	-7.691	0.395	0.00

H2O	5.551e+001	8.086e-001	1.744	-0.092	0.000	18.07
C(4)	4.329e-004					
HCO3-	2.786e-004	2.494e-004	-3.555	-3.603	-0.048	37.56
MgCO3	9.370e-005	9.370e-005	-4.028	-4.028	0.000	-17.09
CO3-2	5.434e-005	5.605e-007	-4.265	-6.251	-1.987	8.68
CO2	6.286e-006	1.380e-005	-5.202	-4.860	0.341	30.26
Ca	6.287e-001					
Ca+2	6.287e-001	3.099e-001	-0.202	-0.509	-0.307	-14.29
Cl	5.070e+000					
Cl-	5.070e+000	5.841e+000	0.705	0.766	0.061	20.09
K	5.945e-001					
K+	5.945e-001	2.470e-001	-0.226	-0.607	-0.381	12.11
Mg	2.642e-001					
Mg+2	2.641e-001	1.973e-001	-0.578	-0.705	-0.127	-17.79
MgCO3	9.370e-005	9.370e-005	-4.028	-4.028	0.000	-17.09
MgOH+	3.283e-005	1.215e-005	-4.484	-4.915	-0.432	(0)
Na	2.642e+000					
Na+	2.642e+000	2.015e+000	0.422	0.304	-0.118	1.41
S(6)	1.100e-003					
SO4-2	1.100e-003	2.414e-005	-2.959	-4.617	-1.659	26.83
HSO4-	5.308e-011	4.686e-011	-10.275	-10.329	-0.054	42.04
Tris	6.010e-002					
(Tris)H+	4.966e-002	2.116e-002	-1.304	-1.674	-0.370	(0)
Tris	1.044e-002	8.839e-003	-1.981	-2.054	-0.072	(0)

-----Saturation indices-----

Phase	SI	log IAP	log K(298 K, 1 atm)		
Anhydrite	-0.90	-5.13	-4.22	CaSO4	
Aragonite	1.46	-6.76	-8.22	CaCO3	
Arcanite	-4.06	-5.83	-1.78	K2SO4	
Bischofite	-4.18	0.27	4.46	MgCl2:6H2O	
Bloedite	-7.35	-9.70	-2.35	Na2Mg(SO4)2:4H2O	
Brucite	-2.62	-13.50	-10.88	Mg(OH)2	
Burkeite	-12.89	-13.66	-0.77	Na6CO3(SO4)2	
Calcite	1.65	-6.76	-8.41	CaCO3	
Carnallite	-3.90	0.43	4.33	KMgCl3:6H2O	
CO2(g)	-3.40	-4.86	-1.46	CO2	Pressure 0.0 atm, phi 1.000
Dolomite	3.37	-13.72	-17.08	CaMg(CO3)2	
Epsomite	-4.09	-5.97	-1.88	MgSO4:7H2O	
Gaylussite	-3.44	-12.86	-9.42	CaNa2(CO3)2:5H2O	
Glaserite	-6.95	-10.75	-3.80	NaK3(SO4)2	
Glauberite	-3.89	-9.13	-5.25	Na2Ca(SO4)2	
Gypsum	-0.73	-5.31	-4.58	CaSO4:2H2O	
H2O(g)	-1.60	-0.09	1.50	H2O	
Halite	-0.50	1.07	1.57	NaCl	
Hexahydrite	-4.24	-5.88	-1.63	MgSO4:6H2O	
Kainite	-5.25	-5.44	-0.19	KMgCISO4:3H2O	
Kalichinite	-4.49	-14.55	-10.06	KHCO3	
Kieserite	-5.29	-5.41	-0.12	MgSO4:H2O	
Labil_S	-7.66	-13.33	-5.67	Na4Ca(SO4)3:2H2O	
Leonardite	-4.80	-5.69	-0.89	MgSO4:4H2O	
Leonite	-7.54	-11.52	-3.98	K2Mg(SO4)2:4H2O	
Magnesite	0.88	-6.96	-7.83	MgCO3	
Mirabilite	-3.72	-4.93	-1.21	Na2SO4:10H2O	
Misenite	-72.52	-83.32	-10.81	K8H6(SO4)7	
Nahcolite	-2.90	-13.64	-10.74	NaHCO3	
Natron	-5.74	-6.57	-0.82	Na2CO3:10H2O	
Nesquehonite	-2.07	-7.23	-5.17	MgCO3:3H2O	
Pentahydrite	-4.50	-5.78	-1.28	MgSO4:5H2O	
Pirssonite	-3.35	-12.59	-9.23	Na2Ca(CO3)2:2H2O	
Polyhalite	-7.85	-21.59	-13.74	K2MgCa2(SO4)4:2H2O	
Portlandite	-8.12	-13.31	-5.19	Ca(OH)2	
Schoenite	-7.38	-11.71	-4.33	K2Mg(SO4)2:6H2O	
Sylvite	-0.74	0.16	0.90	KCl	
Syngenite	-3.60	-11.05	-7.45	K2Ca(SO4)2:H2O	
Trona	-8.08	-19.47	-11.38	Na3H(CO3)2:2H2O	

End of simulation.

Reading input data for simulation 8.

```
USE solution 5
EQUILIBRIUM_PHASES 5
CO2(g) -3.4 10
END
```

Beginning of batch-reaction calculations.

Reaction step 1.

Using solution 5.
Using pure phase assemblage 5.

-----Phase assemblage-----

Phase	SI	log IAP	log K(T, P)	Initial	Final	Delta
CO2(g)	-3.40	-4.86	-1.46	1.000e+001	9.999e+000	-7.130e-004

-----Solution composition-----

Elements	Molality	Moles
C	7.130e-004	7.130e-004
Ca	6.287e-001	6.287e-001
Cl	5.066e+000	5.066e+000
K	5.945e-001	5.945e-001
Mg	2.642e-001	2.642e-001
Na	2.642e+000	2.642e+000
S	1.100e-003	1.100e-003
Tris	6.000e-002	6.000e-002

-----Description of solution-----

pH = 7.849 Charge balance
pe = 11.000 Adjusted to redox equilibrium
Specific Conductance (uS/cm, 25 oC) = 510349
Density (g/cm3) = 1.18209
Volume (L) = 1.10208
Activity of water = 0.809
Ionic strength = 5.962e+000
Mass of water (kg) = 1.000e+000
Total alkalinity (eq/kg) = 1.500e-002
Total CO2 (mol/kg) = 7.130e-004
Temperature (deg C) = 25.00
Electrical balance (eq) = -5.752e-010
Percent error, 100*(Cat-|An|)/(Cat+|An|) = -0.00
Iterations = 18
Gamma iterations = 5
Osmotic coefficient = 1.27279
Density of water = 0.99704
Total H = 1.110575e+002
Total O = 5.551210e+001

-----Distribution of species-----

Species	Molality	Unscaled			Gamma	cm3/mol
		Activity	Unscaled log	log		
OH-	2.288e-006	5.755e-007	-5.641	-6.240	-0.599	3.80

H+	5.713e-009	1.416e-008	-8.243	-7.849	0.394	0.00
H2O	5.551e+001	8.088e-001	1.744	-0.092	0.000	18.07
C(4)	7.130e-004					
HCO3-	4.008e-004	3.590e-004	-3.397	-3.445	-0.048	37.55
MgCO3	1.935e-004	1.935e-004	-3.713	-3.713	0.000	-17.09
CO3-2	1.124e-004	1.161e-006	-3.949	-5.935	-1.986	8.67
CO2	6.286e-006	1.380e-005	-5.202	-4.860	0.341	30.26
Ca	6.287e-001					
Ca+2	6.287e-001	3.089e-001	-0.202	-0.510	-0.309	-14.29
Cl	5.066e+000					
Cl-	5.066e+000	5.836e+000	0.705	0.766	0.061	20.09
K	5.945e-001					
K+	5.945e-001	2.471e-001	-0.226	-0.607	-0.381	12.11
Mg	2.642e-001					
Mg+2	2.640e-001	1.967e-001	-0.578	-0.706	-0.128	-17.79
MgCO3	1.935e-004	1.935e-004	-3.713	-3.713	0.000	-17.09
MgOH+	4.708e-005	1.744e-005	-4.327	-4.758	-0.431	(0)
Na	2.642e+000					
Na+	2.642e+000	2.014e+000	0.422	0.304	-0.118	1.41
S(6)	1.100e-003					
SO4-2	1.100e-003	2.415e-005	-2.959	-4.617	-1.659	26.82
HSO4-	3.688e-011	3.257e-011	-10.433	-10.487	-0.054	42.04
Tris	6.000e-002					
(Tris)H+	4.607e-002	1.963e-002	-1.337	-1.707	-0.371	(0)
Tris	1.394e-002	1.180e-002	-1.856	-1.928	-0.072	(0)

-----Saturation indices-----

Phase	SI	log IAP	log K(298 K, 1 atm)			
Anhydrite	-0.90	-5.13	-4.22	CaSO4		
Aragonite	1.77	-6.45	-8.22	CaCO3		
Arcanite	-4.06	-5.83	-1.78	K2SO4		
Bischofite	-4.18	0.27	4.46	MgCl2:6H2O		
Bloedite	-7.35	-9.70	-2.35	Na2Mg(SO4)2:4H2O		
Brucite	-2.31	-13.19	-10.88	Mg(OH)2		
Burkeite	-12.57	-13.34	-0.77	Na6CO3(SO4)2		
Calcite	1.96	-6.45	-8.41	CaCO3		
Carnallite	-3.90	0.43	4.33	KMgCl3:6H2O		
CO2(g)	-3.40	-4.86	-1.46	CO2	Pressure	0.0 atm, phi 1.000
Dolomite	4.00	-13.09	-17.08	CaMg(CO3)2		
Epsomite	-4.09	-5.97	-1.88	MgSO4:7H2O		
Gaylussite	-2.81	-12.23	-9.42	CaNa2(CO3)2:5H2O		
Glaserite	-6.95	-10.75	-3.80	NaK3(SO4)2		
Glauberite	-3.89	-9.14	-5.25	Na2Ca(SO4)2		
Gypsum	-0.73	-5.31	-4.58	CaSO4:2H2O		
H2O(g)	-1.60	-0.09	1.50	H2O		
Halite	-0.50	1.07	1.57	NaCl		
Hexahydrite	-4.24	-5.88	-1.63	MgSO4:6H2O		
Kainite	-5.25	-5.44	-0.19	KMgClSO4:3H2O		
Kalichinite	-4.33	-14.39	-10.06	KHCO3		
Kieserite	-5.29	-5.42	-0.12	MgSO4:H2O		
Labile_S	-7.66	-13.33	-5.67	Na4Ca(SO4)3:2H2O		
Leonardite	-4.81	-5.69	-0.89	MgSO4:4H2O		
Leonite	-7.54	-11.52	-3.98	K2Mg(SO4)2:4H2O		
Magnesite	1.19	-6.64	-7.83	MgCO3		
Mirabilite	-3.72	-4.93	-1.21	Na2SO4:10H2O		
Misenite	-73.46	-84.27	-10.81	K8H6(SO4)7		
Nahcolite	-2.74	-13.48	-10.74	NaHCO3		
Natron	-5.42	-6.25	-0.82	Na2CO3:10H2O		
Nesquehonite	-1.75	-6.92	-5.17	MgCO3:3H2O		
Pentahydrite	-4.50	-5.78	-1.28	MgSO4:5H2O		
Pirssonite	-2.72	-11.96	-9.23	Na2Ca(CO3)2:2H2O		
Polyhalite	-7.85	-21.59	-13.74	K2MgCa2(SO4)4:2H2O		
Portlandite	-7.80	-12.99	-5.19	Ca(OH)2		
Schoenite	-7.38	-11.71	-4.33	K2Mg(SO4)2:6H2O		
Sylvite	-0.74	0.16	0.90	KCl		
Syngenite	-3.60	-11.05	-7.45	K2Ca(SO4)2:H2O		
Trona	-7.61	-18.99	-11.38	Na3H(CO3)2:2H2O		

End of simulation.

Reading input data for simulation 9.

```
USE solution 6
EQUILIBRIUM_PHASES 6
CO2(g) -3.4 10
END
```

Beginning of batch-reaction calculations.

Reaction step 1.

Using solution 6.

Using pure phase assemblage 6.

-----Phase assemblage-----

Phase	Moles in assemblage					
	SI	log IAP	log K(T, P)	Initial	Final	Delta
CO2(g)	-3.40	-4.86	-1.46	1.000e+001	9.999e+000	-1.447e-003

-----Solution composition-----

Elements	Molality	Moles
C	1.447e-003	1.447e-003
Ca	6.287e-001	6.287e-001
Cl	5.059e+000	5.059e+000
K	5.945e-001	5.945e-001
Mg	2.642e-001	2.642e-001
Na	2.642e+000	2.642e+000
S	1.100e-003	1.100e-003
Tris	6.000e-002	6.000e-002

-----Description of solution-----

pH = 8.057 Charge balance
pe = 11.000 Adjusted to redox equilibrium
Specific Conductance (uS/cm, 25 oC) = 509468
Density (g/cm3) = 1.18206
Volume (L) = 1.10195
Activity of water = 0.809
Ionic strength = 5.956e+000
Mass of water (kg) = 1.000e+000
Total alkalinity (eq/kg) = 2.200e-002
Total CO2 (mol/kg) = 1.447e-003
Temperature (deg C) = 25.00
Electrical balance (eq) = -3.454e-010
Percent error, 100*(Cat-|An|)/(Cat+|An|) = -0.00
Iterations = 19
Gamma iterations = 5
Osmotic coefficient = 1.27224
Density of water = 0.99704
Total H = 1.110506e+002
Total O = 5.551361e+001

-----Distribution of species-----

Species	Molality	Unscaled			cm3/mol
		Activity	Unscaled log	Activity	

OH-	3.691e-006	9.294e-007	-5.433	-6.032	-0.599	3.79
H+	3.544e-009	8.769e-009	-8.450	-8.057	0.393	0.00
H2O	5.551e+001	8.089e-001	1.744	-0.092	0.000	18.07
C(4)	1.447e-003					
HCO3-	6.469e-004	5.798e-004	-3.189	-3.237	-0.048	37.54
MgCO3	5.020e-004	5.020e-004	-3.299	-3.299	0.000	-17.09
CO3-2	2.924e-004	3.028e-006	-3.534	-5.519	-1.985	8.66
CO2	6.287e-006	1.380e-005	-5.202	-4.860	0.341	30.26
Ca	6.287e-001					
Ca+2	6.287e-001	3.073e-001	-0.202	-0.512	-0.311	-14.29
Cl	5.059e+000					
Cl-	5.059e+000	5.826e+000	0.704	0.765	0.061	20.09
K	5.945e-001					
K+	5.945e-001	2.471e-001	-0.226	-0.607	-0.381	12.11
Mg	2.642e-001					
Mg+2	2.637e-001	1.956e-001	-0.579	-0.709	-0.130	-17.79
MgCO3	5.020e-004	5.020e-004	-3.299	-3.299	0.000	-17.09
MgOH+	7.555e-005	2.802e-005	-4.122	-4.553	-0.431	(0)
Na	2.642e+000					
Na+	2.642e+000	2.013e+000	0.422	0.304	-0.118	1.40
S(6)	1.100e-003					
SO4-2	1.100e-003	2.416e-005	-2.959	-4.617	-1.658	26.81
HSO4-	2.284e-011	2.018e-011	-10.641	-10.695	-0.054	42.04
Tris	6.000e-002					
(Tris)H+	4.031e-002	1.717e-002	-1.395	-1.765	-0.371	(0)
Tris	1.969e-002	1.667e-002	-1.706	-1.778	-0.072	(0)

-----Saturation indices-----

Phase	SI	log IAP	log K(298 K, 1 atm)		
Anhydrite	-0.90	-5.13	-4.22	CaSO4	
Aragonite	2.19	-6.03	-8.22	CaCO3	
Arcanite	-4.05	-5.83	-1.78	K2SO4	
Bischofite	-4.19	0.27	4.46	MgCl2:6H2O	
Bloedite	-7.36	-9.70	-2.35	Na2Mg(SO4)2:4H2O	
Brucite	-1.89	-12.77	-10.88	Mg(OH)2	
Burkeite	-12.16	-12.93	-0.77	Na6CO3(SO4)2	
Calcite	2.37	-6.03	-8.41	CaCO3	
Carnallite	-3.90	0.43	4.33	KMgCl3:6H2O	
CO2(g)	-3.40	-4.86	-1.46	CO2	Pressure 0.0 atm, phi 1.000
Dolomite	4.82	-12.26	-17.08	CaMg(CO3)2	
Epsomite	-4.09	-5.97	-1.88	MgSO4:7H2O	
Gaylussite	-1.98	-11.40	-9.42	CaNa2(CO3)2:5H2O	
Glaserite	-6.95	-10.75	-3.80	NaK3(SO4)2	
Glauberite	-3.89	-9.14	-5.25	Na2Ca(SO4)2	
Gypsum	-0.73	-5.31	-4.58	CaSO4:2H2O	
H2O(g)	-1.59	-0.09	1.50	H2O	
Halite	-0.50	1.07	1.57	NaCl	
Hexahydrite	-4.24	-5.88	-1.63	MgSO4:6H2O	
Kainite	-5.25	-5.44	-0.19	KMgClSO4:3H2O	
Kalichinit	-4.12	-14.18	-10.06	KHCO3	
Kieserite	-5.29	-5.42	-0.12	MgSO4:H2O	
Labile_S	-7.66	-13.33	-5.67	Na4Ca(SO4)3:2H2O	
Leonhardite	-4.81	-5.69	-0.89	MgSO4:4H2O	
Leonite	-7.55	-11.52	-3.98	K2Mg(SO4)2:4H2O	
Magnesite	1.61	-6.23	-7.83	MgCO3	
Mirabilite	-3.72	-4.93	-1.21	Na2SO4:10H2O	
Misenite	-74.71	-85.52	-10.81	K8H6(SO4)7	
Nahcolite	-2.53	-13.27	-10.74	NaHCO3	
Natron	-5.01	-5.83	-0.82	Na2CO3:10H2O	
Nesquehonite	-1.34	-6.50	-5.17	MgCO3:3H2O	
Pentahydrite	-4.50	-5.79	-1.28	MgSO4:5H2O	
Pirssonite	-1.89	-11.13	-9.23	Na2Ca(CO3)2:2H2O	
Polyhalite	-7.86	-21.60	-13.74	K2MgCa2(SO4)4:2H2O	
Portlandite	-7.39	-12.58	-5.19	Ca(OH)2	
Schoenite	-7.38	-11.71	-4.33	K2Mg(SO4)2:6H2O	
Sylvite	-0.74	0.16	0.90	KCl	
Syngenite	-3.60	-11.05	-7.45	K2Ca(SO4)2:2H2O	
Trona	-6.98	-18.37	-11.38	Na3H(CO3)2:2H2O	

End of simulation.

Reading input data for simulation 10.

```
USE solution 7
EQUILIBRIUM_PHASES 7
CO2(g) -3.4 10
END
```

Beginning of batch-reaction calculations.

Reaction step 1.

Using solution 7.
Using pure phase assemblage 7.

-----Phase assemblage-----

Phase	Moles in assemblage					
	SI	log IAP	log K(T, P)	Initial	Final	Delta
CO2(g)	-3.40	-4.86	-1.46	1.000e+001	9.997e+000	-2.747e-003

-----Solution composition-----

Elements	Molality	Moles
C	2.747e-003	2.747e-003
Ca	6.287e-001	6.287e-001
Cl	5.051e+000	5.051e+000
K	5.946e-001	5.945e-001
Mg	2.643e-001	2.642e-001
Na	2.643e+000	2.642e+000
S	1.100e-003	1.100e-003
Tris	6.000e-002	6.000e-002

-----Description of solution-----
 pH = 8.232 Charge balance
 pe = 11.000 Adjusted to redox equilibrium
 Specific Conductance (uS/cm, 25 oC) = 508471
 Density (g/cm3) = 1.18204
 Volume (L) = 1.10182
 Activity of water = 0.809
 Ionic strength = 5.949e+000
 Mass of water (kg) = 1.000e+000
 Total alkalinity (eq/kg) = 2.997e-002
 Total CO2 (mol/kg) = 2.747e-003
 Temperature (deg C) = 25.00
 Electrical balance (eq) = 2.213e-009
 Percent error, 100*(Cat-|An|)/(Cat+|An|) = 0.00
 Iterations = 20
 Gamma iterations = 5
 Osmotic coefficient = 1.27153
 Density of water = 0.99704
 Total H = 1.110428e+002
 Total O = 5.551627e+001

-----Distribution of species-----

Species	Molality	Unscaled			Gamma	cm3/mol
		Activity	Unscaled log	Unscaled log		

OH-	5.521e-006	1.392e-006	-5.258	-5.856	-0.598	3.78
H+	2.372e-009	5.855e-009	-8.625	-8.232	0.393	0.00
H2O	5.551e+001	8.092e-001	1.744	-0.092	0.000	18.07
C(4)	2.747e-003					
MgCO3	1.118e-003	1.118e-003	-2.952	-2.952	0.000	-17.09
HCO3-	9.685e-004	8.686e-004	-3.014	-3.061	-0.047	37.52
CO3-2	6.540e-004	6.792e-006	-3.184	-5.168	-1.984	8.65
CO2	6.288e-006	1.380e-005	-5.202	-4.860	0.341	30.26
Ca	6.287e-001					
Ca+2	6.287e-001	3.056e-001	-0.202	-0.515	-0.313	-14.29
Cl	5.051e+000					
Cl-	5.051e+000	5.815e+000	0.703	0.765	0.061	20.09
K	5.946e-001					
K+	5.946e-001	2.472e-001	-0.226	-0.607	-0.381	12.10
Mg	2.643e-001					
Mg+2	2.630e-001	1.942e-001	-0.580	-0.712	-0.132	-17.80
MgCO3	1.118e-003	1.118e-003	-2.952	-2.952	0.000	-17.09
MgOH+	1.122e-004	4.167e-005	-3.950	-4.380	-0.430	(0)
Na	2.643e+000					
Na+	2.643e+000	2.012e+000	0.422	0.304	-0.118	1.40
S(6)	1.100e-003					
SO4-2	1.100e-003	2.417e-005	-2.959	-4.617	-1.658	26.81
HSO4-	1.525e-011	1.348e-011	-10.817	-10.870	-0.054	42.04
Tris	6.000e-002					
(Tris)H+	3.466e-002	1.476e-002	-1.460	-1.831	-0.371	(0)
Tris	2.534e-002	2.146e-002	-1.596	-1.668	-0.072	(0)

-----Saturation indices-----

Phase	SI	log IAP	log K(298 K, 1 atm)			
Anhydrite	-0.91	-5.13	-4.22	CaSO4		
Aragonite	2.54	-5.68	-8.22	CaCO3		
Arcanite	-4.05	-5.83	-1.78	K2SO4		
Bischofite	-4.19	0.27	4.46	MgCl2:6H2O		
Bloedite	-7.36	-9.71	-2.35	Na2Mg(SO4)2:4H2O		
Brucite	-1.54	-12.42	-10.88	Mg(OH)2		
Burkeite	-11.81	-12.58	-0.77	Na6CO3(SO4)2		
Calcite	2.72	-5.68	-8.41	CaCO3		
Carnallite	-3.91	0.42	4.33	KMgCl3:6H2O		
CO2(g)	-3.40	-4.86	-1.46	CO2	Pressure	0.0 atm, phi 1.000
Dolomite	5.52	-11.56	-17.08	CaMg(CO3)2		
Epsomite	-4.09	-5.97	-1.88	MgSO4:7H2O		
Gaylussite	-1.28	-10.70	-9.42	CaNa2(CO3)2:5H2O		
Glaserite	-6.95	-10.75	-3.80	NaK3(SO4)2		
Glauberite	-3.90	-9.14	-5.25	Na2Ca(SO4)2		
Gypsum	-0.73	-5.32	-4.58	CaSO4:2H2O		
H2O(g)	-1.59	-0.09	1.50	H2O		
Halite	-0.50	1.07	1.57	NaCl		
Hexahydrite	-4.25	-5.88	-1.63	MgSO4:6H2O		
Kainite	-5.25	-5.45	-0.19	KMgClSO4:3H2O		
Kalichinit	-3.95	-14.01	-10.06	KHCO3		
Kieserite	-5.30	-5.42	-0.12	MgSO4:H2O		
Labile_S	-7.66	-13.33	-5.67	Na4Ca(SO4)3:2H2O		
Leonardite	-4.81	-5.70	-0.89	MgSO4:4H2O		
Leonite	-7.55	-11.53	-3.98	K2Mg(SO4)2:4H2O		
Magnesite	1.95	-5.88	-7.83	MgCO3		
Mirabilite	-3.72	-4.93	-1.21	Na2SO4:10H2O		
Misenite	-75.76	-86.57	-10.81	K8H6(SO4)7		
Nahcolite	-2.35	-13.10	-10.74	NaHCO3		
Natron	-4.66	-5.48	-0.82	Na2CO3:10H2O		
Nesquehonite	-0.99	-6.16	-5.17	MgCO3:3H2O		
Pentahydrite	-4.50	-5.79	-1.28	MgSO4:5H2O		
Pirssonite	-1.19	-10.43	-9.23	Na2Ca(CO3)2:2H2O		
Polyhalite	-7.86	-21.61	-13.74	K2MgCa2(SO4)4:2H2O		
Portlandite	-7.04	-12.23	-5.19	Ca(OH)2		
Schoenite	-7.38	-11.71	-4.33	K2Mg(SO4)2:6H2O		
Sylvite	-0.74	0.16	0.90	KCl		
Syngenite	-3.61	-11.05	-7.45	K2Ca(SO4)2:H2O		

Trona -6.46 -17.84 -11.38 Na3H(CO₃)₂:2H₂O

End of simulation.

Reading input data for simulation 11.

```
USE solution 8
EQUILIBRIUM_PHASES 8
CO2(g) -3.4 10
END
```

Beginning of batch-reaction calculations.

Reaction step 1.

Using solution 8. Just 1.2x's LSPW (no Tris)
Using pure phase assemblage 8.

-----Phase assemblage-----

Phase	SI	log IAP	log K(T, P)	Initial	Final	Delta
CO ₂ (g)	-3.40	-4.86	-1.46	1.000e+001	1.000e+001	-7.723e-006

-----Solution composition-----

Elements	Molality	Moles
C	7.723e-006	7.723e-006
Ca	6.287e-001	6.287e-001
Cl	5.020e+000	5.020e+000
K	5.945e-001	5.945e-001
Mg	2.642e-001	2.642e-001
Na	2.642e+000	2.642e+000
S	1.101e-003	1.101e-003

-----Description of solution-----
 pH = 5.404 Charge balance
 pe = 11.000 Adjusted to redox equilibrium
 Specific Conductance (uS/cm, 25 oC) = 505300
 Density (g/cm³) = 1.17504
 Volume (L) = 1.10105
 Activity of water = 0.811
 Ionic strength = 5.917e+000
 Mass of water (kg) = 1.000e+000
 Total alkalinity (eq/kg) = 1.696e-014
 Total CO₂ (mol/kg) = 7.723e-006
 Temperature (deg C) = 25.00
 Electrical balance (eq) = 1.808e-014
 Percent error, 100*(Cat-|An|)/(Cat+|An|) = 0.00
 Iterations = 15
 Gamma iterations = 4
 Osmotic coefficient = 1.27274
 Density of water = 0.99704
 Total H = 1.110124e+002
 Total O = 5.551064e+001

-----Distribution of species-----

Species	Molality	Unscaled			Gamma	cm ³ /mol
		Activity	Unscaled log	log		

H+	1.607e-006	3.940e-006	-5.794	-5.404	0.389	0.00
OH-	8.174e-009	2.073e-009	-8.088	-8.683	-0.596	3.75
H2O	5.551e+001	8.107e-001	1.744	-0.091	0.000	18.07
C(4)	7.723e-006					
CO2	6.283e-006	1.380e-005	-5.202	-4.860	0.342	30.26
HCO3-	1.436e-006	1.293e-006	-5.843	-5.888	-0.046	37.47
MgCO3	2.458e-009	2.458e-009	-8.609	-8.609	0.000	-17.09
CO3-2	1.430e-009	1.503e-011	-8.845	-10.823	-1.978	8.61
Ca	6.287e-001					
Ca+2	6.287e-001	3.056e-001	-0.202	-0.515	-0.313	-14.31
Cl	5.020e+000					
Cl-	5.020e+000	5.785e+000	0.701	0.762	0.062	20.08
K	5.945e-001					
K+	5.945e-001	2.465e-001	-0.226	-0.608	-0.382	12.09
Mg	2.642e-001					
Mg+2	2.642e-001	1.930e-001	-0.578	-0.714	-0.136	-17.81
MgOH+	1.652e-007	6.166e-008	-6.782	-7.210	-0.428	(0)
MgCO3	2.458e-009	2.458e-009	-8.609	-8.609	0.000	-17.09
Na	2.642e+000					
Na+	2.642e+000	2.001e+000	0.422	0.301	-0.121	1.39
S(6)	1.101e-003					
SO4-2	1.101e-003	2.429e-005	-2.958	-4.615	-1.656	26.78
HSO4-	1.025e-008	9.117e-009	-7.989	-8.040	-0.051	42.03

-----Saturation indices-----

Phase	SI	log IAP	log K(298 K, 1 atm)		
Anhydrite	-0.90	-5.13	-4.22	CaSO4	
Aragonite	-3.12	-11.34	-8.22	CaCO3	
Arcanite	-4.05	-5.83	-1.78	K2SO4	
Bischofite	-4.19	0.26	4.46	MgCl2:6H2O	
Bloedite	-7.36	-9.71	-2.35	Na2Mg(SO4)2:4H2O	
Brucite	-7.20	-18.08	-10.88	Mg(OH)2	
Burkeite	-17.47	-18.24	-0.77	Na6CO3(SO4)2	
Calcite	-2.93	-11.34	-8.41	CaCO3	
Carnallite	-3.91	0.42	4.33	KMgCl3:6H2O	
CO2(g)	-3.40	-4.86	-1.46	CO2	Pressure 0.0 atm, phi 1.000
Dolomite	-5.79	-22.88	-17.08	CaMg(CO3)2	
Epsomite	-4.09	-5.97	-1.88	MgSO4:7H2O	
Gaylussite	-12.59	-22.01	-9.42	CaNa2(CO3)2:5H2O	
Glaserite	-6.95	-10.75	-3.80	NaK3(SO4)2	
Glauberite	-3.90	-9.14	-5.25	Na2Ca(SO4)2	
Gypsum	-0.73	-5.31	-4.58	CaSO4:2H2O	
H2O(g)	-1.59	-0.09	1.50	H2O	
Halite	-0.51	1.06	1.57	NaCl	
Hexahydrite	-4.24	-5.88	-1.63	MgSO4:6H2O	
Kainite	-5.26	-5.45	-0.19	KMgClSO4:3H2O	
Kalicinite	-6.78	-16.84	-10.06	KHCO3	
Kieserite	-5.30	-5.42	-0.12	MgSO4:H2O	
Labile_S	-7.66	-13.34	-5.67	Na4Ca(SO4)3:2H2O	
Leonardite	-4.81	-5.69	-0.89	MgSO4:4H2O	
Leonite	-7.55	-11.52	-3.98	K2Mg(SO4)2:4H2O	
Magnesite	-3.70	-11.54	-7.83	MgCO3	
Mirabilite	-3.71	-4.92	-1.21	Na2SO4:10H2O	
Misenite	-58.79	-69.59	-10.81	K8H6(SO4)7	
Nahcolite	-5.18	-15.93	-10.74	NaHCO3	
Natron	-10.31	-11.13	-0.82	Na2CO3:10H2O	
Nesquehonite	-6.64	-11.81	-5.17	MgCO3:3H2O	
Pentahydrite	-4.50	-5.78	-1.28	MgSO4:5H2O	
Pirssonite	-12.51	-21.74	-9.23	Na2Ca(CO3)2:2H2O	
Polyhalite	-7.86	-21.60	-13.74	K2MgCa2(SO4)4:2H2O	
Portlandite	-12.69	-17.88	-5.19	Ca(OH)2	
Schoenite	-7.38	-11.71	-4.33	K2Mg(SO4)2:6H2O	
Sylvite	-0.75	0.15	0.90	KCl	
Syngenite	-3.60	-11.05	-7.45	K2Ca(SO4)2:H2O	
Trona	-14.95	-26.33	-11.38	Na3H(CO3)2:2H2O	

End of simulation.

Reading input data for simulation 12.

End of Run after 0.348 Seconds.

B.4 pH BUFFER SOLUTIONS

**Table B.1: As-Made Buffer Solutions for pH and pK'a Measurements
(Units are mol/kg water)**

Details	Solution	pH	mu	Na	K	Ca	Mg	Cl	SO ₄	Tris	si_halite	si_gypsum
NaCl solutions for molar absorptivity coefficient (ϵ) determinations												
no CO ₂	0.05	3.22	0.05	0.050	-	-	-	0.050	-	-	-4.35	-
log PCO ₂ = -3.4	0.05m	3.22	0.05	0.050	-	-	-	0.050	-	-	-4.35	-
no CO ₂	0.05m	11.11	0.12	0.101	-	-	-	0.050	-	-	-4.11	-
log PCO ₂ = -3.4	0.05m	9.61	0.11	0.101	-	-	-	0.050	-	-	-4.10	-
no CO ₂	1.0m	3.10	1.01	1.005	-	-	-	1.005	-	-	-1.93	-
log PCO ₂ = -3.4	1.0m	3.10	1.01	1.005	-	-	-	1.005	-	-	-1.93	-
no CO ₂	1.0m	10.87	1.07	1.050	-	-	-	1.000	-	-	-1.92	-
log PCO ₂ = -3.4	1.0m	9.38	1.06	1.050	-	-	-	1.000	-	-	-1.92	-
no CO ₂	5.0m	2.66	5.04	5.041	-	-	-	5.041	-	-	-0.28	-
log PCO ₂ = -3.4	5.0m	2.66	5.04	5.041	-	-	-	5.041	-	-	-0.28	-
no CO ₂	5.0m	10.69	5.07	5.046	-	-	-	4.996	-	-	-0.29	-
log PCO ₂ = -3.4	5.0m	9.19	5.06	5.047	-	-	-	4.997	-	-	-0.29	-
Buffer solutions containing only Tris/TrisHCl buffer (Just Tris)												
no CO ₂	1	7.10	0.05	-	-	-	-	0.046	-	0.0500	-	-
no CO ₂	2	7.29	0.04	-	-	-	-	0.044	-	0.0500	-	-
no CO ₂	3	7.43	0.04	-	-	-	-	0.042	-	0.0500	-	-
no CO ₂	4	7.43	0.04	-	-	-	-	0.042	-	0.0500	-	-
no CO ₂	5	7.65	0.04	-	-	-	-	0.038	-	0.0500	-	-
no CO ₂	6	7.86	0.03	-	-	-	-	0.033	-	0.0500	-	-
no CO ₂	7	8.04	0.03	-	-	-	-	0.028	-	0.0500	-	-
log PCO ₂ = -3.4	1	7.09	0.05	-	-	-	-	0.046	-	0.0500	-	-
log PCO ₂ = -3.4	2	7.28	0.04	-	-	-	-	0.044	-	0.0500	-	-
log PCO ₂ = -3.4	3	7.42	0.04	-	-	-	-	0.042	-	0.0500	-	-
log PCO ₂ = -3.4	4	7.42	0.04	-	-	-	-	0.042	-	0.0500	-	-
log PCO ₂ = -3.4	5	7.63	0.04	-	-	-	-	0.038	-	0.0500	-	-
log PCO ₂ = -3.4	6	7.84	0.03	-	-	-	-	0.033	-	0.0500	-	-
log PCO ₂ = -3.4	7	8.01	0.03	-	-	-	-	0.028	-	0.0500	-	-
NaCl buffer solutions for pH and pka measurements												
0.1 m NaCl												
no CO ₂	1	7.15	0.10	0.045	-	-	-	0.100	-	0.0600	-4.14	-
no CO ₂	2	7.49	0.10	0.050	-	-	-	0.100	-	0.0601	-4.09	-
no CO ₂	3	7.71	0.10	0.055	-	-	-	0.100	-	0.0599	-4.05	-

**Table B.1: As-Made Buffer Solutions for pH and pK'a Measurements
(Units are mol/kg water)**

Details	Solution	pH	mu	Na	K	Ca	Mg	Cl	SO ₄	Tris	si_halite	si_gypsum
no CO ₂	4	7.95	0.10	0.062	-	-	-	0.100	-	0.0599	-4.00	-
no CO ₂	5	8.13	0.10	0.068	-	-	-	0.100	-	0.0600	-3.96	-
no CO ₂	6	8.33	0.10	0.075	-	-	-	0.100	-	0.0598	-3.91	-
no CO ₂	7	8.49	0.10	0.080	-	-	-	0.100	-	0.0599	-3.89	-
no CO ₂	8	8.89	0.10	0.090	-	-	-	0.100	-	0.0598	-3.83	-
log PCO ₂ = -3.4	1	7.13	0.10	0.045	-	-	-	0.100	-	0.0600	-4.14	-
log PCO ₂ = -3.4	2	7.47	0.10	0.050	-	-	-	0.100	-	0.0601	-4.09	-
log PCO ₂ = -3.4	3	7.70	0.10	0.055	-	-	-	0.100	-	0.0599	-4.05	-
log PCO ₂ = -3.4	4	7.93	0.10	0.062	-	-	-	0.100	-	0.0599	-4.00	-
log PCO ₂ = -3.4	5	8.10	0.10	0.068	-	-	-	0.100	-	0.0600	-3.96	-
log PCO ₂ = -3.4	6	8.29	0.10	0.075	-	-	-	0.100	-	0.0598	-3.92	-
log PCO ₂ = -3.4	7	8.42	0.10	0.080	-	-	-	0.100	-	0.0599	-3.89	-
log PCO ₂ = -3.4	8	8.69	0.10	0.090	-	-	-	0.100	-	0.0598	-3.84	-
1.0 m NaCl												
no CO ₂	1	7.04	1.02	0.962	-	-	-	1.019	-	0.0600	-1.95	-
no CO ₂	2a	7.29	1.02	0.965	-	-	-	1.020	-	0.0599	-1.95	-
no CO ₂	2b	7.28	1.02	0.967	-	-	-	1.022	-	0.0600	-1.95	-
no CO ₂	3	7.51	1.03	0.975	-	-	-	1.027	-	0.0600	-1.94	-
no CO ₂	4	7.85	1.03	0.982	-	-	-	1.027	-	0.0600	-1.94	-
no CO ₂	5	8.02	1.03	0.988	-	-	-	1.028	-	0.0599	-1.93	-
no CO ₂	6	8.18	1.03	0.995	-	-	-	1.030	-	0.0599	-1.93	-
log PCO ₂ = -3.4	1	7.03	1.02	0.962	-	-	-	1.019	-	0.0600	-1.95	-
log PCO ₂ = -3.4	2a	7.27	1.02	0.965	-	-	-	1.020	-	0.0599	-1.95	-
log PCO ₂ = -3.4	2b	7.26	1.02	0.967	-	-	-	1.022	-	0.0600	-1.95	-
log PCO ₂ = -3.4	3	7.49	1.03	0.975	-	-	-	1.027	-	0.0600	-1.94	-
log PCO ₂ = -3.4	4	7.82	1.03	0.982	-	-	-	1.027	-	0.0600	-1.94	-
log PCO ₂ = -3.4	5	7.99	1.03	0.988	-	-	-	1.028	-	0.0599	-1.93	-
log PCO ₂ = -3.4	6	8.13	1.03	0.995	-	-	-	1.030	-	0.0599	-1.93	-
1.0 m NaCl												
no CO ₂	1	6.86	0.99	0.936	-	-	-	0.994	-	0.0600	-1.97	-
no CO ₂	2	7.18	1.00	0.944	-	-	-	1.000	-	0.0600	-1.96	-
no CO ₂	3	7.44	1.00	0.947	-	-	-	1.000	-	0.0600	-1.96	-
no CO ₂	4	7.62	1.00	0.950	-	-	-	1.000	-	0.0600	-1.96	-
no CO ₂	5	7.84	1.00	0.955	-	-	-	1.000	-	0.0600	-1.96	-
no CO ₂	6	8.02	1.00	0.960	-	-	-	1.000	-	0.0600	-1.96	-
log PCO ₂ = -3.4	1	6.84	0.99	0.936	-	-	-	0.994	-	0.0600	-1.97	-
log PCO ₂ = -3.4	2	7.16	1.00	0.944	-	-	-	1.000	-	0.0600	-1.96	-
log PCO ₂ = -3.4	3	7.42	1.00	0.947	-	-	-	1.000	-	0.0600	-1.96	-
log PCO ₂ = -3.4	4	7.60	1.00	0.950	-	-	-	1.000	-	0.0600	-1.96	-
log PCO ₂ = -3.4	5	7.81	1.00	0.955	-	-	-	1.000	-	0.0600	-1.96	-
log PCO ₂ = -3.4	6	7.98	1.00	0.960	-	-	-	1.000	-	0.0600	-1.96	-
5.0 m NaCl												
no CO ₂	1	6.87	5.00	4.942	-	-	-	5.000	-	0.0595	-0.30	-
no CO ₂	2	7.18	5.00	4.942	-	-	-	4.999	-	0.0600	-0.30	-
no CO ₂	3	7.41	5.00	4.944	-	-	-	4.999	-	0.0600	-0.30	-

**Table B.1: As-Made Buffer Solutions for pH and pK'a Measurements
(Units are mol/kg water)**

Details	Solution	pH	mu	Na	K	Ca	Mg	Cl	SO ₄	Tris	si_halite	si_gypsum
no CO ₂	4	7.64	5.00	4.948	-	-	-	5.000	-	0.0600	-0.30	-
no CO ₂	5	7.98	5.00	4.953	-	-	-	4.998	-	0.0600	-0.30	-
no CO ₂	6	8.16	5.00	4.959	-	-	-	4.999	-	0.0600	-0.30	-
log PCO ₂ = -3.4	1	6.84	5.00	4.942	-	-	-	5.000	-	0.0595	-0.30	-
log PCO ₂ = -3.4	2	7.15	5.00	4.942	-	-	-	4.999	-	0.0600	-0.30	-
log PCO ₂ = -3.4	3	7.38	5.00	4.944	-	-	-	4.999	-	0.0600	-0.30	-
log PCO ₂ = -3.4	4	7.61	5.00	4.948	-	-	-	5.000	-	0.0600	-0.30	-
log PCO ₂ = -3.4	5	7.93	5.00	4.953	-	-	-	4.998	-	0.0600	-0.30	-
log PCO ₂ = -3.4	6	8.09	5.00	4.959	-	-	-	4.999	-	0.0600	-0.30	-
L-SPW series buffer solutions for pH and pka measurements												
1.57x's L-SPW												
no CO ₂	1	6.94	7.67	3.405	0.766	0.810	0.341	6.520	0.0011	0.052	-0.11	-0.50
no CO ₂	2	7.12	7.67	3.405	0.766	0.810	0.341	6.520	0.0011	0.053	-0.11	-0.50
no CO ₂	3	7.26	7.67	3.405	0.766	0.810	0.341	6.519	0.0011	0.053	-0.11	-0.50
no CO ₂	4	7.45	7.67	3.405	0.766	0.810	0.341	6.517	0.0011	0.053	-0.11	-0.50
no CO ₂	5	7.65	7.67	3.405	0.766	0.810	0.341	6.514	0.0011	0.053	-0.11	-0.50
no CO ₂	6	7.94	7.66	3.405	0.766	0.810	0.341	6.508	0.0011	0.053	-0.11	-0.51
no CO ₂	7	8.45	7.65	3.405	0.766	0.810	0.341	6.493	0.0011	0.053	-0.11	-0.51
log PCO ₂ = -3.4	1	6.92	7.67	3.405	0.766	0.810	0.341	6.520	0.0011	0.052	-0.11	-0.50
log PCO ₂ = -3.4	2	7.11	7.67	3.405	0.766	0.810	0.341	6.520	0.0011	0.053	-0.11	-0.50
log PCO ₂ = -3.4	3	7.24	7.67	3.405	0.766	0.810	0.341	6.519	0.0011	0.053	-0.11	-0.50
log PCO ₂ = -3.4	4	7.42	7.67	3.405	0.766	0.810	0.341	6.517	0.0011	0.053	-0.11	-0.50
log PCO ₂ = -3.4	5	7.62	7.67	3.405	0.766	0.810	0.341	6.514	0.0011	0.053	-0.11	-0.50
log PCO ₂ = -3.4	6	7.87	7.66	3.405	0.766	0.810	0.341	6.508	0.0011	0.053	-0.11	-0.51
log PCO ₂ = -3.4	7	8.22	7.65	3.405	0.766	0.810	0.341	6.493	0.0011	0.053	-0.11	-0.51
no CO ₂	HCl 1	2.74	6.51	2.908	0.654	0.691	0.291	5.524	0.0010	-	-0.37	-0.69
1.45x's L-SPW												
no CO ₂	unbuffered	5.70	7.03	3.143	0.707	0.746	0.314	5.969	0.0011	0.000	-0.25	-0.58
no CO ₂	unbuffered	5.62	7.03	3.143	0.707	0.746	0.314	5.969	0.0011	0.000	-0.25	-0.59
no CO ₂	3	7.08	7.09	3.143	0.707	0.746	0.314	6.026	0.0011	0.060	-0.24	-0.58
no CO ₂	4	7.31	7.09	3.143	0.707	0.746	0.314	6.024	0.0011	0.060	-0.24	-0.58
no CO ₂	5	7.48	7.09	3.143	0.707	0.746	0.314	6.022	0.0011	0.060	-0.24	-0.58
no CO ₂	6	7.60	7.08	3.143	0.707	0.746	0.314	6.020	0.0011	0.060	-0.24	-0.58
no CO ₂	7	7.87	7.08	3.143	0.707	0.746	0.314	6.014	0.0011	0.060	-0.24	-0.58
no CO ₂	8	8.05	7.07	3.143	0.707	0.746	0.314	6.009	0.0011	0.060	-0.24	-0.59
no CO ₂	9	8.35	7.06	3.143	0.707	0.746	0.314	5.999	0.0011	0.060	-0.24	-0.59
log PCO ₂ = -3.4	3	7.06	7.09	3.143	0.707	0.746	0.314	6.026	0.0011	0.060	-0.24	-0.58
log PCO ₂ = -3.4	4	7.30	7.09	3.143	0.707	0.746	0.314	6.024	0.0011	0.060	-0.24	-0.58
log PCO ₂ = -3.4	5	7.46	7.09	3.143	0.707	0.746	0.314	6.022	0.0011	0.060	-0.24	-0.58
log PCO ₂ = -3.4	6	7.58	7.08	3.143	0.707	0.746	0.314	6.020	0.0011	0.060	-0.24	-0.58
log PCO ₂ = -3.4	7	7.83	7.08	3.143	0.707	0.746	0.314	6.014	0.0011	0.060	-0.24	-0.58
log PCO ₂ = -3.4	8	7.98	7.07	3.143	0.707	0.746	0.314	6.009	0.0011	0.060	-0.24	-0.59
log PCO ₂ = -3.4	9	8.19	7.06	3.143	0.707	0.746	0.314	6.000	0.0011	0.060	-0.24	-0.59
no CO ₂	HCl 1	2.64	7.26	3.244	0.730	0.771	0.324	6.162	0.0011	-	-0.20	-0.58

1.34x's L-SPW

**Table B.1: As-Made Buffer Solutions for pH and pK'a Measurements
(Units are mol/kg water)**

Details	Solution	pH	mu	Na	K	Ca	Mg	Cl	SO ₄	Tris	si_halite	si_gypsum
no CO ₂	1	6.90	6.53	2.890	0.650	0.687	0.289	5.548	0.0011	0.060	-0.37	-0.65
no CO ₂	2	7.32	6.53	2.890	0.650	0.687	0.289	5.546	0.0011	0.060	-0.37	-0.66
no CO ₂	3a	7.55	6.52	2.890	0.650	0.687	0.289	5.542	0.0011	0.060	-0.37	-0.66
no CO ₂	3b	7.55	6.52	2.890	0.650	0.687	0.289	5.543	0.0011	0.060	-0.37	-0.66
no CO ₂	3c	7.55	6.52	2.890	0.650	0.687	0.289	5.543	0.0011	0.060	-0.37	-0.66
no CO ₂	4	7.71	6.52	2.890	0.650	0.687	0.289	5.539	0.0011	0.060	-0.37	-0.66
no CO ₂	5	7.99	6.51	2.890	0.650	0.687	0.289	5.532	0.0011	0.060	-0.37	-0.66
no CO ₂	6	8.36	6.50	2.890	0.650	0.687	0.289	5.520	0.0011	0.060	-0.37	-0.66
no CO ₂	7	8.71	6.49	2.890	0.650	0.687	0.289	5.509	0.0011	0.060	-0.37	-0.67
no CO ₂	unbuffered	5.78	6.47	2.890	0.650	0.687	0.289	5.491	0.0011	0.000	-0.38	-0.66
log PCO ₂ = -3.4	1	6.89	6.53	2.890	0.650	0.687	0.289	5.549	0.0011	0.060	-0.37	-0.65
log PCO ₂ = -3.4	2	7.31	6.53	2.890	0.650	0.687	0.289	5.546	0.0011	0.060	-0.37	-0.66
log PCO ₂ = -3.4	3a	7.53	6.52	2.890	0.650	0.687	0.289	5.543	0.0011	0.060	-0.37	-0.66
log PCO ₂ = -3.4	3b	7.52	6.52	2.890	0.650	0.687	0.289	5.543	0.0011	0.060	-0.37	-0.66
log PCO ₂ = -3.4	3c	7.52	6.52	2.890	0.650	0.687	0.289	5.543	0.0011	0.060	-0.37	-0.66
log PCO ₂ = -3.4	4	7.68	6.52	2.890	0.650	0.687	0.289	5.540	0.0011	0.060	-0.37	-0.66
log PCO ₂ = -3.4	5	7.94	6.51	2.890	0.650	0.687	0.289	5.533	0.0011	0.060	-0.37	-0.66
log PCO ₂ = -3.4	6	8.22	6.50	2.890	0.650	0.687	0.289	5.521	0.0011	0.060	-0.37	-0.66
log PCO ₂ = -3.4	7	8.40	6.49	2.890	0.650	0.687	0.289	5.509	0.0011	0.060	-0.37	-0.66
no CO ₂	HCl 1a	1.42	6.48	2.887	0.650	0.687	0.289	5.499	0.0011	0.000	-0.37	-0.70
no CO ₂	HCl 1a	1.41	6.48	2.887	0.650	0.687	0.289	5.499	0.0011	0.000	-0.37	-0.70
1.22x's L-SPW												
no CO ₂	1	7.09	5.97	2.642	0.595	0.629	0.264	5.078	0.0011	0.060	-0.50	-0.73
no CO ₂	2	7.33	5.97	2.642	0.595	0.629	0.264	5.076	0.0011	0.060	-0.50	-0.73
no CO ₂	3	7.55	5.97	2.642	0.595	0.629	0.264	5.073	0.0011	0.060	-0.50	-0.73
no CO ₂	4	7.72	5.97	2.642	0.595	0.629	0.264	5.070	0.0011	0.060	-0.50	-0.73
no CO ₂	5	7.89	5.96	2.642	0.595	0.629	0.264	5.066	0.0011	0.060	-0.50	-0.73
no CO ₂	6	8.13	5.95	2.642	0.595	0.629	0.264	5.059	0.0011	0.060	-0.50	-0.73
no CO ₂	7	8.36	5.95	2.642	0.595	0.629	0.264	5.051	0.0011	0.060	-0.50	-0.74
no CO ₂	unbuffered	5.89	5.92	2.642	0.595	0.629	0.264	5.021	0.0011	0.000	-0.51	-0.73
log PCO ₂ = -3.4	1	7.07	5.97	2.642	0.595	0.629	0.264	5.078	0.0011	0.060	-0.50	-0.73
log PCO ₂ = -3.4	2	7.31	5.97	2.642	0.595	0.629	0.264	5.076	0.0011	0.060	-0.50	-0.73
log PCO ₂ = -3.4	3	7.53	5.97	2.642	0.595	0.629	0.264	5.073	0.0011	0.060	-0.50	-0.73
log PCO ₂ = -3.4	4	7.69	5.97	2.642	0.595	0.629	0.264	5.070	0.0011	0.060	-0.50	-0.73
log PCO ₂ = -3.4	5	7.85	5.96	2.642	0.595	0.629	0.264	5.066	0.0011	0.060	-0.50	-0.73
log PCO ₂ = -3.4	6	8.06	5.96	2.643	0.595	0.629	0.264	5.059	0.0011	0.060	-0.50	-0.73
log PCO ₂ = -3.4	7	8.23	5.95	2.643	0.595	0.629	0.264	5.051	0.0011	0.060	-0.50	-0.73
log PCO ₂ = -3.4	unbuffered	5.40	5.92	2.642	0.595	0.629	0.264	5.021	0.0011	0.000	-0.51	-0.73
1.22x's L-SPWb												
no CO ₂	1	7.09	5.97	2.642	0.595	0.629	0.264	5.078	0.0011	0.060	-0.50	-0.73
no CO ₂	2	7.33	5.97	2.642	0.595	0.629	0.264	5.076	0.0011	0.060	-0.50	-0.73
no CO ₂	3	7.55	5.97	2.642	0.595	0.629	0.264	5.073	0.0011	0.060	-0.50	-0.73
no CO ₂	4	7.72	5.97	2.642	0.595	0.629	0.264	5.070	0.0011	0.060	-0.50	-0.73
no CO ₂	5	7.89	5.96	2.642	0.595	0.629	0.264	5.066	0.0011	0.060	-0.50	-0.73
no CO ₂	6	8.13	5.95	2.642	0.595	0.629	0.264	5.059	0.0011	0.060	-0.50	-0.73
no CO ₂	7	8.36	5.95	2.642	0.595	0.629	0.264	5.051	0.0011	0.060	-0.50	-0.74

**Table B.1: As-Made Buffer Solutions for pH and pK'a Measurements
(Units are mol/kg water)**

Details	Solution	pH	mu	Na	K	Ca	Mg	Cl	SO ₄	Tris	si_halite	si_gypsum
no CO ₂	unbuffered	5.89	5.92	2.642	0.595	0.629	0.264	5.021	0.0011	0.000	-0.51	-0.73
log PCO ₂ = -3.4	1	7.08	5.97	2.642	0.595	0.629	0.264	5.078	0.0011	0.060	-0.50	-0.73
log PCO ₂ = -3.4	2	7.31	5.97	2.642	0.595	0.629	0.264	5.076	0.0011	0.060	-0.50	-0.73
log PCO ₂ = -3.4	3	7.53	5.97	2.642	0.595	0.629	0.264	5.073	0.0011	0.060	-0.50	-0.73
log PCO ₂ = -3.4	4	7.69	5.97	2.642	0.595	0.629	0.264	5.070	0.0011	0.060	-0.50	-0.73
log PCO ₂ = -3.4	5	7.85	5.96	2.642	0.595	0.629	0.264	5.066	0.0011	0.060	-0.50	-0.73
log PCO ₂ = -3.4	6	8.06	5.96	2.643	0.595	0.629	0.264	5.059	0.0011	0.060	-0.50	-0.73
log PCO ₂ = -3.4	7	8.23	5.95	2.643	0.595	0.629	0.264	5.051	0.0011	0.060	-0.50	-0.73
log PCO ₂ = -3.4	unbuffered	5.40	5.92	2.642	0.595	0.629	0.264	5.021	0.0011	0.000	-0.51	-0.73
L-SPW2 (less CaSO ₄ than LSPW)												
no CO ₂	1	6.92	4.90	2.163	0.487	0.515	0.216	4.167	0.0011	0.060	-0.77	-0.87
no CO ₂	2	7.23	4.90	2.163	0.487	0.515	0.216	4.165	0.0011	0.060	-0.77	-0.87
no CO ₂	3	7.50	4.90	2.163	0.487	0.515	0.216	4.162	0.0011	0.060	-0.77	-0.87
no CO ₂	4	7.68	4.89	2.163	0.487	0.515	0.216	4.159	0.0011	0.060	-0.77	-0.87
no CO ₂	5	7.90	4.89	2.163	0.487	0.515	0.216	4.154	0.0011	0.060	-0.77	-0.87
no CO ₂	6	8.14	4.88	2.163	0.487	0.515	0.216	4.147	0.0011	0.060	-0.77	-0.87
no CO ₂	7	8.37	4.87	2.163	0.487	0.515	0.216	4.139	0.0011	0.060	-0.77	-0.87
no CO ₂	unbuffered	6.11	4.84	2.163	0.487	0.515	0.216	4.109	0.0011	0.000	-0.78	-0.87
log PCO ₂ = -3.4	1	6.90	4.90	2.163	0.487	0.515	0.216	4.167	0.0011	0.060	-0.77	-0.87
log PCO ₂ = -3.4	2	7.22	4.90	2.163	0.487	0.515	0.216	4.165	0.0011	0.060	-0.77	-0.87
log PCO ₂ = -3.4	3	7.48	4.90	2.163	0.487	0.515	0.216	4.162	0.0011	0.060	-0.77	-0.87
log PCO ₂ = -3.4	4	7.65	4.89	2.163	0.487	0.515	0.216	4.159	0.0011	0.060	-0.77	-0.87
log PCO ₂ = -3.4	5	7.86	4.89	2.163	0.487	0.515	0.216	4.154	0.0011	0.060	-0.77	-0.87
log PCO ₂ = -3.4	6	8.08	4.88	2.163	0.487	0.515	0.216	4.147	0.0011	0.060	-0.77	-0.87
log PCO ₂ = -3.4	7	8.26	4.88	2.163	0.487	0.515	0.216	4.139	0.0011	0.060	-0.77	-0.87
log PCO ₂ = -3.4	unbuffered	5.46	4.84	2.163	0.487	0.515	0.216	4.109	0.0011	0.000	-0.78	-0.87
L-SPW												
no CO ₂	1a	6.92	4.95	2.163	0.487	0.525	0.216	4.188	0.0054	0.069	-0.76	-0.16
no CO ₂	1b	6.91	4.88	2.098	0.492	0.525	0.216	4.119	0.0054	0.060	-0.79	-0.17
no CO ₂	2a	7.33	4.94	2.163	0.487	0.525	0.216	4.185	0.0054	0.069	-0.77	-0.16
no CO ₂	2b	7.33	4.88	2.107	0.487	0.524	0.216	4.119	0.0054	0.060	-0.79	-0.17
no CO ₂	3	7.56	4.94	2.163	0.487	0.525	0.216	4.181	0.0054	0.069	-0.77	-0.16
no CO ₂	4	7.68	4.94	2.163	0.487	0.525	0.216	4.179	0.0054	0.069	-0.77	-0.16
no CO ₂	4b	7.68	4.94	2.163	0.487	0.525	0.216	4.179	0.0054	0.069	-0.77	-0.16
no CO ₂	5	8.07	4.93	2.163	0.487	0.525	0.216	4.168	0.0054	0.069	-0.77	-0.17
no CO ₂	6	8.37	4.91	2.163	0.487	0.525	0.216	4.156	0.0054	0.069	-0.77	-0.17
no CO ₂	7	8.67	4.90	2.163	0.487	0.525	0.216	4.145	0.0054	0.069	-0.77	-0.17
no CO ₂	8	9.06	4.89	2.163	0.487	0.525	0.216	4.133	0.0054	0.069	-0.77	-0.17
log PCO ₂ = -3.4	1a	6.91	4.95	2.163	0.487	0.525	0.216	4.188	0.0054	0.069	-0.76	-0.16
log PCO ₂ = -3.4	1b	6.90	4.88	2.098	0.492	0.525	0.216	4.119	0.0054	0.060	-0.79	-0.17
log PCO ₂ = -3.4	2a	7.32	4.94	2.163	0.487	0.525	0.216	4.185	0.0054	0.069	-0.77	-0.16
log PCO ₂ = -3.4	2b	7.32	4.88	2.107	0.487	0.524	0.216	4.119	0.0054	0.060	-0.79	-0.17
log PCO ₂ = -3.4	3	7.55	4.94	2.163	0.487	0.525	0.216	4.182	0.0054	0.069	-0.77	-0.16
log PCO ₂ = -3.4	4	7.66	4.94	2.163	0.487	0.525	0.216	4.179	0.0054	0.069	-0.77	-0.16
log PCO ₂ = -3.4	4b	7.66	4.94	2.163	0.487	0.525	0.216	4.179	0.0054	0.069	-0.77	-0.16
log PCO ₂ = -3.4	5	8.03	4.93	2.163	0.487	0.525	0.216	4.168	0.0054	0.069	-0.77	-0.17

**Table B.1: As-Made Buffer Solutions for pH and pK'a Measurements
(Units are mol/kg water)**

Details	Solution	pH	mu	Na	K	Ca	Mg	Cl	SO ₄	Tris	si_halite	si_gypsum
log PCO ₂ = -3.4	6	8.27	4.92	2.163	0.487	0.525	0.216	4.156	0.0054	0.069	-0.77	-0.17
log PCO ₂ = -3.4	7	8.45	4.91	2.163	0.487	0.525	0.216	4.145	0.0054	0.069	-0.77	-0.17
log PCO ₂ = -3.4	8	8.59	4.90	2.164	0.487	0.525	0.216	4.134	0.0054	0.069	-0.77	-0.17
no CO ₂	HCl 1	3.43	4.78	2.120	0.477	0.515	0.212	4.040	0.0053	-	-0.80	-0.18
no CO ₂	HCl 2	3.06	4.64	2.055	0.462	0.499	0.206	3.916	0.0051	-	-0.84	-0.21
no CO ₂	HCl 3	1.61	4.89	2.161	0.486	0.524	0.216	4.131	0.0054	0.000	-0.77	-0.19
0.73x's L-SPW												
no CO ₂	1	6.91	3.61	1.588	0.357	0.378	0.159	3.075	0.0008	0.060	-1.14	-1.15
no CO ₂	2	7.23	3.61	1.588	0.357	0.378	0.159	3.073	0.0008	0.060	-1.14	-1.15
no CO ₂	3	7.50	3.61	1.588	0.357	0.378	0.159	3.070	0.0008	0.060	-1.14	-1.15
no CO ₂	4	7.68	3.61	1.588	0.357	0.378	0.159	3.067	0.0008	0.060	-1.14	-1.15
no CO ₂	5	7.90	3.60	1.588	0.357	0.378	0.159	3.062	0.0008	0.060	-1.14	-1.15
no CO ₂	6	8.14	3.59	1.588	0.357	0.378	0.159	3.055	0.0008	0.060	-1.14	-1.15
no CO ₂	7	8.38	3.59	1.588	0.357	0.378	0.159	3.047	0.0008	0.060	-1.14	-1.16
no CO ₂	unbuffered	6.36	3.56	1.588	0.357	0.378	0.159	3.017	0.0008	0.000	-1.15	-1.15
log PCO ₂ = -3.4	1	6.90	3.61	1.588	0.357	0.378	0.159	3.075	0.0008	0.060	-1.14	-1.15
log PCO ₂ = -3.4	2	7.22	3.61	1.588	0.357	0.378	0.159	3.073	0.0008	0.060	-1.14	-1.15
log PCO ₂ = -3.4	3	7.48	3.61	1.588	0.357	0.378	0.159	3.070	0.0008	0.060	-1.14	-1.15
log PCO ₂ = -3.4	4	7.66	3.61	1.588	0.357	0.378	0.159	3.067	0.0008	0.060	-1.14	-1.15
log PCO ₂ = -3.4	5	7.87	3.60	1.588	0.357	0.378	0.159	3.062	0.0008	0.060	-1.14	-1.15
log PCO ₂ = -3.4	6	8.09	3.60	1.588	0.357	0.378	0.159	3.055	0.0008	0.060	-1.14	-1.15
log PCO ₂ = -3.4	7	8.28	3.59	1.588	0.357	0.378	0.159	3.047	0.0008	0.060	-1.14	-1.16
log PCO ₂ = -3.4	unbuffered	5.51	3.56	1.588	0.357	0.378	0.159	3.017	0.0008	0.000	-1.15	-1.15
0.48x's L-SPW												
no CO ₂	1	6.90	2.38	1.038	0.234	0.247	0.104	2.030	0.0005	0.060	-1.58	-1.46
no CO ₂	2	7.22	2.38	1.038	0.234	0.247	0.104	2.028	0.0005	0.060	-1.58	-1.46
no CO ₂	3	7.41	2.38	1.038	0.234	0.247	0.104	2.026	0.0005	0.060	-1.58	-1.46
no CO ₂	4	7.67	2.37	1.038	0.234	0.247	0.104	2.022	0.0005	0.060	-1.58	-1.46
no CO ₂	5	7.89	2.37	1.038	0.234	0.247	0.104	2.017	0.0005	0.060	-1.58	-1.46
no CO ₂	6	8.07	2.36	1.038	0.234	0.247	0.104	2.012	0.0005	0.060	-1.59	-1.46
no CO ₂	7	8.37	2.35	1.038	0.234	0.247	0.104	2.002	0.0005	0.060	-1.59	-1.46
no CO ₂	unbuffered	6.58	2.32	1.038	0.234	0.247	0.104	1.972	0.0005	0.000	-1.60	-1.45
log PCO ₂ = -3.4	1	6.89	2.38	1.038	0.234	0.247	0.104	2.030	0.0005	0.060	-1.58	-1.46
log PCO ₂ = -3.4	2	7.21	2.38	1.038	0.234	0.247	0.104	2.028	0.0005	0.060	-1.58	-1.46
log PCO ₂ = -3.4	3	7.39	2.38	1.038	0.234	0.247	0.104	2.026	0.0005	0.060	-1.58	-1.46
log PCO ₂ = -3.4	4	7.65	2.37	1.038	0.234	0.247	0.104	2.022	0.0005	0.060	-1.58	-1.46
log PCO ₂ = -3.4	5	7.86	2.37	1.038	0.234	0.247	0.104	2.017	0.0005	0.060	-1.58	-1.46
log PCO ₂ = -3.4	6	8.03	2.37	1.038	0.234	0.247	0.104	2.012	0.0005	0.060	-1.59	-1.46
log PCO ₂ = -3.4	7	8.29	2.36	1.038	0.234	0.247	0.104	2.002	0.0005	0.060	-1.59	-1.46
log PCO ₂ = -3.4	unbuffered	5.56	2.32	1.038	0.234	0.247	0.104	1.972	0.0005	0.000	-1.60	-1.45
0.24x's L-SPW												
no CO ₂	1	6.87	1.20	0.510	0.115	0.121	0.051	1.026	0.0003	0.060	-2.22	-1.87
no CO ₂	2	7.19	1.20	0.510	0.115	0.121	0.051	1.024	0.0003	0.060	-2.22	-1.87
no CO ₂	3	7.38	1.20	0.510	0.115	0.121	0.051	1.022	0.0003	0.060	-2.22	-1.87
no CO ₂	4a	7.52	1.19	0.510	0.115	0.121	0.051	1.020	0.0003	0.060	-2.22	-1.87

**Table B.1: As-Made Buffer Solutions for pH and pK'a Measurements
(Units are mol/kg water)**

Details	Solution	pH	mu	Na	K	Ca	Mg	Cl	SO ₄	Tris	si_halite	si_gypsum
no CO ₂	4b	7.52	1.19	0.510	0.115	0.121	0.051	1.020	0.0003	0.060	-2.22	-1.87
no CO ₂	4c	7.52	1.19	0.510	0.115	0.121	0.051	1.020	0.0003	0.060	-2.22	-1.87
no CO ₂	5	7.73	1.19	0.510	0.115	0.121	0.051	1.016	0.0003	0.060	-2.22	-1.87
no CO ₂	6	8.03	1.18	0.510	0.115	0.121	0.051	1.008	0.0003	0.060	-2.23	-1.87
no CO ₂	unbuffered	6.77	1.14	0.510	0.115	0.121	0.051	0.968	0.0003	0.000	-2.24	-1.85
log PCO ₂ = -3.4	1	6.85	1.20	0.510	0.115	0.121	0.051	1.026	0.0003	0.060	-2.22	-1.87
log PCO ₂ = -3.4	2	7.18	1.20	0.510	0.115	0.121	0.051	1.024	0.0003	0.060	-2.22	-1.87
log PCO ₂ = -3.4	3	7.36	1.20	0.510	0.115	0.121	0.051	1.022	0.0003	0.060	-2.22	-1.87
log PCO ₂ = -3.4	4a	7.50	1.19	0.510	0.115	0.121	0.051	1.020	0.0003	0.060	-2.22	-1.87
log PCO ₂ = -3.4	4b	7.51	1.19	0.510	0.115	0.121	0.051	1.020	0.0003	0.060	-2.22	-1.87
log PCO ₂ = -3.4	4c	7.50	1.19	0.510	0.115	0.121	0.051	1.020	0.0003	0.060	-2.22	-1.87
log PCO ₂ = -3.4	5	7.71	1.19	0.510	0.115	0.121	0.051	1.016	0.0003	0.060	-2.22	-1.87
log PCO ₂ = -3.4	6	8.00	1.18	0.510	0.115	0.121	0.051	1.008	0.0003	0.060	-2.23	-1.87
log PCO ₂ = -3.4	unbuffered	5.59	1.14	0.510	0.115	0.121	0.051	0.968	0.0003	0.000	-2.24	-1.85
0.09x's L-SPW												
no CO ₂	1a	6.89	0.50	0.202	0.0454	0.0480	0.0202	0.432	0.0001	0.050	-2.96	-2.34
no CO ₂	1b	6.90	0.50	0.202	0.0454	0.0480	0.0202	0.432	0.0001	0.050	-2.96	-2.34
no CO ₂	2	7.21	0.50	0.202	0.0454	0.0480	0.0202	0.429	0.0001	0.050	-2.97	-2.34
no CO ₂	3	7.41	0.50	0.202	0.0454	0.0480	0.0202	0.427	0.0001	0.050	-2.97	-2.34
no CO ₂	4	7.56	0.49	0.202	0.0454	0.0480	0.0202	0.425	0.0001	0.050	-2.97	-2.33
no CO ₂	5	7.78	0.49	0.202	0.0454	0.0480	0.0202	0.422	0.0001	0.050	-2.97	-2.33
no CO ₂	6	8.10	0.48	0.202	0.0454	0.0480	0.0202	0.413	0.0001	0.050	-2.98	-2.33
no CO ₂	unbuffered	6.87	0.45	0.202	0.0454	0.0480	0.0202	0.383	0.0001	0.000	-3.01	-2.30
log PCO ₂ = -3.4	1a	6.87	0.50	0.202	0.0454	0.0480	0.0202	0.432	0.0001	0.050	-2.96	-2.34
log PCO ₂ = -3.4	1b	6.88	0.50	0.202	0.0454	0.0480	0.0202	0.432	0.0001	0.050	-2.96	-2.34
log PCO ₂ = -3.4	2	7.20	0.50	0.202	0.0454	0.0480	0.0202	0.429	0.0001	0.050	-2.97	-2.34
log PCO ₂ = -3.4	3	7.39	0.50	0.202	0.0454	0.0480	0.0202	0.427	0.0001	0.050	-2.97	-2.34
log PCO ₂ = -3.4	4	7.54	0.49	0.202	0.0454	0.0480	0.0202	0.425	0.0001	0.050	-2.97	-2.33
log PCO ₂ = -3.4	5	7.75	0.49	0.202	0.0454	0.0480	0.0202	0.422	0.0001	0.050	-2.97	-2.33
log PCO ₂ = -3.4	6	8.06	0.48	0.202	0.0454	0.0480	0.0202	0.413	0.0001	0.050	-2.98	-2.33
log PCO ₂ = -3.4	unbuffered	5.60	0.45	0.202	0.0454	0.0480	0.0202	0.383	0.0001	0.000	-3.01	-2.30
0.01x's L-SPW												
no CO ₂	1	6.81	0.09	0.020	0.0045	0.0049	0.0020	0.086	0.0001	0.050	-4.55	-2.69
no CO ₂	2	7.13	0.09	0.020	0.0045	0.0049	0.0020	0.084	0.0001	0.050	-4.56	-2.69
no CO ₂	3	7.32	0.09	0.020	0.0045	0.0049	0.0020	0.082	0.0001	0.050	-4.57	-2.68
no CO ₂	4	7.47	0.09	0.020	0.0045	0.0049	0.0020	0.080	0.0001	0.050	-4.58	-2.67
no CO ₂	5	7.68	0.08	0.020	0.0045	0.0049	0.0020	0.076	0.0001	0.050	-4.59	-2.66
no CO ₂	6	7.68	0.08	0.020	0.0045	0.0049	0.0020	0.076	0.0001	0.050	-4.59	-2.66
no CO ₂	7	8.00	0.07	0.020	0.0045	0.0049	0.0020	0.068	0.0001	0.049	-4.64	-2.63
no CO ₂	unbuffered	6.97	0.05	0.020	0.0045	0.0049	0.0020	0.038	0.0001	0.000	-4.85	-2.49
log PCO ₂ = -3.4	1	6.80	0.09	0.020	0.0045	0.0049	0.0020	0.086	0.0001	0.050	-4.55	-2.69
log PCO ₂ = -3.4	2	7.12	0.09	0.020	0.0045	0.0049	0.0020	0.084	0.0001	0.050	-4.56	-2.69
log PCO ₂ = -3.4	3	7.30	0.09	0.020	0.0045	0.0049	0.0020	0.082	0.0001	0.050	-4.57	-2.68
log PCO ₂ = -3.4	4	7.45	0.09	0.020	0.0045	0.0049	0.0020	0.080	0.0001	0.050	-4.58	-2.68
log PCO ₂ = -3.4	5	7.66	0.08	0.020	0.0045	0.0049	0.0020	0.076	0.0001	0.050	-4.59	-2.66
log PCO ₂ = -3.4	6	7.66	0.08	0.020	0.0045	0.0049	0.0020	0.076	0.0001	0.050	-4.59	-2.66

**Table B.1: As-Made Buffer Solutions for pH and pK'a Measurements
(Units are mol/kg water)**

Details	Solution	pH	mu	Na	K	Ca	Mg	Cl	SO ₄	Tris	si_halite	si_gypsum
log PCO ₂ = -3.4	7	7.97	0.08	0.020	0.0045	0.0049	0.0020	0.068	0.0001	0.049	-4.64	-2.63
log PCO ₂ = -3.4	unbuffered	5.60	0.05	0.020	0.0045	0.0049	0.0020	0.038	0.0001	0.000	-4.85	-2.49
S-SPW buffer solutions for pH and pka measurements												
S-SPW												
no CO ₂	1	6.97	8.22	2.702	0.563	1.352	0.282	6.588	0.0011	0.060	-0.14	-0.33
no CO ₂	2	7.31	8.22	2.702	0.563	1.352	0.282	6.585	0.0011	0.060	-0.14	-0.33
no CO ₂	3	7.50	8.22	2.702	0.563	1.352	0.282	6.582	0.0011	0.060	-0.14	-0.33
no CO ₂	4a	7.70	8.21	2.702	0.563	1.352	0.282	6.578	0.0011	0.060	-0.14	-0.33
no CO ₂	4b	7.70	8.21	2.702	0.563	1.352	0.282	6.578	0.0011	0.060	-0.14	-0.33
no CO ₂	5	7.89	8.21	2.702	0.563	1.352	0.282	6.573	0.0011	0.060	-0.14	-0.33
no CO ₂	6	8.05	8.20	2.702	0.563	1.352	0.282	6.568	0.0011	0.060	-0.14	-0.33
no CO ₂	7	8.25	8.20	2.702	0.563	1.352	0.282	6.561	0.0011	0.060	-0.14	-0.33
no CO ₂	unbuffered	5.57	8.17	2.702	0.563	1.352	0.282	6.531	0.0011	0.000	-0.15	-0.33
log PCO ₂ = -3.4	1	6.97	8.22	2.702	0.563	1.352	0.282	6.588	0.0011	0.060	-0.14	-0.33
log PCO ₂ = -3.4	2	7.29	8.22	2.702	0.563	1.352	0.282	6.585	0.0011	0.060	-0.14	-0.33
log PCO ₂ = -3.4	3	7.49	8.22	2.702	0.563	1.352	0.282	6.582	0.0011	0.060	-0.14	-0.33
log PCO ₂ = -3.4	4	7.67	8.21	2.702	0.563	1.352	0.282	6.578	0.0011	0.060	-0.14	-0.33
log PCO ₂ = -3.4	5	7.67	8.22	2.702	0.563	1.352	0.282	6.578	0.0011	0.060	-0.14	-0.33
log PCO ₂ = -3.4	6	7.84	8.21	2.702	0.563	1.352	0.282	6.573	0.0011	0.060	-0.14	-0.33
log PCO ₂ = -3.4	7	7.98	8.21	2.703	0.563	1.352	0.282	6.568	0.0011	0.060	-0.14	-0.33
log PCO ₂ = -3.4	8	8.13	8.20	2.703	0.563	1.352	0.282	6.561	0.0011	0.060	-0.14	-0.33
log PCO ₂ = -3.4	unbuffered	5.38	8.17	2.702	0.563	1.352	0.282	6.531	0.0011	0.000	-0.15	-0.33
no CO ₂	HCl 1	3.16	8.01	2.649	0.552	1.326	0.276	6.402	0.0011	0.000	-0.18	-0.36
log PCO ₂ = -3.4	HCl 1	3.16	8.01	2.649	0.552	1.326	0.276	6.402	0.0011	0.000	-0.18	-0.36
no CO ₂	HCl 2	2.88	7.85	2.598	0.541	1.300	0.271	6.278	0.0011	0.000	-0.21	-0.39
log PCO ₂ = -3.4	HCl 2	2.88	7.85	2.598	0.541	1.300	0.271	6.28	0.0011	0.000	-0.21	-0.39
0.81x's S-SPW												
no CO ₂	1	7.14	6.68	2.190	0.4563	1.0961	0.2282	5.350	0.00091	0.060	-0.48	-0.60
no CO ₂	2	7.34	6.67	2.190	0.4563	1.0961	0.2282	5.348	0.00091	0.060	-0.48	-0.60
no CO ₂	3	7.54	6.67	2.190	0.4563	1.0961	0.2282	5.345	0.00091	0.060	-0.48	-0.60
no CO ₂	4	7.74	6.67	2.190	0.4563	1.0961	0.2282	5.341	0.00091	0.060	-0.48	-0.60
no CO ₂	5	7.93	6.66	2.190	0.4563	1.0961	0.2282	5.335	0.00091	0.060	-0.48	-0.60
no CO ₂	unbuffered	5.24	6.62	2.190	0.4563	1.0961	0.2282	5.294	0.00091	0.000	-0.49	-0.60
log PCO ₂ = -3.4	1	7.14	6.68	2.190	0.4563	1.0961	0.2282	5.350	0.00091	0.060	-0.48	-0.60
log PCO ₂ = -3.4	2	7.33	6.67	2.190	0.4563	1.0961	0.2282	5.348	0.00091	0.060	-0.48	-0.60
log PCO ₂ = -3.4	3	7.52	6.67	2.190	0.4563	1.0961	0.2282	5.345	0.00091	0.060	-0.48	-0.60
log PCO ₂ = -3.4	4	7.71	6.67	2.190	0.4563	1.0961	0.2282	5.341	0.00091	0.060	-0.48	-0.60
log PCO ₂ = -3.4	5	7.89	6.66	2.190	0.4563	1.0961	0.2282	5.336	0.00091	0.060	-0.48	-0.60
log PCO ₂ = -3.4	unbuffered	5.16	6.62	2.190	0.4563	1.0961	0.2282	5.294	0.00091	0.000	-0.49	-0.60
0.60x's S-SPW												
no CO ₂	1	7.05	4.96	1.620	0.338	0.812	0.169	3.974	0.0007	0.060	-0.90	-0.92
no CO ₂	2	7.38	4.95	1.620	0.338	0.812	0.169	3.971	0.0007	0.060	-0.90	-0.92
no CO ₂	3	7.58	4.95	1.620	0.338	0.812	0.169	3.968	0.0007	0.060	-0.90	-0.92
no CO ₂	4	7.77	4.95	1.620	0.338	0.812	0.169	3.964	0.0007	0.060	-0.90	-0.93
no CO ₂	5a	7.96	4.94	1.620	0.338	0.812	0.169	3.959	0.0007	0.060	-0.90	-0.93

**Table B.1: As-Made Buffer Solutions for pH and pK'a Measurements
(Units are mol/kg water)**

Details	Solution	pH	mu	Na	K	Ca	Mg	Cl	SO ₄	Tris	si_halite	si_gypsum
no CO ₂	5b	7.96	4.94	1.620	0.338	0.812	0.169	3.959	0.0007	0.060	-0.90	-0.93
no CO ₂	6	8.18	4.93	1.620	0.338	0.812	0.169	3.952	0.0007	0.060	-0.91	-0.93
no CO ₂	unbuffered	6.19	4.90	1.620	0.338	0.812	0.169	3.917	0.0007	0.000	-0.91	-0.93
log PCO ₂ = -3.4	1	7.04	4.96	1.620	0.338	0.812	0.169	3.974	0.0007	0.060	-0.90	-0.92
log PCO ₂ = -3.4	2	7.36	4.95	1.620	0.338	0.812	0.169	3.971	0.0007	0.060	-0.90	-0.92
log PCO ₂ = -3.4	3	7.56	4.95	1.620	0.338	0.812	0.169	3.968	0.0007	0.060	-0.90	-0.92
log PCO ₂ = -3.4	4	7.75	4.95	1.620	0.338	0.812	0.169	3.964	0.0007	0.060	-0.90	-0.93
log PCO ₂ = -3.4	5a	7.93	4.94	1.620	0.338	0.812	0.169	3.959	0.0007	0.060	-0.90	-0.93
log PCO ₂ = -3.4	5b	7.93	4.94	1.620	0.338	0.812	0.169	3.960	0.0007	0.060	-0.90	-0.93
log PCO ₂ = -3.4	6	8.12	4.94	1.620	0.338	0.812	0.169	3.953	0.0007	0.060	-0.91	-0.93
log PCO ₂ = -3.4	unbuffered	5.56	4.90	1.620	0.338	0.812	0.169	3.917	0.0007	0.000	-0.91	-0.93
0.36x's S-SPW												
	soln	pH	mu	Na	K	Ca	Mg	Cl	S(6)	Tris	si_halite	si_gypsum
no CO ₂	1	7.15	2.96	0.974	0.1591	0.4875	0.1015	2.367	0.00041	0.060	-1.50	-1.35
no CO ₂	2	7.44	2.95	0.974	0.1591	0.4875	0.1015	2.364	0.00041	0.060	-1.50	-1.35
no CO ₂	3	7.63	2.95	0.974	0.1591	0.4875	0.1015	2.360	0.00041	0.059	-1.50	-1.35
no CO ₂	4	7.82	2.95	0.974	0.1591	0.4875	0.1015	2.357	0.00041	0.060	-1.50	-1.35
no CO ₂	5	7.99	2.94	0.974	0.1591	0.4875	0.1015	2.352	0.00041	0.060	-1.51	-1.36
no CO ₂	6	8.22	2.94	0.974	0.1591	0.4875	0.1015	2.345	0.00041	0.060	-1.51	-1.36
no CO ₂	unbuffered	7.12	2.90	0.974	0.1591	0.4875	0.1015	2.310	0.00041	0.000	-1.51	-1.35
log PCO ₂ = -3.4	1	7.14	2.96	0.974	0.1591	0.4875	0.1015	2.367	0.00041	0.060	-1.50	-1.35
log PCO ₂ = -3.4	2	7.42	2.95	0.974	0.1591	0.4875	0.1015	2.364	0.00041	0.060	-1.50	-1.35
log PCO ₂ = -3.4	3	7.62	2.95	0.974	0.1591	0.4875	0.1015	2.360	0.00041	0.059	-1.50	-1.35
log PCO ₂ = -3.4	4	7.79	2.95	0.974	0.1591	0.4875	0.1015	2.357	0.00041	0.060	-1.50	-1.35
log PCO ₂ = -3.4	5	7.96	2.94	0.974	0.1591	0.4875	0.1015	2.352	0.00041	0.060	-1.51	-1.36
log PCO ₂ = -3.4	6	8.17	2.94	0.974	0.1591	0.4875	0.1015	2.345	0.00041	0.060	-1.51	-1.36
log PCO ₂ = -3.4	unbuffered	5.70	2.90	0.974	0.1591	0.4875	0.1015	2.310	0.00041	0.000	-1.51	-1.35
0.03x's S-SPW												
no CO ₂	1	7.04	0.28	0.076	0.0158	0.0381	0.0079	0.231	0.00003	0.050	-3.62	-2.73
no CO ₂	2	7.38	0.27	0.076	0.0158	0.0381	0.0079	0.228	0.00003	0.050	-3.63	-2.73
no CO ₂	3	7.58	0.27	0.076	0.0158	0.0381	0.0079	0.225	0.00003	0.050	-3.63	-2.73
no CO ₂	4	7.79	0.27	0.076	0.0158	0.0381	0.0079	0.221	0.00003	0.050	-3.64	-2.72
no CO ₂	5	7.99	0.26	0.076	0.0158	0.0381	0.0079	0.216	0.00003	0.050	-3.64	-2.72
no CO ₂	6	8.24	0.25	0.076	0.0158	0.0381	0.0079	0.209	0.00003	0.050	-3.66	-2.71
no CO ₂	unbuffered	7.05	0.23	0.076	0.0158	0.0381	0.0079	0.184	0.00003	0.000	-3.70	-2.68
log PCO ₂ = -3.4	1	7.03	0.28	0.076	0.0158	0.0381	0.0079	0.231	0.00003	0.050	-3.62	-2.73
log PCO ₂ = -3.4	2	7.36	0.27	0.076	0.0158	0.0381	0.0079	0.228	0.00003	0.050	-3.63	-2.73
log PCO ₂ = -3.4	3	7.57	0.27	0.076	0.0158	0.0381	0.0079	0.225	0.00003	0.050	-3.63	-2.73
log PCO ₂ = -3.4	4	7.76	0.27	0.076	0.0158	0.0381	0.0079	0.221	0.00003	0.050	-3.64	-2.73
log PCO ₂ = -3.4	5	7.96	0.26	0.076	0.0158	0.0381	0.0079	0.216	0.00003	0.050	-3.64	-2.72
log PCO ₂ = -3.4	6	8.19	0.26	0.076	0.0158	0.0381	0.0079	0.209	0.00003	0.050	-3.66	-2.71
log PCO ₂ = -3.4	unbuffered	5.62	0.23	0.076	0.0158	0.0381	0.0079	0.184	0.00003	0.000	-3.70	-2.68

B.5 POTENTIOMETRIC pH MEASUREMENTS

Table B.2: Results from Potentiometric pH Measurements of HCl and Tris Buffer Series

Just Tris	Ross 815600 + Barnant 20 meter							
	1	2	3	4	5a	5b	6	° C
<i>I</i> (mol/kg)	0.05	0.04	0.04	0.04	0.04	0.03	0.03	
modelled pH, no CO ₂	7.10	7.29	7.43	7.43	7.65	7.86	8.04	25.00
modelled pH, log PCO ₂ = -3.4	7.09	7.28	7.42	7.42	7.63	7.84	8.01	25.00
measured pH	9-Jan-14	7.08	7.28	7.42	7.42	7.64	7.86	8.04
measured pH	10-Jan-14	7.08	7.28	7.42	7.42	7.64	7.86	8.04
measured pH	10-Jan-14	7.06	7.26	7.41	7.41	7.63	7.85	8.03
measured pH	Mean	7.07	7.27	7.42	7.42	7.64	7.86	8.04
measured pH	σ	0.01	0.01	0.01	0.01	0.01	0.01	0.26
mV	9-Jan-14	-18	-30	-38	-38	-51	-63	-74
mV	10-Jan-14	-18	-30	-38	-38	-51	-64	-74
mV	10-Jan-14	-17	-29	-38	-38	-51	-63	-74
mV	Mean	-18	-30	-38	-38	-51	-63	-74
mV	σ	1	1	0	0	0	1	0
SureFlow + Jenco Model-5005 meter								
	1	2	3	4	5a	5b	6	
measured pH	9-Jan-14	7.08	7.28	7.42	7.43	7.65	7.86	8.05
measured pH	10-Jan-14	7.08	7.28	7.43	7.43	7.65	7.87	8.06
measured pH	10-Jan-14	7.06	7.26	7.41	7.41	7.63	7.85	8.03
measured pH	Mean	7.07	7.27	7.42	7.42	7.64	7.86	8.05
measured pH	σ	0.01	0.01	0.01	0.01	0.01	0.01	0.02
mV	9-Jan-14	1	-10	-18	-18	-31	-44	-54
mV	10-Jan-14	1	-10	-18	-18	-31	-44	-55
mV	10-Jan-14	2	-9	-18	-18	-31	-43	-54
mV	Mean	1	-10	-18	-18	-31	-44	-54
mV	σ	1	1	0	0	0	1	1
0.1m NaCl	Ross 815600 + Barnant 20 meter							
	1	2	3	4	5	6	7	8
<i>I</i> (mol/kg)	0.10	0.10	0.10	0.10	0.10	0.10	0.10	0.10
modelled pH, no CO ₂	7.15	7.49	7.71	7.95	8.13	8.33	8.49	8.89
modelled pH, log PCO ₂ = -3.4	7.13	7.48	7.69	7.93	8.10	8.29	8.42	8.69
measured pH	9-Sep-13	7.14	7.49	7.71	7.95	8.14	8.34	8.50
measured pH	11-Sep-13	7.12	7.47	7.70	7.94	8.13	8.33	8.49
measured pH	13-Sep-13	7.10	7.44	7.68	7.92	8.10	8.31	8.47
measured pH	Mean	7.12	7.47	7.70	7.94	8.12	8.33	8.49
measured pH	σ	0.02	0.03	0.02	0.02	0.02	0.02	0.01
mV	9-Sep-13	-13	-33	-46	-60	-70	-83	-92
mV	11-Sep-13	-13	-33	-46	-60	-70	-83	-92
mV	13-Sep-13	-11	-32	-44	-59	-69	-81	-91
mV	Mean	-12	-33	-45	-60	-70	-82	-92
mV	σ	1	1	1	1	1	1	0
1.0m NaCl	Ross 815600 + Barnant 20 meter							
	1	2	3	4	5	6	° C	
<i>I</i> (mol/kg)	1.02	1.02	1.03	1.03	1.03	1.03		
modelled pH, no CO ₂	7.04	7.28	7.51	7.85	8.02	8.18	25.00	
modelled pH, log PCO ₂ = -3.4	7.03	7.26	7.49	7.82	7.99	8.13	25.00	

Table B.2: Results from Potentiometric pH Measurements of HCl and Tris Buffer Series

measured pH	18-Sep-13	6.98	7.24	7.47	7.81	7.99	8.14	23.70
measured pH	24-Sep-13	6.94	7.19	7.42	7.77	7.95	8.11	25.10
measured pH	24-Sep-13	6.94	7.19	7.42	7.77	7.95	8.11	24.60
measured pH	Mean	6.95	7.21	7.44	7.78	7.96	8.12	
measured pH	σ	0.02	0.03	0.03	0.02	0.02	0.02	
mV	18-Sep-13	-5	-20	-33	-52	-63	-72	
mV	24-Sep-13	-2	-16	-30	-50	-61	-70	
mV	24-Sep-13	-3	-17	-30	-50	-60	-70	
mV	Mean	-3	-18	-31	-51	-61	-71	
mV	σ	2	2	2	1	2	1	
<hr/>								
1.0m NaCl	Ross 815600 + Barnant 20 meter							
		1	2	3	4	5	6	° C
	I (mol/kg)	0.99	1.00	1.00	1.00	1.00	1.00	
modelled pH, no CO ₂		6.86	7.18	7.44	7.62	7.84	8.02	25.00
modelled pH, log PCO ₂ = -3.4		6.84	7.16	7.42	7.60	7.81	7.98	25.00
measured pH	13-Jan-14	6.77	7.10	7.37	7.55	7.78	7.96	24.61
measured pH	13-Jan-14	6.76	7.08	7.36	7.54	7.77	7.95	24.69
measured pH	14-Jan-14	6.75	7.08	7.35	7.53	7.76	7.94	24.64
measured pH	Mean	6.76	7.09	7.36	7.54	7.77	7.95	24.65
measured pH	σ	0.01	0.01	0.01	0.01	0.01	0.01	0.04
mV	18-Sep-13	0	-19	-35	-46	-59	-69	
mV	24-Sep-13	1	-18	-34	-45	-58	-68	
mV	24-Sep-13	1	-18	-34	-45	-58	-68	
mV	Mean	1	-18	-34	-45	-58	-68	
mV	σ	1	1	1	1	1	1	
	SureFlow + Jenco Model-5005 meter							
measured pH	13-Jan-14	6.84	7.16	7.42	7.60	7.81	7.98	
measured pH	13-Jan-14	6.76	7.09	7.36	7.54	7.76	7.94	
measured pH	14-Jan-14	6.75	7.07	7.35	7.53	7.76	7.93	
measured pH	Mean	6.73	7.07	7.34	7.52	7.75	7.93	
measured pH	σ	6.75	7.08	7.35	7.53	7.76	7.93	
mV	18-Sep-13	0.02	0.01	0.01	0.01	0.01	0.01	
mV	24-Sep-13	19	0	-15	-25	-39	-49	
mV	24-Sep-13	20	1	-14	-25	-38	-48	
mV	Mean	20	1	-14	-27	-38	-48	
mV	σ	20	1	-14	-26	-38	-48	
		1	1	1	1	1	1	
<hr/>								
5.0m NaCl	Ross 815600 + Barnant 20 meter							
	I (mol/kg)	5.00	5.00	5.00	5.00	5.00	5.00	° C
modelled pH, no CO ₂		6.87	7.18	7.41	7.64	7.98	8.15	25.00
modelled pH, log PCO ₂ = -3.4		6.84	7.15	7.38	7.61	7.93	8.09	25.00
measured pH	27-Sep-13	6.63	6.94	7.18	7.42	7.76	7.94	25.55
measured pH	30-Sep-13	6.62	6.93	7.17	7.41	7.75	7.93	25.32
measured pH	1-Oct-13	6.63	6.94	7.18	7.41	7.76	7.94	25.20
measured pH	Mean	6.63	6.94	7.18	7.41	7.76	7.94	25.36
measured pH	σ	0.01	0.01	0.01	0.01	0.01	0.01	0.18
mV	27-Sep-13	15	-3	-17	-31	-51	-61	
mV	30-Sep-13	16	-3	-17	-30	-50	-61	
mV	1-Oct-13	15	-3	-17	-31	-50	-61	
mV	Mean	15	-3	-17	-31	-50	-61	
mV	σ	1	0	0	1	1	0	

Table B.2: Results from Potentiometric pH Measurements of HCl and Tris Buffer Series

1.57x's L-SPW		Ross 815600 + Barnant 20 meter										
		HCl	1	2	3a	3b	4	5	6	7a	7b	° C
	I (mol/kg)	7.26	7.67	7.67	7.67	7.67	7.67	7.67	7.66	7.65	7.65	
modelled pH, no CO ₂		2.64	6.94	7.12	7.26	7.26	7.45	7.65	7.94	8.45	8.45	25.00
modelled pH, log PCO ₂ = -3.4		2.64	6.92	7.11	7.24	7.24	7.42	7.62	7.87	8.22	8.22	25.00
measured pH	13-Nov-13	-	6.4	6.58	6.72	6.72	6.91	7.12	7.41	7.94	7.94	25.07
measured pH	14-Nov-13	-	6.38	6.56	6.69	6.69	6.89	7.1	7.39	7.92	7.92	25.08
measured pH	15-Nov-13	-	6.36	6.55	6.7	6.7	6.9	7.11	7.4	7.93	7.93	25.09
measured pH	21-Nov-13	2.14	-	-	-	-	-	-	-	-	-	
measured pH	Mean	2.14	6.38	6.56	6.70	6.70	6.90	7.11	7.40	7.93	7.93	25.08
measured pH	σ	NA	0.02	0.02	0.02	0.02	0.01	0.01	0.01	0.01	0.01	0.01
mV	13-Nov-13	-	26	16	8	8	-4	-16	-32	-63	-63	
mV	14-Nov-13	-	27	17	9	9	-3	-15	-32	-63	-63	
mV	15-Nov-13	-	28	18	9	9	-3	-15	-32	-63	-63	
mV	Mean	272	27	17	9	9	-3	-15	-32	-63	-63	
mV	σ	NA	1	1	1	1	1	1	0	0	0	

Table B.2: Results from Potentiometric pH Measurements of HCl and Tris Buffer Series

		HCl	1	2	3a	3b	4	5	6	7a	7b	
measured pH	13-Nov-13	-	6.39	6.57	6.70	6.70	6.90	7.10	7.39	7.92	7.92	
measured pH	14-Nov-13	-	6.38	6.55	6.69	6.69	6.89	7.1	7.39	7.92	7.92	
measured pH	15-Nov-13	-	6.34	6.53	6.68	6.68	6.88	7.09	7.38	7.9	7.91	
measured pH	21-Nov-13	2.15	-	-	-	-	-	-	-	-	-	
measured pH	Mean	2.15	6.37	6.55	6.69	6.69	6.89	7.10	7.39	7.91	7.92	
measured pH	σ	NA	0.03	0.02	0.01	0.01	0.01	0.01	0.01	0.01	0.01	0.01
mV	13-Nov-13	-	45	34	27	27	15	3	-13	-43	-43	
mV	14-Nov-13	-	45	35	27	27	16	4	-12	-43	-43	
mV	15-Nov-13	-	47	36	28	28	16	4	-12	-43	-43	
mV	Mean	291	46	35	27	27	16	4	-12	-43	-43	
mV	σ	NA	1	1	1	1	1	1	1	0	0	0
1.45x's L-SPW		Ross 815600 + Barnant 20 meter										
		HCl	1	2	3	4	5	6	7a	°C		
	I (mol/kg)	6.51	7.09	7.09	7.09	7.08	7.08	7.07	7.06			
modelled pH, no CO ₂	2.74	7.08	7.31	7.48	7.60	7.87	8.05	8.35	25.00			
modelled pH, log PCO ₂ = -3.4	2.74	7.06	7.30	7.46	7.58	7.83	7.98	8.19	25.00			
measured pH	19-Nov-13	-	6.55	6.80	6.96	7.09	7.37	7.55	7.86	24.64		
measured pH	20-Nov-13	-	6.54	6.79	6.95	7.08	7.36	7.54	7.85	25.19		
measured pH	20-Nov-13	-	6.55	6.80	6.96	7.09	7.38	7.56	7.86	24.34		
measured pH	21-Nov-13	2.23	-	-	-	-	-	-	-			
measured pH	Mean	2.23	6.55	6.80	6.96	7.09	7.37	7.55	7.86	24.72		
measured pH	σ	NA	0.01	0.01	0.01	0.01	0.01	0.01	0.01	0.01	0.43	
mV	19-Nov-13	-	16	3	-7	-15	-31	-41	-59			
mV	20-Nov-13	-	17	3	-7	-14	-30	-41	-59			
mV	20-Nov-13	-	16	3	-7	-15	-31	-42	-60			
mV	21-Nov-13	267	-	-	-	-	-	-	-			
mV	Mean	267	16	3	-7	-15	-31	-41	-59			
mV	σ	NA	1	0	0	1	1	1	1			
SureFlow + Jenco Model-5005 meter		Ross 815600 + Barnant 20 meter										
		HCl	1	2	3	4	5	6	7			
measured pH	19-Nov-13	-	6.55	6.79	6.95	7.08	7.36	7.54	7.84			
measured pH	20-Nov-13	-	6.53	6.77	6.94	7.06	7.33	7.52	7.83			
measured pH	20-Nov-13	-	6.54	6.78	6.95	7.08	7.36	7.54	7.85			
measured pH	21-Nov-13	2.24	-	-	-	-	-	-	-			
measured pH	Mean	2.24	6.54	6.78	6.95	7.07	7.35	7.53	7.84			
measured pH	σ	NA	0.01	0.01	0.01	0.01	0.02	0.01	0.01			
mV	19-Nov-13	-	35	21	12	5	-11	-21	-39			
mV	20-Nov-13	-	36	22	13	5	-10	-20	-38			
mV	20-Nov-13	-	36	22	12	5	-11	-21	-39			
mV	Mean	286	36	22	12	5	-11	-21	-39			
mV	σ	NA	1	1	1	0	1	1	1			
1.34x's L-SPW		Ross 815600 + Barnant 20 meter										
		HCl1a	HCl1b	1	2	3a	3b	3c	4	5	6	7 °C
	I (mol/kg)	6.48	6.48	6.53	6.53	6.52	6.52	6.52	6.51	6.50	6.49	###
modelled pH, no CO ₂	1.42	1.41	6.90	7.32	7.55	7.55	7.55	7.71	7.99	8.36	8.71	25.00
modelled pH, log PCO ₂ = -3.4	1.42	1.41	6.89	7.31	7.53	7.52	7.52	7.68	7.94	8.22	8.40	25.00
measured pH	27-Nov-13	-	6.40	6.83	7.07	7.07	7.07	7.23	7.52	7.90	8.27	24.73
measured pH	28-Nov-13	-	6.41	6.84	7.08	7.08	7.07	7.25	7.53	7.91	8.28	24.88
measured pH	28-Nov-13	-	6.40	6.83	7.07	7.07	7.06	7.23	7.52	7.90	8.27	24.87
measured pH	3-Feb-14	0.94	0.94	-	-	-	-	-	-	-	-	25.18
measured pH	4-Feb-14	0.95	0.95	-	-	-	-	-	-	-	-	24.96
measured pH	4-Feb-14	0.95	0.95	-	-	-	-	-	-	-	-	25.18
measured pH	Mean	0.95	0.95	6.40	6.83	7.07	7.07	7.07	7.24	7.52	7.90	24.83
measured pH	σ	0.01	0.01	0.01	0.01	0.01	0.01	0.01	0.01	0.01	0.01	0.18
mV	27-Nov-13	-	-	24	0	-14	-14	-14	-24	-41	-62	-84
mV	28-Nov-13	-	-	25	0	-14	-14	-13	-24	-40	-62	-84
mV	28-Nov-13	-	-	25	0	-14	-14	-14	-24	-40	-62	-84
mV	3-Feb-14	337	337	-	-	-	-	-	-	-	-	-
mV	4-Feb-15	337	337	-	-	-	-	-	-	-	-	-
mV	4-Feb-15	337	337	-	-	-	-	-	-	-	-	-
mV	Mean	337	337	25	0	-14	-14	-14	-24	-40	-62	-84
mV	σ	0	0	1	0	0	0	1	0	1	0	0
SureFlow + Jenco Model-5005 meter		Ross 815600 + Barnant 20 meter										
		HCl1a	HCl1b	1	2	3a	3b	3c	4	5	6	7
measured pH	27-Nov-13	-	-	6.40	6.83	7.06	7.06	7.06	7.23	7.52	7.89	8.27

Table B.2: Results from Potentiometric pH Measurements of HCl and Tris Buffer Series

measured pH	28-Nov-13	-	-	6.39	6.83	7.06	7.06	7.06	7.24	7.54	7.92	8.31
measured pH	28-Nov-13	-	-	6.39	6.81	7.05	7.05	7.05	7.22	7.51	7.80	8.25
measured pH	3-Feb-14	0.93	0.93	-	-	-	-	-	-	-	-	-
measured pH	4-Feb-14	0.95	0.95	-	-	-	-	-	-	-	-	-
measured pH	4-Feb-14	0.95	0.96	-	-	-	-	-	-	-	-	-
measured pH	Mean	0.94	0.95	6.39	6.82	7.06	7.06	7.06	7.23	7.52	7.87	8.28
measured pH	σ	0.01	0.02	0.01	0.01	0.01	0.01	0.01	0.01	0.02	0.06	0.03
mV	27-Nov-13	-	-	44	19	6	5	6	-3	-20	-42	-64
mV	28-Nov-13	-	-	44	19	6	6	6	-4	-20	-42	-64
mV	28-Nov-13	-	-	44	19	6	6	6	-3	-20	-42	-63
mV	3-Feb-14	356	356	-	-	-	-	-	-	-	-	-
mV	4-Feb-14	355	355	-	-	-	-	-	-	-	-	-
mV	4-Feb-14	356	355	-	-	-	-	-	-	-	-	-
mV	Mean	356	355	44	19	6	6	6	-3	-20	-42	-64
mV	σ	1	1	0	0	0	1	0	1	0	0	1
1.22x's L-SPW	Ross 815600 + Barnant 20 meter											
		1	2	3	4	5	6	7	°C			
	I (mol/kg)	5.97	5.97	5.97	5.97	5.96	5.95	5.95	25.00			
modelled pH, no CO ₂		7.09	7.33	7.55	7.72	7.89	8.13	8.36	25.00			
modelled pH, log PCO ₂ = -3.4		7.07	7.31	7.53	7.69	7.85	8.06	8.23	25.00			
measured pH	3-Dec-13	6.64	6.88	7.11	7.28	7.45	7.70	7.94	24.36			
measured pH	4-Dec-13	6.63	6.87	7.10	7.27	7.44	7.69	7.93	24.87			
measured pH	4-Dec-13	6.63	6.87	7.10	7.27	7.45	7.69	7.93	24.83			
measured pH	6-Dec-13	6.63	6.87	7.11	7.28	7.45	7.70	7.94	24.57			
measured pH	Mean	6.63	6.87	7.11	7.28	7.45	7.70	7.94	24.69			
measured pH	σ	0.00	0.00	0.01	0.01	0.00	0.01	0.01	0.24			
mV	3-Dec-13	10	-4	-17	-27	-37	-51	-65				
mV	4-Dec-13	11	-3	-17	-26	-37	-51	-65				
mV	4-Dec-13	11	-3	-17	-27	-37	-51	-65				
mV	6-Dec-13	11	-3	-17	-27	-37	-51	-65				
mV	Mean	11	-3	-17	-27	-37	-51	-65				
mV	σ	1	1	0	1	0	0	0				
	SureFlow + Jenco Model-5005 meter											
		1	2	3	4	5	6	7				
measured pH	3-Dec-13	6.63	6.87	7.10	7.27	7.45	7.69	7.93				
measured pH	4-Dec-13	6.62	6.86	7.10	7.26	7.44	7.68	7.93				
measured pH	4-Dec-13	6.62	6.86	7.09	7.26	7.43	7.68	7.92				
measured pH	6-Dec-13	6.62	6.86	7.09	7.26	7.44	7.69	7.94				
measured pH	Mean	6.62	6.86	7.10	7.26	7.44	7.68	7.93				
measured pH	σ	0.00	0.00	0.01	0.00	0.01	0.01	0.01				
mV	3-Dec-13	30	16	2	-7	-17	-31	-45				
mV	4-Dec-13	30	16	3	-6	-16	-30	-45				
mV	4-Dec-13	30	16	3	-6	-16	-30	-44				
mV	6-Dec-13	30	16	3	-6	-17	-31	-45				
mV	Mean	30	16	3	-6	-17	-31	-45				
mV	σ	0	0	1	1	1	1	1				
1.22x's L-SPWb	Ross 815600 + Barnant 20 meter											
		1	2	3	4	5	6	7	temp			
	I (mol/kg)	5.97	5.97	5.97	5.97	5.96	5.95	5.95	25.00			
modelled pH, no CO ₂		7.09	7.33	7.55	7.72	7.89	8.13	8.36	25.00			
modelled pH, log PCO ₂ = -3.4		7.08	7.31	7.53	7.69	7.85	8.06	8.23	25.00			
measured pH	4-Mar-14	6.63	6.87	7.11	7.27	7.45	7.69	7.94	25.07			
measured pH	5-Mar-14	6.61	6.86	7.09	7.26	7.44	7.68	7.92	24.95			
measured pH	5-Mar-14	6.61	6.86	7.09	7.26	7.43	7.68	7.92	25.00			
measured pH	Mean	6.62	6.86	7.10	7.26	7.44	7.68	7.93	25.01			
measured pH	σ	0.01	0.01	0.01	0.01	0.01	0.01	0.01	0.06			
mV	4-Mar-14	5	-9	-23	-32	-42	-57	-71				
mV	5-Mar-14	6	-9	-22	-32	-42	-57	-70				
mV	5-Mar-14	6	-9	-22	-32	-42	-57	-70				
mV	Mean	6	-9	-22	-32	-42	-57	-70				
mV	σ	1	0	1	0	0	0	1				
L-SPW2	Ross 815600 + Barnant 20 meter											
		1	2	3	4	5	6	7	°C			
	I (mol/kg)	4.90	4.90	4.90	4.89	4.89	4.88	4.87	25.00			
modelled pH, no CO ₂		6.92	7.23	7.50	7.68	7.90	8.14	8.37	25.00			

Table B.2: Results from Potentiometric pH Measurements of HCl and Tris Buffer Series

modelled pH, log PCO ₂ = -3.4	6.91	7.22	7.48	7.65	7.86	8.08	8.26	25.00
measured pH 9-Dec-13	6.52	6.84	7.11	7.29	7.52	7.76	8.00	24.87
measured pH 10-Dec-13	-	-	-	-	-	-	-	24.91
measured pH 10-Dec-13	6.52	6.84	7.11	7.30	7.52	7.77	8.01	24.58
measured pH Mean	6.52	6.84	7.11	7.30	7.52	7.77	8.01	24.79
measured pH σ	0.00	0.00	0.00	0.01	0.00	0.01	0.01	0.18
mV 9-Dec-13	16	-2	-18	-29	-42	-56	-70	
mV 10-Dec-13	-	-	-	-	-	-	-	
mV 10-Dec-13	17	-2	-18	-29	-41	-56	-70	
mV Mean	17	-2	-18	-29	-42	-56	-70	
mV σ	1	0	0	1	0	0	0	
SureFlow + Jenco Model-5005 meter								
	1	2	3	4	5	6	7	
measured pH 9-Dec-13	6.51	6.84	7.11	7.29	7.52	7.76	8.00	
measured pH 10-Dec-13	6.50	6.83	7.10	7.28	7.51	7.75	7.99	
measured pH 10-Dec-13	6.51	6.83	7.10	7.28	7.51	7.76	8.00	
measured pH Mean	6.51	6.83	7.10	7.28	7.51	7.76	8.00	
measured pH σ	0.01	0.01	0.01	0.01	0.01	0.01	0.01	
mV 9-Dec-13	36	17	2	-8	-21	-35	-49	
mV 10-Dec-13	37	18	2	-8	-21	-35	-49	
mV 10-Dec-13	36	18	2	-8	-21	-35	-49	
mV Mean	36	18	2	-8	-21	-35	-49	
mV σ	1	1	0	0	0	0	0	
0.75x L-SPW	Ross 815600 + Barnant 20 meter							
	1	2	3	4	5	6	7	°C
I (mol/kg)	3.61	3.61	3.61	3.61	3.60	3.59	3.59	
modelled pH, no CO ₂	6.91	7.23	7.50	7.68	7.90	8.14	8.38	25.00
modelled pH, log PCO ₂ = -3.4	6.90	7.22	7.48	7.66	7.87	8.09	8.28	25.00
measured pH 12-Dec-13	6.61	6.93	7.20	7.39	7.61	7.86	8.10	24.87
measured pH 13-Dec-13	6.60	6.92	7.20	7.38	7.61	7.85	8.09	24.49
measured pH 13-Dec-13	6.59	6.91	7.19	7.37	7.60	7.84	8.08	24.86
measured pH Mean	6.60	6.92	7.20	7.38	7.61	7.85	8.09	24.74
measured pH σ	0.01	0.01	0.01	0.01	0.01	0.01	0.01	0.22
mV 12-Dec-13	12	-7	-23	-34	-47	-61	-75	
mV 13-Dec-13	12	-7	-23	-34	-47	-61	-75	
mV 13-Dec-13	13	-7	-23	-33	-46	-61	-75	
mV Mean	12	-7	-23	-34	-47	-61	-75	
mV σ	1	0	0	1	1	0	0	
SureFlow + Jenco Model-5005 meter								
	1	2	3	4	5	6	7	
measured pH 12-Dec-13	6.59	6.92	7.19	7.37	7.60	7.84	8.08	
measured pH 13-Dec-13	6.60	6.92	7.19	7.38	7.61	7.86	8.11	
measured pH 13-Dec-13	6.58	6.90	7.18	7.37	7.59	7.84	8.08	
measured pH Mean	6.59	6.91	7.19	7.37	7.60	7.85	8.09	
measured pH σ	0.01	0.01	0.01	0.01	0.01	0.01	0.02	
mV 12-Dec-13	31	12	-2	-13	-26	-40	-54	
mV 13-Dec-13	31	12	-3	-13	-26	-41	-55	
mV 13-Dec-13	32	13	-2	-13	-26	-40	-54	
mV Mean	31	12	-2	-13	-26	-40	-54	
mV σ	1	1	1	0	0	1	1	
0.48x's L-SPW	Ross 815600 + Barnant 20 meter							
	1	2	3	4	5	6	7	°C
I (mol/kg)	2.38	2.38	2.38	2.37	2.37	2.36	2.35	
modelled pH, no CO ₂	6.90	7.22	7.41	7.67	7.89	8.07	8.37	25.00
modelled pH, log PCO ₂ = -3.4	6.89	7.21	7.39	7.65	7.86	8.03	8.29	25.00
measured pH 17-Dec-13	6.68	7.00	7.20	7.46	7.68	7.86	8.16	24.17
measured pH 18-Dec-13	6.66	6.97	7.17	7.43	7.66	7.84	8.14	24.90
measured pH 18-Dec-13	6.65	6.97	7.17	7.43	7.66	7.84	8.15	25.04
measured pH 27-Dec-13	6.68	7.01	7.20	7.46	7.68	7.86	8.17	24.91
measured pH Mean	6.67	6.99	7.19	7.45	7.67	7.85	8.16	24.70
measured pH σ	0.01	0.02	0.02	0.02	0.01	0.01	0.01	0.40
mV 17-Dec-13	6	-12	-24	-39	-52	-62	-80	
mV 18-Dec-13	8	-11	-22	-38	-51	-61	-79	
mV 18-Dec-13	9	-10	-22	-37	-51	-61	-79	
mV 27-Dec-13	6	-13	-24	-39	-52	-62	-80	
mV Mean	7	-12	-23	-38	-52	-62	-80	

Table B.2: Results from Potentiometric pH Measurements of HCl and Tris Buffer Series

mV	σ	2	1	1	1	1	1	1
SureFlow + Jenco Model-5005 meter								
		1	2	3	4	5	6	7
measured pH	17-Dec-13	6.67	7.00	7.19	7.45	7.67	7.85	8.16
measured pH	18-Dec-13	6.65	6.97	7.17	7.43	7.66	7.84	8.14
measured pH	18-Dec-13	6.64	6.96	7.16	7.43	7.65	7.83	8.14
measured pH	27-Dec-13	6.66	6.99	7.18	7.44	7.66	7.84	8.15
measured pH	Mean	6.65	6.98	7.17	7.44	7.66	7.84	8.15
measured pH	σ	0.01	0.02	0.01	0.01	0.01	0.01	0.01
mV	17-Dec-13	26	7	-3	-18	-31	-42	-59
mV	18-Dec-13	27	9	-2	-17	-30	-41	-59
mV	18-Dec-13	28	9	-2	-17	-30	-40	-58
mV	27-Dec-13	26	7	-3	-18	-31	-42	-60
mV	Mean	27	8	-3	-18	-31	-41	-59
mV	σ	1	1	1	1	1	1	1
0.24x's L-SPW								
Ross 815600 + Barnant 20 meter								
		1	2	3	4a	4b	4c	5
	I (mol/kg)	1.20	1.20	1.20	1.19	1.19	1.19	1.19
modelled pH, no CO ₂		6.87	7.19	7.38	7.52	7.52	7.73	8.03
modelled pH, log PCO ₂ = -3.4		6.85	7.18	7.36	7.50	7.51	7.71	8.00
measured pH	19-Dec-13	6.73	7.05	7.24	7.38	7.38	7.60	7.90
measured pH	20-Dec-13	6.71	7.03	7.23	7.37	7.37	7.58	7.89
measured pH	20-Dec-13	6.70	7.03	7.22	7.37	7.37	7.59	7.89
measured pH	Mean	6.71	7.04	7.23	7.37	7.37	7.59	7.89
measured pH	σ	0.02	0.01	0.01	0.01	0.01	0.01	0.01
mV	19-Dec-13	4	-15	-26	-34	-34	-46	-64
mV	20-Dec-13	6	-13	-25	-33	-33	-46	-64
mV	20-Dec-13	6	-13	-25	-33	-33	-46	-64
mV	Mean	5	-14	-25	-33	-33	-46	-64
mV	σ	1	1	1	1	0	0	0
SureFlow + Jenco Model-5005 meter								
		1	2	3	4a	4b	4c	5
measured pH	19-Dec-13	6.71	7.04	7.23	7.37	7.37	7.36	7.58
measured pH	20-Dec-13	6.69	7.02	7.22	7.36	7.36	7.36	7.57
measured pH	20-Dec-13	6.68	7.02	7.21	7.36	7.36	7.36	7.58
measured pH	Mean	6.69	7.03	7.22	7.36	7.36	7.36	7.58
measured pH	σ	0.02	0.01	0.01	0.01	0.01	0.00	0.01
mV	19-Dec-13	23	5	-6	-14	-14	-14	-26
mV	20-Dec-13	25	6	-5	-13	-13	-13	-26
mV	20-Dec-13	25	6	-4	-13	-13	-13	-26
mV	Mean	24	6	-5	-13	-13	-13	-26
mV	σ	1	1	1	1	1	0	1
0.09x's L-SPW								
Ross 815600 + Barnant 20 meter								
		1a	1b	2	3	4	5	6
	I (mol/kg)	0.50	0.50	0.50	0.50	0.49	0.49	0.48
modelled pH, no CO ₂		6.89	6.90	7.21	7.41	7.56	7.78	8.10
modelled pH, log PCO ₂ = -3.4		6.87	6.88	7.20	7.39	7.54	7.75	8.06
measured pH	2-Jan-14	6.80	6.81	7.13	7.33	7.48	7.70	8.03
measured pH	3-Jan-14	6.79	6.78	7.11	7.32	7.46	7.69	8.02
measured pH	3-Jan-14	6.78	6.79	7.12	7.31	7.46	7.69	8.02
measured pH	Mean	6.79	6.79	7.12	7.32	7.47	7.69	8.02
measured pH	σ	0.01	0.02	0.01	0.01	0.01	0.01	0.15
mV	2-Jan-14	-2	-2	-21	-32	-41	-54	-73
mV	3-Jan-14	-1	-1	-20	-31	-40	-53	-72
mV	3-Jan-14	-1	-1	-20	-32	-40	-53	-73
mV	Mean	-1	-1	-20	-32	-40	-53	-73
mV	σ	1	1	1	1	1	1	1
SureFlow + Jenco Model-5005 meter								
		1a	1b	2	3	4	5	6
measured pH	2-Jan-14	6.80	6.81	7.13	7.33	7.48	7.70	8.03
measured pH	3-Jan-14	6.78	6.78	7.11	7.31	7.46	7.69	8.02
measured pH	3-Jan-14	6.78	6.78	7.11	7.31	7.46	7.68	8.02
measured pH	Mean	6.79	6.79	7.12	7.32	7.47	7.69	8.02
measured pH	σ	0.01	0.02	0.01	0.01	0.01	0.01	0.01
mV	2-Jan-14	18	17	0	-12	-21	-34	-53
mV	3-Jan-14	19	19	0	-11	-20	-33	-52

Table B.2: Results from Potentiometric pH Measurements of HCl and Tris Buffer Series

mV	3-Jan-14	19	19	0	-11	-20	-33	-52		
mV	Mean	19	18	0	-11	-20	-33	-52		
mV	σ	1	1	0	1	1	1	1		
0.01x's L-SPW										
Ross 815600 + Barnant 20 meter										
<i>I</i> (mol/kg)										
modelled pH, no CO ₂		0.09	0.09	0.09	0.09	0.08	0.08	0.07		
modelled pH, log PCO ₂ = -3.4		6.81	7.13	7.32	7.47	7.68	7.68	8.00		
measured pH	7-Jan-14	6.80	7.12	7.30	7.45	7.66	7.66	7.97		
measured pH	8-Jan-14	6.77	7.10	7.29	7.44	7.66	7.66	7.99		
measured pH	8-Jan-14	6.76	7.08	7.28	7.43	7.66	7.66	7.99		
measured pH	Mean	6.77	7.09	7.29	7.44	7.66	7.66	7.99		
measured pH	σ	0.01	0.01	0.01	0.01	0.01	0.01	0.10		
mV	7-Jan-14	0	-19	-31	-39	-52	-52	-71		
mV	8-Jan-14	1	-19	-30	-39	-52	-52	-71		
mV	8-Jan-14	1	-18	-30	-38	-51	-51	-70		
mV	Mean	1	-19	-30	-39	-52	-52	-71		
mV	σ	1	1	1	1	1	1	1		
SureFlow + Jenco Model-5005 meter										
1 2 3 4 5a 5b 6										
measured pH	7-Jan-14	6.77	7.10	7.30	7.44	7.67	7.67	8.00		
measured pH	8-Jan-14	6.76	7.09	7.28	7.43	7.65	7.65	7.98		
measured pH	8-Jan-14	6.75	7.07	7.27	7.42	7.65	7.65	7.97		
measured pH	Mean	6.76	7.09	7.28	7.43	7.66	7.66	7.98		
measured pH	σ	0.01	0.02	0.02	0.01	0.01	0.01	0.02		
mV	7-Jan-14	19	0	-11	-19	-32	-32	-51		
mV	8-Jan-14	19	0	-10	-19	-32	-32	-51		
mV	8-Jan-14	20	1	-10	-18	-31	-31	-51		
mV	Mean	19	0	-10	-19	-32	-32	-51		
mV	σ	1	1	1	1	1	1	0		
S-SPW										
Ross 815600 + Barnant 20 meter										
HCl1 HCl2 1 2 3 4a 4b 5 6 7 ° C										
<i>I</i> (mol/kg)										
modelled pH, no CO ₂		8.01	7.85	8.22	8.22	8.21	8.21	8.21	8.20	8.20
modelled pH, log PCO ₂ = -3.4		3.16	2.88	6.97	7.31	7.50	7.70	7.70	7.89	8.05
measured pH	15-Jan-14	-	-	6.30	6.63	6.84	7.04	7.04	7.23	7.40
measured pH	16-Jan-14	-	-	6.30	6.63	6.84	7.04	7.04	7.24	7.40
measured pH	17-Jan-14	2.6	2.25	6.30	6.63	6.83	7.04	7.03	7.23	7.40
measured pH	Mean	2.60	2.25	6.30	6.63	6.84	7.04	7.04	7.23	7.40
measured pH	σ	NA	NA	0.00	0.00	0.01	0.00	0.01	0.01	0.00
mV	15-Jan-14	-	-	26	7	-5	-16	-16	-28	-37
mV	16-Jan-14	-	-	26	7	-4	-16	-16	-28	-37
mV	17-Jan-14	242	262	27	8	-4	-16	-16	-28	-37
mV	Mean	242	262	26	7	-4	-16	-16	-28	-37
mV	σ	NA	NA	1	1	1	0	0	0	0
SureFlow + Jenco Model-5005 meter										
HCl1 HCl2 1 2 3 4a 4b 5 6 7										
measured pH	15-Jan-14	-	-	6.31	6.64	6.84	7.04	7.04	7.24	7.40
measured pH	16-Jan-14	-	-	6.31	6.64	6.84	7.04	7.04	7.24	7.40
measured pH	17-Jan-14	2.61	2.27	6.3	6.62	6.83	7.04	7.03	7.23	7.39
measured pH	Mean	2.61	2.27	6.31	6.63	6.84	7.04	7.04	7.24	7.40
measured pH	σ	NA	NA	0.01	0.01	0.01	0.00	0.01	0.01	0.01
mV	15-Jan-14	-	-	45	26	14	2	3	-8	-17
mV	16-Jan-14	-	-	45	26	14	2	3	-8	-18
mV	17-Jan-14	260	280	46	27	15	3	3	-8	-17
mV	Mean	260	280	45	26	14	2	3	-8	-17
mV	σ	NA	NA	1	1	1	0	0	1	1
0.81x's S-SPW										
using 6m old (a) or freshly made (b) phenol red stock solution										
Ross 815600 + Barnant 20 meter										
1a 1b 2a 2b 3a 3b 4a 4b 5a 5b ° C										
<i>I</i> (mol/kg)										
modelled pH, no CO ₂		6.68	6.68	6.67	6.67	6.67	6.67	6.66	6.66	6.66
modelled pH, P _{CO₂} = -3.4		7.14	7.14	7.34	7.34	7.54	7.54	7.74	7.74	7.93
measured pH	27-Feb-14	6.56	6.56	6.76	6.75	6.96	6.96	7.16	7.16	7.36
measured pH	28-Feb-14	6.57	6.56	6.76	6.76	6.96	7.17	7.17	7.36	7.36

Table B.2: Results from Potentiometric pH Measurements of HCl and Tris Buffer Series

measured pH	28-Feb-14	6.56	6.56	6.76	6.75	6.96	6.96	7.16	7.17	7.36	7.36	25.26
measured pH	Mean	6.56	6.56	6.76	6.75	6.96	6.96	7.16	7.17	7.36	7.36	25.15
measured pH	σ	0.01	0.00	0.00	0.01	0.00	0.00	0.01	0.01	0.00	0.00	0.10
mV	27-Feb-14	9	9	-2	-2	-14	-14	-26	-26	-37	-37	
mV	28-Feb-14	9	9	-2	-2	-14	-14	-26	-26	-38	-38	
mV	28-Feb-14	9	9	-2	-2	-14	-14	-26	-26	-37	-37	
mV	Mean	9	9	-2	-2	-14	-14	-26	-26	-37	-37	
mV	σ	0	0	0	0	0	0	0	0	1	1	
SureFlow + Jenco Model-5005 meter												
		1a	1b	2a	2b	3a	3b	4a	4b	5a	5b	
measured pH	27-Feb-14	6.56	6.56	6.76	6.75	6.96	6.96	7.16	7.16	7.36	7.36	
measured pH	28-Feb-14	6.56	6.56	6.75	6.75	6.96	6.96	7.16	7.16	7.35	7.35	
measured pH	28-Feb-14	6.55	6.55	6.74	6.74	6.95	6.95	7.15	7.15	7.35	7.35	
measured pH	Mean	6.56	6.56	6.75	6.75	6.96	6.96	7.16	7.16	7.35	7.35	
measured pH	STD	0.01	0.01	0.01	0.01	0.01	0.01	0.01	0.01	0.01	0.01	
mV	27-Feb-14	27	27	15	15	3	3	-7	-7	-19	-19	
mV	28-Feb-14	27	27	15	15	3	3	-8	-7	-19	-19	
mV	28-Feb-14	27	27	16	16	3	4	-7	-7	-18	-18	
mV	Avg	27	27	15	15	3	3	-7	-7	-19	-19	
mV	STD	0	0	1	1	0	1	1	0	1	1	

0.60x's S-SPW

Ross 815600 + Barnant 20 meter												
		1	2	3	4	5a	5b	6		$^{\circ}\text{C}$		
$I \text{ (mol/kg)}$	4.96	4.95	4.95	4.95	4.94	4.94	4.94	4.93				
modelled pH, no CO ₂	7.05	7.38	7.58	7.77	7.96	7.96	8.18	25.00				
modelled pH, P _{CO2} = -3.4	7.04	7.36	7.56	7.75	7.93	7.93	8.12	25.00				
measured pH	18-Feb-14	6.58	6.92	7.12	7.31	7.51	7.51	7.74	24.98			
measured pH	19-Feb-14	6.57	6.92	7.11	7.31	7.50	7.50	7.73	25.24			
measured pH	19-Feb-14	6.56	6.91	7.11	7.31	7.50	7.50	7.73	25.41			
measured pH	Mean	6.57	6.92	7.11	7.31	7.50	7.50	7.73	25.21			
measured pH	σ	0.01	0.01	0.01	0.00	0.01	0.01	0.01	0.22			
mV	19-Feb-14	9	-12	-23	-34	-46	-46	-59				
mV	19-Feb-14	9	-11	-23	-34	-45	-45	-59				
mV	19-Feb-14	10	-11	-22	-34	-45	-45	-58				
mV	Mean	9	-11	-23	-34	-45	-45	-59				
mV	σ	1	1	1	0	1	1	1				
SureFlow + Jenco Model-5005 meter												
		1	2	3	4	5a	5b	6				
measured pH	19-Feb-14	6.58	6.92	7.12	7.31	7.51	7.51	7.74				
measured pH	19-Feb-14	6.56	6.92	7.11	7.31	7.51	7.51	7.74				
measured pH	19-Feb-14	6.55	6.91	7.10	7.30	7.49	7.49	7.72				
measured pH	Mean	6.56	6.92	7.11	7.31	7.50	7.50	7.73				
measured pH	σ	0.02	0.01	0.01	0.01	0.01	0.01	0.01				
mV	19-Feb-14	27	7	-4	-15	-27	-27	-40				
mV	19-Feb-14	28	7	-3	-15	-26	-26	-39				
mV	19-Feb-14	28	8	-3	-14	-25	-25	-39				
mV	Mean	28	7	-3	-15	-26	-26	-39				
mV	σ	1	1	1	1	1	1	1				

0.36x's S-SPW

Note: there were unusual laboratory temperature fluctuations during the measurements

Ross 815600 + Barnant 20 meter												
		1	2	3	4	5	6		$^{\circ}\text{C}$			
$I \text{ (mol/kg)}$	2.96	2.95	2.95	2.95	2.94	2.94						
modelled no CO ₂	7.15	7.44	7.63	7.82	7.99	8.22	25.00					
modelled PCO ₂ = -3.4	7.14	7.42	7.62	7.79	7.96	8.17	25.00					
measured pH	11-Mar-14	6.74	7.07	7.28	7.48	7.67	7.90	25.36				
measured pH	12-Mar-14	6.74	7.07	7.28	7.48	7.68	7.90	25.45				
measured pH	12-Mar-14	6.76	7.10	7.30	7.50	7.70	7.93	24.14				
pH	Mean	6.75	7.08	7.29	7.49	7.68	7.91	24.98				
pH	σ	0.01	0.02	0.01	0.01	0.02	0.02	0.73				
mV	11-Mar-14	-2	-21	-33	-45	-56	-69					
mV	12-Mar-14	-3	-22	-34	-46	-57	-70					
mV	12-Mar-14	-4	-23	-35	-47	-58	-71					
mV	Avg	-3	-22	-34	-46	-57	-70					
mV	STD	1	1	1	1	1	1					
SureFlow + Jenco Model-5005 meter												
		1	2	3	4	5a	6					

Table B.2: Results from Potentiometric pH Measurements of HCl and Tris Buffer Series

measured pH	11-Mar-14	6.73	7.06	7.26	7.46	7.65	7.88
measured pH	12-Mar-14	6.72	7.05	7.26	7.46	7.65	7.88
measured pH	12-Mar-14	6.74	7.07	7.28	7.48	7.67	7.90
pH	Mean	6.73	7.06	7.27	7.47	7.66	7.89
pH	σ	0.01	0.01	0.01	0.01	0.01	0.01
mV	11-Mar-14	15	-3	-15	-26	-38	-51
mV	12-Mar-14	15	-3	-15	-27	-38	-51
mV	12-Mar-14	14	-4	-16	-28	-39	-53
mV	Avg	15	-3	-15	-27	-38	-52
mV	STD	1	1	1	1	1	1
0.03x's S-SPW							
Ross 815600 + Barnant 20 meter							
I (mol/kg)							
1 2 3 4 5 6 ° C							
modelled pH, no CO ₂		7.04	7.38	7.58	7.79	7.99	8.24 25.00
modelled pH, P _{CO2} = -3.4		7.03	7.36	7.57	7.76	7.96	8.19 25.00
measured pH	20-Feb-14	6.97	7.31	7.52	7.73	7.94	8.19 24.37
measured pH	21-Feb-14	6.96	7.30	7.51	7.72	7.93	8.18 25.16
measured pH	21-Feb-14	6.95	7.29	7.5	7.71	7.92	8.18 25.46
measured pH	Avg	6.96	7.30	7.51	7.72	7.93	8.18 25.00
measured pH	STD	0.01	0.01	0.01	0.01	0.01	0.56
mV	20-Feb-14	-14	-34	-46	-58	-70	-85
mV	21-Feb-14	-13	-33	-46	-58	-70	-85
mV	21-Feb-14	-13	-33	-45	-57	-69	-84
mV	Mean	-13	-33	-46	-58	-70	-85
mV	σ	1	1	1	1	1	1
SureFlow + Jenco Model-5005 meter							
1 2 3 4 5 6							
measured pH	20-Feb-14	6.97	7.31	7.52	7.73	7.93	8.19
measured pH	21-Feb-14	6.95	7.28	7.5	7.71	7.91	8.17
measured pH	21-Feb-14	6.94	7.28	7.49	7.7	7.91	8.16
measured pH	Mean	6.95	7.29	7.50	7.71	7.92	8.17
measured pH	σ	0.02	0.02	0.02	0.02	0.01	0.02
mV	20-Feb-14	4	-15	-27	-39	-52	-66
mV	21-Feb-14	5	-14	-26	-38	-50	-66
mV	21-Feb-14	5	-13	-26	-38	-50	-65
mV	Mean	5	-14	-26	-38	-51	-66
mV	σ	1	1	1	1	1	1

" - " means not measured; NA mean Not Applicable

B.6 PHENOL RED pK'a DETERMINATION RESULTS

Table B.3: pK'a Measurement Results Based on Modelled pH Assuming No Effect from Atmospheric CO_{2(g)}

pK'a				pK'a			
°C	Measured	Temperature Corrected	°C	Measured	Temperature Corrected		
Just Tris				0.1m NaCl			
<i>Mean I = 0.04 mol/kg</i>				<i>Mean I = 0.10 mol/kg</i>			
9-Jan-14	24.88	7.80	7.80	9-Sep-13	24.0	7.69	7.72
10-Jan-14	24.48	7.79	7.81	11-Sep-13	24.8	7.72	7.72
10-Jan-14	24.98	7.81	7.81	13-Sep-13	25.5	7.73	7.72
Mean	24.78	7.80	7.81	Mean	24.8	7.71	7.72
σ	0.26	0.01	0.004	σ	0.8	0.02	0.004
RSD	1.07%	0.11%	0.05%	RSD	3%	0.25%	0.05%
1.0m NaCl				1.0m NaCl			
<i>Mean I = 1.02 mol/kg</i>				<i>Mean I = 1.00 mol/kg</i>			
18-Sep-13	23.70	7.55	7.59	13-Jan-14	24.61	7.59	7.60
24-Sep-13	25.10	7.59	7.59	13-Jan-14	24.69	7.61	7.61
24-Sep-13	24.60	7.59	7.60	14-Jan-14	24.64	7.59	7.60
Mean	24.47	7.58	7.59	Mean	24.65	7.60	7.60
σ	0.71	0.02	0.008	σ	0.04	0.01	0.01
RSD	3%	0.29%	0.11%	RSD	0.16%	0.11%	0.12%
5.0m NaCl				L-SPW			
<i>Mean I = 5.00 mol/kg</i>				<i>Mean I = 4.92 mol/kg</i>			
27-Sep-13	25.55	7.68	7.67	24-Oct-13	25.01	7.73	7.73
30-Sep-13	25.32	7.68	7.67	25-Oct-13	24.60	7.70	7.71
1-Oct-13	25.20	7.69	7.69	28-Oct-13	24.70	7.70	7.71
Mean	25.36	7.69	7.67	Mean		7.71	7.71
σ	0.18	0.00	0.01	σ		0.02	0.01
RSD	0.70%	0.06%	0.13%	RSD		0.25%	0.17%
1.57x's L-SPW				1.45x's L-SPW			
<i>Mean I = 7.66 mol/kg</i>				<i>Mean I = 7.08 mol/kg</i>			
13-Nov-13	25.07	7.79	7.79	19-Nov-13	24.64	7.79	7.80
14-Nov-13	25.08	7.78	7.78	20-Nov-13	25.19	7.77	7.77
15-Nov-13	25.09	7.79	7.79	15-Nov-13	24.34	7.75	7.77
Mean	25.08	7.79	7.79	Mean	24.72	7.77	7.78
σ	0.01	0.01	0.01	σ	0.43	0.02	0.02
RSD	0.04%	0.09%	0.09%	RSD	1.75%	0.30%	0.27%
1.34x's L-SPW				1.22x's L-SPW			
<i>Mean I = 6.52 mol/kg</i>				<i>Mean I = 5.96 mol/kg</i>			
27-Nov-13	24.73	7.77	7.78	3-Dec-13	24.21	na	na
28-Nov-13	24.88	7.75	7.75	4-Dec-13	24.93	na	na
15-Nov-13	24.87	7.77	7.78	4-Dec-13	24.86	7.73	7.74
Mean	24.83	7.76	7.77	6-Dec-13	24.52	na	na
σ	0.09	0.01	0.01	Mean	24.63	7.73	7.74
RSD	0.35%	0.15%	0.17%	σ	0.33	na	na
				RSD	1.35%	na	na

("na" means there were issues with the flow through)

Table B.3: pK'a Measurement Results Based on Modelled pH Assuming No Effect from Atmospheric CO_{2(g)}

pK'a Measured Temperature °C Corrected				pK'a Measured Temperature °C Corrected			
1.22x's L-SPWb <i>Mean I = 5.96 mol/kg</i>				LSPW2 <i>Mean I = 4.89 mol/kg</i>			
4-Mar-14	25.07	7.74	7.74	9-Dec-13	24.87	7.70	7.71
5-Mar-14	24.95	7.73	7.73	10-Dec-13	24.91	7.67	7.68
5-Mar-14	25.00	7.73	7.73	10-Dec-13	24.58	7.72	7.73
Mean	25.01	7.73	7.73	Mean	24.79	7.70	7.71
σ	0.06	0.01	0.01	σ	0.18	0.02	0.03
RSD	0.24%	0.10%	0.08%	RSD	0.72%	0.29%	0.35%
0.73x's L-SPW <i>Mean I = 3.60 mol/kg</i>				0.48x's L-SPW <i>Mean I = 2.38 mol/kg</i>			
12-Dec-13	24.87	7.64	7.64	17-Dec-13	24.17	7.59	7.62
13-Dec-13	24.49	7.64	7.66	18-Dec-13	24.90	7.60	7.61
13-Dec-13	24.86	7.66	7.66	18-Dec-13	25.04	7.62	7.62
Mean	24.74	7.65	7.65	27-Dec-13	24.91	7.61	7.61
σ	0.22	0.01	0.01	Mean	24.75	7.61	7.61
RSD	0.88%	0.12%	0.11%	σ	0.40	0.01	0.005
				RSD	1.60%	0.16%	0.06%
0.24x's L-SPW <i>Mean I = 1.19 mol/kg</i>				0.09x's L-SPW <i>Mean I = 0.49 mol/kg</i>			
19-Dec-13	24.89	7.60	7.61	2-Jan-14	25.26	7.61	7.60
20-Dec-13	24.96	7.62	7.62	3-Jan-14	25.08	7.63	7.63
20-Dec-13	25.02	7.62	7.62	3-Jan-14	24.97	7.64	7.64
Mean	24.96	7.61	7.61	Mean	25.10	7.63	7.62
σ	0.07	0.01	0.01	σ	0.15	0.01	0.02
RSD	0.27%	0.11%	0.08%	RSD	0.58%	0.16%	0.22%
0.01x's L-SPW <i>Mean I = 0.09 mol/kg</i>				S-SPW <i>Mean I = 8.21 mol/kg</i>			
7-Jan-14	24.83	7.74	7.74	15-Jan-14	24.76	7.80	7.80
8-Jan-14	24.78	7.75	7.76	16-Jan-14	24.70	7.82	7.83
8-Jan-14	24.97	7.75	7.75	17-Jan-14	24.79	7.82	7.83
Mean	24.86	7.75	7.75	Mean	24.75	7.81	7.82
σ	0.10	0.01	0.01	σ	0.05	0.01	0.01
RSD	0.40%	0.11%	0.11%	RSD	0.19%	0.17%	0.17%
0.81x's S-SPWa (using 6m old phenol red indicator stock) <i>Mean I = 4.95 mol/kg</i>				0.81x's S-SPWb (using freshly made phenol red indicator stock) <i>Mean I = 4.95 mol/kg</i>			
27-Feb-14	25.08	7.74	7.74	27-Feb-14	25.08	7.75	7.74
28-Feb-14	25.10	7.76	7.76	28-Feb-14	25.10	7.76	7.76
28-Feb-14	25.26	7.77	7.76	28-Feb-14	25.26	7.77	7.76
Mean	25.22	7.76	7.75	Mean	25.22	7.76	7.76
σ	0.20	0.01	0.01	σ	0.20	0.01	0.01
RSD	0.81%	0.18%	0.15%	RSD	0.81%	0.18%	0.15%

Table B.3: pK'a Measurement Results Based on Modelled pH Assuming No Effect from Atmospheric CO_{2(g)}

		pK'a				pK'a	
	°C	Measured	Temperature Corrected		°C	Measured	Temperature Corrected
0.60x's S-SPW							
<i>Mean I = 4.95 mol/kg</i>							
18-Feb-14	24.98	7.68	7.68	11-Mar-14	25.36	7.65	7.64
19-Feb-14	25.24	7.69	7.68	12-Mar-14	25.45	7.67	7.65
19-Feb-14	25.41	7.71	7.70	12-Mar-14	24.14	7.65	7.67
Mean	25.21	7.69	7.69	Mean	24.98	7.66	7.66
σ	0.22	0.02	0.01	σ	0.73	0.01	0.02
RSD	0.86%	0.20%	0.12%	RSD	2.9%	0.13%	0.21%
0.36x's S-SPW							
<i>Mean I = 2.95 mol/kg</i>							
20-Feb-14	24.37	7.65	7.65	Notes:			
21-Feb-14	25.16	7.67	7.66	<i>I</i> = ionic strength; σ = standard deviation			
21-Feb-14	25.46	7.67	7.66				
Mean	25.00	7.66	7.65				
σ	0.56	0.01	0.00				
RSD	2.3%	0.13%	0.04%				